

ResearchOnline@JCU

This file is part of the following reference:

Wilkes, Mark Christopher (2016) *Regulation of transforming growth factor beta (TGF β) at the level of nuclear entry*. PhD thesis, James Cook University.

Access to this file is available from:

<https://researchonline.jcu.edu.au/51506/>

The author has certified to JCU that they have made a reasonable effort to gain permission and acknowledge the owner of any third party copyright material included in this document. If you believe that this is not the case, please contact

ResearchOnline@jcu.edu.au and quote

<https://researchonline.jcu.edu.au/51506/>

Regulation of Transforming Growth Factor beta (TGF β) at the Level of Nuclear Entry

Thesis submitted by

Mark Christopher WILKES

B.Sc (Biochemistry)

James Cook University

March 2016

for the degree of Doctor of Philosophy
in the College of Public Health, Medical and Veterinary Sciences
James Cook University

ACKNOWLEDGEMENTS

First and foremost I would like to thank my two mentors. Firstly, Dr Catherine Rush, who supervised and advised on the academic and institutional matters, as well as oversaw the thesis construction, on the Australian side of the Pacific at James Cook University. Secondly, Professor Edward Leof who oversaw the majority of bench work and manuscript preparation, and provided the freedom to explore and discover, yet focused me when my pursuits became too diffuse. Professor Jules Dore's insight was instrumental in allowing me to bring the thesis to an acceptable level and mentorship invaluable. The advice, friendship and support from Noriko Daneshtalab during times of hardship and frustration will never be forgotten. At James Cook University I also need to thank Professors Helene Marsh and Jeff Warner who worked tirelessly to provide me the best possible situation in which to write up my thesis and overcome adversity. Assistance in the preparation and organization of my confirmation and exit seminars was provided by Ben Crowley and Professor Alan Baxter.

Furthermore, Professors Jim Burnell and Subhash Vasudevan who's enthusiasm and passion piqued my curiosity in biochemistry, Drs Jules Dore, Nandor Garamszegi and Diying Yao who nurtured my early scientific thoughts, and Drs Deepak Sharma and Claire Repellin that made investigating scientific questions and pursuing experimental results fun. The technicians, students, postdocs and principal investigators I have worked with in my time at Mayo Clinic have all contributed beyond what I can express and I shall always be indebted. Drs Mark McNiven, Dave Katzmann and Dan Billadeau provided helpful discussion, both professional and personal, that helped me through challenging times. Without saying, the support, guidance and love from my parents, brother, wife, children, friends and family have been, and continue to be instrumental. To all, thank you.

Finally, the study would not have been possible without the generous sharing of reagents and support from funding agencies. Thank you to Drs. Sven Carlsson, Ralf Janknecht, Katie Ullman and André Hoelz respectively, for the indicated SNX9, Smad, Nup153-HA, and Nup214-HA constructs. Additionally I would like to thank the late Dr Anita Roberts (NIH, Bethesda, MD) for supplying Smad2^{-/-} mouse embryo fibroblasts and Dr Jinhua Li (Monash University, Australia) for supplying Phospho-PAK2 site specific R-Smad antibody and Dr Jeff Wrana for providing the sequence of a functional extracellular epitope-tagged TGF β R2. This work was supported by Public Health

Service grants GM-55816 and GM-54200 from the National Institute of General Medical Sciences, the Scleroderma Foundation, and the Mayo Foundation awarded to Edward B. Leof. There is no actual, potential or apparent conflict of interest that we are aware.

STATEMENT OF THE CONTRIBUTION OF OTHERS

Nature of Assistance	Contribution	Names
Intellectual Support	Proposal Writing	Edward Leof,, Jules Dore
	Data Analysis	Edward Leof, Claire Repellin, Jules Dore
	Experimental Design	Edward Leof, Mark McNiven, David Katzman, Dan Billadeau
	Editorial Assistance	Edward Leof, Claire Repellin, Cathy Rush, Jon Gollege
Financial Support		NIH General Medicine Schleroderma Foundation Mayo Clinic and Foundation
	Grant Write Up	Edward Leof, Cathy Rush
Data Collection	Research Assistance	Claire Repellin, Jeung Han Kang
	Confocal Microscopy Assistance	Jeung Han Kang
	Stable Cell Generation	Xuiqien Yi, Claire Repellin
	Validation of Results	Jeung Han Kang, Claire Repellin

ABSTRACT

Transforming Growth Factor β (TGF β) has broad reaching biological actions spanning development, homeostasis and disease. Whilst our understanding of many of the molecules involved in the TGF β signalling cascade is growing, precisely how these factors deliver their messages into the nucleus remain elusive.

The aim of this study was to investigate the cellular machinery and mechanisms involved in delivering proteins involved in the TGF β cascade into the nucleus. Using novel constructs and diverse cell biology tools and techniques, the effects and consequences of TGF β stimulation on the expression, activity, sub-cellular localisation and molecular associations of various proteins within the cell were assessed.

The primary mediators of TGF β responses from the receptors into the nucleus are the two Smad proteins, Smad2 and Smad3. Despite significant sequence homology and apparently identical receptor regulation and DNA sequence recognition sequences, knockout and overexpression studies indicate each of these proteins have very differing roles in homeostasis, tumour/fibrosis suppression and driving tumour/fibrosis progression (Yamamoto 1999, Santiago 2005, Hoot 2008, Meng 2010). Here (Chapter 4), we identify SNX9 as being required for Smad3 (but not Smad2) nuclear translocation and cell stimulation. SNX9 principally interacts with phosphorylated (p) Smad3 independent of Smad2 or Smad4 and promotes more rapid nuclear delivery from that observed independent of ligand. Although SNX9 does not bind Imp7, Imp β , Nup153 or Nup214, it mediates the association of pSmad3 with Imp8 and the nuclear membrane via Phox Homology (PX) and Bin, Amphiphysin, Rvs (BAR) domain phosphoinositide binding motifs. This facilitates recruitment of pSmad3/SNX9 to the nuclear pore, heterodimerization of Imp8 with Imp β , and nuclear translocation of pSmad3, but not SNX9. The demonstration that Smad3 is regulated in a distinct manner from Smad2 provides the opportunity to develop intervention strategies to enhance or dampen specific aspects of the cellular response to TGF β .

Smad phosphorylation in response to TGF β stimulation occurs in all cell types expressing TGF β receptors, however in a number of mesenchymal cell lines TGF β receptors also activate PAK2, contributing to a distinct fibroblastic TGF β response (Wilkes 2003, Sato 2013). Within this study (Chapter 5), we document PAK2 phosphorylation of R-Smads at a site distinct from the C terminal SSxS motif recognized by TGF β R1. Furthermore, R-Smad phosphorylation at the PAK2 site

prolongs the duration of the receptor-recognized phosphorylation sites, by preventing binding of PPM1A, the nuclear phosphatase that dephosphorylates the R-Smad receptor sites.

For many cytokines, the accepted model of signal propagation requires a transmembrane receptor complex that becomes enzymatically active upon binding the extracellular ligand, to transmit the signal through enzymatic modification of soluble, cytoplasmic proteins that are either directly transported to the nucleus, or initiate a cascade of enzymatic reactions that ultimately lead to transcriptional alterations. The accepted model of TGF β signalling fits well within that paradigm. However, in recent years, a number of plasma membrane-embedded tyrosine kinase receptors have been documented to traffic from the cell surface to the nucleus, in addition to activating signalling cascades in soluble, cytoplasmic proteins. Evidence is accumulating that a pool TGF β receptors are also trafficking to the nucleus upon ligand stimulation (Mu 2011, Chandra 2012, Gudey 2014). We document (in Chapter 6) nuclear trafficking of TGF β receptors occurs in normal and transformed cells with both TGF β R1 and TGF β R2 required for nuclear entry. Receptors pass through the Golgi apparatus, COPI vesicles, endoplasmic reticulum, retrotranslocon and nuclear pore *en route* to the nucleus. Upon nuclear entry, receptors are not soluble, instead residing in the inner nuclear membrane before incorporation into Promyolecytic Leukemia (PML) nuclear bodies. In the nucleus, TGF β R1 phosphorylates a number of transcription factors, including ATF/CREB and are required for the robust induction of a subset of TGF β /Smad genes.

Being that many of the genes we identified as requiring the presence of nuclear TGF β receptors for TGF β regulation have previously been reported as being Smad-dependent, we sought to investigate this apparent data conflict. We document (in Chapter 7), TGF β receptors in the nucleus maintain kinase activity, and the phosphorylation of transcription factors such as ATF2, CREB and sp1 increases the histone acetyltransferase (HAT) activity of these transcription factors, leading to the exposure of Smad Binding Elements (SBEs) in the promoter regions surrounding the phosphorylated ATF2/CREB/sp1. Once exposed, nuclear pSmad2/3 bind these SBEs in the promoters, prompting a full transcriptional response. In this way the presence of nuclear receptors works in co-operation with the Smads, each being required (but not sufficient) for the TGF β -induced effect.

Additionally (in Chapter 6), we report a short region of 14 amino acids in TGF β R2 that binds to the retromer complex is required for nuclear translocation of the receptors.

While retromer binding is maintained in TGF β superfamily members, such as BMPR2 and ActR2, these receptors fail to translocate to the nucleus upon stimulation. We report a single lysine (K488) that is not present in BMPR2 or ActR2 is responsible for conferring nuclear trafficking ability. We also present evidence ubiquitination of this site may be the cue to select the nuclear-bound subset of receptors from the larger pool being degraded.

Our aim has been to examine how the various components of the TGF β pathway are relayed into the nucleus, the routes, the factors and the mechanisms. Along the way we have stumbled onto unexpected results that have been problematic to explain, as well as pieces of information that have helped unite seemingly contradictory data within the field. As with most studies our answers have opened up as many questions as we've answered but, at least in some small part, we have gained insight too.

Uncovering differential mechanisms for nuclear translocation of Smad2 and Smad3 gives validity to models claiming cells actively balance these two signals in various cell contexts. Extending the duration of nuclear signalling of Smads by phosphorylation at non-receptor sites by kinases activated only in select cell types also provides a mechanism for cells to balance and fine tune Smad signals to meet the needs of the cell. Uncovering the nuclear translocation of the TGF β receptors adds another TGF β activated kinase that contributes to the nuclear message. Reports of differential expression and multiple mechanisms to deliver these active kinases to the nucleus imply this too is actively regulated to balance with Smad and other non-Smad signals. As we move forward in our attempts to manage disease states driven by aberrant TGF β signalling we might do well if we switch our thinking from general inhibitors of all TGF β signalling or blocking the activity of single components of the pathway, but rather look to influence interactions that influence the balance of these factors.

Admittedly our understanding of the mechanisms regulating the balance between these factors are in their infancy but with concept of tumour microenvironment and stromal interactions already firmly in place amongst cancer researchers, it seems plausible this way of thinking will permeate throughout research and influence those of us advancing TGF β understanding. While the age of identifying new TGF β -specific signalling factors may be at its twilight, a new exciting age of exploring the mechanisms that balance these factors and how other cell stimuli cross talk and influence the TGF β signal is just beginning. We contend a major bottleneck to regulation is importing these factors into and out of the nucleus and factors like SNX9, retromer complex and kinases such as PAK2 play an important role in this process.

Insight from these studies sheds light on new regulatory controls utilized to fine tune the TGF β signalling cascade with only a limited number of core protein components, with the potential to adapt to a wide range of environmental cues across numerous cell types. Modulating the TGF β signal at the level of nuclear entry or exit not only enhances our knowledge of how this powerful signal impacts the cell, but also provides essential insight into therapeutic strategies for management of the numerous clinical manifestations that occur due to imbalances in TGF β signalling that regularly occur in human disease.

TABLE OF CONTENTS

ACKNOWLEDGEMENTS	i
STATEMENT OF THE CONTRIBUTION OF OTHERS	iii
ABSTRACT	iv
LIST OF TABLES	xiv
LIST OF FIGURES	xv
LIST OF ABBREVIATIONS	xix
CHAPTER 1: GENERAL INTRODUCTION.....	2
1.1 Thesis rationale and hypothesis.....	3
CHAPTER 2: LITERATURE REVIEW.....	6
2.1 Ligands of the Transforming Growth Factor-beta Superfamily.....	6
2.2 Receptors of the TGF β Superfamily.....	12
2.2.1 Ligand binding to Type I and Type II Receptors	12
2.2.2 Receptor-mediated signal transduction	13
2.2.3 Co-receptors for Type I and II receptors	16
2.3 Activating the signalling cascades of the TGF β Superfamily.....	18
2.3.1 Smad domain structure	20
2.3.2 Linker and non-receptor mediated Smad phosphorylation.....	21
2.4 Smad translocation into the nucleus	25
2.5 Role of Smads in transcription	28
2.5.1 DNA binding	28
2.5.2 Transcriptional co-activators of Smads.....	28
2.5.3 Histone acetyltransferases and histone deacetylases.....	31
2.6. TGF β signal termination.....	31
2.6.1 Smad dephosphorylation for signal termination	32
2.6.2 Smad ubiquitination for signal termination.....	33
2.7. TGF β receptor deactivation, downregulation and degradation.....	35
2.8. Nuclear entry of soluble proteins.....	38
2.9. Nuclear entry of cleaved membrane-embedded proteins.....	41
2.10 Nuclear entry of full-length membrane-embedded proteins.....	43
2.10.1 Endocytosis.....	44
2.10.2 Receptor entry into and exit from the Golgi.....	46
2.10.3 Endoplasmic reticulum and retrotranslocon	49
2.10.4 Receptor intracellular chaperones	51
CHAPTER 3: GENERAL MATERIALS AND METHODS.....	56

3.1	Generation of plasmids and purified proteins	57
3.1.1	Plasmid construction and preparation	61
3.1.2	Gene Cloning	62
3.1.2.1	Polymerase Chain Reaction (PCR) cloning	62
3.1.2.2	Gel electrophoresis and plasmid purification.....	62
3.1.2.3	Ligation.....	62
3.1.2.4	Transformation of <i>E.coli</i>	62
3.1.2.5	Construct validation.....	63
3.1.3	Site direct mutagenesis.....	63
3.1.4	Preparation of fusion proteins from <i>E. coli</i>	63
3.2	Generation and culture of cell lines and viruses	64
3.2.1	GM-CSF/TGF β chimeric receptors: rationale and strategy	67
3.2.2	Culture conditions	69
3.2.3	Transfection of cell lines.....	69
3.2.3.1	Lipofectamine® 2000	69
3.2.3.2	FuGENE® 6	69
3.2.3.3	TransIT® 2020	69
3.2.4	Generation of recombinant Adenovirus	70
3.2.5	Generation of recombinant Lentivirus.....	70
3.2.6	Infection of cell lines.....	70
3.2.7	Gene silencing	71
3.3	TGF β stimulation of cell lines.....	71
3.4	Experimental analysis.....	71
3.4.1	Cell-based assays.....	72
3.4.1.1	[³ H] Thymidine incorporation proliferation assay	72
3.4.1.2	Soft agar assays.....	72
3.4.2	Visual analysis of intracellular compartments and trafficking	72
3.4.3	Gene expression analysis	73
3.4.3.1	Luciferase reporter assays	73
3.4.3.2	Quantitative Reverse Transcriptase-Polymerase Chain Reaction (qRT-PCR).....	73
3.4.4	Protein analysis.....	73
3.4.4.1	Cellular compartment fractionation	76
3.4.4.1.1	Golgi and Endoplasmic Reticulum fractionation.....	76
3.4.4.1.2	COPI vesicle fractionation	76
3.4.4.1.3	Inner nuclear membrane fractionation	77
3.4.4.1.4	Nuclear membrane, soluble and chromatin-bound fractionation	77
3.4.4.1.5	Nuclear fractions	77
3.4.4.2	Immunoprecipitation	79
3.4.4.3	Kinase assays	80
3.4.4.4	Western blotting	80
3.4.4.5	Co-immunoprecipitation.....	80
3.4.4.6	GST fusion protein pull-down assays	81

CHAPTER 4: SORTING NEXIN 9 DIFFERENTIATES LIGAND-ACTIVATED SMAD3 FROM SMAD2 FOR NUCLEAR TRANSLOCATION AND TGF β SIGNALLING

		84
4.1	BACKGROUND	84
4.2	MATERIALS AND METHODS	87

4.2.1	Cell culture and stimulation	87
4.2.2	Gene silencing and expression of mutant SNX9 constructs	88
4.2.3	Role of SNX9 in TGF β -induced anchorage-independent growth in fibroblasts	89
4.2.4	Role of SNX9 in TGF β induced growth arrest in epithelial cells.....	90
4.2.5	Role of SNX9 in the TGF β -induced transcriptional regulation of Smad2 and Smad3 responsive Genes.....	90
4.2.6	Western blotting and immunoprecipitation.....	91
4.2.7	Isolation of SNX9/Smad protein complexes using GST-pull-down.....	91
4.2.8	Isolating nuclear compartments to determine the role of SNX9 in trafficking of Smads into the nucleus.....	92
4.2.9	Visualization of SNX9 and Smads using immunofluorescence microscopy	92
4.2.10	Generation of TAT-Smad fusion proteins.....	92
4.2.11	Isotope labelling of unphosphorylated and phosphorylated TAT-Smad proteins.....	94
4.2.12	Determining Smad3/pSmad3 nuclear entry kinetics using TAT-Smad3	94
4.2.13	SNX9/pSmad3 binding to lipid membranes.....	95
4.2.14	Determination of Dynamin GTPase activity.....	96
4.3	RESULTS.....	97
4.3.1	Sorting Nexin 9 Specifically Regulates Smad3-dependent TGF β Signalling.....	97
4.3.2	SNX9 required for Smad3 but not Smad2 nuclear translocation.....	101
4.3.3	SNX9 specifically impacts phosphorylated Smad3 nuclear entry.....	104
4.3.4	SNX9 preferentially binds phosphorylated Smad3.....	107
4.3.5	SNX9 requirements for nuclear membrane association.....	113
4.3.6	SNX9 is required for Smad3/Importin 8 complex formation	113
4.3.7	Importin 8 links pSmad3 to Importin- β for nuclear entry.....	117
4.3.8	pSmad3/SNX9 is recruited to nuclear membrane by SNX9 PIP2 binding domain.....	119
4.4	DISCUSSION.....	123

CHAPTER 5: ROLE OF p21-ACTIVATED KINASE 2 (PAK2) IN

DEPHOSPHORYLATION OF SMAD2 IN TGF β SIGNALLING..... 129

5.1	BACKGROUND	129
5.2	MATERIALS AND METHODS	133
5.2.1	Cell culture and stimulation	133
5.2.2	Phosphorylation of Smads by activated PAK2.....	134
5.2.3	Detection of Smad phosphorylation by western blotting	134
5.2.4	p21-Activated Kinase-2 (PAK2) expressing adenovirus production and infection	134
5.2.5	Smad mutant construction and validation.....	135
5.2.6	Smad Co-Immunoprecipitations	135
5.2.7	Nuclear fractionations	136
5.3	RESULTS.....	136
5.3.1	TGF β -induced R-Smads contain conserved PAK2 phosphorylation consensus sequences and can be phosphorylated by activated PAK2 <i>in vitro</i> and <i>in vivo</i>	136
5.3.2	Phosphorylation of Smad2 at Threonine 430 only occurs in fibroblasts.....	137
5.3.3	Phosphorylation at Threonine 430 decreases the susceptibility of Smad2 to dephosphorylation at Serines 465/467	138

5.3.4 Smad2 phosphorylation at Threonine 430 has no impact on nuclear translocation, heterodimerization with Smad4, or sensitivity to ligand.....	140
5.3.5 Phosphorylation at Threonine 430 prevents the phosphatase PPM1A from binding Smad2 and dephosphorylating Serines 465/467.....	142
5.4 DISCUSSION.....	143

CHAPTER 6: RETROGRADE TRAFFICKING OF TGF β RECEPTOR POOL

TO THE NUCLEUS UPON TGF β STIMULATION..... 151

6.1 BACKGROUND 151

6.2 MATERIALS AND METHODS 154

6.2.1 Cell culture and stimulation 154

6.2.2 Visualization of surface receptors and intracellular compartments using immunofluorescence confocal microscopy 155

6.2.3 Isolation of intracellular compartments via fractionation..... 157

6.2.3.1 Nuclear fractions 157

6.2.3.2 Inner nuclear membrane fractions 157

6.2.3.3 COPI vesicle fractions 157

6.2.3.4 Golgi and Endoplasmic Reticulum fractions..... 157

6.2.3.5 Nuclear membrane, soluble nuclear and chromatin associated fractions..... 158

6.2.4 Generation of TGF β receptor constructs for receptor trafficking analysis 158

6.2.4.1 TGF β receptors expressing extracellular epitope for use in immunofluorescence confocal microscopy imaging..... 158

6.2.4.2 TGF β receptors expressing intracellular FLAG epitope 159

6.2.4.3 GM-CSF/TGF β chimeric receptors 159

6.2.4.4 TGF β R1 expressing di-Lysine mutations 159

6.2.4.5 TGF β R2 truncations, Δ 484-498 deletion, K488Q mutant and DUB fusion mutants..... 160

6.2.5 Biotinylation of surface proteins for detection of Activin and TGF β receptors in subcellular compartments..... 160

6.2.6 Disruption of retrograde trafficking components 161

6.2.6.1 Gene silencing of retrograde trafficking components 163

6.2.6.2 Pharmacological disruption of clathrin and caveolar endocytosis and polymyeloid leukemia (PML) body formation 164

6.2.7 Activin and TGF β receptor co-immunoprecipitation with retromer subunits 164

6.3 RESULTS..... 165

6.3.1 Upon TGF β stimulation, a subset of surface receptors traffic to the nucleus through the golgi and endoplasmic reticulum 165

6.3.1.1 TGF β R1 and TGF β R2 translocate from the cell surface to the nucleus after TGF β stimulation in different cell types, from different species and in transformed and non-transformed lines as full-length proteins 165

6.3.1.2 Nuclear TGF β Receptors enter the cell via clathrin-mediated endocytosis.... 168

6.3.1.3 TGF β Receptors translocate to the nucleus via the Golgi and Endoplasmic Reticulum..... 169

6.3.2 TGF β receptors traffic to nucleus together: TGF β R2 facilitates Golgi entry, while TGF β R1 is required for COPI vesicle entry and subsequent nuclear delivery 170

6.3.3. Golgi sorting requires TGF β R2 domain interacting with retromer complex 174

6.3.4 TGF β Type II receptor superfamily share retromer binding but Lys488 confers nuclear targeting in TGF β R2 but not other superfamily members..... 176

6.3.4.1 Retromer binds TGF β R2 and Activin Type II receptor..... 177

6.3.4.2 Activin Type II Receptor does not traffic to the nucleus after Activin stimulation.....	177
6.3.4.3 Lysine 488 in TGF β R2 confers Golgi targeting, possibly via ubiquitination ...	178
6.3.5 Di-Lysines in TGF β R1 required for COPI vesicle sorting of both TGF β receptors.....	180
6.3.6 Receptors are delivered to the inner nuclear membrane through the retrotranslocon and nuclear pore.....	183
6.3.7 TGF β receptors enter PML bodies from the inner nuclear membrane	186
6.4 DISCUSSION	189

CHAPTER 7: ROLE OF NUCLEAR TGF β RECEPTORS IN REGULATION OF TGF β -RESPONSIVE GENES 195

7.1 BACKGROUND	195
7.2 MATERIALS AND METHODS	197
7.2.1 Cell culture and stimulation	197
7.2.2 Transcription Factor phosphorylation by TGF β Receptors.....	197
7.2.3 Comparison of kinase activity between plasma membrane and nuclear TGF β R1	198
7.2.4 The role of kinase activity in nuclear trafficking of TGF β Receptors	198
7.2.5 Effect of TGF β R1 mediated phosphorylation on histone acetyltransferase (HAT) activity of Transcription Factors	199
7.2.6 Determination of the role of di-Lysine motifs in TGF β R1-mediated Smad phosphorylation, nuclear translocation and binding to Smad Binding Elements.....	200
7.2.6.1 Comparison of TGF β R1 WT and 2xDiK Smad3 phosphorylation <i>in vitro</i>	200
7.2.6.2 Comparison of TGF β R1 WT and 2xDiK Smad2 and Smad3 phosphorylation <i>in vivo</i>	200
7.2.6.3 Comparison of TGF β R1 WT- and 2xDiK-mediated Smad2 and Smad3 nuclear translocation	200
7.2.6.4 Comparison of TGF β R1 WT- and 2xDiK-mediated Smad2 and Smad3 binding to SBES	201
7.2.7 Effect of diLysine mutations in TGF β R1 on pSmad3 promoter binding using Chromatin Immunoprecipitation (ChIP)	202
7.2.8 qRT-PCR of TGF β -induced genes	203
7.2.9 Anaysis of gene and chromatin array data	204
7.3 RESULTS	205
7.3.1 Kinase activity of TGF β R2 (but not TGF β R1) is required for nuclear entry	205
7.3.2 TGF β R1 kinase activity is maintained after trafficking to the nucleus	206
7.3.3 TGF β R1 phosphorylates ATF-CREB Transcription Factors <i>in vitro</i>	207
7.3.4 Nuclear delivery of activated TGF β R1 is required for the phosphorylation and increased P300 binding of ATF-CREB Transcription Factors in response to TGF β	208
7.3.5 Nuclear delivery of active TGF β R1 is required for activation of a subset of TGF β responsive genes.....	210
7.3.6 Cross talk between nuclear receptors and Smads in gene regulation.....	211
7.4 DISCUSSION.....	215

CHAPTER 8: GENERAL DISCUSSION 223

REFERENCES.....	240
APPENDICES.....	275
Appendix I: Gene Silencing.....	276
Appendix II: Site – Directed Mutagenesis	277
Appendix III: Cell Culture	279
Appendix IV: Buffer Recipes	280
Appendix V: Quantitative Reverse Transcriptase Polymerase Chain Reaction.....	286
Appendix VI: Antibody Validation	289
Appendix VII: Bolton-Hunter Reaction.....	290
Appendix VII: Statistical Calculations for Chapter 4	291
Appendix IX: Validating Smad Purity of Immunoprecipitation	295
Appendix X: Validating Disruption of Trafficking Compartments.	295
Appendix XI: Pharmacological Inhibitor Protocols.....	297
Appendix XII: Bead Preparation for Chromatin Immunoprecipitation Assay	298

LIST OF TABLES

Table 3.1	Plasmids utilised in this study.....	57
Table 3.2	Cell lines utilised in this study.....	64
Table 3.3	Antibodies utilised in this study.....	74
Table 7.1	Genes examined and grouped by association with transcription factor	204

LIST OF FIGURES

Figure 2.1 TGF β Superfamily members.....	6
Figure 2.2 Formation of TGF β large latency complex.....	9
Figure 2.3 Activation of latent TGF β by integrins.....	10
Figure 2.4 Complexity of TGF β superfamily ligands, type I and type II receptors.....	13
Figure 2.5 Model of TGF β R1 phosphorylation of regulatory Smads.....	15
Figure 2.6 Homology of Smad protein family.....	19
Figure 2.7 Conformational changes of Smad proteins after TGF β stimulation.....	20
Figure 2.8 Comparison between phosphorylation sites in R-Smads linker regions. ...	22
Figure 2.9 Phosphorylation sites and kinases of the Smad family of proteins.....	25
Figure 2.10 Examples of Smad transcriptional regulation.....	30
Figure 2.11 Structure of the nuclear pore complex.....	39
Figure 2.12 Complex assembly and disassembly in nuclear translocation.....	41
Figure 2.13 Endocytosis and vesicular fates of EGFR.....	45
Figure 2.14 Model of retromer structure and cargo recognition.....	47
Figure 2.15 Proposed model of EGFR transit from the ER into the nucleus.....	53
Figure 3.1 Overview of experimental design and generation of reagents and analysis.	56
Figure 3.2 Advantage of introducing mutations and truncations into GM-CSFR/TGF β chimeric receptors over tagged native receptors.....	68
Figure 3.3 Flowchart of protein analysis in this study.....	74
Figure 3.4 Determining purity of organelle enrichment fractionation.....	79
Figure 4.1 Domains of SNX9 and binding partners.....	85
Figure 4.2 Design of SNX9 escape constructs to evade SNX9 shRNA.....	89
Figure 4.3 SNX9 regulates soft agar colony formation, growth inhibition, and Smad3- dependent transcriptional activity.....	99
Figure 4.4 SNX9 knockdown and dominant negatives distinguish Smad3 from Smad2 responses.....	100
Figure 4.5 SNX9 functions downstream of R-Smad phosphorylation.....	102
Figure 4.6 Smad2 and Smad3 phosphorylation is unaffected by dominant negative SNX9.....	103
Figure 4.7 SNX9 is required for enhanced pSmad3 nuclear entry.....	105
Figure 4.8 Differing kinetics of nuclear entry between phosphorylated and unphosphorylated Smad3.....	106
Figure 4.9 SNX9 specifically binds pSmad3 but not pSmad2.....	109

Figure 4.10 pSmad3/SNX9 binding is independent of Smad2 or Smad4.....	110
Figure 4.11 TGF β induces perinuclear/nuclear SNX9/pSmad3 localization.	111
Figure 4.12 Increased co-localization of SNX9 and Smad3 upon TGF β stimulation in different cell types.	112
Figure 4.13 SNX9 is required for pSmad3/Imp8 Binding but SNX9/pSmad3 association is independent of Imp8.	115
Figure 4.14 Nucleoporins and Imp β have distinct roles in R-Smad nuclear accumulation.	116
Figure 4.15 SNX9 and Imp8 differentially regulate pSmad3 association with the nuclear membrane and pore.	118
Figure 4.16 SNX9 does not enter the soluble nuclear fraction but does co-purify with the nuclear pore in an Imp8-dependent manner.	119
Figure 4.17 Nuclear membrane association of pSmad3/SNX9 is dependent upon phosphoinositide binding motifs in SNX9 and independent of SNX9 homodimerization.	122
Figure 4.18 Schematic representations of SNX9/pSmad3 interaction and mechanism of nuclear entry.	123
Figure 5.1 Fibroblast specific signalling in response to TGF β	132
Figure 5.2 Smad2 constructs.....	135
Figure 5.3 Smad2 and Smad3 can be phosphorylated by PAK2 <i>in vitro</i> and possess PAK2 phosphorylation consensus sequences.	137
Figure 5.4 Smad2 phosphorylation at Threonine 430 is induced by TGF β when PAK2 activation occurs and correlates with extended duration of phosphorylation at Serines 465/467.	138
Figure 5.5 Receptor site phosphorylation is not required for PAK2 site phosphorylation whereas PAK2 phosphorylation extends duration of receptor site phosphorylation.	140
Figure 5.6 Phosphorylation of Smad2 at Thr430 has no impact on TGF β induced nuclear translocation of Smad2.	141
Figure 5.7 Smad2 wild type and those unable to be phosphorylated by PAK2 have the same ability to form heterodimers with Smad4 upon TGF β stimulation.....	141
Figure 5.8 Phosphorylation of Smad2 at Threonine 430 has no impact on ligand sensitivity to TGF β	142
Figure 5.9 Smad2 mutants are unable to be phosphorylated at Threonine 430 and have increased association with phosphatase PPM1A which correlates with dephosphorylation at receptor sites.	143

Figure 5.10 Structural analysis of the carboxy terminus of Smad2.	146
Figure 5.11 Differences in Smad2 phosphorylation and dephosphorylation in fibroblast and epithelial cells.	149
Figure 6.1 Diagrammatic representation of tracking surface-derived TGF β receptors after ligand stimulation.....	156
Figure 6.2 Detection of cell surface derived receptors in nuclear fractions using sulfo- NHS-SS-biotin.....	161
Figure 6.3 Retrograde trafficking pathway and gene silencing and pharmacological inhibitors designed to disrupt specific compartments along the trafficking route.....	162
Figure 6.4 A subset of surface receptors translocate to the nucleus in cells derived from different species, tissues and healthy or diseased organs.	167
Figure 6.5 Receptors in the nucleus are full length and not cleaved fragments.	168
Figure 6.6 TGF β receptors enter the nucleus through clathrin-mediated endocytosis.	169
Figure 6.7 TGF β receptors travel from cell surface to nucleus through Golgi and ER.	170
Figure 6.8 TGF β R2 can enter the Golgi after TGF β stimulation in the absence of TGF β R1.	172
Figure 6.9 While TGF β R2 can enter the Golgi alone, both TGF β receptors are required to enter the ER and nucleus.	173
Figure 6.10 Residues 485-498 in TGF β R2 are required for Golgi and subsequent nuclear delivery.	175
Figure 6.11 Alignment of TGF β superfamily Type II receptors and predicted secondary structure at retromer binding region.....	176
Figure 6.12 Activin Type II receptor and TGF β R2 can bind retromer but only TGF β R2 can traffic to the nucleus upon stimulation.....	177
Figure 6.13 The absence of a lysine 488 or prevention of ubiquitination of TGF β R2 does not impact binding to retromer but does prevent nuclear delivery. ...	179
Figure 6.14 COPI vesicle transport required for receptors to exit Golgi and reach ER and nucleus.....	181
Figure 6.15 TGF β R1 facilitates receptor pair moving from Golgi to ER through sorting into COPI vesicles.....	182
Figure 6.16 TGF β Receptors bind to and require retrotranslocon and nuclear pore factors for nuclear entry.....	184
Figure 6.17 Receptors require intact retrotranslocon and nuclear pore complex for nuclear delivery to the inner nuclear membrane.	185

Figure 6.18 TGF β Receptors are present in inner nuclear membrane and PML nuclear bodies.	187
Figure 6.19 TGF β Receptors enter PML bodies from the inner nuclear membrane. .	188
Figure 6.20 Diagrammatic representation of route of nuclear trafficking of TGF β receptors after ligand stimulation.	193
Figure 7.1 Comparison between the promoters of endogenous TGF β -responsive genes and the 6xSBE responsive Luciferase reporter gene.	201
Figure 7.2 Kinase activity of TGF β R2 required for nuclear delivery of receptors, while TGF β R1 kinase is irrelevant.	206
Figure 7.3 TGF β R1 kinase activity is intact in the nucleus.	207
Figure 7.4 TGF β R1 kinase activity is intact in the nucleus and is able to phosphorylate ATF/CREB family member Transcription Factors.	208
Figure 7.5 Nuclear TGF β R1 is required for phosphorylation of ATF/CREB but not Smad2 signalling <i>in vivo</i>	209
Figure 7.6 Nuclear TGF β R1 phosphorylation of ATF/CREB is required for full induction of subset of TGF β regulated genes.	211
Figure 7.7 Activated TGF β R1 phosphorylates and increases Histone Acetyltransferase (HAT) activity of ATF2, CREB and AP1.	212
Figure 7.8. Of promoters bound by CREB, only those additionally bound by Smads are induced by TGF β	213
Figure 7.9 Multiple Smad Binding Elements are clustered around CREB binding elements in PAI-1 promoter.	214
Figure 7.10 Correlation between gene induction and presence of Smad3 on promoters in the presence and absence of nuclear TGF β Receptors.	215
Figure 7.11 Model of proposed mechanism of nuclear receptor crosstalk with Smads at the promoter level.	218

LIST OF ABBREVIATIONS

ActR-I	Activin Receptor 1
ActR-II	Activin Receptor 2
ADAM	A Disintegrin and metalloprotease domain-containing protein
AIG	Anchorage-independent Growth
ALK	Activin-like Kinase
AP1	Activator Protein 1
ARC105	Activator-recruited complex 105
ARF1	ADP Ribosylation Factor 1
ATF2	Activating Transcription Factor 2
ATP	Adenine triphosphate
BAMBI	BMP and activin membrane-bound inhibitor
BiP	Binding immunoglobulin Protein
BMP	Bone Morphogenic Proteins
BMPR-I	Bone Morphogenic Protein Receptor 1
BMPR-II	Bone Morphogenic Protein Receptor 2
c-Abl	cellular-Abelson Tyrosine Kinase
CIP	calf alkaline phosphatase
CaMKII	Calcium/Calmodulin-dependent Protein Kinase 2
CBP	CREB Binding Protein
Cdc42	Cell Division Control Protein 42
CK1 γ 2	Casein Kinase 1 gamma 2
CK1 ϵ	Casein Kinase 1 epsilon
CDK2	Cyclin-Dependent Kinase 2
CDK4	Cyclin-Dependent Kinase 4
CHIP	Carboxyl terminus of Hsc70-Interacting Protein
COPI	coatamer protein 1
CREB	cAMP-Response Element Binding Protein
CRM1	Chromosome Region Maintenance 1
CSF-1	Colony Stimulating Factor 1
DEPC	diethylpyrocarbonate
DME	Dulbecco's modified Eagle

DN	Dominant Negative
DNA	Deoxyribonucleic Acid
DUSP	Dual Specificity Phosphatase
EDEM	ER degradation-enhancing α -mannosidase
EDTA	ethylenediaminetetraacetic acid
EEA1	Early Endosome Antigen 1
EGF	epidermal growth factor
EGFR	epidermal growth factor receptor
EMT	Epithelial to Mesenchymal Transition
ETF	Electron Transferring Flavoprotein
ER	endoplasmic reticulum
ERAD	endoplasmic reticulum associated degradation
ERK	extracellular signal regulated kinase
ERQC	endoplasmic reticulum quality control
ESCRT	Endosomal Sorting Complex Required for Transport
FAST1	Forkhead Activin Signal Transducer 1
FAK	Focal Adhesion Kinase
FBS	Fetal Bovine Serum
FGF R1/R2	Fibroblast Growth Factor Receptors 1 and 2
FKBP12	FK506 Binding Protein 12
FSH	follicle stimulating hormone
FYVE	Fab1/YOTB/Vac1/EEA1 (first 4 proteins discovered with the domain)
GADD34	Growth Arrest and DNA Damage 34
GDF	Growth Differentiation Factors
GDNF	Glial-derived Neurotrophic Factors
GIPC	GAIP interacting protein, C terminus
GPI	Glycosylphosphatidylinositol
GPI-RGM	Glycosylphosphatidylinositol-anchored Repulsive Guidance Molecule
GRK2	G-protein Coupled Receptor Kinase 2
GSK3 β	Glycogen synthase kinase 3 β
GST	Glutathione S-transferase
GTP	guanine triphosphate
HAT	histone acetyl transferase
HBSS	Hank's balanced salt solution

HDAC	histone deacetylases
HIV	human immunodeficiency Virus
HRP	horse radish peroxidase
HRS	Hepatocyte Growth Factor Regulated Substrate
HSP70	Heat Shock Protein 70
ICD	intracellular domain
ID1	Inhibitor of DNA binding 1
IGF1	Insulin-like Growth Factor
INM	inner nuclear membrane
IPTG	isopropyl β -d-thiogalactopyranoside
IRF4	Interferon Regulatory Factor 4
I-Smad	Inhibitory Smad
JNK	c-Jun N-terminal Kinases
KD	Kinase Dead or Knockdown
LAP	latency associated peptide
LB	Liquid Broth
LLC	Large Latent Complex
LTBP	Latent TGF β Binding Protein
MAD	Mothers against Decapentaplegic
MAPK	mitogen activated protein kinase
MBP	myelin basic protein
MDa	Mega Daltons
MEKK	MAP Kinase Kinase Kinase (MAP3K)
MEM	Minimal essential media
MH1	Mad Homology 1
MH2	Mad Homology 2
MIS	Müllerian Inhibitory Substance
MISR-II	Müllerian Inhibitory Substance Receptor 2
MMP	Matrix Metalloprotease
MNS1	α -mannosidase
MOI	multiplicity of infection
MSG1	Melanocyte Specific Gene 1
MT1MMP	Membrane-associated type-1 Transmembrane Matrix metalloprotease
MTMR4	Myotubularin Related Protein 4

NES	Nuclear Export Sequence
NHS	N-hydroxysuccinimide
NLS	nuclear localization sequence
NPC	Nuclear Pore Complex
OAZ	Olf/EBF-associated zinc-finger Protein
Otub1	Otubain 1
PAK2	p21-activated Kinase 2
PBS	phosphate buffered saline
P/CAF	P300/CBP Associated Factor
PDP	Pyruvate Dehydrogenase Phosphatase
PDZ	PSD95/Dlg1/zo-1 (first 3 proteins discovered with the domain)
PI3K	Phosphoinositide 3 Kinase
PIP	Phosphoinositide Phosphate
PIX	PAK interacting and exchange factor
PKC	Protein Kinase C
PML	Promyolecytic Leukemia
PP1	Protein Phosphatase 1
PP2A	Protein Phosphatase 2A
PPM1A	Protein Phosphatase Mg ²⁺ /Mn ²⁺ dependent 1A
PVDF	polyvinylidene fluoride
RanBP3	Ran Binding Protein 3
RanGAP	Ran GTPase activating protein
RanGDP	Guanosine Diphosphate bound Ran
RanGEF	Ran Guanosine exchange factor
RanGTP	Guanosine 5' Triphosphate- bound Ran
RCC1	Regulator of Chromosome Condensation 1
RIPA	radioimmunoprecipitation assay buffer
RNAi	inhibitory ribonucleic acid
ROCK	Rho Associated Kinase
ROS	Reactive Oxygen Species
R-Smad	Receptor Smad
RUNX	Runt-related transcription Factor
SARA	Smad Anchor for Receptor Activation
SBE	Smad Binding Element

SCP	Small C-terminal domain phosphatase
Sec61	Secretory Protein 61
siRNA	short inhibitor ribonucleic acid
SIRT1	Sirtuin 1
Ski	Sloan Kettering Institute (Institution where Identified)
SLC	Small Latent Complex
SNARE	Soluble NSF Attachment Protein Receptor
SnoN	Ski-related Novel Protein N
SNX	Sorting Nexin
Sp1	Specificity Protein 1
STAT5	Signal Transducer and Activator of Transcription 5
TACE	Tumour Necrosis Factor Alpha Converting Enzyme
TAK1	TGF β Activated Kinase 1
TAT	Trans-Activator of Transcription
TBST	Tris-Buffered Saline with Tween
TFE3	Transcription Factor E3
TGF β	Transforming Growth Factor β
TGF β R1	Transforming Growth Factor β Receptor 1
TGF β R2	Transforming Growth Factor β Receptor 2
TGIF	TG Interacting Factor
TGN	Trans Golgi Network
Tie1	Tyrosine kinase with immunoglobulin-like and EGF-like domains
TRIM33	Tripartite Motif Containing 33
TrkA	Tropomyocin receptor kinase A
VEGF	Vascular Endothelial Growth Factor
Vps26	Vascular Protein sorting associated protein 26
WT	Wild Type
WWP1	WW Domain containing E3 Ubiquitin Ligase Protein 1

CHAPTER 1

GENERAL INTRODUCTION

CHAPTER 1: GENERAL INTRODUCTION

Transforming Growth Factor- β is a cytokine with broad reaching biological actions spanning development, homeostasis and disease. A cytokine released by and stimulating virtually all cell types and present throughout all multicellular life, this cytokine is an essential messenger that began co-evolving with multicellular organisms many millions of years ago. Through that time TGF β superfamily members have diverged and the signals they stimulate have also evolved to serve different stimulatory needs of various cell types to different environmental conditions. While much work remains to understand the different factors involved in mitigating this signal through the cells, a number of key proteins have been identified. The ligands themselves initiate signalling from the cell surface when they bind receptors. This activates a kinase signalling cascade that transmits that signal from the cell surface to the nucleus, where genetic alterations occur. Whilst our understanding of many of the proteins involved in this cascade is coming to light, the mechanisms of how these factors deliver their messages into the nucleus remains elusive.

Much of the last 30 years has been focused on looking at the individual TGF β -specific components of the pathway in isolation and searching for up-regulations, mutation or loss-of-function to explain why TGF β can be so beneficial to the organism but cause such problems when things go wrong. Dramatic changes in these factors are rare in disease and have little impact on differences in the varied responses to TGF β . Evidence has begun to accumulate suggesting disease states actually result from imbalances between the various factors (Hoot 2008, Meng 2010) but how do these imbalances occur? Where are these signals regulated? What are the factors that regulate them?

With only a limited number of components, the TGF β signalling pathway commands cells to undertake a tremendous range of different cellular changes. Instead of evolving vast numbers of pathway specific components, the TGF β pathway appears to tap into (and be very sensitive to) cellular context and delivers a message to the nucleus appropriate to that cell type and the conditions it finds itself in. There appears to be multiple levels of regulation of every component of the pathway. Proteins can be phosphorylated, monoubiquitinated, polyubiquitinated, sumoylated, neddylated, acetylated, dephosphorylated, deubiquitinated, desumoylated, deneddylated, deacetylated, cleaved, complexed, relocalized (Derynck 2014) and reorganized in

countless ways, before we even consider splice variant isoforms and allelic variations. Many of these modifications can occur at numerous sites by more than one catalytic enzyme, all feeding into a complex web of interaction evolved to enable a cell to interact symbiotically with the cells around it and the organism within which it is both dependent upon and essential to.

1.1 Thesis rationale and hypothesis

The overall aim of this study was to examine how the various components of the TGF β pathway are relayed into the nucleus and the routes, the factors and the mechanisms involved in this signalling cascade.

We will test the general hypothesis that TGF- β signalling is regulated by the coordinate action of membrane proximal and nuclear TGF- β receptor (TGF- β R) activity. It is our contention that cellular signals emanating from both membrane proximal and nuclear receptors require specific nuclear trafficking machinery and this defines new models for regulating TGF- β action.

Exactly what TGF β receptors are doing in the nucleus and how they're traffick there remains a mystery, and even their presence in the nucleus remains controversial. Recently new tools have been developed to address these questions, particularly how the receptors get into the nucleus and how that process is regulated. Regulation of how TGF β receptors get to the nucleus is completely unknown. Even the rudimentary aspects of Smad nuclear trafficking are misunderstood and the literature full of contradictions. Furthermore, nuclear trafficking mechanisms may help explain why some cell types have sustained or diminished kinetics of TGF β signalling. It is for these reasons we have chosen to focus our studies on the regulatory mechanisms of nuclear trafficking of TGF β signalling components focusing on three aspects.

Firstly, we examine R-Smad nuclear trafficking in a study to explore preliminary data suggesting that Sorting Nexin 9 (SNX9) may have a role in R-Smad nuclear trafficking. Intriguing data suggests that Smad2 and Smad3 nuclear trafficking may be regulated differently, which may have significant academic and clinical impacts.

Secondly, again focused on R-Smads, we examine why Smad phosphorylation and nuclear retention is longer in cell types that activate PAK2, rather than those that do not. A number of kinases phosphorylate R-Smads in the linker region (where there is a PAK2 consensus sequence) which can impact nuclear localization. Our study aims to

test the hypothesis that PAK2 may phosphorylate the Smad linker region to increase nuclear retention.

Finally we examine the route of delivery for TGF β receptors, comparing and contrasting the routes with EGFR nuclear trafficking and attempting to determine TGF β specific regulation mechanisms and downstream consequences.

Although this study has been compartmentalized into three distinct sections (nuclear targeting of the Smads, nuclear retention of Smads between cell types, and nuclear targeting of the receptors), my intention is to illuminate a central theme, that being that TGF β is not ONLY regulated at the plasma membrane proximal level by phosphorylation of certain factors, but also at the level of nuclear entry. Smad2/3 do not just travel directly (without regulation) to the nucleus and the cell can modulate Smad and receptor nuclear entry to respond to different cellular cues. The very fact there are multiple fates for receptors after ligand stimulation (degradation and nuclear trafficking) indicates cells do actively sort and traffic receptors which has a significant input on the biological input of TGF β stimulation.

It is hoped that by recognizing and understanding the role of factors that regulate nuclear delivery of TGF β signalling components, manipulation of these mechanisms will lead to clinical therapies of tremendous benefit in the plethora of diseases driven by perturbed TGF β signalling.

CHAPTER 2

LITERATURE REVIEW

CHAPTER 2: LITERATURE REVIEW

2.1 Ligands of the Transforming Growth Factor-beta Superfamily

The Superfamily of Transforming Growth Factor beta (TGF β) cytokines is comprised of proteins such as TGF β s, Activins, Inhibins, Bone Morphogenic Proteins (BMPs), Growth Differentiation Factors (GDFs), Glial-derived Neurotrophic Factors (GDNFs), Lefty, Nodal and Müllerian Inhibitory Substance (MIS). Over 40 members have been added to this family since the prototypic member of the group (TGF β 1) was characterized in 1983 (Assoian 1983), with all family members possessing a cysteine knot domain and existing as dimers. Evolutionarily they can be divided into 4 groups differentiated by sequence homology; (see Fig 2.1) TGF β s, Activins and Inhibins, BMPs and MIS (Santibañez 2011).

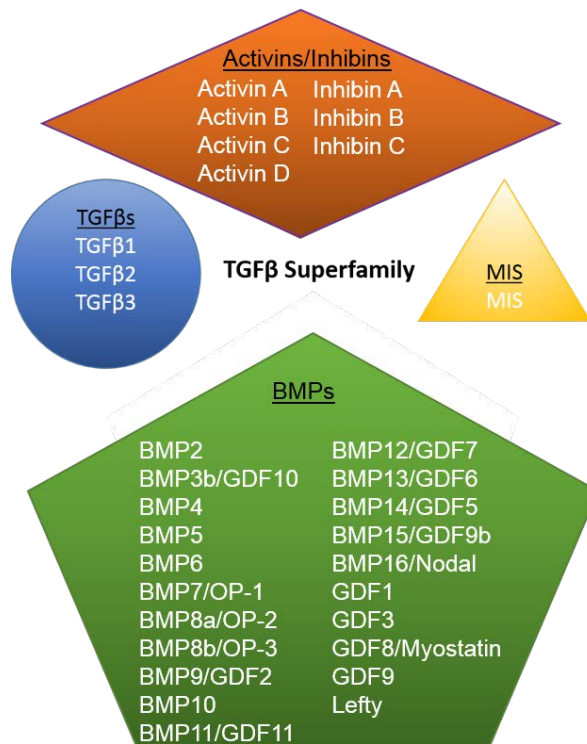


Figure 2.1 TGF β Superfamily members. The superfamily can be divided into 4 distinct groups based on sequence homology, although MIS is often grouped with BMPs.

Activins were originally purified from gonadal fluids that stimulated the release of pituitary follicle stimulating hormone (FSH) (Ying 1988). Despite this original gonadal-pituitary axis function, Activins have been shown to have a broad range of biological activities including regulating hematopoiesis (Shav-Tel and Zipori 2002), neural cell differentiation (Suzuki 2010), mesoderm induction (Cerdan 2012), and bone remodeling (Alves 2013). Like other TGF β superfamily members, Activins and Inhibins are dimers. While Activins consist of homodimers or heterodimers of the five different beta subunits, Inhibins consist of a single beta subunit bound to a unique alpha subunit. The nomenclature of Activin/Inhibins reflects the various subunit linkages with Activin A (beta A-beta A), Activin B (beta B-beta B), Activin AB (beta A-beta B), Inhibin A (alpha A-beta A), Inhibin B (alpha A-beta B) and so forth (Weiss and Attisano 2013).

The largest group consists of the Bone Morphogenic Proteins (BMPs) made up of classical BMPs, GDNFs and GDFs. BMPs were originally identified as having a role in bone and cartilage development with over 20 recognized BMPs having numerous roles in morphogenesis and embryogenesis (Lee 2014). The GDNF subgroup consists of 4 members, which are GDNF, Aremin, neuturin, and persephin. They are all distantly related to other TGF β members, and impact survival and growth by acting in many cell types, including neurons (Sariola and Saarma 2003). Due to sequence conservation, Lefty and Nodal (important in embryonic development) are usually grouped with BMPs. Nodal is essential in mesoderm formation and anterior-posterior as well as left-right axis formation during development (Katsu 2013). The Lefty proteins act as antagonists of Nodal (Sun 2014).

Often grouped with the BMPs, although distinctly different, Müllerian Inhibitory substance (MIS) is another distantly related member of the family with limited expression, being restricted to granulosa cells of the postnatal ovary and Sertoli cells of the testis (Meyers-Wallen 1993). MIS' primary role is in sex determination by inhibiting development of the Müllerian ducts in male testis (Taketo 1993).

Transforming Growth Factor betas are powerful cytokines and the prototype and namesake of the TGF β superfamily of cytokines. There are three members expressed in mammals; TGF β 1, 2, and 3 which have roles in multicellular organisms ranging from directing early development and homeostasis to immune and wound healing

responses . Biologically relevant concentrations of TGF β are in the femto-molar range and both the ligand and receptors are expressed in virtually all cell types (Shi and Massagué 2003). Although a great deal of redundancy appears to exist between the three TGF β isoforms, targeted deletion studies in mice demonstrate a number of non-redundant roles as well. For instance, TGF β 1 has a unique role in hematopoiesis and endothelial differentiation (Challen 2010), TGF β 2 is strongly implicated in lung, heart, limb, eye, ear, urogenital, and craniofacial development (Ishtiaq 2014), while TGF β 3 uniquely affects pulmonary development and palatogenesis (Jalali 2012).

Furthermore, the abundance of TGF β in the body is significantly higher than that required for cell stimulation, and to ensure receptor activation occurs only when and where it is required, the ligand is produced in an inactive, latent form. TGF β produced in this conformation cannot bind receptors, and it is also enveloped by a large latency-associated peptide. This ensures a very rapid, highly localized and significant stimulatory event can be generated without the time delay and delivery complications related to *de novo* ligand synthesis (Shi and Massagué 2003).

Activation of the TGF β pathways has significant cellular effects and is highly regulated. The ligand is produced and secreted as a propeptide dimeric precursor (Miyazono 1993, Lack 2003; Chen 2006) with the carboxy-terminal destined to become the active peptide once the amino-terminal region is released by proteolytic cleavage (Fig 1.2) (Miyazono 1993). Once cleaved, the amino terminus forms an inhibitory compound known as the latency associated peptide (LAP) that stays covalently bound to the active ligand, folding around it. This complex (formed within the cell) is called the small latent complex (SLC) and it remains in the cell until binding the latent TGF β binding protein (LTBP) via disulfide bonds to form the large latent complex (LLC) (Lack 2003, Chen 2005). The role of the latency complex is to physically envelope the ligand, preventing it binding to the receptors (Lack 2003, Shi and Massagué 2003). The LLC is then secreted from the cell into the extracellular milieu. Interestingly, there are four LAP proteins with differing affinities for the different isoforms of TGF β ligands (Jobling 2006) each suggested to show differential activation properties to different stimuli (Fig 2.2).

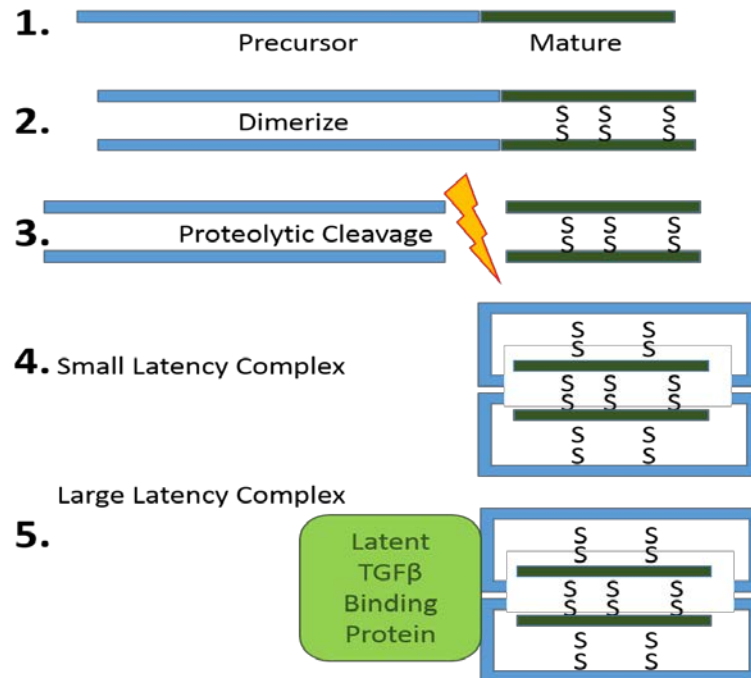


Figure 2.2 Formation of TGFβ large latency complex. (1) The precursor is translated with the active and inhibitory components on one molecule. (2) Two precursors form disulfide bridges to generate a dimer. (3) Proteolytic cleavage separates the inhibitory (LAP) from the active forms of the ligand. (4) The inhibitory fragment folds over and encapsulates the active ligand and disulfide bridges secure the small latency fragment. (5) Finally, binding of the LTBP generates the LLC which is secreted into the extracellular matrix. Activation occurs when the active ligand is released from the LAP and LTBP.

Our understanding of the activation of TGFβ ligands remains poor, despite the importance of the process in disease and homeostasis. The first step of ligand activation is to free the large latent complex from the extracellular matrix. A number of different proteins have been implicated in this process, including matrix metalloproteases (Dallas 2002), thrombospondin (Bourd-Boittin 2011), reactive oxygen species (ROS) (Jobling 2006) and integrins (Munger and Sheppard 2011).

Matrix metalloproteases (such as MMP2 and MMP9) have been shown to cleave the LAP and activate ligand (Dallas 2002). However, mice deficient in both these enzymes are still able to activate TGFβ, indicating other factors are involved or redundant pathways exist. Thrombospondin (Bourd-Boittin 2011) and ROS (Jobling 2006) play roles in ligand activation by causing conformational changes and assisting proteolysis. The role of integrins in activation of latent TGFβ is probably a widespread phenomenon. It has been demonstrated to be essential for development and

progression in pulmonary lung fibrosis (Munger and Sheppard 2011). Two mechanisms have been uncovered; one that activates ligand for a neighbouring cell (using mechanical force generated by the actin cytoskeleton) and the other that uses a combination of mechanical force and proteolytic cleavage that yields free active ligand (Morris 2003).

In homeostatic conditions the first mechanism of ligand activation by integrins is established across two neighbouring cells. The integrin $\alpha V\beta 6$ of one cell binds to the LAP of the latent complex, while TGF β receptors of a neighbouring cell loosely bind a small, exposed region of the active ligand. During inflammation and extracellular matrix deposition cells experience forces that can pull them apart. Integrins are bound to the cytoskeleton and act to anchor the LAP to one cell as the other cell (bound to an exposed part of the active ligand) pulls away due to the forces induced by inflammation or extracellular matrix deposition. This counter-lever mechanism provides enough force to disrupt the disulfide bonds between the LAP and the active ligand and present a fully active ligand to the TGF β receptors of the neighbouring cell (see Fig 2.3A). The above mechanism provides a tight degree of regulation, limiting activation to during the active process of separation, and only to cells immediately impacted by inflammatory processes where separating neighbouring cells is disruptive (such as epithelial layers). The other mechanism involves the integrin $\alpha V\beta 8$, bound to the LAP of the latent ligand, presenting the latent ligand complex to the transmembrane metalloprotease MT1MMP, which then cleaves the LAP and releases free active TGF β (see Fig 2.3B).

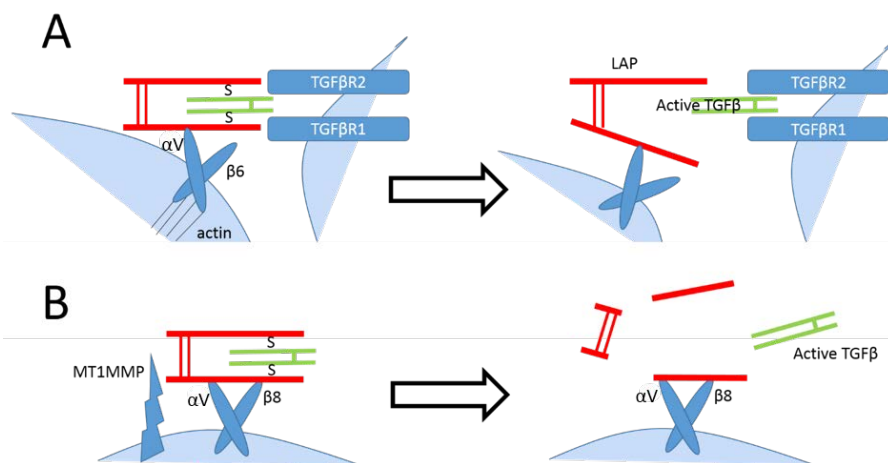


Figure 2.3 Activation of latent TGF β by integrins. (A) Integrin $\alpha V\beta 6$ of one cell binds the LAP while TGF β receptors of a neighbouring cell bind an exposed portion of the active ligand. As the two cells are pushed apart that force (and the counter force of integrins bound to the actin cytoskeleton) mechanically overwhelm the disulfide bonds binding the LAP to the active ligand, exposing an active ligand to the receptors. (B) Integrin $\alpha V\beta 8$ binds the LAP and concurrently recruits the metalloprotease MT1MMP which cleaves the LAP and releases active TGF β .

BMPs and Activins do not form latent complexes and are thus secreted as active ligands (Miyazano 2000). However cells have evolved numerous mechanisms to limit signalling to the required locations. Negative regulation of BMP and Activin is achieved by two basic categories of antagonists; those that bind and/or sequester ligand, or those that bind receptors and block ligand-induced receptor activation. There are many antagonists, reflecting the need for subtle regulation and gradient formation in many cellular processes during development and growth. Noggin, chordin, follistatin, cerberus, gremlin, and the Dan family of proteins (such as caronte) as well as a host of other proteins all bind to BMP ligands to negatively regulate BMP signalling (Dean 2010, Stabile 2007, Mine 2008). Proteins of the DAN family share the cysteine knot motif conserved in all TGF β s and BMPs (Nolan and Thompson 2014) but most share no other sequence homology with TGF β superfamily members (Miyazono 2000).

Antagonists play essential roles during development; Cerberus facilitates head structure formation (Rodriguez Esteban 1999), caronte is essential for establishment of left-right asymmetry (Yokouchi 1999), and limb development is regulated through the combined effects of multiple BMP antagonists including gremlin, chordin, noggin, and follistatin (McMahon 1998, Capdevila 1999). Noggin and chordin have additional roles in regulating neural tissue development (Piccolo 1996). These antagonists have differing affinities for different BMPs or Activins (Li and Ge 2013) and diffuse through tissues at different rates (Piccolo 1996) which simultaneously allows the establishment of multiple gradients for multiple ligands. For example, follistatin has a high affinity for Activin A with low binding to BMPs (Yamashita 1995, Iemura 1999), caronte binds BMP4, BMP7, and nodal but not Activin A (Rodriguez Esteban 1999), and Noggin binds BMP2, BMP4, and GDF6 with high affinity but has low affinity to BMP7 (Zimmerman 1996). Additionally, Activins can be inhibited by pseudoligands that mimic Activin and bind to the receptors to negatively compete with the natural ligand. Lefty1, Lefty and activin are essential for left-right patterning and are currently the only members of this type of antagonist (Miyazono 2000). It is evident that cells have adapted a myriad of processes to maximally utilize the TGF β superfamily system to elicit the required response appropriate to specific extracellular stimuli using a complex activation of checks and safeguards.

2.2 Receptors of the TGF β Superfamily

2.2.1 Ligand binding to Type I and Type II Receptors

All TGF β superfamily ligands utilize essentially the same receptor activation process to relay the ligand signal into the cell. The ligands are non-cell permeable and while affinity is high for the receptors, TGF β is very “sticky” with low specificity and low affinity binding to extracellular and membrane associated components (Shi and Massagué 2003). However, high affinity binding is restricted to a very limited number of receptors. The core signalling cassette is a complex that forms between two proteins, known as the type I and type II receptors. While ligand does bind the type I receptor in the absence of the type II, there is only high affinity binding to the type II receptors. In the presence of both receptors the binding affinity is increased even more.

There are seven recognized type I receptors for the TGF β superfamily of ligands (Attisano and Wrana 2002) designated Activin-like kinases (ALKs) and they can be classified into three groups; BMPR-I group, ALK-1 group and TGF β R1 group (Attisano and Wrana 2002). The BMPR-I group includes BMPR-1A and BMPR-1B, also called ALK3 and ALK6 respectively. The ALK-1 group includes ALK1 and ALK2 while the TGF β R1 group includes ActR-1B, TGF β R1 (also called ALK4 and ALK5 respectively), and ALK7. There are two basic signalling cascades initiated by TGF β superfamily ligands, the Smad1/5/8 pathway and the Smad2/3 pathway. The BMPR-I and ALK1 group both activate the Smad1/5/8 pathway while TGF β R1 group activates Smad2/3. BMP ligands have differing affinities for each of the receptors (Miyazono 2010). BMP2 and BMP4 bind BMPR-IA and BMPR-IB while BMP6 and BMP7 bind strongly to ALK2 and weakly to BMPR-IB. BMP9 and BMP10 bind ALK1 and ALK2 while GDF5 binds only BMPR-IB (Miyazono 2010). Activin ligands bind ALK1 group as well as ActR1B and TGF β binds TGF β R1 receptor (Attisano and Wrana 2002) and ALK1 occasionally (Bertolino 2005).

As mentioned previously, the presence of the specific type II receptor has a large bearing on which type I receptor is engaged by the ligand, with five distinct type II receptors having been described. For example, MIS can engage any one of three type I receptors, ALK2, BMPR-IA or BMPR-IB depending on the cellular conditions, but only if MISR-II is present and has bound the ligand (Wu 2012). TGF β R2 and MISR-II are

specific for binding of TGF β 1/2/3 and MIS, respectively (Attisano and Wrana 2002), while BMPR-II is specific for BMPs, whereas ActR-II and ActR-IIB are shared by Activins, myostatins and BMPs (Yu 2005). The complicated mix of ligand, type I and type II receptor adds sensitivity and responsiveness to a wide variety of cellular signals as described in Figure 2.4.

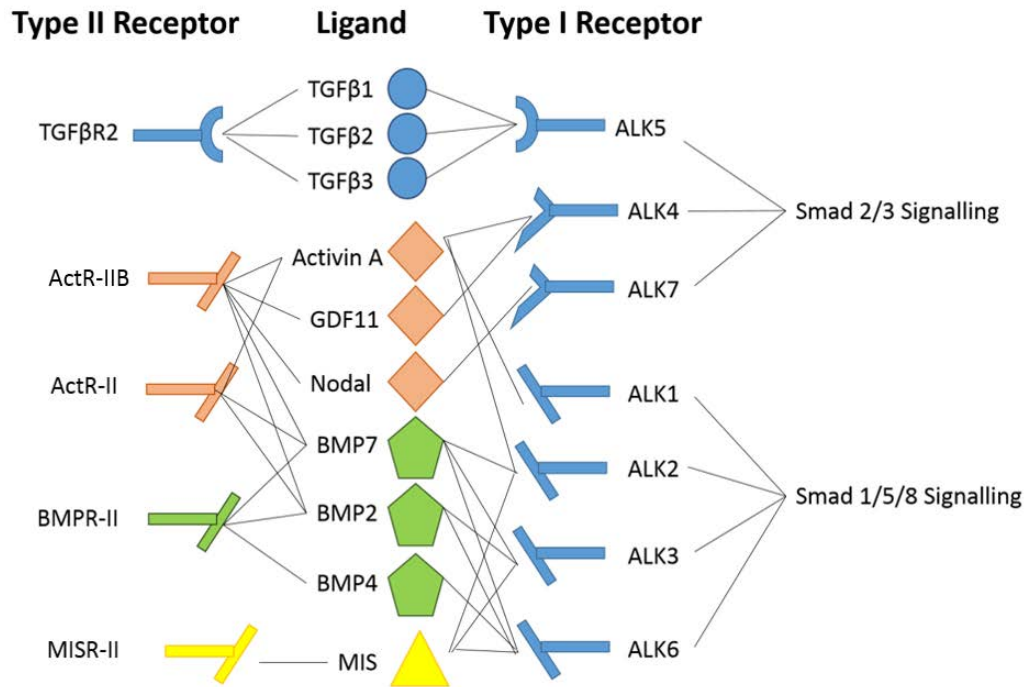


Figure 2.4 Complexity of TGF β superfamily ligands, type I and type II receptors. BMP, Activin, TGF β , MIS and other ligands are recognized by specific type II receptors with further specificity generated through pairings with other type I receptors. ALK5=TGF β R1

2.2.2 Receptor-mediated signal transduction

All TGF β superfamily receptors are single-pass transmembrane receptors. The core TGF β signalling receptor complex (TGF β R1 and TGF β R2) is believed to consist of a heterotetramer of two type I and two type II receptors bound to a TGF β ligand dimer (Shi and Massagué 2003). However, the receptor complex does not exist in high abundance in the absence of ligand, with the receptor complement believed to be broken into homodimers of type I and type II respectively. However compelling single molecule imaging data indicates they may exist as monomers at the plasma membrane (Zhang 2009) until ligand addition. Both of these receptors have significant intracellular domains with kinase enzymatic activity; while the type II receptor has

intrinsic kinase activity, the type I receptor must be complexed with the complement type II receptor and ligand for activation of its kinase domain.

Upon binding ligand, type II receptor's binding affinity for type I receptor dimers is dramatically increased leading to rapid recruitment into the signalling complex. As the type II receptor kinase has high specificity for type I receptor, it rapidly phosphorylates numerous serine residues (with the highest concentration of trans-phosphorylation events in a glycine and serine rich region known as the GS domain). As well as this transphosphorylation capacity, type II receptor also has auto-phosphorylation capacity that likely serves to stabilize the receptor homodimeric complex. Once phosphorylated, type I receptor kinase domain becomes enzymatically active to phosphorylate downstream signalling components (Shi and Massagué 2003, Attisano and Wrana 2002).

While the activation of the receptors occurs rapidly on the cell surface, the intracellular components of the TGF β signal cascade cannot be phosphorylated by receptors at the plasma membrane (Penheiter 2002). Indeed multiple studies indicate both TGF β (Penheiter 2002, Hayes 2002, Di Guglielmo 2003) and BMP (Gleason 2014) receptors need to internalize through clathrin-mediated endocytosis before phosphorylation of these downstream components can occur (Fig 2.5). Activation probably occurs between endosome scission by the pinchase dynamin, and early endosome formation. While it has been reported that downstream signalling components can be found complexed with receptors at the cell surface (Penheiter 2002), growing evidence suggests these downstream factors are not compartmentalized together with activated receptors until they are in early or very early endosomes (Panopoulou 2002, Hayes 2002). The likelihood of this compartment serving as the signalling locale stems from the properties of an accessory protein, Smad Anchor for Receptor Activation (SARA) that binds to TGF β R1 and the downstream Smad proteins, thereby acting as a scaffold between the two. SARA, and including Hepatocyte Growth Factor Regulated Substrate (HRS), have a FYVE domain (Fab1/YOTB/Vac1/EEA1, the first 4 proteins examined with this domain) that recruit these proteins to phosphoinositide-3-phosphate (PIP3) groups in membranes (Panopoulou 2002). These membranes are not exposed when encapsulated by the clathrin coat but are exposed with disassembly. The PIP3 groups target many trafficking proteins involved in various endosome formations, including Early Endosome Antigen 1 (EEA1) and Rabs. SARA's FYVE domain has less

affinity for PIP3 than these other proteins (including EEA1, and sorting nexins), and therefore we can presume that SARA binding is limited to very early endosomes. Experimental data supports the idea of the very early endosome being the site of activation, as dominant negative Rab5 (which prevents early endosomes maturation) not only supports, but also increases, Smad activation. (E.Leof, (Mayo Clinic) *personal communication*).

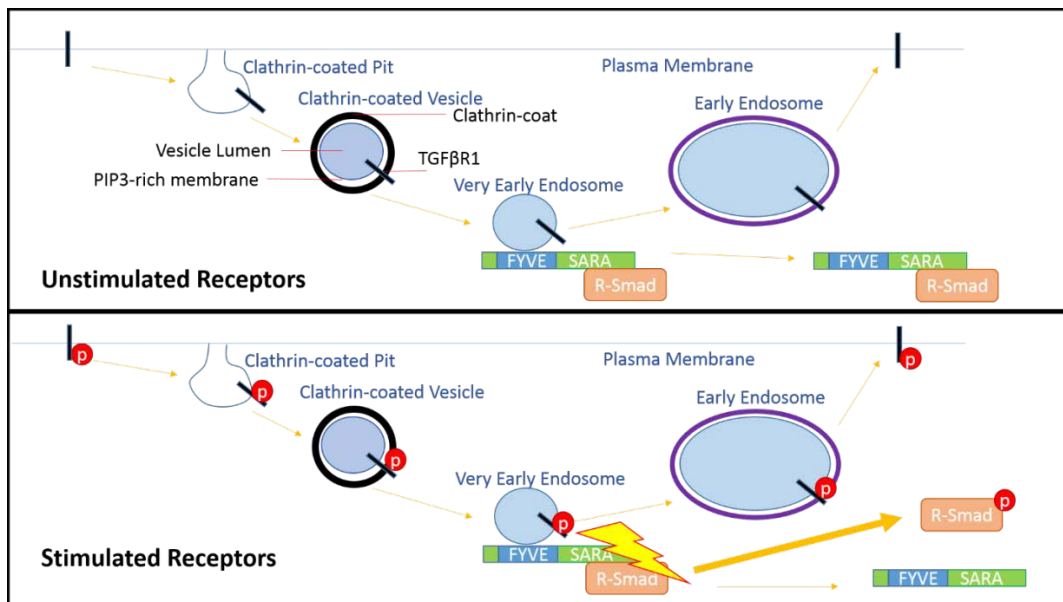


Figure 2.5 Model of TGFβR1 phosphorylation of regulatory Smads. Through the FYVE domain, SARA binds to PIP3 in naked membranes exposed after clathrin coat disassembly. In this way the associated regulatory Smads can sample the phosphorylation status of TGFβR1 prior to the binding of EEA1, Rabs and other proteins that direct endosome trafficking. As the receptors are constantly recycling this sensory allows a rapid response. In the case of unstimulated receptors (Top) SARA/Smad are not modified on contact with internalized receptor. In the case of activated receptors (bottom), Smad is phosphorylated (indicated by lightning bolt) causing dissociation of SARA, Smad and the receptor.

Which Smad signalling cascade becomes engaged depends on the type I receptor activated. Although these proteins share significant residue conservation, particularly in the kinase domain, there is a single region that differs between Smad1/5/8 signalling receptors and those that signal through Smad2/3. This region forms a loop in the tertiary structure of the protein and has the designation L45 Loop. Studies interchanging the loops between receptors could switch a Smad2/3 signalling receptor to a Smad1/5/8 response and vice versa (Chen 1998). This simple mechanism is fine tuned in BMP signal responses as BMPR-I and BMPR-IB have slightly different downstream responses despite both activating the Smad1/5/8 pathway (Attisano and Wrana 2002) indicating additional levels of regulation, probably involving other molecules.

Regulation of signalling also involves endogenous antagonists; just as there are antagonists that sequester ligands or outcompete ligand for receptor binding, there are antagonists at the receptor level also. The most characterized of these is BMP and Activin membrane-bound inhibitor (BAMBI) in *Xenopus* embryos but the mammalian homologue *nma* seems to play a similar role (Gonzales 2010). The antagonists share a strong sequence homology with TGF β type I receptors but lack an intracellular domain. Both BAMBI and *nma* interact with numerous type I and type II receptors and their expression abolishes TGF β , Activin, and BMP signalling (Sekiya 2004). Expression is induced by members of the TGF β superfamily (Gonzales 2010) and may therefore serve as a negative feedback loop to switch off signalling once it is no longer needed. FK506 Binding Protein 12 (FKBP12) is another antagonist which binds to inactive TGF β R1 and serves to prevent ligand-independent activation through unstimulated TGF β R2 (which has active kinase activity) occurring through random binding events between the two receptors. While FKBP12 is bound to TGF β R1, unstimulated TGF β R2 is unable to phosphorylate TGF β R1. When TGF β R2 binds to ligand, there is increased affinity between TGF β R1 and TGF β R, causing FKBP12 to disengage, allowing TGF β R1 to be phosphorylated (Yao 2000).

2.2.3 Co-receptors for Type I and II receptors

While the essential signalling receptors consist of the type I and type II receptors and cells can signal through their respective Smad1/5/8 or Smad2/3 pathways in the absence of other factors, there are a number of co-receptors that can positively or negatively impact the signal. The TGF β type III receptor (also called betaglycan) is an 853 amino acid transmembrane proteoglycan with a very short (42 amino acid) intracellular region (Gatza 2011). Within this intracellular region lies a PDZ domain (PSD95/DIg1/zo-1 are the first 3 proteins identified with this domain) and β -arrestin2 interacting domain. The extracellular domain is heavily glycosylated with a single O-linked, 3 N-linked, and 2 glycosaminoglycan side chains in the mature type III protein. Type III receptors are expressed in almost all cell types but expression levels differ considerably. In most cell types, type III receptors are expressed at much higher levels than the signalling receptors. However hematopoietic and endothelial cells express virtually undetectable levels and decreased expression is commonly observed in breast (Kershaw 2013), colorectal (Bellone 2010), prostate (Breen 2013), ovarian (Xu 2013), pancreatic (Yoshitomi 2008) and non-small cell lung cancers (Kopczyńska

2012) as well as hepatocellular (Yu 2007), renal cell (Dubinsk 2012) oral squamous cell carcinomas (Marioni 2006), multiple myeloma (Pappa 2013), and a number of sarcomas (Boeuf 2012, Hara 2012, Mitsui 2013) where it is considered a tumour suppressor.

The transmembrane type III receptor binds to the ligands TGF β 1/2/3, BMP2/4/7, GDF5 and inhibin and presents these ligands to the appropriate type I and type II receptors to facilitate and enhance signalling (or inhibit it in the case of inhibin) (Gatza 2011). However type III can also be cleaved, shedding the ectodomain as the so-called soluble type III receptor (sT β RIII). Soluble receptor is inhibitory to signalling as it acts as a sink (or trap) for ligand and reduces availability to cells. Little is known about the mechanisms that regulate shedding of the receptor but inhibition of phosphatases and/or ADAM family of proteases prevents shedding (Kaitu'u-Lino 2012). Likewise the interactions with GIPC and β -arrestin2 are not well defined but GIPC binding appears to stabilize type III expression at the cell surface while β -arrestin2 interaction has implications in BMP signalling, particularly involving ALK6 (Lee 2008).

The importance of the type III receptor is underscored by the correlation with loss of this receptor in various human cancers, and one would predict similar observations will be observed in other TGF β -driven diseases in the future. Another related protein that functions as a co-receptor is endoglin. Endoglin binds a number of TGF β family ligands including TGF β 1 and 3, Activin A and BMP2 and 7. Our understanding of endoglin in signalling is undeveloped, but data implies it has an antagonistic impact on TGF β signalling while enhancing BMP responses (Schemer 2007).

DRAGON and hemojuvelin are members of the glycosylphosphatidylinositol-anchored repulsive guidance molecule family (GPI-RGM family) and bind to both BMP2 and BMP4 but not BMP7, other Activins, or TGF β s (Babbit 2005, Babbit 2006). In the absence of the RGM proteins, BMP2/4 can only signal through BMPR-II but when present, these ligands can utilize both BMPR-II and ActR-II, implying these GPI proteins somehow facilitate binding to ActR-II (Xia 2007). There are likely many other co-receptors to be found as more and more genetic studies come online. Currently however, our understanding of how they function remains very much in its infancy.

2.3 Activating the signalling cascades of the TGF β Superfamily

The core of intracellular TGF β signalling involves a remarkably small family of proteins. The Smad proteins derive their name from a fusion between the *Drosophila melanogaster* homologue MAD (mothers against decapentaplegic) and *Caenorhitis elegans* SMA genes. These proteins are found ubiquitously across all animalae with homologues discovered throughout the animal phyla, from mammalia to hydras (Hobmeyer 2001) and cnidarians (corals and jellyfish) (Samuel 2001).

Following activation by the type II receptor, the L45 loop of the type I receptor becomes exposed and able to recognize either Smad1/5/8 (for BMPs) or Smad2/3 (TGF β s or Activins). Accessory proteins such as SARA or HRS can help facilitate these interactions, and activation can also occur in the absence of these proteins both *in vivo* (Chang 2014) and *in vitro* (Bakkebø 2012). The now activated kinase domain of the type I receptor catalyzes the transfer of a phosphate group from ATP onto the Smad. The phosphorylated Smad undergoes a conformational change, loses affinity for the receptor, and gains affinity for other binding partners (Shi and Massagué 2003).

Not all Smad proteins are phosphorylated by TGF β receptors, but those that are phosphorylated are termed Receptor (or Regulatory) Smads (R-Smads) (Fig 2.6); In TGF β and Activin signalling they are Smad2 and Smad3, while BMPs phosphorylate Smad1, Smad5 and Smad8. Prior to phosphorylation these proteins exist as monomers, and phosphorylation dramatically favours formation of multimers (predominantly trimers). These can consist of homotrimers or heterotrimers made up of two phosphorylated R-Smads and one Smad4. Smad 4, (otherwise known as Co-Smad) is not phosphorylated by the receptors but is crucial for DNA binding and initiation of transcription at many TGF β responsive gene promoters. Smad4 binds to R-Smads phosphorylated by either BMP or TGF β (Wrana 2013), thus the term Co-Smad. The ratio of homotrimers to heterotrimers *in vivo* is unknown but the formation of the R-Smad/Co-Smad heterotrimer is more energetically favourable *in vitro* and *in silico* (Chacko 2004).

The other group of Smads are the inhibitory Smads (I-Smads; Smad 6/7). They are not phosphorylated by the receptors, and compete for receptor intracellular binding thus antagonizing the phosphorylation of R-Smads (Yan 2009). Smad6 binds to BMP type I receptors and inhibits Smad1/5/8 phosphorylation (Estrada 2011) while Smad7 binds to BMP, TGF β , and Activin type I receptors and inhibits Smad2/3 and Smad1/5/8 phosphorylation (Yan 2009). There is also evidence that Smad6 can compete with Smad4 for binding to phosphorylated Smad1, thereby inhibiting BMP signalling by more than one mechanism (Hata 1998). To further inhibit signalling, I-Smads recruit the E3 ubiquitin ligases (SMURF1/2) to activated receptors to facilitate receptor degradation (Soond and Chantry 2011) as well as compete with R-Smads for binding to gene promoters within the nucleus (Yan 2014), thus antagonizing signalling in many ways.

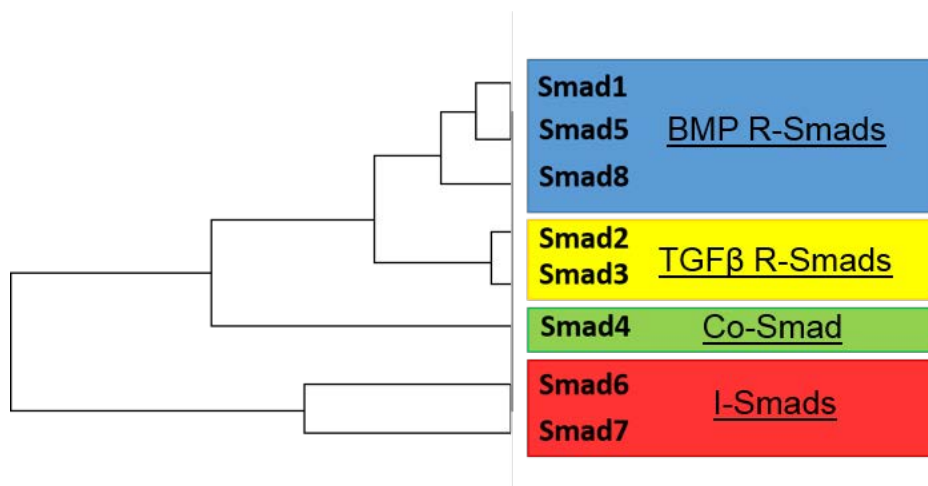


Figure 2.6 Homology of Smad Protein Family. Within the Regulatory Smads (R-Smads) there are two conserved groups, one that is phosphorylated by BMP receptors and one that is phosphorylated by TGF β /Activin Receptors. The Co-Smad shares significant homology while the Inhibitory Smads (I-Smads) are a related pair that are distinctly different to the other Smad family members.

2.3.1 Smad domain structure

R-Smads all share two defined domains known as Mad Homology domains linked together by a linker region. In the unphosphorylated, monomeric form the MH1 and MH2 domains are folded upon one another. At the extreme carboxy terminus of the R-Smad is an SSXS motif in which the serines (S) are recognized and phosphorylated by the activated type I receptor. Upon phosphorylation, MH1 and MH2 domains uncouple allowing the favoured trimeric complex (Fig 2.7). The region of R-Smads that interacts with type I receptors is a highly conserved loop (L3 loop) within the MH2 domain that differs only by 2 amino acids between Smad1 and Smad2. Although switching these residues switches their interactions between BMPRI and TGF β R1 (Chen 1998), other regions have an influence over receptor affinity. It is therefore likely that a combination of multiple sites determine specificity (Chen 1999).

Smad4 also possesses conserved MH1 and MH2 domains, however there is no SXSS motif and the MH1 and MH2 domains do not interact with one another as unphosphorylated R-Smads do (Shi and Massagué 2003). Although Smad4 shares a high degree of similarity with the R-Smads at the L3 loop, it is different enough that Smad4 can't bind the receptors (Chen 1998). The L3 loop is also the region of the Smads that allow interaction with one another after phosphorylation (see Fig 2.7).

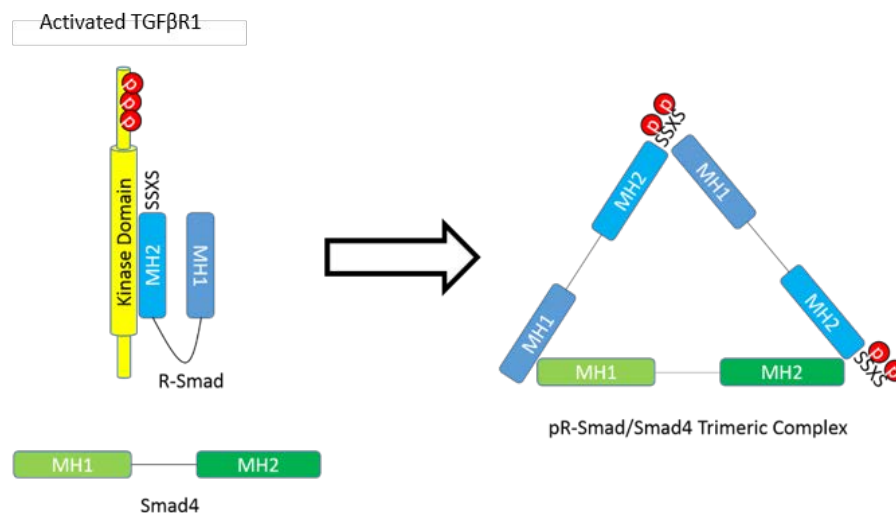


Figure 2.7 Conformational changes of Smad Proteins after TGF β Stimulation. When the G/S domain of the type I receptor is phosphorylated the kinase domain is activated and associated R-Smad proteins are phosphorylated. The MH1 and MH2 domains of R-Smads are folded upon one another when unphosphorylated but when the SSXS motif is phosphorylated it linearizes, releases from the receptor and associates with the constitutively unfolded Smad4.

Inhibitory Smads are less conserved than the R-Smads and Co-Smad and while they share an MH2 domain, the amino terminus has very little conservation. Unlike Smad4, the L3 loop of I-Smads binds the receptor but without a SSXS motif it cannot be phosphorylated. In fact, the L3 loop binding affinity of I-Smads is higher than that of R-Smads (Kamiya 2010). I-Smad expression levels are generally low but TGF β stimulation induces their expression (Attisano and Wrana 2002) acting as a negative feedback mechanism to turn off prolonged TGF β signalling.

2.3.2 Linker and non-receptor mediated Smad phosphorylation

There have been reports of involvement of numerous factors that either interact with Smads or completely independent of them including Ras (Mulder and Morris 1992, Suzuki 2005), extracellular signal regulated kinase (ERK) (Suzuki 2005, Cheng 2014), p38 (Gal 2008), c-Jun N-terminal Kinases (JNK) (Hocevar 1999), Focal Adhesion Kinase (FAK) (Hong 2011), p21-activated Kinase 2 (PAK2) (Wilkes 2003), cellular-Abelson Tyrosine Kinase (c-Abl) (Daniels 2004, Wilkes 2006), Phosphoinositide 3 Kinase (PI3K) (Wilkes 2005, Bakin 2000), (cdc42)/rac (Wilkes 2003) TGF β Activated Kinase 1 (TAK1) (Choi 2012) and others, but often this is in a cell type or disease context. At our current level of understanding, it appears these non-Smad signals allow cells to fine tune the core Smad response but there is certainly much more to understand with Smad independent signals and how other cell signals interact with and impact the TGF β signal.

Although we have a limited understanding of how R-Smads enter the nucleus, cells have evolved a number of mechanisms to influence it. While receptor phosphorylation is the mitigator of ligand binding and receptor activation, the Smads can be phosphorylated at a number of other sites. This is an active area of research and new sites are being uncovered with regularity and we are only in the infancy of elucidating the kinases responsible and biology associated with these phosphorylation events. Many of these sites are contained within the linker region (between the MH1 and MH2 domains – see Fig 2.7), which is the least conserved region in the Smad family. A

screen of Smad proteins revealed numerous mitogen activated protein kinase (MAPK) consensus phosphorylation motifs (PXS/TP) that are phosphorylated by ERK *in vivo* (Kretzschmar 1997). Similar sequence screens have been performed for a plethora of kinases including JNK, p38, Glycogen Synthase kinase 3 β (GSK3 β), Cyclin-Dependent Kinases (CDKs), Protein Kinase C (PKC), G-protein Coupled Receptor Kinase 2 (GRK2), Calcium/Calmodulin-dependent Protein Kinase 2 (CaMKII) and Casein Kinase 1 gamma 2 (CK1 γ 2) and have been confirmed to phosphorylate Smads under physiological conditions. Figure 2.8 illustrates a region of the linker of human R-Smads indicating the presence of MAPK, GSK3 β , general proline-targetted kinase, and the E3 ubiquitin ligase SMURF1 sites. The abundance and overlap of these sequences hints at the possibility of the incredible complexity in crosstalk and attenuation of Smads with other signalling stimuli.

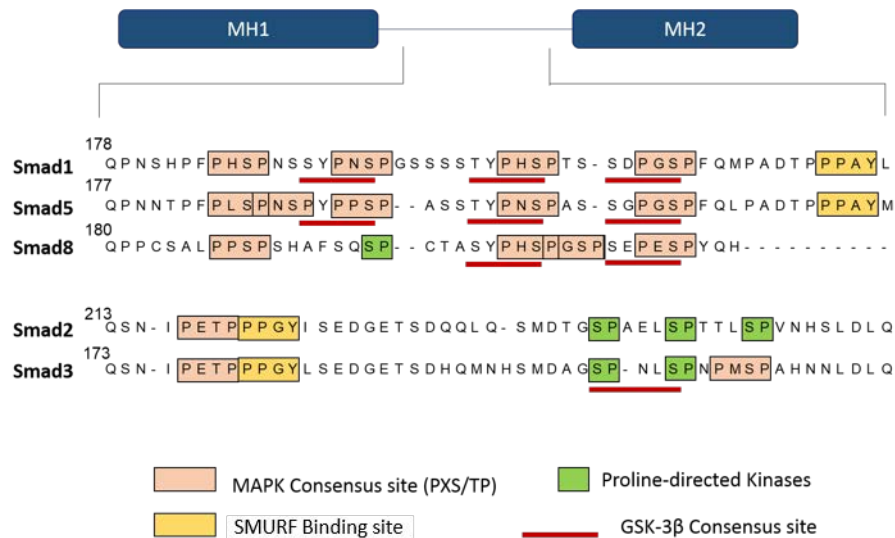


Figure 2.8 Comparison between phosphorylation sites in R-Smads linker regions. Linker region of Smads 1,2,3,5 and 8 are aligned and MAPK (orange box), general proline-directed kinases (green box), GSK3 β (red line) and SMURF (yellow box) consensus binding sites are marked.

Within the linker regions of Smad2 and Smad3, ERK has been demonstrated to phosphorylate T220, S245, S250, S255 in Smad2 and T179, S204, S208 in Smad3 respectively. Mutational analysis has suggested ERK phosphorylation dampens the ability of Smad3 to activate target genes (Kretzschmar 1999). ERK has also been shown to phosphorylate Smad2 at T8 but phosphorylation at this site enhanced Smad2 transcriptional activity (Funaba 2002). Smad1 has been shown to be phosphorylated by

ERK at 4 sites (S187, S195, S206 and S214) with 2 other potential sites (S209 and S210). Mutations at these sites leads to increased Smad1 transcription (Aubin 2004), suggesting phosphorylation of these sites is inhibitory. A mechanism that has been proposed is that phosphorylation of the ERK sites primes Smad1 for phosphorylation at S191 and S210 by GSK3 β which in turn facilitates ubiquitin-mediated degradation (Fuentealba 2007).

While R-Smads have been examined in some detail, we know much less about Smad4 phosphorylation. Although not all the phosphorylation sites are known, Smad4 is constitutively phosphorylated in cells. ERK has been shown to phosphorylate T277 and mutation at this site leads to reduced nuclear accumulation after BMP or TGF β stimulation (Roelen 2003). Although the mechanism is unknown, Smad4 phosphorylation appears to play a role in certain cancer cells with some link to ubiquitination (Liang 2004).

Original studies on linker phosphorylation by ERK suggested phosphorylation inhibited nuclear translocation of both TGF β (Kretzschmar 1999) and BMP (Massagué 2003) induced Smads. However, these observations have not held up in all experimental settings. Indeed as the list of phosphorylation sites grows, and the number of kinases that can phosphorylate each of these sites increases, questions as to how these phosphorylated sites impact one another become crucial, suggesting the phosphorylation state of certain sites will impact how a Smad will respond after each successive phosphorylation event. Add to this that phosphorylation, either in the cytoplasm or the nucleus, could greatly impact available binding partners and the potential for an intricate cross talking network.

Smad1 phosphorylation serves as an example of how compartmental phosphorylation can play a significant role. Smad1 is phosphorylated at the C-terminus by BMP-RI which results in translocation to the nucleus. In one experimental context, once within the nucleus it is phosphorylated in the linker region by ERK, p38, and/or JNK which primes the Smad1 for subsequent phosphorylation by GSK3 β (Fuentealba 2007). This phosphorylation enhances ubiquitination-driven degradation resulting in repressed transcriptional activity. It is important to note that ERK/p38/JNK and GSK3 β

phosphorylation occur within the nucleus, and after nuclear translocation. In contrast, another study confirms that phosphorylation at the same linker residues of Smad1 causes transcriptional repression but in this experimental context ERK phosphorylation occurs prior to nuclear translocation while still in the cytoplasm, Smad1 binding with nucleoporins is diminished and results in nuclear exclusion (Sapkota 2007). Similarities are found with Smad2/3 signalling also, as ERK phosphorylation in the linker region of cytoplasmic Smad2/3 inhibits transcriptional upregulation of Smad2/3 genes by nuclear exclusion of the phosphorylated Smads (Kreuzschmar 1999). Interestingly, when ERK was present in the nucleus, there was negligible impact on Smad nuclear exclusion yet there was still reduced transcriptional activity. In this case it was reportedly due to nuclear ERK phosphorylation of the Smad interacting partner TG Interacting Factor (TGIF) (Lo 2001). Why ERK activation is cytoplasmic in one model and nuclear in another may be related to variables like the concentrations of both TGF β and EGF used to stimulate the cells, the cell type, and/or culture conditions.

As mentioned earlier, kinases not involved in the ERK pathway appear to affect Smad signalling; kinases such as Casein Kinase 1 gamma 2 (CK1 γ 2), Casein Kinase 1 epsilon (CK1 ϵ), Calcium/Calmodulin-dependent Protein Kinase 2 (CaMKII), Protein Kinase C (PKC), G-protein Coupled Receptor Kinase 2 (GRK2), and MEKK1 (MAP Kinase Kinase Kinase (MAP3K) (Wrighton 2009) have also been demonstrated as *in vivo* kinases for Smads. The cyclin dependent kinases Cyclin-Dependent Kinase 2 and 4 (CDK2/4) phosphorylate Smad3 at many of the same residues as ERK (within the nucleus) and likewise has a negative impact on transcription (Matsuura 2004).

While most studies indicate linker phosphorylation attenuates Smad transcriptional responses, phosphorylation of Smad3 at S208 and S213 (analogous to S250 and S255 in Smad2) by JNK and S204, S208, and S213 by Rho Associated Kinase (ROCK) enhances Smad2/3 transcriptional activity yielding a more robust response (Kamaraju and Roberts 2005, Engel 1999). Our current understanding of the residues and kinases involved is shown below (see Fig 2.9).

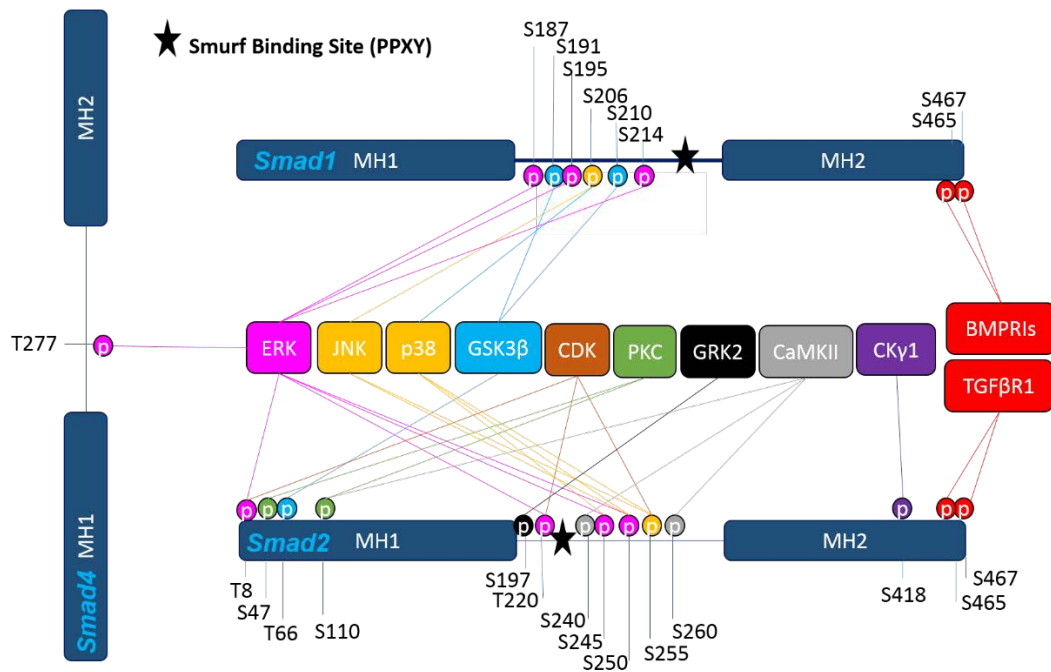


Figure 2.9 Phosphorylation sites and kinases of the Smad family of proteins. Smad1,2 and 4 are arranged around a number of kinases that have been characterized as kinases for the Smads. The residues reported to be phosphorylated are indicated as well as the site of the E3 ubiquitin ligase SMURF2 (designated with a star).

Interestingly, some of these non-receptor phosphorylation sites can be phosphorylated in response to TGFβ (Wrighton and Feng 2008, Hough 2012) in a cell type-dependent manner by “Smad-independent” factors providing a way for cells to tweak the generic Smad response to suit different cellular roles. Unfortunately, as with other Smad-independent signals, our understanding of how TGFβ transmits these signals from the receptors into the nucleus is poor. PAK2 is a Smad-Independent factor activated by TGFβ specifically in fibroblasts. Smads contain a consensus sequence for potential PAK2 phosphorylation, however, if this site is phosphorylated or has any physiological role is not known.

2.4 Smad translocation into the nucleus

Regulating R-Smad nuclear trafficking is critical as TGFβ exerts its effects at the transcriptional level inside the nucleus. As the nuclear membrane excludes macromolecules like Smads to enter and exit the nucleus they must utilize cylindrical pores composed of proteins that span both lipid bilayers, called nuclear pore complexes (NPC) (Holden 2014). These pores consist of over 30 proteins, many of

which contain multiple repeats of phenylalanine and glycine. These regions align the inside of the nuclear pore tunnel and provide a highly hydrophobic environment to restrict flow in and out (Ribbeck and Görlich 2001), so in order for proteins to get through these pores they need to bind a karyopherin carrier (importin or exportin). There are numerous karyopherins that share little sequence homology but usually share structural characteristics (Ström and Weis 2001) and recognize distinct sequences on target proteins. Our understanding of the roles of individual karyopherins in R-Smad trafficking remains incomplete and controversial.

Some of the confusion about Smad nucleo-shuttling stems from over-simplified dogma arising through early observations of Smad trafficking after TGF β stimulation. It was proposed that R-Smads were phosphorylated by receptors and then formed complexes with Smad4, and that this complex was then able to translocate to the nucleus and initiate transcriptional changes (Massagué 1998). This dogma persists in reviews and schematics today but poorly reflects our understanding of cellular events. Notably, cells deficient in Smad4 remain responsive to TGF β and R-Smads continue to accumulate in the nucleus (Sirard 2000), although the TGF β response in the absence of Smad4 *is* altered and Smad4 mutations and deletions *are* common in disease, particularly colon and pancreatic cancers (Wain 2014).

Unphosphorylated R-Smads shuttle between the cytosol and nucleus (Inman 2002, Schmierer and Hill 2005, Xu 2002). However, upon receptor mediated phosphorylation, R-Smads redistribute exclusively to the nucleus (Shi and Massagué 2003). In contrast, Smad4, the only Smad containing a classical leucine-rich nuclear export sequence (NES), is restricted to the cytoplasm in unstimulated cells, only entering nuclei once cells have been exposed to ligand (Pierreux 2000). This sequence is recognized by the nuclear exportin Chromosome Region Maintenance 1 (CRM1) and exported from the nucleus by RanGTP hydrolysis (Pierreux 2000). As mentioned above, R-Smads and Smad4 have no affinity in unstimulated cells, however upon phosphorylation R-Smads rapidly associate with Smad4. The NES in Smad4 becomes masked when phosphorylated R-Smads bind, allowing the pR-Smad/Smad4 complex to remain in the nucleus (Pierreux 2000). This nuclear retention ends upon dephosphorylation of R-Smad, leading to Smad4 dissociation and exposure of the Smad4 NES (Pierreux 2000).

The inhibitory Smads have an opposite localization profile to R-Smads, being predominately nuclear until TGF β stimulation when the I-Smads re-localize to bind the receptors at the plasma membrane and endosomes (Asano 2004). The mechanisms regulating Smad7 nuclear trafficking are unknown.

As R-Smads shuttle between the cytosol and the nucleus in an unstimulated state, there must be both nuclear import and export signals. Whether the phosphorylated R-Smads accumulate in the nucleus (Shi and Massagué 2003) due to: (1) increased nuclear import, (2) increased nuclear retention (decreased export), or (3) a combination thereof, is controversial. All have experimental evidence to support and/or refute each mechanism (Chen 2005, Kurisaki 2001, Schmierer and Hill 2007, Inman 2002, Nicolas 2004, Schmierer and Hill 2005, Schmierer 2008).

Early work suggested Importin- β was the karyopherin responsible for R-Smad nuclear entry (Kurisaki 2001, Xiao 2000) but subsequent genome-wide siRNA and RNAi screens have yielded other candidates. Most of these candidates were originally identified in screens in model organisms and translated to mammalian models (Xu 2007, Yao 2008). Candidates include Importin7 and Importin8 (Xu 2007), secretory protein 13 (sec13) (Chen and Xu 2010), Nucleoporin 93 (Nup93) (Chen and Xu 2010), Nup153 and Nup214 (Xu 2002) and others (Chen and Xu 2010).

The nuclear export machinery for R-Smads remains just as uncertain with the only consensus being that export is not mediated by CRM1 (Hill 2009). Exportin4 (Kurisaki 2006) and Ran-binding protein 3 (RanBP3) (Dai 2009, Dai 2011), which were identified via high throughput screens, show potential as export karyopherins for dephosphorylated Smads. One compounding variable that needs to be considered is the possibility of different factors playing roles in different cell types or disease states. For example, in fibroblast and carcinoma lines, R-Smad phosphorylation (and subsequent nuclear accumulation) lasts much longer than in healthy epithelial cells (Rahimi 2009, Dr Jules Doré (Memorial University of Newfoundland) *pers comm*).

2.5 Role of Smads in transcription

2.5.1 DNA binding

TGF β , Activin, and BMP ligands exert their actions through the Smads. Phosphorylated Smads enter the nucleus and bind DNA altering gene transcription (Shi and Massagué 2003) but Smads are unable to modulate transcription without accessory proteins. The reality is that the role of Smads as transcription factors is far more complicated than initially thought and the complex array of interactions with other transcription factors accounts for many the pleiotropic effects of TGF β ligands. Smad4, and all R-Smads except Smad2, can independently bind DNA (Gaarenstroom and Hill 2014) through a β -hairpin structure in the MH1 domain which inserts into the major groove of the DNA forming 3 hydrogen bonds (Shi 1998). Smad2 contains the conserved residues comprising the β -hairpin but contained within it is an extra exon (denoted exon 3) that serves to disrupt formation of the hairpin structure and therefore prevent DNA binding (Yagi 1999). Being unable to bind DNA directly does not mean Smad2 is not involved in transcription; as with all phosphorylated R-Smads, Smad2 forms heteromeric complexes with Smad4 which binds DNA with high affinity. Cells also express a splice variant of Smad2 missing exon 3 that can bind DNA in its own right (Yagi 1999) but this form is expressed at much lower levels (10 fold lower) than the full length version (Dunn 2005).

Since the β -hairpin is conserved across all R-Smads and Smad4, it confers no DNA sequence specificity (Massagué 2005). The sequences Smads bind were first defined as 5'-GTCTAGAC-3' (Zawel 1998) and 5'-CAGACA-3' (Jonk 1998). However, they were further refined to CAGA(C), with contributions to the affinity by surrounding residues (Chen 2002) as more promoters were analysed. The binding affinity of Smads to a single Smad Binding Element (SBE) is too low to detect *in vivo* (Shi 1998) but can be forced through the generation of concatamers of multiple (between 6 and 11) copies of SBEs (Zawel 1998). *In vivo*, even promoters with multiple SBEs require other cooperating factors for high affinity DNA binding and transcriptional changes (Seoane 2004).

2.5.2 Transcriptional co-activators of Smads

A large number of Smad coactivators and corepressors have been described and the list continues to grow. The first characterized example is Forkhead Activin Signal

Transducer 1 (FAST1), (renamed FoxH1) that binds the MH2 domain of Smad2 (Chen 1996). FoxH1 is recruited to a pSmad2/Smad4 complex and is responsible for Smad2-mediated induction of the gene *Mix2* (Chenet 1996). Other members of the forkhead family of transcription factors, such as FoxO and FoxG1, have been implicated as Smad coactivators (Seoane 2004) cooperating with both pSmad2-Smad4 and pSmad3-Smad4 complexes. As expected from the variety of cellular responses to TGF β superfamily members, a large number of other transcription factors have also been shown to modulate Smad regulated transcription, and include; Runt-related transcription Factor (RUNX) family members (Hanai 1999, Aliston 2001, Agas 2013), Olf/EBF-associated zink-finger Protein (OAZ) (Hata 2000), Activator Protein 1 (AP1) family (Zhang 1998, Sunqvist 2013), Electron Transferring Flavoprotein (ETF) family members (Chen 2002), Activating Transcription Factor and cAMP-Response Element Binding Protein (ATF/CREB) family members (Kang 2003, Topper 1998, Warner 2004), p53 (Cordenonsi 2003), Interferon Regulatory Factor 4 (IRF4) (Tamiya 2013), Transcription Factor E3 (TFE3) (Brodin 2000) and Specificity Protein 1 (Sp1) (Jungert 2006, Poncelet and Schnaper 2001, Ellenrieder 2008). Because promoters have both SBEs and elements for the associated transcription factors within a specific proximity, they provide highly specific regulation. To recruit the specific complexes, those genes regulated by Smads are dependent on the expression, abundance, and availability of any number of transcription factor partners. This has led to a highly specific, highly regulated system at the transcriptional level. Further modulation of the activity of these transcription factors by other cellular signals that can impact their ability to either bind Smads or their DNA element, such as phosphorylation of TGIF (by ERK) and c-jun (by JNK), thus serving as a potential mechanism for cross talk from other cellular signals.

As well as associating with DNA binding transcription factors, Smads can also bind non-DNA-binding proteins in the nucleus to impact transcription either positively (co-activators), or negatively (co-repressors). Of the co-activators, the most characterized are the p300 and CREB-binding protein (CBP) proteins. P300/CBP binds Smads1, 2, 3, 4 at the MH2 domain (Pouponnot 1998, Topper 1998) and is required for full gene induction of many transcription factors, including P/CAF, SRC1, TFIIE and TFIIIF (Bannister and Kouzarides 1996). Other co-activators identified include the chromatin assembly factor P300/CBP Associated Factor (P/CAF) (Itoh 2000), Activator-recruited complex 105 (ARC105) (Kato 2002), Melanocyte Specific Gene 1 (MSG1) (Shioda 1998), and Swift (Shimizu 2001). Both MSG1 and Swift are not general transcriptional co-activators and require binding to Smad4 before they can induce transcription (Bai

2002). Transcriptional co-repressors like Sloan Kettering Institute protein (Ski), Ski-related Novel Protein N (SnoN), as well as TGIF all bind nuclear Smads and dampen TGF β -mediated transcription. Ski and SnoN are able to bind phosphorylated and unphosphorylated Smads in the nucleus, but upon TGF β stimulation are rapidly degraded (Sun 1999). TGIF binding appears limited to phosphorylated R-Smads and inhibits their activity by competing for binding with co-activators (Lo 2001). The strength of the transcriptional response can be modulated through a balance between co-activator and co-repressor expression/binding and the subsequent competition for Smad binding (Miyazono 2000). A further degree of complexity is added when Smads upregulate other repressors or activators (see Fig 2.10).

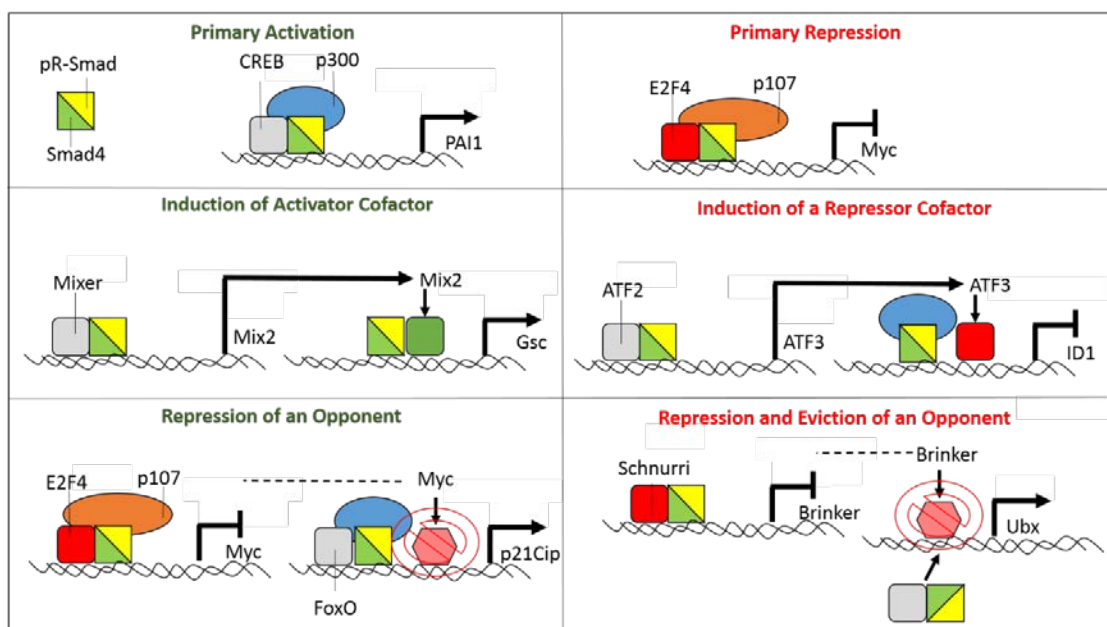


Figure 2.10 Examples of Smad transcriptional regulation. **Primary Activation:** Phosphorylated R-Smad/Smad4 complexes in combination with different transcription factors target specific gene promoters. In the case of one activation site of PAI1, CREB and p300 act as cofactors with the Smad complex to initiate gene induction. **Primary Repression:** Instead of promoting gene expression, repressors inhibit them. In TGF β -mediated repression of Myc, E2F4 and p107 partner with the Smads to repress the c-myc gene. **Induction of Activator Cofactor:** In this two-step process (otherwise known as self-enabling gene responses) the Smad complex couples with the transcription factor Mixer to bind the promoter of Mix2 and induce it. Mix2 protein then binds Smad complexes at the Goosecoid (Gsc) promoter for its induction. **Induction of a Repressor Cofactor:** Another self-enabling gene response; However, in this case ATF2 and Smads bind at the promoter of ATF3 for its induction. ATF3 protein then complexes with the Smads to repress Inhibitor of DNA binding 1 (ID1). **Repression of an Opponent:** Upon initial stimulation the gene p21CIP is inhibited by the presence of Myc at the promoter. The Smads, complexed with E2F4 and p107 bind the Myc promoter and induce its repression. Due to the quick turnover of Myc protein there is not enough Myc to repress the p21CIP promoter and the Smad/FoxO complex is able to induce p21CIP. **Repression and Eviction of an Opponent:** This mechanism is similar to the repression of an opponent model, except the inhibitor (Brinker) occupies the same region of the promoter (in this case ubx) as the Smads, except with higher affinity. The repressor schnurri binds Smads at the Brinker promoter and inhibits it which in turn makes the ubx promoter accessible to the Smads.

2.5.3 Histone acetyltransferases and histone deacetylases

The Smads' ability to modulate transcription has been shown to partially require Histone Acetyltransferases (HATs). HATs are enzymes that facilitate the transfer of an acetyl group from acetyl-CoA to lysine residues on histone proteins (Dahlin 2014) which are the structural, proteinaceous component of chromatin. In order for DNA to be contained in a cell nucleus it needs to be condensed into dense coils that are wrapped onto larger coils with histones making up the core that the DNA is wound upon (Fransz and de Jong 2011). Densely packed chromatin is not accessible to transcription factors and is not actively transcribed (termed heterochromatin), while less densely packed chromatin facilitates transcription by allowing transcription factors access to the DNA (termed euchromatin). Upon acetylation, histones lower the affinity for one another, relaxing the DNA coils and allowing transcription initiation complexes to assemble (Fransz and de Jong 2011). P300/CBP (discussed above) which binds pSmad complexes in the nucleus, also has histone acetyltransferase activity (Bannister and Kouzarides 1996) and in this way, Smads may be able to modulate the chromatin around SBEs. In addition, some of the other transcription factors associated with Smads have histone acetyltransferase activity, including the ATF/CREB family (Kang 2003, Topper 1998, Warner 2004) and Sp1 (Hilton 2005). In support of the hypothesis that histone acetylation has a role in TGF β signalling, phosphorylation of these transcription factors in response to TGF β increases their acetyltransferase activity (Dekker and Haisma 2009., Fukushima 2007). As that Smads have no intrinsic kinase activity, a critical question is what are the TGF β -induced kinases responsible for phosphorylating these nuclear factors?

In contrast to HATs, histone deacetylases (HDACs) facilitate the removal of acetyl groups from histones (Kroeson 2014) and have also been shown to be associated with Smads in the nucleus. The class II histone deacetylase HDAC4 (Kang 2005) binds RUNX/smad3/smad4 complexes and represses TGF β induction of the *osteocalcin* gene while HDAC1 and 2 complex with mSin3/ Nkx3.2/Smad1/Smad4 as a repressor (Kim and Lassar 2003).

2.6. TGF β signal termination

As TGF β receptors are kinases and signal initiation begins with phosphorylation of the Smads, termination of TGF β requires two crucial termination steps; (1) the

phosphorylated Smads already in the nucleus need to be “turned off”, and (2) further activation of Smads needs to be switched off (receptor deactivation). For each of these steps there are multiple theoretical mechanisms proposed.

2.6.1 Smad dephosphorylation for signal termination

Observations between years 2000 and 2002 provided strong evidence for a model of Smad dephosphorylation in the nucleus, with dephosphorylated Smads quickly returned to the cytoplasm (Xu 2000; Inman 2002, Xu 2002). It should be noted that proteasomal inhibitors also had a mild impact on the observed loss of phosphorylated Smads, suggesting some role for ubiquitination-mediated proteasomal degradation in dampening the phosphorylated Smad signal (Knockaert 2006). The search for a nuclear phosphatase was performed with a screen of 39 phosphatases that yielded a single candidate known as Protein Phosphatase Mg²⁺/Mn²⁺dependent 1A or PPM1A (Lin 2006). PPM1A was found to bind phosphorylated Smads and, when overexpressed, reduced Smad phosphorylation while silencing the PPM1A gene increased both the intensity and duration of Smad phosphorylation (Lin 2006). Overexpression of PPM1A in *Xenopus* also caused biological consequences reminiscent of disrupted TGFβ signalling (Lin 2006). Despite this, two groups who have generated PPM1A-null mice have not directly indicated altered Smad phosphorylation; one group observed no morphological phenotypes (Yang 2011), and the other group made no statement about Smad dephosphorylation, but instead reported that PPM1A dephosphorylates RanBP, a protein required for Smad nuclear export (Dai 2011). Whether redundancy exists in mammals or other complexities are at play is yet to be determined. Another point of contention is whether or not PPM1A is localized in the nucleus. In an initial study performed in the human keratinocyte HaCaT cell line, PPM1A was determined to be exclusively nuclear (Lin 2006), while another group claimed that in over ten cell lines (including HaCaTs), PPM1A is exclusively cytoplasmic (Bruce and Sapkota 2012). Although generally accepted in the field that PPM1A is the Smad phosphatase, it is wise to be mindful that our understanding of Smad dephosphorylation is not yet complete, as evidenced by the role of other phosphatases involved in Smad signalling. Perhaps there are specific phosphatases involved in regulating specific Smad subtypes, or conditions in which other phosphatases are recruited for Smad dephosphorylation.

In hypoxic conditions the most promiscuous of phosphatases, PP2A, can selectively dephosphorylate Smad3 (not Smad2) but this does not occur in normal conditions (Heikkinnen 2010). Surprisingly, the DUSP-family member phosphatase Myotubularin Related Protein 4 (MTMR4) was shown to bind to phosphorylated Smads in early endosomes and sequester them there, thereby preventing them entering the nucleus (Yu 2010). As nonphosphorylated Smads apparently can enter the nucleus it is unclear how MTMR4 is actually preventing nuclear entry. Pyruvate dehydrogenase phosphatase (PDP), which is confined to mitochondria, can dephosphorylate Smad1 (Chen 2006). How PDP exerts its effects from the mitochondria remains unknown. Differential dephosphorylation of Smad families is evident, with the Small C-terminal domain phosphatases (SCPs) localized in the nucleus and specifically recognizing and dephosphorylating the receptor sites of Smad1 but not Smad2 or Smad3 (Knockaert 2006). They may, however, have a more significant role as a phosphatase for the Smad linker region (Wrighton 2006, Sapkota 2006). Interestingly, PPM1A has been implicated in both Smad2/3 (Lin 2006) and Smad1 dephosphorylation (Duan 2006),

Unfortunately we currently lack the phospho-specific antibodies to thoroughly investigate how linker sites and other Smad sites are regulated, particularly the phosphatases, but certainly there are multiple mechanisms. Kinetics of phosphorylation, dephosphorylation and the locales where these events happen (Wrighton 2009, Sapkota 2007) all vary greatly, suggesting multiple regulatory mechanisms. As antibodies become available our understanding of how these phosphorylation events are regulated and impact on TGF β signalling will become clearer.

2.6.2 Smad ubiquitination for signal termination

Although dephosphorylation of Smads is an important component of terminating Smad signalling, there is also a role for ubiquitin-mediated degradation (Knockaert 2006). In BMP signalling ubiquitination appears to be critical. The E3-ubiquitin ligase SMURF1 was shown to bind to both unphosphorylated and phosphorylated Smads (Zhu 1999), and BMP-regulated developmental processes were disrupted in the absence of SMURF1 during development (Ying 2003, Shi 2004). SMURF1 recognizes and binds a PPXY motif in the linker domain of Smad1 (see Fig 2.8), although the binding requires phosphorylation of a number of serine/threonine residues surrounding it (Alarcón

2009). These residues can be phosphorylated by a number of different kinases including CDK8/9 (Alarcón 2009) and GSK-3 β (Aragón 2011), which allow non-BMP signals to prime cells to increase or decrease their BMP responsiveness by influencing Smad levels. The nature of the ubiquitin linkages and the specific lysine residues ubiquitinated is unknown, but leads to rapid degradation. Another E3 ubiquitin ligase, Carboxyl terminus of Hsc70-Interacting Protein (CHIP), has also been shown to ubiquitinate and cause degradation of Smad1 (Li 2004) indicating that there may be redundancy and/or a contextual component to how E3 ubiquitin ligases regulate Smad1 levels.

At least three E3 ubiquitin ligases have been described for Smad2/3, including SMURF2 (also known to act on Smad1) (Lo and Massagué 1999), NEDDL4 (Kuratomi 2005), and WW Domain containing E3 Ubiquitin Ligase Protein 1 (WWP1) (Ito 2010). Again these ligases recognize a PPXY motif but not in the same region of the linker as in Smad1 (Gao 2009). As with Smad1, NEDDL4 binding requires phosphorylation of residues in the linker region by kinases such as CDK8/9 (Al-Sahih 2012). However, an unidentified kinase induced by TGF β can phosphorylate the linker region and lead to a ligand induced degradation of Smad2/3 (Gao 2009). CHIP has also been shown to ubiquitinate and lead to degradation of Smad2 and Smad3 but, unlike NEDDL4, does not differentiate between phosphorylated and unphosphorylated forms (Li 2004). Rapid degradation of phosphorylated forms of Smad2 and Smad3 in the nucleus occurs when the transcriptional repressor Ski is bound. The Smad/Ski complex is recognized by ARKADIA (Yuzawa 2008). Interestingly, an inhibitor of ubiquitination, Otubain 1 (Otub1), binds phosphorylated Smad2 and Smad3 and prevents ubiquitination-mediated degradation (Herhaus 2013).

Smad4, despite lacking a PPXY motif, can be ubiquitinated by SMURF1/2, NEDDL4, and WWP1. This occurs after the ligase is recruited by phosphorylated Smad2 and Smad3 (Morén 2005). Tripartite Motif Containing 33 (TRIM33) is another E3 ubiquitin ligase that can mono-ubiquitinate Smad4 at Lysine519 (Dupont 2005) but this event only occurs after binding to chromatin where Smad4 binding to R-Smads has been disrupted. There is no evidence this ubiquitin modification impacts Smad4 stability or degradation (Agricola 2011).

The Inhibitory Smads, Smad6 and Smad7, also contain a PPXY motif and can indeed bind the NEDD4-like E3 ubiquitin ligases but these are not the primary targets for ubiquitination. Instead, the target is the activated receptors with the receptors and I-Smads degraded as a complex (Kavsak 2000). ARCADIA has also been implicated in Smad7 degradation with a role in renal fibrosis and hypertension (Fukasawa 2004, Lui 2012) when TGF β signalling is hyperactivated. The Lysine residues on Smad7 that are targets for ubiquitination (Lys64 and Lys70) are also targeted by the histone acetyltransferase p300. When acetylated, these residues can not be ubiquitinated and are therefore protected from degradation (Grönroos 2002). These sites can also be deacetylated by SIRT1 that controls the degradative fate of Smad7 (Simonsson 2005). The biological relevance of Smad ubiquitination has led to multiple intricate positive and negative regulatory mechanisms.

2.7. TGF β receptor deactivation, downregulation and degradation

In an unstimulated state, TGF β receptor surface levels are maintained by a balance of constitutive recycling and continual degradation and replacement (Mitchell 2004). Early studies revealed cells exposed to TGF β rapidly internalized both TGF β R1 and TGF β R2 receptors from the cell surface (Engel 1998). However, these assays utilized radiolabelled TGF β ligand cross-linked with the two receptors. More recent studies based on non-cell permeable biotinylation indicate only TGF β R2 surface levels are reduced while TGF β R1 levels stay constant (Chen 2011). In either case, ligand cannot bind the initiating partner so essentially the cell is unable to respond further to external ligand. The definition of receptor activation is ambiguous, particularly when involving a receptor pair like TGF β receptors. While initial ligand binding is considered to be critical in the activation of receptors, experiments where receptors were pre-bound with ligand at 4°C (when endocytosis is inhibited) and then ligand was immediately removed by acid stripping (before allowing the cells to return to 37°C), signalling was still optimal (Zwaagstra 2001), indicating ligand does not need to remain bound to the receptors for kinase activity. The kinase activity of TGF β R2 is required for TGF β signalling, but this activity is not impacted by the presence of ligand. Rather, ligand acts as a scaffold to recruit TGF β R1 to TGF β R2. An activated kinase domain of TGF β R1 is required for R-Smad phosphorylation and although a mutation at Thr204 to Aspartate introduces mild kinase activity, full kinase activation corresponds with multiple phosphorylation events both within and outside the G/S domain (Willis and Mathews 1997). For the sake of this study, receptor activation will be defined as

phosphorylation of TGF β R1, so an obvious potential deactivation mechanism would be receptor dephosphorylation. Smad7 interacts with Growth Arrest and DNA Damage 34 (GADD34), which is a regulatory subunit of the phosphatase protein phosphatase 1 (PP1), shown to dephosphorylate TGF β R1 when Smad7 is recruited to the active receptor (Shi 2004). Components of the PP2A phosphatase also bind, and have been implicated in, dampening the TGF β response through direct interaction with TGF β R1 (Griswold-Prenner 1998, Batut 2008).

Dephosphorylation is only one way to remove active receptors. As with the phosphatase GADD34, a number of E3-ubiquitin ligases are recruited to active receptors by Smad7. The Smad7-associated ligases (including SMURF1/2 and NEDDL4) poly-ubiquitinate the active receptors and the whole complex is subsequently degraded (Kavsak 2000). The balance between dephosphorylation and ubiquitin-directed degradation is not known, but total cellular levels of both TGF β receptors are significantly reduced within 8-12 hours of the initial ligand addition (DiGuglielmo 2003), indicating the steady state balance between recycling, degradation and replacement is disrupted. Transcriptional repression of either receptor gene has not been demonstrated after TGF β stimulation, suggesting the reduction is due to enhanced degradation. The increase in degradation may be due to the receptors being shunted from the recycling route to the degradative one upon activation. However recycling assays indicate that ligand stimulation does not alter the rate by which receptors return back to the cell surface after internalization, but very rapidly surface levels decline (Doré 2001, Mitchell 2004). This would imply recycling is not impacted by ligand, rather pre-activated receptors are being targeted to a degradative pathway upon returning to the cell surface.

Degradation of the receptors has been reported through both lysosomal and proteosomal pathways (Huang and Chen 2012), and may not always require ubiquitination (Zhang and Cohen 2004). However, there is a major discrepancy between how rapidly receptors are removed from the cell surface (downregulated) and the time it takes for degradation to occur. Maximal downregulation of receptors (ie. loss of receptors from the cell surface) occurs within 2 hours (Anders 1997, Doré 2001, Garemszegi 2001), while degradation (loss of receptors from intracellular compartments) isn't maximal until 12-16 hours (Di Guglielmo 2003, Luga 2009).

Another, perhaps more puzzling, conundrum occurs when comparing the extent of downregulated versus degraded surface receptors. Almost 80% of surface receptors are downregulated (Anders 1997, Doré 2001, Garamszegi 2001) but only about 40% end up degraded (Ebisawa 2001, Di Guglielmo 2003, Kavsak 2000).

Comparing downregulation and degradation studies (Anders 1997, Doré 2001, Garamszegi 2001, Ebisawa 2001, Di Guglielmo 2003, Kavsak 2000), biochemical results tell us only that the receptors aren't on the cell surface, and they are not yet degraded, leaving the question of where they are. While a direct comparison between downregulation and degradation has not been conducted, some have argued it is simply a delayed degradation process. Addressing the question using immunofluorescence microscopy has proved as challenging as biochemical approaches. Low receptor expression levels hamper trafficking studies following fluorescent tagged receptors. Antibodies generated against receptors, particularly the extracellular domain, are notoriously non-specific. Even inserting a small epitope sequence at the amino-terminal (extracellular) end of the receptors causes problems as it hampers the ability of the ligand to bind. Nevertheless, John Zwaagstra and colleagues reported a significant increase in TGF β R1 antibody staining in the nucleus (Zwaagstra 2000) upon ligand stimulation. Recently two independent groups have also reported some TGF β R1 localizes to the nucleus after ligand stimulation using more specific antibodies, at least in some cell types and conditions (Chandra 2012, Mu 2011).

However, a number of contradictions have arisen between the three studies regarding the kinetics of nuclear entry, the cell types in which it occurs, and if the receptors are full length or truncated. TGF β R1 nuclear localization is observed within 10 minutes in 59 of 66 prostate cancer tissues, renal cell carcinoma, and bladder tumours, as well as human breast and lung carcinoma cell lines but not noncancerous tissue or untransformed cell lines. Receptors localized to the nucleus are reported to be a truncated form consisting of only the intracellular domain (Mu 2011). A much slower rate of nuclear accumulation is observed in HER2 positive-transformed, but not untransformed or HER2-negative transformed lines, peaking at after two hours post stimulation and full-length receptors observed (Chandra 2012). Slower again was the

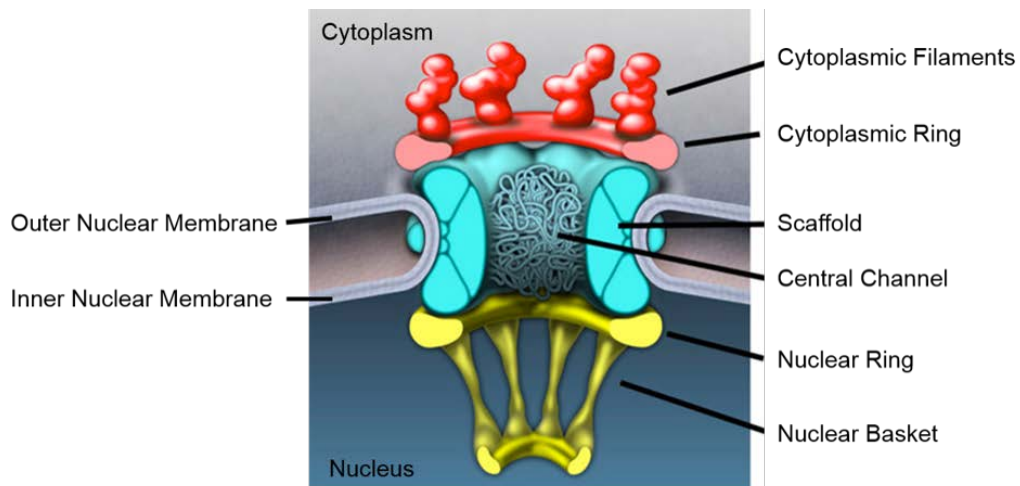
earlier observations with full-length nuclear receptors observed in two lung epithelial cell lines after 24 hours TGF β stimulation (Zwaagstra 2000).

Regarding TGF β R1's translocation to the nucleus, it remains a mystery exactly what they are doing in the nucleus and how that process is regulated. Even their presence in the nucleus remains controversial. Regulation of how receptors get to the nucleus is completely unknown and even the rudimentary aspects of Smad nuclear trafficking are misunderstood, with the literature full of conjecture and contradictions. Furthermore, nuclear trafficking mechanisms may help explain why some cell types have sustained, and others have diminished kinetics of signalling.

In this study we will define nuclear trafficking as the regulated (not passive) transfer of macromolecules from another cellular compartment fully across the nuclear membrane and mechanisms contributing to delivery to, passage through, retention within, and export out of the nucleus. Mechanisms employed in nuclear transport are broken into two broad categories, (1) soluble proteins and (2) membrane embedded proteins.

2.8. Nuclear entry of soluble proteins

In order for soluble proteins to enter the nucleus, they must bypass the one major obstacle, the double lipid bilayer. The double lipid bilayer nuclear membrane does not permit passive diffusion of macromolecules. Therefore, proteins and RNA are required to pass through proteinaceous structures known as nuclear pores. Each nuclear pore is an approximately 125 MDa macromolecular complex made up of about 30 soluble proteins, referred to as nucleoporins, (D'Angelo and Hetzer 2008). The nucleoporins are arranged into an octagonal pore composed of two rings, (one on the cytoplasmic side and the other on the nuclear side of the nuclear membrane) with a central scaffold bridging the two (see Fig 2.11). Being octagonal, each nucleoporin is present in copies of 8, or multiples of 8 with 3 transmembrane proteins that anchor the pore complex into the lipid membrane (Mansfeld 2006).



Adapted from "Structure, dynamics and function of nuclear pore complexes" by M.A. D'Angelo and M.W. Hetzer, 2008, Trends in Cell Biology, Vol 18, p456-466. Copyright Elsevier 2008. Adapted with Permission

Figure 2.11 Structure of the nuclear pore complex. An octagonal structure forms 2 rings at the cytoplasmic and nuclear sides of the membranes. Between them is a scaffold region and a central channel runs the length of it. These pores form where the inner and outer nuclear membranes fuse.

Ions and macromolecules smaller than approximately 40 kDa can freely diffuse through nuclear pores (Patel 2007) while larger proteins need to be actively transported. The exclusion factor is not size, rather a meshwork of weak hydrophobic interactions introduced by the core of FG-containing nucleoporins (Ribbeck 2001). These FG-containing proteins contain multiple repeats of the amino acids GLFG, FXFG, PXFG or SFXG that line the central channel and make up approximately a third of the nuclear pore complex (Isgro and Schulten 2007). While restricting unwanted cargo, these pores can facilitate approximately 1000 translocation events per second, shuttling a mass of over 100 MDa in that time (Ribbeck 2001).

Through interactions with the nucleoporins, a group of proteins facilitate this active transport of desired proteins. These facilitator proteins are referred to as β -karyopherins. The β -karyopherins can be further subdivided into importins (bring cargo from the cytoplasm to the nucleus) or exportins (take cargo from the nucleus to the cytoplasm) (Mosammamarast and Pemberton 2004). The energy required to drive this active transport is provided by a Ras-like protein, Ran. A strong gradient exists across the nuclear membrane of RanGTP and RanGDP. Within the nucleus Ran is almost

exclusively bound to GTP, due to the exclusive nuclear localization of the RanGEF (exchanges GDP for GTP on Ran), Regulator of Chromosome Condensation 1 (RCC1), and the exclusive cytoplasmic localization of the Ran GAP (exchanges GTP for GDP on Ran) (Ohtsubo 1989).

There are over 22 putative β -karyopherins described in mammals (Ström and Weis 2001) ranging in size from 90 and 130 kDa, but sharing relatively low sequence homology (less than 20% amino acid identity). They are characterized by having an acidic isoelectric point and the ability to bind RanGDP (Ström and Weis 2001). The karyopherins bind RanGDP via a domain in the amino terminal and the cargo towards the carboxy terminal (Cingolani 1999). After binding RanGDP and cargo the karyopherins bind multiple FXFG repeats of the nucleoporins to facilitate entry. When bound to RanGDP, the importins are able to complex with their cargo and translocate into the nucleus but as soon as the GTP displaces GDP on Ran, the complex is rapidly disassembled, releasing the cargo into the nucleoplasm (Kobe 1999).

In order for importins to traffic cargo through the nuclear pore, they must first recognize them in a process which may be direct or indirect. All proteins that enter the nucleus must therefore possess a sequence that somehow connects them to the import machinery. This amino acid sequence is referred to as a Nuclear Localization Sequences (NLS) (Lange 2007). The best characterized is the classical NLS consisting of either monopartite (one) or bipartite (two) stretches of basic amino acids. Comparisons of numerous classical NLS sequences has resulted in a minimal consensus sequence of K(K/R)X(K/R), however variation does exist. An example of a monopartite NLS is found in the SV40 T antigen at residues 126-132 and is PKKKRRV (Lange 2007), while an example of a bipartite NLS is found in nucleoplasmin in residues 155-170 and is KRPAATKKAGQAKKKKK (the underscored residues are the essential residues for nuclear import) (Lange 2007). For minimal NLS sequences, the NLS is not directly bound to Importin- β , but rather by a scaffold protein known as Importin- α . Unbound Importin- α is in a folded state in which the C- and N-terminal are folded back upon one another but rapidly unfolds upon binding RanGDP-bound Importin- β in the cytoplasm. This exposes a domain in Importin- α that can recognize classic NLS sequences in potential cargo. The cargo/Importin- α /Importin- β complex now translocates into the nucleus. Once shuttled across the nuclear membrane

RanGTP is exchanged for Ran GDP causing a complete complex dissociation (Lange 2007). Importin- α has low affinity for RanGTP-bound Importin- β , the N-terminal of Importin- α now binds to the C-terminal dislodging the cargo (described in Fig 2.12).

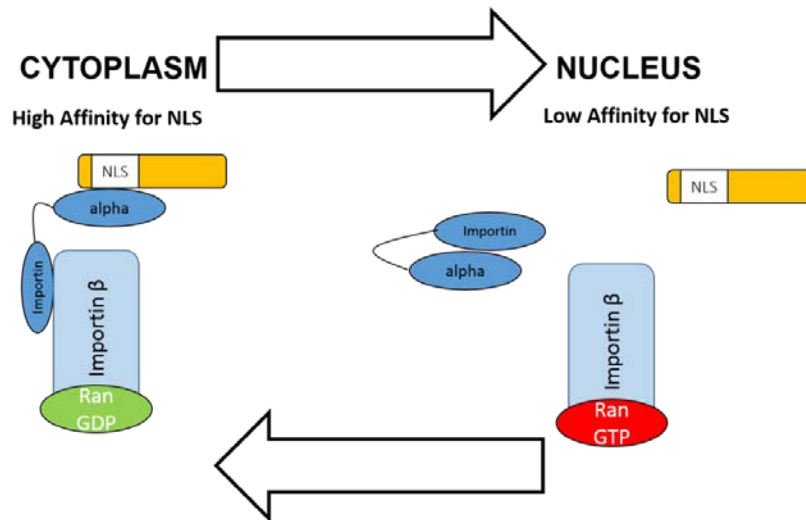


Figure 2.12 Complex assembly and disassembly in nuclear translocation. In the cytoplasm Importin- β is bound the RanGDP. This facilitates binding to the N-terminal of Importin- α which maintains the protein in a conformation that allows it to recognize and bind proteins carrying a classical NLS. This complex crosses into the nucleus where RanGDP is very rapidly exchanged for RanGTP and the properties of Importin- β changes. The affinity for Importin- α is removed and the N-terminal of Importin- α binds back across the C-terminal and dislodges the cargo freely inside the nucleus.

While this is the classic nuclear entry model, there are many variations of this, including direct binding of proteins to Importin- β . As a result there are many non-classical NLS, with the only thing in common being they confer binding to an importin- β either directly or indirectly (Ström and Weis 2001).

2.9. Nuclear entry of cleaved membrane-embedded proteins

Moving transmembrane proteins from their membrane compartment into the nucleus is more problematic than soluble proteins. However passage across the nuclear membrane still requires the same nuclear pore complexes, nucleoporins, karyopherins, and RanGTP/GDP, as soluble proteins. The initial problem is moving a membrane-embedded protein, with at least one span of hydrophobic residues, to a nuclear pore. Four billion years of evolution has evolved a multitude of ways to achieve this goal but in our current understanding there are only two characterized mechanisms. The first is

simply cleaving the membrane-embedded protein on the cytoplasmic side of the transmembrane region, yielding a truncated, soluble protein. The second involves a process that essentially reverses the trafficking route these peptides followed during synthesis and delivery to their cellular locale. Within the Epidermal Growth Factor Receptor (EGFR) family of transmembrane receptors are classic and well characterized examples of both mechanisms of nuclear delivery and we will therefore focus our attention within this group as it has not been well described for serine/threonine kinase receptors.

The classic example of cleaved receptors undergoing nuclear transport is the Notch receptor (Bray 2006), in which ligand binding at the cell surface results in sequential proteolytic cleavage. The first step is extracellular (ectodomain) cleavage, by α -secretase, followed by cleavage within the transmembrane domain by γ -secretase. This step releases a soluble intracellular domain (ICD) fragment that enters the nucleus via karyopherins and the nuclear pore to act as a transcription factor (Bray 2006). Within the EGFR family, ErbB-4 receptor traffics to the nucleus via a virtually identical mechanism (Carpenter 2008). While ectodomain cleavage of this receptor occurs at a low basal level, it is greatly increased by the addition of the cognate ligand neuregulin (heregulin) (Vecchi 1996). This cleavage event is mediated by A Disintegrin and metalloprotease domain-containing protein 17 (ADAM17) (also called Tumour Necrosis Factor Alpha Converting Enzyme or TACE) (Cheng 2003) and yields a 120 kDa fragment released extracellularly and an 80 kDa fragment remaining within the membrane. Further cleavage by γ -secretase at the endo-juxtamembrane (just inside the membrane) region releases the ICD (Cheng 2003).

Once the Erb-B4 ICD is transported into the nucleus, nuclear ErbB-4 has been shown to play a significant role in control of astrogenesis in the developing mouse brain (Sardi 2006) and mammary differentiation, in conjunction with Signal Transducer and Activator of Transcription 5 (STAT5) (Jones 2008). An almost identical mechanism to generate intracellular soluble fragments has been reported for ephrin receptor (Litterst 2007), Colony Stimulating Factor 1 (CSF-1) receptor (Glenn and van der Geer 2007), Vascular Endothelial Growth Factor (VEGF) receptor (Cai 2006), Tyrosine kinase with immunoglobulin-like and EGF-like domains 1 (Tie 1) (Marron 2007), Insulin-like Growth Factor 1 (IGF-1), and insulin receptors (Kasuga 2007). In all of these cases, nuclear

trafficking is the same as any other soluble protein and is regulated as such at the nuclear pore.

2.10 Nuclear entry of full-length membrane-embedded proteins

While more and more examples of full length plasma-membrane derived transmembrane proteins are being discovered in the nucleus, the most characterized and understood is the EGFR or ErbB-1.

EGFR has been observed in the nucleus of many cell types and tissues including mouse uterus, developing mouse embryos, rat liver, placentas, thyroids, and immortalized epithelia cells of ovary and kidney origin (Cao 1995, Lin 2001, Marti 2001). The correlation between nuclear EGFR and cancer prognosis is particularly alarming and has been observed in multiple solid tumour types (Wang and Hung 2012). In bladder and cervical cancer, nuclear expression was significantly correlated with increased tumour grade, mitotic frequency, and cellular proliferation (Lipponen and Eskelinen 1994), with 31% (Lipponen and Eskelinen 1994) to 37% (Tervahauta 1994) of tumour samples examined having EGFR present in the nucleus. In breast cancer, 38% of patients showed nuclear EGFR staining and patients with higher levels of nuclear expression demonstrated poor overall survival. The results statistically correlated with tumour size, lymph node involvement, and Nottingham prognostic index (prognostic evaluation after surgery). The patients also had a 3.4 fold higher mortality risk than patients with no detectable nuclear staining (Lo 2005). In ovarian cancers, nuclear receptors were detected in 28% of patient samples and significantly correlated with poorer overall survival (Xia 2009). Poor overall survival was also reported to correlate with nuclear EGFR expression in squamous carcinoma (Lo 2005), gallbladder carcinoma (Li 2011), and oropharyngeal carcinomas (Psyrrri 2005) where 49% of patients expressed nuclear receptors. Interestingly, 88% of patients that reported poor or no response to first line chemotherapy regimens also expressed high levels of nuclear EGFR (Psyrrri 2005). At present our understanding of how EGFR in the nucleus impacts cancer progression and drug resistance is in its infancy but based on the number of different cancers and relationship to poor prognosis, determining its affects promises tremendous therapeutic benefits.

2.10.1 Endocytosis

This first step for any intracellular trafficking is endocytosis (bringing in) the receptor from the cell surface. While EGFR has been linked with both clathrin-dependent and clathrin-independent endocytosis (Orth 2006; Mayer and Pagano 2007), the major pathway of endocytosis (at least for receptor downregulation after ligand stimulation) is through a clathrin-dependent mechanism (Sorkin 2004). In this process, the membrane invaginates around the receptor due to a cytoplasmic surface coating of the protein, clathrin. The interlocking of the triskelion structure of clathrin deepens the curvature of the pit. Eventually this pit encases the membrane bound receptor and is completely “coated” (thus the term “clathrin coated pit”) in clathrin while a thin “neck” maintains connectivity with the rest of the plasma membrane (see Fig 2.13). The final scission of this “neck” is performed by the dynamin proteins, utilizing GTP hydrolysis to pinch the clathrin vesicle from the plasma membrane freeing the vesicle to move into the cytoplasm (McNiven 1998). This movement is not passive diffusion but is, in fact, highly regulated by the intracellular domain of EGFR and accessory proteins in the clathrin framework. The immediate fate of EGFR-containing clathrin-coated vesicles is to uncoat (disassembly of the clathrin matrix) and fuse with larger endosomes. From here the receptors can be directed to rapid or slower recycling endosomes, shuttled towards the Golgi, or late endosomes *en route* to the lysosome for degradation (See Fig 2.13).

The master proteins that determine vesicular fate are the Rab proteins, a family of small GTPase relatives of Ras (Maxfield and McGraw 2004). The routing of the uncoated clathrin vesicle to the early endosome is mediated by Rab5 and Rab4. These Rab proteins direct vesicles containing cargo to be sorted for rapid recycling or further processing, while Rab9 directs cargos that returns to the surface somewhat slower (Ceresa 2006). Vesicles leaving the early endosome to the late endosome (usually a checkpoint prior to degradation) are directed by Rab7. Experiments impacting clathrin-mediated endocytosis (by gene silencing of clathrin or mutant dynamin that cannot facilitate vesicle scission) suggest the pool of EGFR that translocates to the nucleus is dependent on clathrin-mediated endocytosis (Giri 2005, Bryant and Stow 2005) with inferred evidence indicating this trafficking occurs after entry into the early endosome (Giri 2005).

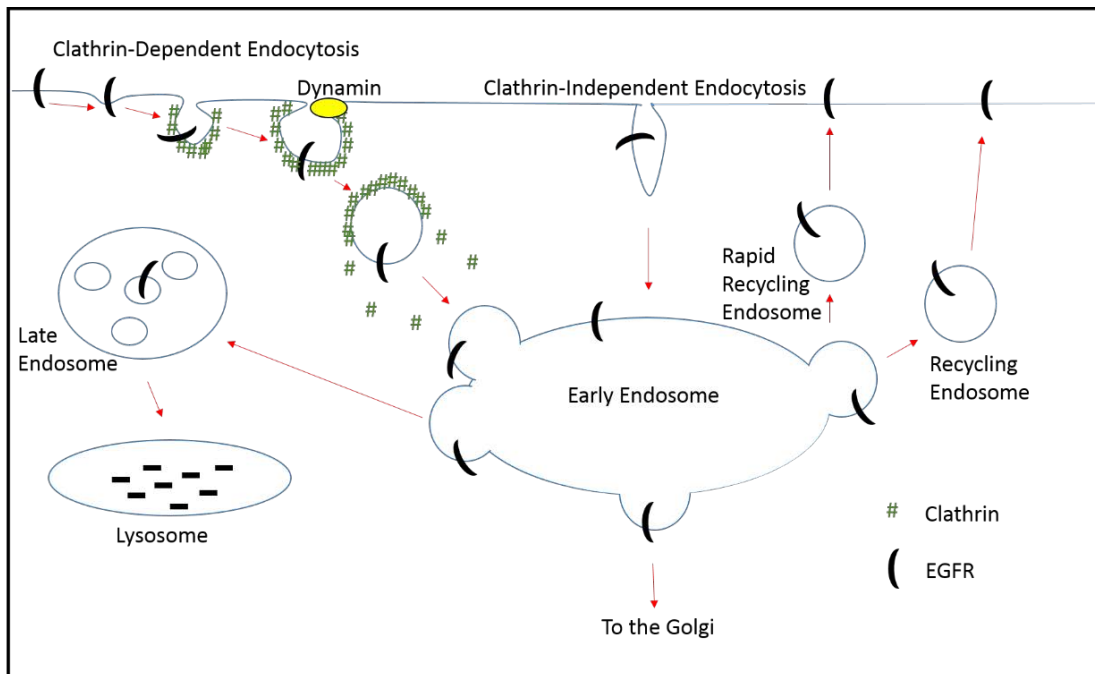


Figure 2.13 Endocytosis and vesicular fates of EGFR. As the membrane around EGFR begins to curve and surround the receptor, clathrin forms a structural coat that encapsulates the receptor and membrane around it. The pinchase dynamin then severs the plasma membrane from that within the vesicle, allowing the vesicle to endocytose, uncoat, and fuse with the early endosome. From the early endosome the receptors can be directed to recycling endosomes, the Golgi, or the late endosome prior to degradation in the lysosome.

Although Rabs direct vesicles, it is the EGFR that determines which compartment it is shunted into with post-translational modifications phosphorylation and ubiquitination being the major determinants. While a number of groups have shown the nuclear EGFR is phosphorylated (Cao 1995, Cordero 2002, Ditmann 2005), the necessity of these phospho-residues in labelling the receptor for nuclear transport has not yet determined. Ubiquitinated EGFR receptors are sorted into intraluminal vesicles within multivesicular bodies of the late endosome (Sorkin and Goh 2009) destined to fuse with lysosomes. This pathway is regulated by the Endosomal Sorting Complex Required for Transport (ESCRT) machinery comprised of 4 multicomponent complexes named ESCRT-0, ESCRT-I, ESCRT-II, and ESCRT-III (Gruenberg and Stenmark 2004). As well as being essential in degradation of EGFR, they have also been shown to be important in EGFR recycling (Baldys and Raymond 2009), yet the role of ubiquitination in nuclear delivery has not been determined.

2.10.2 Receptor entry into and exit from the Golgi

The first clear insights into the nuclear delivery pathway of EGFR came from the observation that, upon EGF stimulation, full-length EGFR was anchored to the membranes of both the Golgi and the endoplasmic reticulum (ER) (Wang 2010) with the carboxy terminus exposed and the amino terminus inserted into the lumen of these organelles, an inverted position relative to that on the plasma membrane and *de novo* synthesis. As proteins are synthesized and delivered to the various cellular destinations they travel from the ER to the Golgi and link into the exocytic or secretory pathways (termed anterograde transport) (Bonafacino and Rojas 2006). However our understanding of so-called retrograde transport of proteins from the endocytic vesicular network back to the Golgi has been limited to a small number of proteins including acid-hydrolase receptors (Mannose-6-phosphate in mammals), a few transmembrane enzymes (such as furin), and certain Soluble NSF Attachment Protein Receptors (SNAREs) (Bonafacino and Rojas 2006). This retrograde trafficking is also hijacked by a number of protein toxins such as Shiga toxin, cholera toxin, and ricin (Bonafacino and Rojas 2006) for delivery of their destructive cargo. The discovery of EGFR delivery from the Golgi to the ER was heralded as the first example of retrograde transport of a plasma membrane protein to the nucleus (Wang and Hung 2012).

While little has been done examining the exact machinery responsible for retrograde trafficking of EGFR from the endocytic network to the Golgi, the same is not true for other cargoes, as retrograde transport has become acknowledged as crucial for lysosomal biogenesis, ion and glucose transport, processing and secretion of polypeptide precursors, and secretion of signalling proteins that regulate development (Chia and Gleeson 2011). Through yeast genetics and mutagenesis studies examining retrograde sorting of acid-hydrolases, the key components of the retromer were first discovered (Restrepo 2007) and it seems these retromer subunits are conserved in all eukaryotes (Bonafacino and Rojas 2006). This multi-subunit complex consists of a number of membrane curvature sensing sorting nexins (SNXs) present in various combinations, depending on the cargo (Burd and Cullen 2014), as well as a cargo-sensing component, comprised of 3 proteins; Vascular sorting protein 26 (Vps26), Vps29, and Vps35. A working model of retromer structure and cargo association is presented in Figure 2.14.

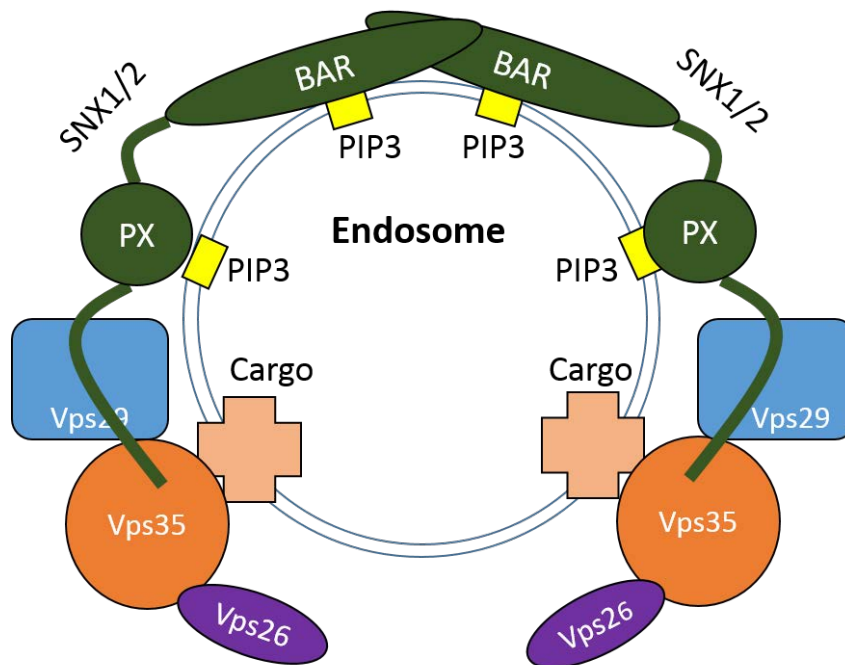


Figure 2.14 Model of retromer structure and cargo recognition. The Vps35 subunit recognizes the cargo while Vps26 and Vps29 comprise the rest of the structural component. The Sorting Nexins (SNXs) recognize phosphoinositides in the endosome membrane and the specific vesicle curvature to target the retromer complex to the appropriate location.

Other proteins that have been implicated in retrograde trafficking from endosomes to the Golgi are Rab9 and its effector tail-interacting protein of 47kDa (TIP47). Rab9 has been associated with vesicles that bud from late endosomes and fuse with the Trans-Golgi Network (TGN). These two proteins (Rab9 and TIP47) have only been shown to be involved in retrograde trafficking of the Mannose-6-phosphate (Lombardi 1993) although are likely involved in trafficking other cargoes as well.

Retromer complexes have been shown to play a role in the generation of tubular extensions from the early endosome towards the Golgi (Harbour 2010) with Rab9 as the driver of these extensions (Lombardi 1993). In order to fuse with the Golgi, the vesicular extensions first need to tether and dock at the TGN (Chia and Gleeson 2011). In contrast to other cisternae of the Golgi stack, the TGN is an extensive membrane network (Ladinski 1999) composed of dynamic tubular extensions, likely organized into distinct membrane subdomains for the various anterograde and retrograde pathways. This organizational subdomain thus protects the anterograde

pathways from inadvertent mixing of newly arrived retrograde cargo. It is suggested that retrograde “hotspots” would establish and maintain TGN domains that contain appropriate SNAREs and tethers to recognize incoming vesicular cargo (Chia and Gleeson 2011). There have been a number of tethers and Golgins identified that are restricted to processing retrograde cargo (Chia and Gleeson 2011). It seems implausible that EGFR and any other nuclear bound membrane-embedded protein would target to the Golgi without utilizing these tethering factors.

In anterograde delivery of newly synthesized cargo, the Golgi serves in glycan processing with virtually all glycoproteins being subject to glycan tree trimming and/or extension as they exit the Golgi (Moremen 2012). Whether glycosylation state or glycan modification has any role in nuclear translocation of EGFR (or any other nuclear-bound receptor) has not been examined.

The cell is thought to recycle most components of the anterograde pathway to conserve energy (Lanoix 2001). This is achieved by two distinct retrograde trafficking mechanisms that shunt cargo back from the Golgi to the ER. The two mechanisms are known as coatamer protein 1 (COPI)-independent and a COPI-dependent pathways (Lanoix 2001). While COPI-independent retrograde trafficking is poorly defined, our understanding of the COPI-dependent pathway is extensive. COPI vesicles form at the cis-end of the Golgi. This process is initiated by the membrane binding of the small GTPase ADP Ribosylation Factor 1 (ARF1). At this point, activated ARF1 recruits a preassembled coatamer complex composed of 7 subunits (COP α , β , β' , λ , δ , ϵ and ξ) and cargo proteins are recognized and assembled into the vesicle based on recognition of specific consensus sequences (Ostermann 1993). Although there are other motifs, the major COPI loading motif consists of K(X)KXX (Sohn 1996, Jackson 1990). The vesicle disassembles when the ARF hydrolyses the GTP (Goldberg 1999), after ER docking.

In studies using the chemical inhibitor of COPI vesicle formation (Brefeldin A) or dominant-negative forms of ARF1, retrograde trafficking of EGFR to the nucleus and ER was prevented (Wang 2010), strongly suggesting EGFR utilizes COPI vesicles to shunt from the Golgi to the ER. Furthermore, co-immunoprecipitation experiments

yielded an association between EGFR and γ -COP that occurred only after EGF stimulation, strengthening support the EGFR transits between the Golgi and ER is via COPI vesicles (Wang 2010).

2.10.3 Endoplasmic reticulum and retrotranslocon

As with the Golgi, EGFR is detected in the ER membrane after ligand addition in the N-terminal luminal and the C-terminal cytosolic orientation (Wang 2010). Elegant studies utilizing endoglycosidase H and glycosidase indicate the surface-derived receptor is indeed a full-length and mature receptor, possessing seven complex and 3 high mannose glycan chains (Liao and Carpenter 2007). With over a third of newly synthesized proteins translocating into the ER for delivery to other cellular compartments (Ghaemmaghami 2003), the main role of the ER is to ensure the correct folding before passage to the Golgi (Nakatsukasa and Brodsky 2008). However, many of these proteins never fold correctly and are subject to ER qulity control (ERQC) in which polypeptides are on a folding “timer”. Those that fail to fold in ER within a timely manner are expelled, labelled for degradation, and destroyed (Nakatsukasa and Brodsky 2008). Therefore, at any given time, a large number of proteins are undergoing retrograde transport with the specific purpose of degradation, and thus we require a clearer understanding of the ER itself and retrograde trafficking of the ER-associated degradation (ERAD) pathway.

The influx of proteins into the ER is prodigious and is the first line of defence against mutant or improperly translated proteins. As such, the system is prone to the potentially catastrophic consequences associated with misfolded protein accumulation (Nakatsukasa and Brodsky 2008). The primary disposal mechanism is the above mentioned ERAD pathway, during which misfolded proteins are transported to the 26S proteasome in the cytoplasm via retrograde trafficking. In most cases this delivery is facilitated by ubiquitination and ATP hydrolysis (Jarosch 2002).

In normal conditions within the ER, proteins must remain bound to chaperones, such as the ER luminal specific Heat Shock Protein 70 (HSP70) family member Binding immunoglobulin Protein (BiP), to prevent aggregation. Either during, or immediately

after, polypeptide insertion into the ER, the N-linked oligosaccharide (NAc-Gln₂-Man₉-Glc₃) is bound to a core glycosylation consensus sequence found on almost all proteins. Shortly thereafter, two of the three glucose residues in the N-glycan are trimmed sequentially by glucosidase I and glucosidase II. This crucial step allows the polypeptide to be recognized by calnexin (and later calreticulin) to catalyze protein folding (Yoshida and Tanaka 2010). But this is not the end of a role for glycan groups as two opposing enzymes regulate repeated cycles of deglycosylation-reglycosylation until the glycoprotein reaches the native structure. Glucosyltransferase II removes glycan groups while glucosyl-transferase adds them.

Misfolded proteins cannot bind calnexin and while they may be given subsequent chances to fold by addition of glycan groups by glucosyl-transferase, if they continue to fail to fold, the final glycan group will be removed by α -mannosidase (MNS1) irreversibly, labelling the protein for destruction. The rapid kinetics of calnexin and glucosyl-transferase quickly removes a correctly folding protein away from the degradative pathway. However, the slow acting MNS1 serves as a timer to sense peptide chains that have existed in the monoglucosylated form for too long (Yoshida and Tanaka 2010, Nakatsukasa and Brodsky 2008), marking the failed peptide ready for degradation.

The doomed peptide is bound by ER degradation-enhancing α -mannosidase (EDE1) and is now targeted for exit from the ER. Virtually all ERAD substrates are ubiquitinated prior to degradation, which poses a problem as E1, E2 and E3 ubiquitin ligases are localized in the cytoplasm (Biederer 1997) and the ER is a membrane-encased structure. Entry of nascent polypeptide chains is through a pore-like complex known as the Secretory Protein 61 (Sec61) translocon complex (Schnell and Hebert 2003) but determining the site of retrograde exit remains unsettled (Yoshida and Tanaka 2010).

The Sec61 translocon forms a hydrophilic channel through the ER membrane (Meyer 2000) and is composed of a large subunit (Sec61 α) with 10 transmembrane spans, and two smaller subunits (Sec61 β and Sec61 γ). The pore may exist as a single set of these factors or multiples of each, depending on the size the cargo being transported

(Mandon 2009). During protein synthesis, ribosomes have been reported to bind to the pore and the newly forming polypeptides to be directly imported into the ER through the pore (Rapoport 2008).

Although some defined integral membrane proteins in the ER have been shown to interact with ERAD substrates *en route* to degradation, the identity of the retrotranslocon remains contentious (Nakatsukasa and Brodsky 2008). However increasing evidence suggests the retrotranslocon may simply be a Sec61 complex accommodating retrograde transport (Rapoport 2007). While this sets up the intriguing possibility that the same pore may serve both forward and reverse transport, experimental evidence suggests this is not the case, with each pore being “assigned” a single role (either forward OR reverse) in both time and space (Mandon 2009). Supporting that hypothesis, a number of ubiquitin ligases and the ATPase Cdc48/p97 (which produces the energy to extract peptides from the Sec61 pore) have been found to physically interact with Sec61 at the cytoplasmic side of the ER (Jarosch 2002, Hiller 1996). Even the proteasome itself has been shown to physically interact with the Sec61 pore (Ng 2007).

Through co-immunoprecipitation and gene silencing experiments it was reported EGFR nuclear entry required a physical interaction between Sec61 and surface-derived EGFR (Liao and Carpenter 2007). The requirement of Sec61 was independently confirmed (Wang 2012) strongly suggesting that if Sec61 is not the retrotranslocon for all ERAD and retrograde cargos, it at least functions that way for EGFR *en route* to the nucleus. How EGFR avoids being ubiquitinated and inserted directly into the proteasome upon exit from the retrotranslocon pore remains unanswered.

2.10.4 Receptor intracellular chaperones

While exit from the ER via the Sec61 retrotranslocon is generally agreed upon, two distinct models have been proposed for what happens next (Liao and Carpenter 2007, Wang 2012) and are summarized in Figure 2.15. The first model proposed (Liao and Carpenter 2007) suggests receptors exit the retrotranslocon and enter the cytosol,

although experimentally EGFR could not be detected there. The chaperone HSP70 was determined to be required for nuclear transport and was suspected to be involved in masking the hydrophobic transmembrane domain to allow solubilization of the receptor. The karyopherin Importin- β , is required for nuclear entry of a soluble EGFR. Once in the nucleus EGFR bound Cyclin D and other cell cycle promoters (Liao and Carpenter 2007). In a second model, the receptors never fully exit the ER into the cytoplasm but rather slide along the contiguous membrane of the rough ER to where it joins the outer nuclear membrane, eventually encountering a nuclear pore (Wang 2012). Both models found HSP70 and Importin- β crucial to nuclear entry but while the first model, by Graham Carpenter and colleagues, suggest the Sec61 retrotranslocon exits into the cytosol, the second model, by Mien-Chi Hung's team, provide data indicating the Sec61 retrotranslocon is embedded in the Inner Nuclear Membrane (INM) and therefore receptors have no transient cytoplasmic localization (Wang 2012). As EGFR has been determined to be soluble in the nucleus, an unknown mechanism to extract and solubilize EGFR from the INM must be operative if the latter model is indeed valid.

Interestingly, ATP addition inhibited the ability of EGFR to translocate to the nucleus (Liao and Carpenter 2007), which contrasts with many other retrotranslocation events (Tsai and Rapoport 2002). The chaperoning function of HSP70 requires ATP hydrolysis, so the observation ATP inhibits the process of EGFR nuclear trafficking implies HSP70 is only required in its capacity to bind hydrophobic substrate regions, most likely the transmembrane domain (Liao and Carpenter 2007). Keeping in mind the karyopherins and nucleoporins of the central channel of the nuclear pore are all soluble, perhaps the masking of the hydrophobic region of EGFR by HSP70 simply keeps EGFR from precipitating allowing passage through the nuclear pore.

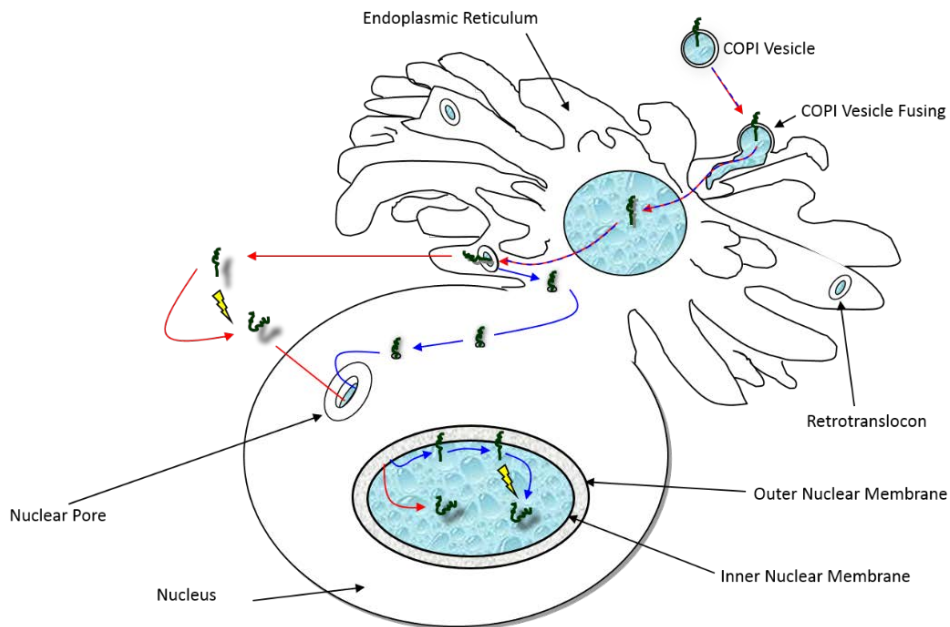


Figure 2.15 Proposed model of EGFR transit from the ER into the nucleus. In both models, EGFR enters the ER via COPI vesicles and travels along the ER membrane until it reaches the Sec61 translocon. In one model EGFR completely exits the ER into the cytosol where it undergoes a conformational change to mask the hydrophobic domain before entering the nucleus as a soluble protein through the nuclear pore. In an alternate model, EGFR does not completely exit the ER membrane but rather slides along the membrane (NB, the rough ER membrane is contiguous with the outer nuclear membrane) until a nuclear pore is encountered. In this case EGFR enters the nucleus as a transmembrane protein and, upon entry, is contained within the Inner Nuclear Membrane. Solubilization occurs via an unknown nuclear event.

Regardless of which model regulates EGFR nuclear trafficking, the main mystery is whether any of these factors are involved in TGF β receptor nuclear trafficking, as a number of striking differences between the two receptors are evident. Firstly, the kinetics of nuclear trafficking is dramatically different between the two types of receptors. EGFR nuclear entry occurs within minutes (Wang 2010) while TGF β receptors accumulate in the nucleus after a number of hours (Mu 2011). Secondly, EGFR is a tyrosine kinase and is phosphorylated on tyrosine residues upon ligand stimulation (Carpenter and Liao 2009) whereas TGF β receptors are serine/threonine kinases and are phosphorylated on serine residues (Shi and Massagué 2003). EGF receptors are homodimers (Carpenter and Liao 2009) but TGF β receptors are a complex of heteromers (Anders 1997) that may or may not stay together for nuclear trafficking. Still, the trafficking of a number of other kinase receptors have been shown to follow a similar pathway to the nucleus as EGFR (Carpenter and Liao 2009), making this pathway an ideal starting place to examine TGF β receptor nuclear translocation.

Indeed the nuclear translocation of TGF β receptors may be closely linked to mechanisms regulating nuclear transport of the Smads and work together to integrate TGF β signalling into the nucleus. It is therefore prudent to examine trafficking of both sets of signalling molecules to obtain a comprehensive picture of TGF β signalling.

In this study we have focused on the nuclear import mechanisms of Smads and TGF β receptors but it is also important to recognize, Smad-independent factors contribute to the overall TGF β signal and should not be ignored.

CHAPTER 3

GENERAL MATERIALS AND METHODS

CHAPTER 3: GENERAL MATERIALS AND METHODS

The methods presented in this Chapter include:

- (1) Generation of plasmid and virus vectors for bacterial transformation, cell transfection and infection studies; generation of purified proteins and oligopeptides;
- (2) Generation of cell lines transiently or stably expressing delivery vectors;
- (3) Stimulation of diverse cell types with TGF β for various times and under different experimental conditions;
- (4) Determination of the impact of the experimental conditions on the expression, activity, sub-cellular localization and molecular associations of various proteins and genes within the cell.

Methods associated with (1) and (2) above can be considered generating reagents for input into experiments and are summarised diagrammatically in Figure 3.1. The assays associated with analysing the effects of the experimental conditions on proteins and genes of interest can be considered the output of experiments (Fig 3.1).

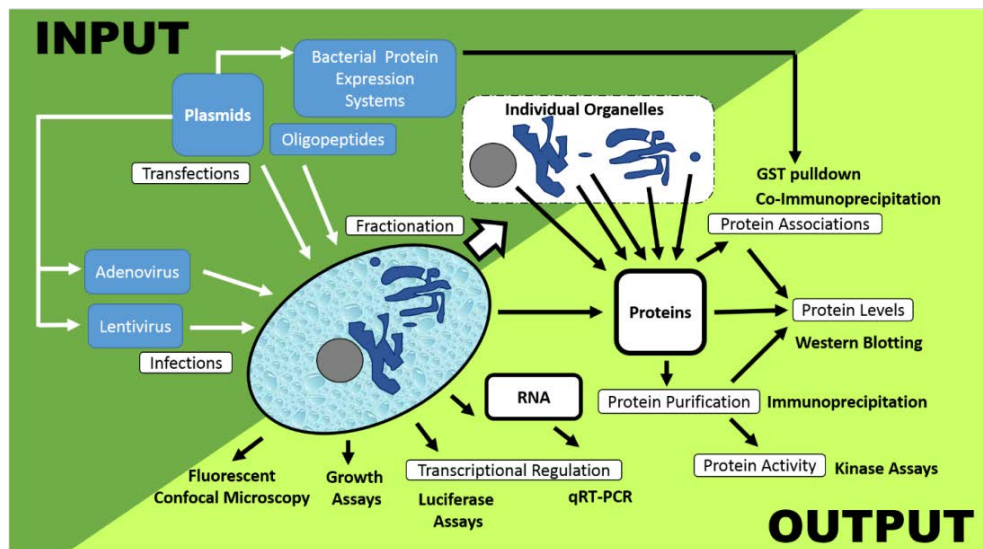


Figure 3.1 Overview of experimental design and generation of reagents and analysis. Assays designed to generate reagents and cell lines to be utilized to experimentally test our outlined objectives are designated as INPUT. Assays designed to analyse and interpret the results of the experimental manipulations are designated OUTPUT. The oval at the centre of the image represents a cell with nuclei and other organelles contained within it. Arrows indicate experimental workflow.

3.1 Generation of plasmids and purified proteins

Plasmid vectors utilised throughout this thesis were either constructed as part of this study or generously provided by collaborators. A complete list of the plasmids utilized in this study can be found in Table 3.1. Plasmid vectors contained either wildtype or mutant genes, or siRNA/shRNA for target genes. Delivery of constructs into various mammalian cell lines was achieved using viral infection (Adenovirus and Lentivirus) or non-viral plasmid transfection methods. Bacterial expression systems were used to express and purify fusion proteins.

Table 3.1 Plasmids utilised in this study

	Construct	Description	Vector backbone	Source
Adenoviral Expression	Ad.eGFP-PAK2 WT	Wild type PAK2 with N-tagged eGFP	pAdCMV	Provided by Rolf Jakobi (University of Wisconsin - Milwaukee)(
	Ad.eGFP-PAK2 K278R	PAK2 with K278R mutation with N-tagged eGFP (Dominant Negative)	pAdCMV	Provided by Rolf Jakobi University of Wisconsin - Milwaukee)(
	Ad.GFP	Green Fluorescent Protein	pAdCMV	Provided by Riken Genbank
Lentiviral Expression	Short hairpin SNX9-77	shRNA against SNX9	pLKO.1 puro	Generated by Claire Repellin (Mayo Clinic) (See Appendix I for sequence)
	Short hairpin SNX9-78	shRNA against SNX9	pLKO.1 puro	Generated by Claire Repellin (Mayo Clinic) (See Appendix I for sequence)
	Short hairpin Sec61	shRNA against Sec61	pLKO.1 puro	Generated by Xueqien Yi (Mayo Clinic) (See Appendix I for sequence)
	Short hairpin Importin β	shRNA against Importin β	pLKO.1 puro	Generated by Xueqien Yi (Mayo Clinic) (See Appendix I for sequence)

	Short hairpin Importin8	shRNA against Importin8	pLKO.1 puro	This study (See Appendix I for sequence)
siRNA	Small interfering RNA COP α	siRNA oligomer against cop α		Purchased from Invitrogen (See Appendix I for sequence)
Receptors Constructs	TGF β R1-FLAG	TGF β R1 with C-terminus-tagged FLAG epitope	pCMV5	Generated by Diying Yao (Mayo Clinic)
	Myc-TGF β R1	TGF β R1 with N-terminus Myc tag	pBabe puro	Generated by Xueqien Yi (Mayo Clinic)
	Myc-TGF β R1-DiK1	TGF β R1 with K342A,K343A mutations and N-terminus Myc tag	pBabe puro	This study; Site Directed mutagenesis (see Appendix II for primer sequences)
Mammalian Expression	Myc-TGF β R1-DiK2	TGF β R1 with K489A,K490A mutations and N-terminus Myc tag	pBabe puro	This study; Site Directed mutagenesis (see Appendix II for primer sequences)
	Myc-TGF β R1-2xDiK	TGF β R1 with K342A,K343A and K489A,K490A mutations and N-terminus Myc tag	pBabe puro	This study; Site Directed mutagenesis (see Appendix II for primer sequences)
	GM-CSFR α /TGF β R1	Extracellular domain of GM-CSFR α fused with transmembrane and intracellular domain of TGF β R1	pNa	Generated by Bob Anders (Mayo Clinic)
Receptors Constructs	GM-CSFR α /TGF β R1-K232R	Extracellular domain of GM-CSFR α fused with transmembrane and intracellular domain of TGF β R1 bearing K232R (kinase deficient)	pNa	Generated by Bob Anders (Mayo Clinic)
	TGF β R2-FLAG	TGF β R2 with C-tagged FLAG	pCMV5	Generated by Nandor Gareszegi (Mayo Clinic)
	HA-TGF β R2	TGF β R2 with HA tag just in from N-terminal	pcDNA3.1 hygro	Generated by Xueqien Yi (Mayo Clinic)
Mammalian Expression	HA-TGF β R2-K488Q	TGF β R2 with HA tag just in from N-terminal bearing K488Q mutation	pcDNA3.1 hygro	This study; Site Directed mutagenesis (see Appendix II for primer sequences)
	HA-TGF β R2-	TGF β R2 with HA tag just in	pcDNA3.1	Provided by Dave

Receptors Constructs Mammalian Expression	DUB	from N-terminal fused to deubiquitination domain	hygro	Katzmann (Mayo Clinic)
	GM-CSFCR β /TGF β R 2	Extracellular domain of GM-CSFR β fused with transmembrane and intracellular domain of TGF β R2	pHa	Generated by Bob Anders (Johns Hopkins University)
	GM-CSFCR β /TGF β R 2-K277R	Extracellular domain of GM-CSFR β fused with transmembrane and intracellular domain of TGF β R2 bearing K277R (kinase deficient)	pHa	Generated by Bob Anders (Mayo Clinic)
	GM-CSFCR β /TGF β R 2- Δ 474	Extracellular domain of GM-CSFR β fused with transmembrane and intracellular domain of TGF β R2 with 3X stop codons after 474	pHa	Generated by Youli Wang (Mayo Clinic)
	GM-CSFCR β /TGF β R 2- Δ 484	Extracellular domain of GM-CSFR β fused with transmembrane and intracellular domain of TGF β R2 with 3X stop codons after 484	pHa	Generated by Youli Wang (Mayo Clinic)
	GM-CSFCR β /TGF β R 2- Δ 498	Extracellular domain of GM-CSFR β fused with transmembrane and intracellular domain of TGF β R2 with 3X stop codons after 498	pHa	Generated by Youli Wang (Mayo Clinic)
	GM-CSFCR β /TGF β R 2- Δ 517	Extracellular domain of GM-CSFR β fused with transmembrane and intracellular domain of TGF β R2 with 3X stop codons after 517	pHa	Generated by Youli Wang (Mayo Clinic)
	GM-CSFCR β /TGF β R 2- Δ 485-498	Extracellular domain of GM-CSFR β fused with transmembrane and intracellular domain of TGF β R2 with residues 485-498 deleted	pHa	Generated by Youli Wang (Mayo Clinic)
	Smad Constructs Mammalian Expression	Smad2-myc WT	Smad2 fused to C-tagged Myc	pcDNA3.1 hygro
Smad2-GFP WT		Smad2 fused to C-tagged GFP	pcDNA3.1 hygro	This study; excised myc from pcDNA3.1Smad2-myc using BamH1 and Sal1 then sub-cloned in GFP from pAdCMV-eGFP

	Smad2-myc-C sites	Smad2 fused to C-tagged Myc baring S465A,S467A	pcDNA3.1 hygro	This study; Site Directed mutagenesis (see Appendix II for primer sequences)
	Smad2-myc T430A	Smad2 fused to C-tagged Myc baring T430A	pcDNA3.1 hygro	This study; Site Directed mutagenesis (see Appendix II for primer sequences)
Smad Constructs Bacterial Expression	Smad3-HA-TAT	Smad3 tagged with HA and TAT sequence	pHA-TAT	Generated by Jeung-Han Kang (Mayo Clinic)
	Smad3-GST	Smad3 fused to C-tagged GST	pGEX-4T-2	Provided by Ralf Janknecht (Mayo Clinic)
	Smad2-GST	Smad2 fused to C-tagged GST	pGEX-4T-2	Provided by Ralf Janknecht (Mayo Clinic)
SNX9 Constructs Mammalian Expression	Myc-SNX9-WT	SNX9 fused to N-tagged Myc (Wild Type)	pBabe puro	Provided by Sven Carlsson (Umeå University)
	Myc-SNX9-SH3LC	Amino half of SNX9 fused to N-tagged Myc (Dom Neg)	pBabe puro	Provided by Sven Carlsson (Umeå University)
	Myc-SNX9-PXBAR	Carboxy half of SNX9 fused to N-tagged Myc (Dom Neg)	pBabe puro	Provided by Sven Carlsson (Umeå University)
	Myc-SNX9-WT escape	SNX9 fused to N-tagged Myc with C1374T, G1383, A1389G conserved mutations in DNA (avoid shRNA-77)	pBabe puro	This study; Site Directed mutagenesis (see Appendix II for primer sequences)
	Myc-SNX9-PIP Mut escape	Myc-SNX9escape baring R286K,Y287A, K288R,R426E,K433E,K437 E mutations	pBabe puro	This study; Site Directed mutagenesis (see Appendix II for primer sequences)
	Myc-SNX9Δ13 escape	Myc-SNX9escape with 3x stop codons introduced 13 residues from C terminus	pBabe puro	This study; Site Directed mutagenesis (see Appendix II for primer sequences)
	SNX9-YFP	SNX9 fused with C-terminus tagged YFP	pBabe puro	This study; Excised myc from pBabe-myc-SNX9 using HindIII and BamH1 and subcloned in YFP from pYFP
	SNX9-PXBAR-	Carboxy half of SNX9 fused	pGEX-4T-2	This study; SNX9-PXBAR subcloned

SNX9 Constructs Bacterial Expression	GST	to C-terminus tagged GST		into pGEX-4T-2 using Sal1 and Not1
	SNX9-SH3LC-GST	Amino half of SNX9 fused to C-tagged GST	pGEX-4T-2	This study; SNX9-SH3LC subcloned into pGEX-4T-2 using Sal1 and Not1
	SNX9-GST	SNX9 fused to C-tagged GST	pGEX-4T-2	Generated by Claire Repellin (Mayo Clinic)
Misc. Mammalian Expression	Nup153-HA	Nucleoporin153 with C-terminus tagged HA*	pCMV5	Provided by Katie Ullman (University of Utah)
	Nup213-HA	Nucleoporin213 with C-terminus tagged HA*	pCMV5	Provided by André Hoelz (California Institute of Technology)
	3TP luciferase	3TP (PAI1) Promoter driving luciferase	pCMV5	Provided by Hal Moses (Vanderbilt University)
	SBE luciferase	6 x SBE driving luciferase	pCMV5	Provided by Jeff Wrana (University of Toronto)
	βGal	CMV-driven β-Galactosidase	pCMV5	Provided by Hal Moses (Vanderbilt University)
	pBabe puro	Puromycin expression cassette	pBabe puro	Purchased from Sigma
	YFP	Yellow Fluorescent Protein	pcDNA3.1 neo	Purchased from Invitrogen
Misc. Bacterial Expression	pGEX-4T-2	Protein expression Vector	pGEX-4T-2	Purchased from Amersham

* HA: Human influenza hemagglutinin

3.1.1 Plasmid construction and preparation

Plasmid were prepared using QIAGEN® mini, midi and maxi Prep kits (QIAGEN, Venlo, The Netherlands) as per the manufacturer's instructions, the choice of kit was based upon the scale of the DNA stocks desired. When large amounts or high purity of plasmid were required, the caesium chloride-based method was employed using standard techniques (Cold Spring Harbor Protocols). After determining absorbance at 260 and 280nm, DNA purity and concentration was calculated and sequences validated by Sanger sequencing (Mayo Clinic).

3.1.2 Gene Cloning

When plasmids containing the desired gene sequences could not be obtained, standard molecular biology techniques were used to clone or subclone sequences into the plasmids of interest (see Table 3.1). When possible, subcloning by restriction digest taking advantage of existing restriction sites was employed. However most often, useful restriction sites needed to be engineered (by PCR) to insert the sequence in the correct orientation.

3.1.2.1 Polymerase Chain Reaction (PCR) cloning

Primers were designed incorporating desired restriction sites flanking the gene sequence of interest and amplified from the template plasmid by PCR using standard methods. Following digestion of both the insert and plasmid to receive the insert and calf alkaline phosphatase (CIP) treatment, the insert was ligated into the vector.

3.1.2.2 Gel electrophoresis and plasmid purification

Linearized DNA was run on agarose gels containing ethidium bromide using standard electrophoresis and visualized with ultraviolet light. With the agarose gel illuminated with ultraviolet light, the band/s of interest were excised with a scalpel and placed in a microfuge tube and purified using a Geneclean® II kit (MP biomedical, Santa Ana, California) as per manufacturer instructions.

3.1.2.3 Ligation

Ligations were catalysed by the T4 DNA ligase (New England Biolabs, Ipswich, Massachusetts) using standard procedures. The reaction was allowed to proceed overnight at 16°C with a ratio of 1:3 of vector to insert. Prior to ligation, plasmid digest products were treated with CIP (New England Biolabs, Ipswich, Massachusetts) to dephosphorylate 5' and 3' ends of the DNA.

3.1.2.4 Transformation of *E.coli*

Competent Max-Efficiency® DH5α™ (Life Technologies, Grand Island, New York) or TOP10 (Invitrogen, Carlsbad, California) cells were mixed with 1 to 5 µl of DNA (10 pg

- 100 ng) and treated as per manufacturer instructions. Transformed cells were plated on LB-agar plates with the appropriate antibiotic for overnight incubation.

3.1.2.5 Construct validation

Standard molecular biology techniques were used to screen and confirm plasmid cloning. A minimum of ten colonies were cultured and plasmids purified by QIAGEN® mini Prep kits (QIAGEN, Venlo, The Netherlands) as recommended, followed by restriction enzyme digest and DNA sequencing.

3.1.3 Site direct mutagenesis

The introduction of SNX9, Smad2 and TGFβ receptor proteins carrying various mutations was necessary to elucidate mechanisms regulating TGFβ signalling. Conserved mutations in the DNA codons (without impacting the amino acid sequence), single point mutations whereby the DNA sequence was modified to reflect a change in the amino acid sequence or stop codons, or changes resulting in multiple amino acid changes were all generated using the same method. Point mutations were introduced across an approximately 15-25 nucleotide sequence and then validated by DNA sequencing. In the event further mutations were required, the process would be repeated sequentially until each of the desired mutations was introduced.

Point mutagenesis was performed using Quikchange® II XL (Agilent Technologies, Santa Clara, California) site-directed mutagenesis kits following manufacturer recommendations. Mutagenesis reaction and cycling parameters were followed as suggested in a thermocycler with hot top assembly. Primers used for mutagenesis are listed in Appendix II. To ensure the methylated, non-mutated parental DNA was not present, *Dpn1* (New England Biolabs, Ipswich, Massachusetts) was added to the mix and incubated at 37°C for 1 hour before transformation into the supplied XL1-Blue competent cells (Agilent Technologies, Santa Clara, California).

3.1.4 Preparation of fusion proteins from *E. coli*.

In order to address a number of experimental questions we required the production of high concentrations of purified proteins. We utilized the bacterial high protein

expression *E.coli* strain BL21 (Novogen, Hornsby, Australia) and validated expression on sodium dodecyl sulfate polyacrylamide gel electrophoresis (SDS PAGE).

GST and HA-TAT fusion Proteins were cloned into pGEX-4T-2 (Amersham Pharmacia Biotechnology, Piscataway, New Jersey)(Table 3.1) and used to transform BL21 (DE3) cells (Novogen, Hornsby, Australia). Bacterial cultures were grown at 37°C to OD₆₀₀ of approximately 0.3, shifted to 30°C for continued growth to OD₆₀₀ between 0.6 and 0.8, and induced with 0.1 mM IPTG for 2 hours at 30°C. As per standard practice, bacterial pellets were subjected to extensive sonication and mixed with glutathione-agarose bead slurry (50% vol/vol in PBS) and eluted, concentrated and exchanged with storage buffer in Centricon Plus-20 (EMD Millipore, Darmstadt, Germany).

Purified proteins were separated by size by transfer through a SDS-PAGE using standard methods (Cold Spring Harbor Protocols) and visualized by Bio-Safe™ Coomassie Blue (Bio-Rad, Hercules, California).

3.2 Generation and culture of cell lines and viruses

Once generated and the sequences confirmed, expression vectors were delivered into cells. The cell type utilized depended on the experimental question being addressed, however all lines were immortalized adherent cells. The AKR-2B mouse fibroblast line has been well characterized in response to TGFβ and consequently was used throughout this study. A variety of transformed and immortalized cells from healthy and diseased tissues in a multitude of species were used as needed to address specific questions as they arose. Both the parental and derived cell lines are presented in Table 3.2.

Table 3.2 Cell lines utilised in this study

Cell Line	Description	Culture conditions	Source	Section
AKR-2B	Immortalized mouse fibroblast	10% FBS-DME	Supplied Hal Moses	Ch 4,6,7 5.3.1
AKR-2B SNX9 WT	AKR-2B stably expressing Wild Type SNX9	10% FBS-McCoy's puromycin	Generated by stable transfection of pSNX9 using Lipofectamine® 2000	4.3.1 4.3.2 4.3.4

AKR-2B SNX9 SH3LC	AKR-2B stably expressing Dominant-Negative SNX9	10% FBS-McCoy's puromycin	Generated by stable transfection of pSNX9 SH3LC using Lipofectamine® 2000	4.3.1 4.3.2 4.3.4
AKR-2B SNX9 PXBAR	AKR-2B stably expressing Dominant-Negative SNX9	10% FBS-McCoy's puromycin	Generated by stable transfection of pSNX9 PXBAR using Lipofectamine® 2000	4.3.1 4.3.2 4.3.4
AKR-2B shSNX9 77 clones	AKR-2B with SNX9 knocked down through stable expression of shRNA	10% FBS-DME puromycin	Generated by stable integration of shRNA sequence against SNX9 after lentiviral infection	4.3.1-4 4.3.6-8
AKR-2B shSNX9 78 clones	AKR-2B with SNX9 knocked down through stable expression of shRNA	10% FBS-DME puromycin	Generated by stable integration of shRNA sequence against SNX9 after lentiviral infection	4.3.1 4.3.2 4.3.4
AKR-2B shNT clones	AKR-2B stably expressing non-targeting shRNA	10% FBS-DME puromycin	Generated by stable integration of non-targeting shRNA sequence after lentiviral infection	4.3.1-4 4.3.6-8 6.3.3 6.3.4
AKR-2B shIMP8 clones	AKR-2B with Importin8 knocked down through stable expression of shRNA	10% FBS-DME puromycin	Generated by stable integration of shRNA sequence against IMP8 after lentiviral infection	4.3.6 4.3.7
AKR-2B shIMPβ clones	AKR-2B with Importinβ knocked down through stable expression of shRNA	10% FBS-DME puromycin	Generated by stable integration of shRNA sequence against impβ after lentiviral infection	4.3.6 4.3.7 6.3.3 6.3.4
AKR-2B shSEC61 clones	AKR-2B with Sec61 knocked down through stable expression of shRNA	10% FBS-DME puromycin	Generated by stable integration of shRNA sequence against sec61 after lentiviral infection	6.3.3
A105 clones*	AKR-2B stably expressing Wild Type αGM-CSF/TGFβR1 and Wild Type βGM-CSF/TGFβR2	10% FBS-McCoy's neomycin/hygromycin	Supplied by Bob Anders (Johns Hopkins)	6.3.5
A615 clones*	AKR-2B stably expressing Kinase-Dead αGM-CSF/TGFβR1 and Wild Type βGM-CSF/TGFβR2	10% FBS-McCoy's neomycin/hygromycin	Supplied by Bob Anders (Johns Hopkins)	6.3.5
A708 clones*	AKR-2B stably expressing Wild Type αGM-CSF/TGFβR1 and Kinase-Dead βGM-CSF/TGFβR2	10% FBS-McCoy's neomycin/hygromycin	Supplied by Bob Anders (Johns Hopkins)	6.3.5
NMuMg	Immortalized Mouse Mammary Epithelial Cell	10% FBS-DME +insulin+EGF	Supplied by Phil Howe	4.3.4
NMuMg shSNX9 77	NMuMg with SNX9 knocked down	10% FBS-DME +Insulin+EGF	Generated by stable integration of shRNA	4.3.1

clones	through stable expression of shRNA	puromycin	sequence to SNX9 after lentiviral infection	
NMuMg shSNX9 78 clones	NMuMg with SNX9 knocked down through stable expression of shRNA	10% FBS-DME +Insulin+EGF puromycin	Generated by stable integration of shRNA sequence to SNX9 after lentiviral infection	4.3.1
NMuMG shNT clones	NMuMg stably expressing non-targeting shRNA	10% FBS-DME +Insulin+EGF puromycin	Generated by stable integration of non-targeting shRNA after lentiviral infection	4.3.1
Smad2^{-/-} Mouse Embryo Fibroblasts	Immortalized Mouse Embryo Fibroblast with targeted deletion of Smad2	10% FBS-DME	Supplied by Anita Roberts	4.3.1 5.3.2 5.3.3 5.3.4
Smad3^{-/-} Mouse Embryo Fibroblasts	Immortalized Mouse Embryo Fibroblast with targeted deletion of Smad3	10% FBS-DME	Supplied by Anita Roberts	4.3.4 4.3.5 4.3.6
Smad4^{-/-} Mouse Embryo Fibroblasts	Immortalized Mouse Embryo Fibroblast with targeted deletion of Smad4	10% FBS-DME	Supplied by Phil Howe	4.3.4
NIH3T3	Immortalized Mouse Fibroblast	10% FBS-DME	Purchased from ATTC	4.3.4
WI38	Immortalized Human Lung Fibroblast	10% FBS-Eagle's MEM	Supplied by Hal Moses	4.3.4
Mv1Lu	Immortalized Mink Lung Epithelial Cell	10% FBS-DME	Supplied by Juan Massagué	6.3.1 6.3.2 6.3.4 7.3.1
MDCK	Immortalized Dog Epithelial Cell	10% FBS-Eagle's MEM	Purchased from ATCC	6.3.1
MD-1*	MDCK stably expressing Wild Type α GM-CSF/TGF β R1 and Wild Type β GM-CSF/TGF β R2	10% FBS-DME neomycin/hygromycin	Supplied by Jules Dore	6.3.2
MD shVPS35	MDCK with Vps35 knocked down through stable expression of shRNA	10% FBS-Eagle's MEM puromycin	Generated by stable integration of shRNA sequence to Vps35 after lentiviral infection	6.3.2
MD shNT	MDCK stably expressing non-targeting shRNA	10% FBS-Eagle's MEM puromycin	Generated by stable integration of non-targeting shRNA after lentiviral infection	6.3.2
MD-1 truncations*	MDCK stably expressing Wild Type α GM-CSF/TGF β R1 and truncated and deleted forms of β GM-CSF/TGF β R2	10% FBS-DME neomycin/hygromycin	Generated by stable transfection of pSNX9 using Lipofectamine® 2000	6.3.2
Cos7	SV40-transformed Green Monkey Fibroblast-like cells	10% FBS-DME	Purchased from ATCC	6.3.1 6.3.2 6.3.4 7.3.1

				7.3.2
293 FT	SV40 Large T antigen-transformed Human Kidney Cell Hec293	10% FBS-DME neomycin	Purchased from Invitrogen	3.2.4
293 Cre	Hec293 expressing Cre recombinase	10% FBS-DME neomycin	Purchased from Invitrogen	3.2.3
MCF10A	Human Breast Epithelial	MEBM + MEGM	Supplied by Ruth Lupu	6.3.1
MCF10A/Neu	MCF 10A transformed with ErbB2	MEBM + MEGM	Supplied by Ruth Lupu	6.3.1
MDA MB231	Human Breast Adenocarcinoma	MEBM + MEGM	Supplied by Ruth Lupu	6.3.1
IMR90	Human Lung Fibroblast	10% FBS-Eagle's MEM	Purchased from ATCC	6.3.1
A549	Human Lung Adenocarcinoma	10% FBS-F12K	Purchased from ATCC	6.3.1
PC-3	Human Prostate Cancer	10% FBS-F12K	Supplied by Don Tindal	6.3.1
Eph4	Mouse Breast Cancer (transformed with constitutively active ERK) from metastatic xenograft	10% FBS-DME	Supplied by Anita Roberts	4.3.4

* Rationale for use of GM-CSF/TGF β chimeric receptors is outlined in section 3.2.1

3.2.1 GM-CSF/TGF β chimeric receptors: rationale and strategy

The GM-CSF and TGF β receptor signalling mechanisms share many features. Both consist of a pair of single-pass transmembrane receptors with extracellular, transmembrane and intracellular components. Both require the two receptors being brought together by ligand binding to initiate signalling and both internalize through clathrin-mediated endocytosis. However, while TGF β receptors are expressed on virtually all cells, GM-CSF receptor expression is limited to myeloid cells. Furthermore TGF β receptors initiate Smad signalling whereas GM-CSF receptors activate STAT5 and STAT3. Importantly in the context of this study, antibodies with high specificity and affinity are available that recognize the extracellular domains of both GM-CSF receptors, whilst no such antibodies exist for TGF β receptors.

Fusion of the extracellular domains of GM-CSF receptors to the transmembrane and intracellular domains of TGF β receptors creates a system by which the TGF β signalling pathway can be initiated by GM-CSF and the trafficking of the receptors can be easily observed by antibody binding to the extracellular domains (Anders 1996). This system provides benefits that other epitope tagged constructs do not.

TGF β receptors exist as homodimers (two TGF β R1s and two TGF β R2s) prior to ligand stimulation and TGF β binding brings these homodimers together into the signalling heterotetramer complex (Anders 1996). Because TGF β receptors are expressed on virtually all cells, when mutations or truncations are introduced into tagged TGF β receptor constructs, these can homodimerize with themselves or with the endogenous receptors, which makes it difficult to decipher the true impacts of the introduced mutation/truncation (Fig 3.2). This only becomes amplified when both TGF β R1 and TGF β R2 tagged constructs are introduced. Importantly, neither α GM-CSFR/TGF β R1 nor β GM-CSFR/TGF β R2 receptors interact or associate with endogenous TGF β R1 or TGF β R2, meaning that within a cell, distinct endogenous TGF β and GM-CSF/TGF β receptor complexes will be activated in response to either ligand (Fig 3.2). In this way, in the same cell type, the wild type TGF β response can be observed by stimulating with TGF β , while the impacts of a mutation/truncation can be observed through the addition of GM-CSF (Anders 1996).

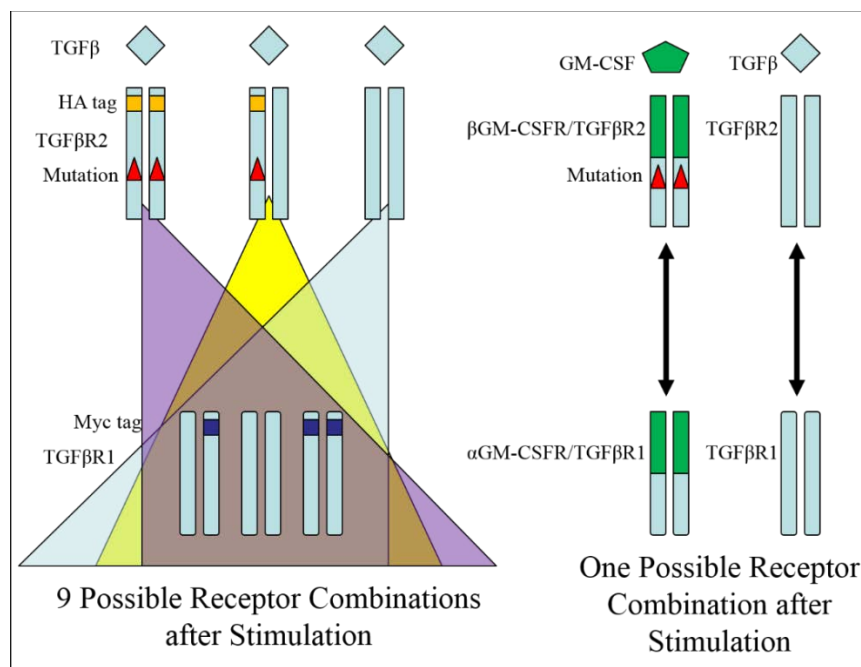


Figure 3.2 Advantage of introducing mutations and truncations into GM-CSF/TGF β chimeric receptors over tagged native receptors. Because chimeric receptors do not interact with endogenous receptors, mutant receptors can be kept distinct (and assayed separately) from native, wild type receptors. The use of antibodies to GM-CSF extracellular domains allows visualization of mutated receptors and the addition of GM-CSF facilitates examination of how the receptor mutations impact the intracellular TGF β signal.

3.2.2 Culture conditions

Standard cell culture techniques were employed and all assays were carried out in sterile flow hoods with cells maintained at 37°C with 5% carbon dioxide and fixed humidity. Cell lines were cultured in culture media (Table 3.2. and Appendix III) recommended for optimal growth by the supplier and supplemented with 10% Fetal Bovine Serum (FBS) (Gibco® Life Technologies, Grand Island, New York) with regular passaging (as per ATCC suggestions) before expansion for freezing down stocks or experimental manipulation. A large seed stock (approximately 20 cryovials) of each cell line was banked and maintained in liquid nitrogen storage.

3.2.3 Transfection of cell lines

A number of different transfection protocols were utilized in these studies. Different protocols performed better on certain cell types, with determinants including plasmids copy number, amount of DNA required and the confluency of the cells prior to transfection.

3.2.3.1 Lipofectamine® 2000 (Invitrogen, Carlsbad, California)

Lipofectamine® 2000 was purchased from Invitrogen™ and the protocol was based on the recommended procedure with modifications designed to optimize transfection in the cell types utilized. Transfections were either performed in 6 well or 10 cm² dishes with cells grown to 90% confluency prior to transfection however, in cases when large volumes of DNA (and associated lipid) were required to be transfected, cells were less prone to toxic effects if allowed two days to reach confluency. In this case cells were seeded at ¼ the number seeded to reach confluency at 24 hours. Rather than removal of the transfection media (as recommended) less toxicity was observed by directly adding 20% FBS-DMEM and allowing overnight recovery in this media, prior to experimental manipulation.

3.2.3.2 FuGENE® 6 (Promega, Madison, Wisconsin)

The protocol followed was essentially the same as recommended by the manufacturer except transfection was allowed to proceed for 24 hours. This protocol allowed transfection of large amounts of DNA and in sparse cell cultures.

3.2.3.3 TransIT® 2020 (Thermo Fisher Scientific, Waltham, Massachusetts)

TransIT® 2020 was utilized to improve transfection efficiency in hard to transfect cells such as Mouse Embryo Fibroblasts (MEFs) and when higher transfection efficiency was required in fibroblast cell lines and was performed essentially as recommended by the manufacturer.

3.2.4 Generation of recombinant Adenovirus

After subcloning the genes of interest into the pAd.CMV shuttle vector DNA was transfected into 293Cre cells using Lipofectamine® 2000 and incubated for 48 hours. Adenovirus-containing cells and supernatant was harvested and pipetted into 15 ml sterile tubes and stored at -80°C. Recombinant clones were determined in 293Cre monolayers by induction of cytopathic effects, isolated and plaque purified. Cell-free viral supernatants were prepared by multiple freeze-thaw centrifugations prior to determination of the viral titre.

Virus titering was achieved through serial dilution of virus supernatants and addition to confluent 293 cultures, with individual cytopathic plaques as a readout of infectious virus determining the Plaque Forming Units (PFUs) per volume of viral supernatant. This was converted to Multiplicity of Infection (MOI).

3.2.5 Generation of recombinant Lentivirus

Lentivirus production was achieved using the ViraPower™ Lentiviral Expression System (Invitrogen, Carlsbad, California). Once purified, plasmid constructs carrying shRNA sequences were transfected into 293FT cells and packaged using ViraPower reagents (Invitrogen, Carlsbad, California) as described by the manufacturer using Lipofectamine® 2000 along with the three plasmids contained in the ViraPower™ Packaging Mix (pLP1, pLP2 and pLP/VSFG). Virus-containing supernatant was harvested by pipetting media into sterile 15 ml tubes and centrifuging for 15 minutes at 3000 rpms at 4°C and aliquoted into 1 ml cryovials for storage at -80°C.

3.2.6 Infection of cell lines

For viral transduction the cell lines of interest (either AKR-2B or NMuMg) were plated at 2.5×10^5 or 4×10^5 cells in each 6 well plate, respectively and allowed to attach and divide for 24 hours. The following day the media was removed and 1 ml of lentiviral

stock and 6 µg/ml of Polybrene® (Santa Cruz Biotechnology, Santa Cruz, California) added prior to overnight incubation. The virus-containing media was then removed and replaced with 10% FBS-DME containing 1.2 µg/ml puromycin to begin selecting clones. When lentiviral strategies were used for RNA interference, non-targeting (NT) shRNAs viruses were used as controls.

3.2.7 Gene silencing

Gene silencing was achieved primarily by lentiviral transduction of shRNA sequences supplied by Sigma's MISSION library purchased from the Mayo Clinic Jacksonville RNA Interference Technology Resource (see Appendix I for shRNA sequences). In the case of silencing components of the coatamer complex (section 6.3.5), generation of stable knockdown clones using shRNA was unsuccessful so transient expression of siRNA to Copβ was introduced by transfection with Lipofectamine® 2000 (Invitrogen, Carlsbad, California).

3.3 TGFβ stimulation of cell lines

Having generated reagents and cell lines, our experimental questions could be examined in cell cultures. Most assays simply required parallel cell lines harbouring wild type sequence or various mutations being exposed to TGFβ for varying lengths of time (as indicated in figure legends). TGFβ1 was supplied by R&D Systems (Minneapolis, Minnesota) and used at 10 ng/ml. Upon completion of the experiment, cells were either fixed or lysed immediately, or snap frozen awaiting further processing and analysis.

3.4 Experimental analysis

The final step in the experimental process outlined in Figure 3.1 involves analyzing the results. We have sought to examine the impacts on TGFβ signalling by analyzing changes in cell growth, gene transcription and protein trafficking, expression, associations, and activity. A number of different techniques were employed to examine these specific events and the links between the specific technique and the readout are visually represented in Figures 3.1 and 3.3.

3.4.1 Cell-based assays

3.4.1.1 [3H] Thymidine incorporation proliferation assay

Thymidine incorporation proliferation assays were performed essentially as described (Wilkes 2003). Four μCi of free [^3H] thymidine was added to cycling cells in the presence or absence of TGF β for 2 hours. Thymidine-containing media was replaced with fresh media and incubated for 22 hours, prior to washing and addition of 2 ml 5% Trichloroacetic acid (TCA), 1N NaOH and 1N HCl and transferred to a scintillation vial. After addition of 4 ml of scintillation fluid, the vial was shaken well and counted in a scintillation beta counter.

3.4.1.2 Soft agar assays

The ability of cells to grow in anchorage-independent conditions was assessed through the ability of cells to form colonies in a gel of culture media and polymerized Sea Plaque $^{\text{®}}$ agarose (Lonza, Basel, Switzerland) as described (Wilkes 2006). Soft agar gels were poured in 6-well plates with a base layer of firmer polymerized agarose. The base plug was 0.5% agar while the cell-containing top layer was 0.3%. Cell colonies were counted using a Gel Count $^{\text{®}}$ cell colony counter (Oxford Optronix, Oxford, UK) with 100 μm set as the minimal diameter to define a colony.

3.4.2 Visual analysis of intracellular compartments and trafficking

Microscopy was performed using standard techniques on a LSM510 confocal microscope. Cells were plated onto coverslips and after experimental manipulation were immersed in wash/fixation/permeabilization/blocking buffer and fixed in 4% formaldehyde, permeabilized with 0.1% Triton X100 (in PBS) for 3 minutes, and blocked in wash buffer containing 10% donkey serum for 1 hour, all at room temperature. Antibodies were prepared in 0.5% BSA/PBS, 5% normal donkey serum with the concentration of the specific antibody/s listed in Table 3.3. Coverslips with incubated with primary antibody for 1 hour and quenched in 50 mM NH_4Cl for 10 minutes prior to quench background fluorescence. Following an additional wash buffer rinse, the samples were blocked in wash buffer containing 10% donkey serum for 10 minutes prior to incubation in fluorophore-labelled secondary antibody. After mounting, fluorescence images were collected on the LSM510 confocal microscope (Zeiss, Heidenheim, Germany) followed by MetaMorph $^{\text{®}}$ analysis (Molecular Devices, Sunnyvale, California) of fluorescence intensities.

3.4.3 Gene expression analysis

TGF β signalling is conveyed from the cell surface to the nucleus where it regulates gene transcription. The regulation of a number of TGF β -regulated genes was analysed in this study and examined using either luciferase reporter assays or qRT-PCR.

3.4.3.1 Luciferase reporter assays

AKR-2B or Mv1Lu cells devoid of TGF β R1 (R1B) were transfected with 2 μ g of luciferase reporter (either 3TP or 6xSBE luc) and 0.5 μ g of cytomegalovirus- β -galactosidase with Lipofectamine[®] 2000 (Invitrogen, Carlsbad, California)(section 3.2.3.1). 1.0 μ g of additional experimental constructs were transfected as needed. Cultures were subjected to the indicated experimental manipulations and stimulated with TGF β for 24 hours and harvested in 200 μ l of reporter lysis buffer (Promega, Madison, Wisconsin). Luciferase activity was determined in a Lumat 9501 luminometer (Berthold Technologies, Bad Wildbad, Germany) after standardization for protein levels and transfection efficiency with β -galactosidase.

3.4.3.2 Quantitative Reverse Transcriptase-Polymerase Chain Reaction (qRT-PCR)

Total RNA was extracted from cells either using Trizol[®] (Invitrogen, Carlsbad, California) or the RNeasy Plus Mini Kit with gDNA eliminator spin columns to remove genomic DNA (QIAGEN, Velno, The Netherlands). RNA was converted to cDNA for quantitative PCR using Superscript III Reverse Transcriptase (Life Technologies, Grand Island, New York). Quantitative real time PCR was performed using the CFX96 Real-Time PCR detection system (Bio-Rad, Hercules, California) using the SYBR[®] Green PCR Master Mix (Life Technologies, Grand Island, New York). Primers (0.2 μ M final concentration) are listed in Appendix V. The experimental mRNA levels were normalized to GAPDH mRNA using the comparative threshold cycle (CT) method, in which the fold difference is $2^{-\Delta\Delta CT}$ of target gene - $\Delta\Delta CT$ of reference gene).

3.4.4 Protein analysis

A central focus of our TGF β signalling and trafficking study is protein biology. Investigation of protein activity, expression, localization and interactions requires a number of different assays. Most of these require SDS-PAGE resolution of proteins

into bands in a gel prior to visualization either by western blotting or autoradiography. Because of the overlap in techniques utilized in the various assays, a schematic flowchart of the various protein analyses undertaken and the assays used are presented in Figure 3.3. Antibodies used for protein analysis are listed in Table 3.3.

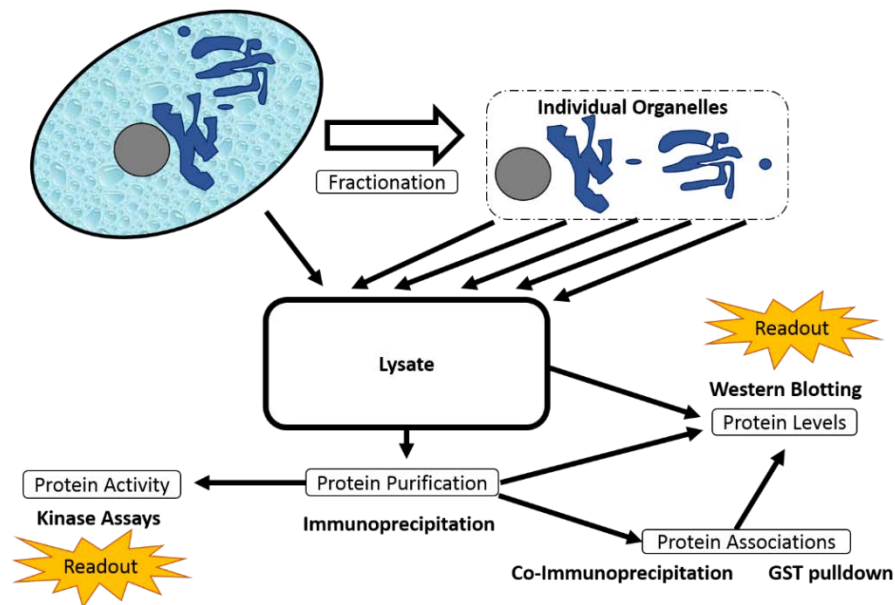


Figure 3.3 Flowchart of protein analysis in this study. Schematic representation of the methods of protein analysis employed and how they relate to protein expression, associations and kinase activity. While the final readout of a kinase assay is autoradiography, all other assays are ultimately resolved via western blotting. Each is subject to SDS-PAGE.

Table 3.3 Antibodies utilised in this study

Antibody	Company (Catalog Number)	WB* Dilution	IP* Dilution	IF* Dilution	Secondary antibody
ActR11a	Abcam (ab96793)	1:500	-	-	
ATF2	Cell Signalling (9226)	1:1000	-	-	Rabbit
Calnexin	Abcam (ab31290)	1:3000	-	1:800	Mouse
Calnexin	Abcam (ab22595)	-	-	1:1000	Rabbit
Clathrin HC	Santa Cruz (sc-6579)	1:2000	-	-	Goat
Copα	Abcam (ab2913)	1:1000	-	-	Rabbit

CREB	Millipore (06-863)	1:2000	-	-	Rabbit
Cytochrome C	Abcam (ab13575)	1:2000	-	-	Mouse
Dynamin	Henley et al., 1998	1:3000	-	-	Mouse
E2F4	Santa Cruz (sc-866)	1:500	-	-	Rabbit
EGFR	Millipore (06-847)	1:1000	-	-	Rabbit
Elk1	Santa Cruz (sc-355)	1:300	-	-	Rabbit
Emerin	Abcam (ab40688)	1:500	-	1:200	Rabbit
FLAG	Sigma (F3165-5MG)	1:1000	1 µg/ml	-	Mouse
Fos	Santa Cruz (sc-52)	1:1000	-	-	Rabbit
GAPDH	Chemicon (MAB374)	1:15 000	-	-	Mouse
GFP	Roche (11814460001)	1:1000	1 µg/ml	-	Mouse
Giantin	Abcam (ab24586)	1:2500	-	1:000	Rabbit
Giantin	Abcam (37266)	-	-	1:1000	Mouse
GM130	Abcam (ab52649)	1:3000	-	-	Rabbit
GM-CSFRα	Santa Cruz (sc-456)	1:800	4 µg/ml	1:200	Mouse
GM-CSFRβ	Santa Cruz (sc-676)	1:1000	2 µg/ml	-	Rabbit
GM-CSFRβ	Santa Cruz (21766)	-	-	1:200	Mouse
HA	Roche (11666606001)	1:1000	1 µg/ml	1:200	Mouse
HDAC1	Cell Signalling (2062)	1:1000	-	-	Rabbit
Histone H2B	Santa Cruz (sc-10808)	1:1500	-	-	Rabbit
H2B	Millipore (07-371)	1:1000	-	-	Mouse
Importin-7	AbCam (ab15840)	1:1000	2 µg/ml	-	Goat
Importin-8	AbCam (ab72109)	1:1000	2 µg/ml	-	Rabbit
Importin-β	Abcam (ab36775-50)	1:1500	1 µg/ml	-	Rabbit
Myc	Roche (11667149001)	1:500	1 µg/ml	-	Mouse
Myc	Cell Signalling (2276)	-	-	1:100	Mouse
P300	Cell Signalling (7389)	1:1000	-	-	Rabbit
PAK2	Santa Cruz (sc-1872)	1:500	2 µg/ml	-	Goat
Phospho-Smad2	Millipore (07-408)	1:1000	-	-	Rabbit
Phospho-Smad3	Wilkes et al,2003	1:3000	-	-	Rabbit
pSmad3	Cell Signalling (9520)	1:1000	-	-	Rabbit
pSmad PAK site	Jinhua Li,2014	1:2500	-	-	Rabbit
Phospho-S/T	BD Bio (612548)	1:500	-	-	Rabbit
PML	Santa Cruz (sc966)	-	-	1:100	Mouse
PML	Abcam (ab53773)	-	-	1:200	Rabbit

PPM1A	Abcam (114824)	1:350	5 µg/ml	-	Mouse
Sec61	Abcam (ab15037)	1:2500	2 µg/ml	-	Rabbit
Sec63	Abcam (ab99031)	1:1000	-	-	Rabbit
Smad2	Calbiochem (5664165)	1:1000	2 µg/ml	-	Rabbit
Smad2	AbCam (ab63576)	1:1000	-	-	Rabbit
Smad3	Abcam (ab28379-100)	1:3000	2 µg/ml	-	Rabbit
Smad2/3	Millipore (07-408)	1:1000	-	-	Rabbit
Smad4	Cell Signalling (9515)	1:2000	4 µg/ml	-	Rabbit
SNX9	Santa Cruz (sc49143)	1:1000	3 µg/ml	-	Goat
TGFβR1	Santa Cruz (sc-398)	1:500	-	-	Rabbit
TGFβR2	Santa Cruz (sc-220)	1:400	-	-	Rabbit
VPS26	Abcam (Ab23892)	1:350	2 µg/ml	-	Rabbit
YFP Tag	Santa Cruz (sc32897)	1:1000	1 µg/ml	-	Rabbit
Mouse-Alex488	Invitrogen (715-165-150)	-	-	1:200	Goat
Mouse-Cy3	Jackson Labs (A11011)	-	-	1:200	Donkey
Rabbit-Alex488	Invitrogen (711-165-152)	-	-	1:200	Goat
Rabbit-Cy3	Jackson Labs (A11008)	-	-	1:200	Donkey

*WB= western blotting; IP = immunoprecipitation; IF = immunofluorescence

3.4.4.1 Cellular compartment fractionation

3.4.4.1.1 Golgi and Endoplasmic Reticulum fractionation

Purification of the Golgi was adapted for cell lysates using the Golgi Isolation Kit (Sigma-Aldrich, St Louis, Missouri). Endoplasmic Reticulum (ER) fractions were obtained by performing essentially as per manufacturer instructions using the Endoplasmic Reticulum Isolation Kit (Sigma-Aldrich, St Louis, Missouri). Purity was determined by western blotting (see Fig 3.4E) for the presence of GM130 or giantin (localization is restricted to the Golgi), calnexin (restricted to the ER), or Cytochrome C (which is restricted to mitochondria). Mitochondrial contamination is the most common contaminant in these fractions.

3.4.4.1.2 COPI vesicle fractionation

COPI vesicle fractionation was performed essentially as described in Sönnichsen et al, (1996) except that cells were suspended in 1 ml 0.25 M sucrose supplemented with Complete® protease inhibitor cocktail, and passed through a 27-G needle 12 times to lyse cells by shear stress. The fraction containing the most COPα was considered the

Copl vesicle fraction. Possible contamination with clathrin-coated vesicles was screened by western blotting analysis for clathrin heavy chain (see Fig 3.4C).

3.4.4.1.3 Inner nuclear membrane fractionation

Nuclei were isolated (by hypotonic extraction) and the isolated nuclei were suspended in 0.25 M Sucrose, 50 mM Tris-HCl (pH7.4), 10 mM MgCl₂, 1 mM DTT with Complete® Protease inhibitor. The resulting suspended pellet was dissolved in 1% (by weight/volume) sodium citrate with gentle agitation at 4°C for 30 minutes before centrifugation at 10000 x *g* for 2 hours. The digested pellet was submitted to ultracentrifugation at 100000 x *g* for 20 minutes on a sucrose gradient. The inner nuclear membrane fraction was collected from the 0.25 – 1.6 M sucrose interface. While Emerin is detected in both nuclear membrane and inner nuclear membrane fractions, Sec63 is restricted in localization to the rough ER and outer nuclear membrane, so inner nuclear membrane purity is determined by the absence of Sec63 contamination (see Fig 3.4D).

3.4.4.1.4 Nuclear membrane, soluble and chromatin-bound fractionation

The nuclear soluble and chromatin-bound fractions were derived completely as directed by the manufacturer while the nuclear membrane fraction was generated from the membrane prep (as per the manufacturers' recommendations) on purified nuclei. Nuclei were obtained using NE-PER followed by membrane extraction using the Subcellular Protein Fractionation Kit for Cultured Cells (Thermo Fisher Scientific, Waltham, Massachusetts). Nuclei were suspended in ice-cold Membrane Extraction Buffer Suffer (supplied) and disrupted using 12 passes through a 27-gauge syringe and subjected to centrifugation at 1000 x *g* for 2 minutes at 4°C. Purity of the fractions was confirmed by the presence or absence of Sec63 (outer nuclear membrane and rough ER marker), HDAC (Largely soluble in the nucleus but some chromatin binding) and Histone1 (restricted to chromatin) as determined by western blot analysis (Fig 3.4G).

3.4.4.1.5 Nuclear fractions

A number of techniques were employed to extract nuclear fractions, depending on how intact the purified nuclei needed to be.

Nuclear extracts (soluble nuclear components with only limited nuclear membrane and chromatin-associated components) were obtained using NE-PER™ Nuclear and Cytoplasmic Extraction Reagents (Pierce Biotechnology, Rockford, Illinois) supplemented with Complete® protease inhibitor. 2) To obtain purer, intact nuclei confluent 10 cm² dishes were washed twice in PBS, scraped and pipetted into a 15 ml culture tube and centrifuged for 10 minutes at 2500 x *g* at 4°C. The supernatant was discarded and roughly 5 times the volume of the pellet worth of hypotonic buffer (see Appendix IV) was added to the tube and rapidly centrifuged for 5 minutes at 2500 x *g* at 4°C. This rapid wash step was followed by adding 3 times the volume of hypotonic buffer with cells allowed to swell on ice for 10 minutes. Cells were transferred to a dounce homogenizer and homogenized with 10 – 12 up-and-down strokes before centrifugation at 3300 x *g* for 15 minutes with the pellet representing the nuclei. 3) Cells were lysed in hypotonic buffer with Nonident-p40 (NP-40) detergent added before spinning in a 1.8 M sucrose cushion for 30 minutes at 100000 x *g*. Nuclear fraction purity was determined by western blotting with the exclusion of the cytosolic protein GAPDH and enrichment of HDAC (or histone1) indicative of successful fractionation (see Fig 3.4A).

Crude nuclear pores and nuclear membranes were generated as described by Aaronson and Blobel (Aaronson 1975, Aaronson and Blobel 1975). The purity of nuclear pore fractions was determined by the exclusion of the outer nuclear membrane and rough ER component Sec63 and the intranuclear HDAC. The enrichment of the nuclear shuttling proteins Importinβ was also confirmed (see Fig 3.4F).

A number of protocols were tested to determine which yielded the purest and most enriched plasma membrane fractions. The most successful was based on a commercial kit that was determined to give a higher plasma membrane enrichment. The procedure was performed as per manufacturer instructions using Qproteome Plasma Membrane Protein Kit (QIAGEN, Venlo, The Netherlands). The enrichment of EGFR and exclusion of Calnexin (ER marker), GM130 (Golgi marker) and HDAC (nuclear marker) was utilized to determine the purity of plasma membrane fractions obtained (see Fig 3.4B).

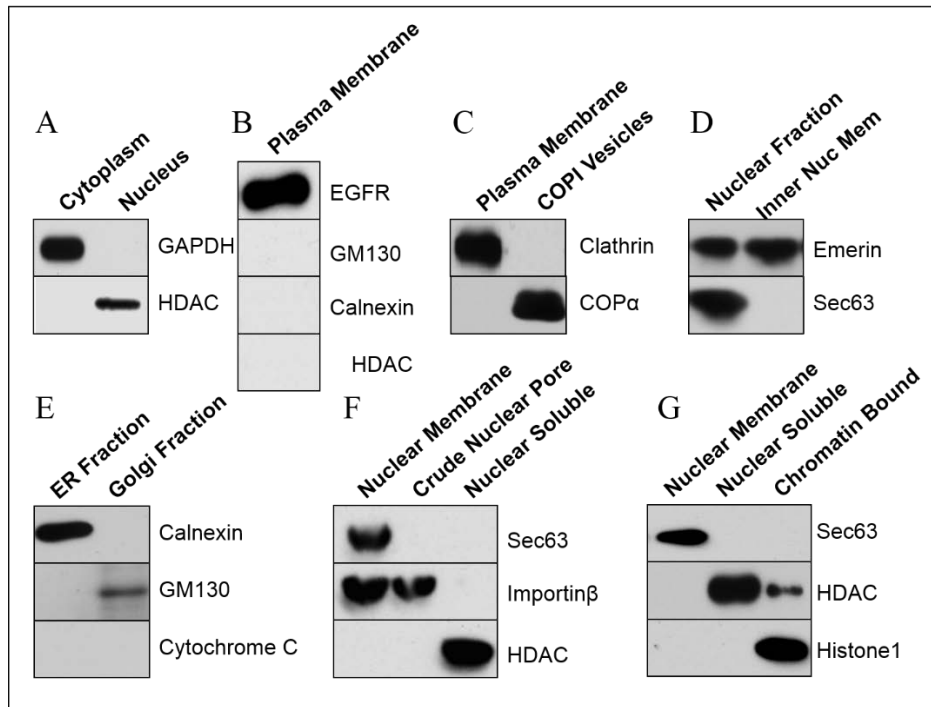


Figure 3.4 Determining purity of organelle enrichment fractionation. (A) Nuclear fraction purity was determined through the enrichment of HDAC (or histone) and exclusion of GAPDH (B) Plasma Membrane purity was determined by high enrichment of EGFR and exclusion of calnexin, GM130 and HDAC (C) Cop1 vesicle fractions were determined by enrichment of COP α and the absence of Clathrin (D) Inner nuclear membrane contains emerin but Sec63 is excluded (E) calnexin is restricted to the ER while GM130 is restricted to the Golgi. (F) The crude nuclear pore fraction excludes outer nuclear membrane/ER markers such as Sec63 and soluble nuclear proteins such as HDAC, yet Importin β is enriched. (G) Nuclear membrane fractions exclude HDAC and Histone1 with Sec63 enrichment. The nuclear soluble fraction has enriched HDAC and an absence of Sec63 and histone1. Chromatin bound fractions excluded Sec63 with enrichment of histone1 and moderate detection of HDAC.

3.4.4.2 Immunoprecipitation

Cell lysates were prepared using a number of standard techniques using various lysis buffers, French Press lysis or passage of cell pellets through a syringe multiple times, depending on the cell type and assay requirements. After normalizing for protein concentration lysates were pre-cleared with 50% Protein A/G Sepharose/Agarose slurry before incubation with antibody overnight at 4 °C. Antibody/protein complex was precipitated with 50% Protein A/G Sepharose/Agarose slurry and washed in preparation for kinase analysis (kinase assay), protein expression (western blotting with same antibody used in immunopurification) or analyzing the associated with other proteins (western blotting with antibody against a protein other than the one immunopurified).

3.4.4.3 Kinase assays

Purified immune complexes were precipitated (see immunoprecipitation) with the addition of 50 μ l Protein G (goat) or Protein A (mouse) agarose beads (50% slurry vol/vol). Washed pellets were suspended in 50 μ l of kinase buffer containing 5 μ M ATP, 5 μ Ci [γ -³²P]ATP per reaction and 10 μ g of substrate. The kinase reaction was brought to 37°C and allowed to proceed for 30 minutes prior to being terminated with 50 μ l 2xLaemmli buffer. Samples were then subjected to SDS-PAGE and resolved by autoradiography after destained gels were dried on Whatman paper.

3.4.4.4 Western blotting

After separation by SDS-PAGE, proteins were transferred from the gel to either nitrocellulose (Bio Rad, Hercules, California) or polyvinylidene fluoride (PVDF) (EMD Millipore, Darmstadt, Germany) using a wet transfer method (Cold Spring Harbor Protocols) at 90 volts and transfer apparatus cooled in a circulating bath of 10°C water to dissipate heat. Membrane blots were blocked in Tris-Buffered Saline with Twen (TBST) with either 5% milk or BSA before incubation with primary antibody overnight (see Table 3.3 for list of antibodies and working dilutions). After incubation in secondary antibody conjugated to horse radish peroxidase (HRP), the membrane was immersed in ECL HRP-substrate (Amersham, Pittsburgh, Pennsylvania) for 5 minutes prior to processing for chemiluminescence detection.

In some cases membranes were stripped of bound antibody and subject to a second round of probing with a different antibody. Likewise, single membranes were often cut and probed with different antibodies if the proteins of interest were significantly different sizes.

3.4.4.5 Co-immunoprecipitation

Standard co-immunoprecipitation (Co-IP) techniques were followed (Cold Spring Harbor Protocols) although Co-IP of specific protein complexes required optimisation. A general protocol is described below.

Cells were plated in 10 cm² dishes (allow enough plates to yield approximately 1 mg of protein) to reach 90% confluency the following day. After experimental manipulation

cells were lysed using lysis conditions optimized for the association being examined (ranging from the shear stress generated by multiple passes through a syringe, or pressure of a French Press, or buffers that either use detergents to disrupt the membranes or high/low salt to induce osmotic swelling).

After normalizing for protein concentration and pre-clearing the first protein of the complex was immunoprecipitated (see section 3.4.4.2) by incubation with antibody (Table 3.3) and 50% Protein A/G Sepharose/Agarose slurry. The pellet was washed 1-4 times with the same lysis buffer used for cell lysis with the detergent subtracted (protease inhibitors included) with the number of washes, mixing and centrifugal speed between washes dependent on the interaction being investigated with 10000 x *g* for 1 minute as the starting point. Co-immunoprecipitated proteins were eluted in 1x Laemmli buffer and analysed by Western blotting.

In cases where either the directly or indirectly associated protein ran at the same size as the antibody light or heavy chain on a SDS-PAGE gel (i.e. the strong IgG band masked the presence of our desired protein), the immunoprecipitating antibody was cross-linked prior to addition to the immunoprecipitation sample with BS³ (Thermo Fisher Scientific, Waltham, Massachusetts) per manufacturer's instructions using a 15 fold molar excess of cross linker (final cross linker concentration of 0.25 mM).

3.4.4.6 GST fusion protein pull-down assays

GST pull-downs were performed as per standard procedure (Cold Spring Harbor Protocols). Generally 500 µg to 1 mg of protein from cell lysates was used per pull-down reaction and lysates were probed with 10 µg GST-fusion protein (see Table 3.1 for list of GST-fusion proteins) or GST alone. On occasion proteins were eluted from the beads using 50 µl of 20 mM reduced glutathione in Tris-Cl (pH 8.0) however usually dissociation and denaturation was achieved when Laemmli buffer was added prior to SDS-PAGE. Association of proteins of interest were examined by western blotting.

In those assays requiring GST-fusion proteins be phosphorylated by TGFβR1 prior to pull-down (or HAT assay –see Chapter 6.2) the desired fusion protein was mixed with activated TGFβR1 in conditions favourable for an *in vitro* kinase reaction to proceed (see kinase assays). Purification of activated TGFβR1 was achieved by transfection of Cos7 cells with FLAG-TGFβR2 and HA-TGFβR1 using Lipofectamine® 2000

(Invitrogen, Carlsbad, California) and the HA-tagged TGF β R1 purified by HA immunoprecipitation and per manufacturer's recommendation using Catch and Release[®] v2.0 (Upstate Biotechnology, Lake Placid, New York) (see section 3.4.4.3 for details).

CHAPTER 4

SORTING NEXIN 9 DIFFERENTIATES LIGAND-ACTIVATED SMAD3 FROM SMAD2 FOR NUCLEAR TRANSLOCATION AND TGF β SIGNALLING

CHAPTER 4: SORTING NEXIN 9 DIFFERENTIATES LIGAND-ACTIVATED SMAD3 FROM SMAD2 FOR NUCLEAR TRANSLOCATION AND TGF β SIGNALLING

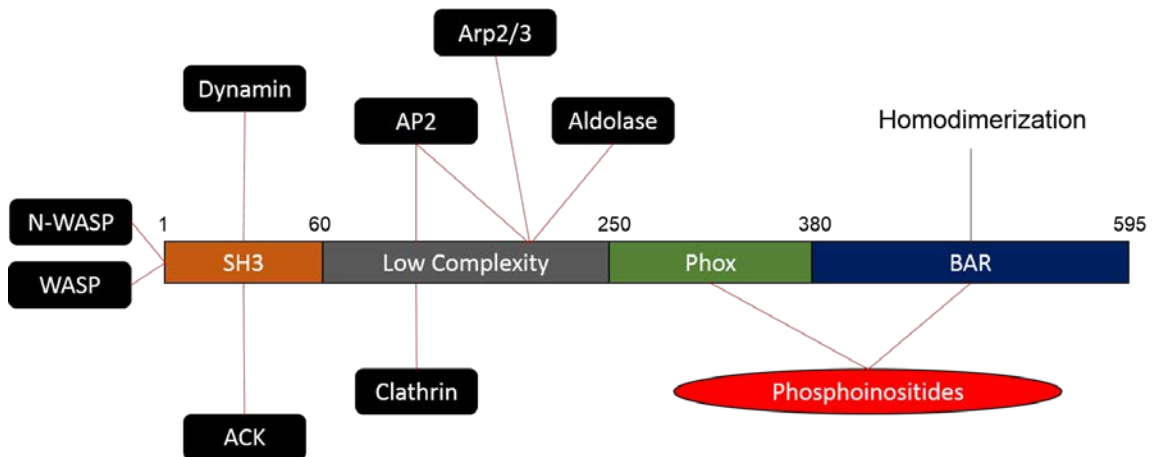
4.1 BACKGROUND

TGF β is a 25 kDa polypeptide that regulates a variety of cellular processes including matrix deposition, mitosis, development, differentiation and apoptosis (Roberts 2003, Elliott 2005). The primary intracellular mediators of TGF β action are the Smad proteins although non-Smad pathways have been reported, often in a cell-type specific context (Rahimi 2007, Ross 2008). Three general categories of Smad proteins have been identified: receptor-regulated Smads (R-Smads; Smads2 and 3 for TGF β or Activin and Smads1, 5, and 8 for BMPs); common-mediator Smad (Co-Smad; Smad4); and inhibitory Smads (I-Smads; Smads6 and 7). The R- and Co-Smad proteins shuttle continuously between the nucleus and cytoplasm in unstimulated cells as well as in the presence of TGF β (Inman 2002, Xu 2002, Schmierer 2005). Of particular note, it is presently unclear whether nuclear R-Smad accumulation results primarily from enhanced nuclear retention (Schmierer 2005, Schmierer 2007, Varelas 2008) and/or an increased rate of nuclear entry following TGF β stimulation (Kurisaki 2001, Schmierer 2008). Although a great deal of information concerning Smad trafficking has been generated, and there is evidence for the dynein light chain km23-2 in TGF β /Smad3 signalling (Jin 2009), it is still unclear how, or even whether, distinct mechanisms are utilized by Smad2 and Smad3. The diversity of cellular responses initiated when TGF β binds to its cell surface receptors may be explained by differences between Smad2 and Smad3 nuclear signalling and/or nuclear trafficking.

Smad2 and Smad3 are virtually identical in the regions phosphorylated and that bind to TGF β -receptors and Smad4. Furthermore the Smad Binding Elements (SBE) and the kinetics of phosphorylation and nuclear entry are the same for both proteins (Massagué 2005, Zawel 1998). Despite these similarities there appears to be dramatic differences in how these two proteins regulate the cell and these have differences have significant clinical implications: for example Smad2 has been suggested to act as a tumour and fibrosis suppressor whereas Smad3 acts as a putative tumour and fibrosis promoter (Yamamoto 1999, Santiago 2005, Hoot 2008, Meng 2010). With conventional phosphorylation and activation studies revealing no major differences

between the two proteins, we focused our studies on other proteins that may differentially regulate TGFβ-induced receptor and R-Smad activation and trafficking.

The sorting nexins (SNXs) are involved in various aspects of intracellular protein trafficking (Carlton 2005, Badour 2007, Verges 2007) and have been linked to TGFβ signalling components (Parks 2001). While no direct role in regulating *nuclear* translocation has been reported, SNXs represent a large family (>30 in human) of structurally related proteins with proposed roles in membrane transport and cell signalling through receptor degradation, sorting, internalization, and recycling (Carlton 2005, Badour 2007, Verges 2007). All SNXs are defined by the presence of a Phox (PX) domain which binds phosphoinositides and aids in targeting SNXs to particular membranes (Worby 2002). SNX9, however, also contains an amino terminal SH3 domain required for membrane recruitment and dynamin, cdc42-associated kinase (ACK2), WASp, and Itch binding, a Bin/Amphiphysin/Rvs (BAR) domain which senses membrane curvature and is required for dimerization, as well as a low complexity region which binds AP-2α and clathrin (Fig 4.1) (Worby 2002, Carlton 2005, Badour 2007, Lundmark 2009, Baumann 2010).



Sorting Nexin 9

Figure 4.1 Domains of SNX9 and binding partners. Sorting Nexin 9 can be broken into 4 distinct regions. The SH3 domain binds dynamin, N-WASP and WASP as well as ACK. The region of low complexity binds AP2, Arp2/3, aldolase and clathrin. The Phox and BAR domains bind phospholipids and allow homodimerization and are responsible for recognizing the curvature of the plasma membrane and early endosomes.

Objectives

As SNX9 is known to modulate the trafficking responses of several transmembrane receptors (Worby 2002, Verges 2007), and since TGF β endocytic activity and Smad phosphorylation have been shown to be coupled in various systems (Hayes 2002, Di Guglielmo 2003), studies were initiated to examine the role(s) of SNX9 in TGF β receptor action, Smad2/3 signalling and trafficking and in different cell types.

The specific Aims were:

1. To determine the role of SNX9 in TGF β -mediated responses in fibroblast and epithelial cell types by silencing SNX9 gene expression.
2. To determine if SNX9 impacts Smad2/3 signalling, and if so, determine if any lesion in signalling is at the level of phosphorylation, hetero-oligomerization with Smad4, or nuclear translocation.
3. To characterize the mechanism in which SNX9 exerts its effects by investigating the molecular interactions of SNX9 with nuclear pore proteins (NUPs) and Importins (Imps) recognized as playing a role in Smad nuclear translocation.
4. To investigate the role of SNX9 in events at the plasma membrane and determine how this impacts TGF β signalling.

Although we found negligible effects on TGF β receptor activity, we observed SNX9 has an obligate role in TGF β signalling. We present evidence to support a role for SNX9 in facilitating the accelerated nuclear translocation of Smad3 (and not Smad2) upon its phosphorylation. Inhibition of SNX9 significantly reduced pSmad3 nuclear accumulation, downstream gene responses and biological responses to TGF β that are attributed to pSmad3. SNX9 performs this role by binding pSmad3 and transporting it to the nuclear membrane. pSmad3-bound SNX9 bound the nuclear membrane via phosphoinositides contained within the outer membrane which led to the formation of a complex with the nuclear pore protein Importin8. This complex bound the main nuclear pore transport protein, Importin β which then facilitated the entry of pSmad3 into the nucleus while releasing SNX9 back to the cytoplasm. The data presented in this Chapter supports a novel role for SNX9 downstream of its canonical plasma membrane action and its central role in TGF β signalling.

4.2 MATERIALS AND METHODS

4.2.1 Cell culture and stimulation

A range of immortalized cells from different tissues and species were utilized in this study (Table 3.2) with extensive utilization of AKR-2B cells. AKR-2B cells are an immortalized mouse fibroblast line that demonstrate a robust signalling and morphologic response to TGF β and furthermore possess a more stable genome than other fibroblast lines (including NIH3T3 fibroblasts). Short hairpin RNA (shRNA) to silence genes suspected to be associated with SNX9 in TGF β signalling were introduced to AKR-2B cell lines via lentiviral infection (AKR-2B shSNX9 77 clones, AKR-2B shSNX9 78 clones, AKR-2B shIMP8 clones and AKR-2B shIMP β clones) along with the appropriate cell line to control for initiation of short hairpin machinery (AKR-2B shNT clones). Cell lines carrying GM-CSF/TGF β chimeric receptors (A105) or dominant negative SNX9 expression constructs (AKR-2B SNX9 PXBAR, AKR-2B and SNX9 SH3LC), or both (A105 SNX9 PXBAR and A105 SNX9 SH3LC) were generated in conjunction with cell lines expressing the appropriate wild type SNX9 (AKR-2B SNX9 WT and A105 SNX9 WT) as described in Chapter 3 (Table 3.2). Myc- and YFP-epitope tagged SNX9 was also introduced into cells by standard transfection methods. The re-introduction of SNX9 into cell lines expressing shRNA against SNX9 was achieved by generating SNX9 constructs bearing conserved DNA mutations, in which the codons encoded the same amino acids as the native, but utilized different nucleic acids. Along with wild type SNX9, mutants failing to bind phosphoinositides (Mut^{PIP₂}) or homodimerize (Δ 13C) were generated (Table 3.2)

Mouse embryo fibroblasts (MEFs) with Smad2, Smad3 or Smad4 genes deleted (Smad2^{-/-}, Smad3^{-/-} and Smad4^{-/-}) and appropriate sibling matched wild type controls fibroblasts (Smad2^{+/+}, Smad3^{+/+}) were utilized to examine the role these Smad proteins play in the observed SNX9-impacted phenotypes (NB: No Smad4^{+/+} MEFs were available to us at the time of this study). To confirm findings observed in Smad2^{-/-} and Smad3^{-/-} lines were due to the absence of the respective Smads, (and not a clonal artifact) Smad2-GFP and Smad3-GFP were re-introduced via transient transfection (described in Chapter 3) into Smad2^{-/-} and Smad3^{-/-} lines respectively. The nucleoporins Nup153 and Nup214 are believed to play a role in Smad nuclear import (Xu 2002) with the potential to bind SNX9. As antibodies raised against these proteins failed to immunoprecipitate, we expressed HA-epitope tagged Nup153 and Nup214 generously provided by Katie Ullman and André Hoelz.

Because the cellular response to TGF β differs between cell types, conclusions drawn from experiments performed using AKR-2B cultures were often extended to include other cell lines (NMuMg, NIH3T3, WI38 and Eph4). NMuMg are an immortalized cell line derived from mouse mammary epithelial cells. Upon TGF β stimulation these cells undergo an EMT-like morphological transformation and growth arrest (Bakin 2000). Clones stably expressing short hairpin RNA sequences to silence SNX9 were generated (NMuMg shSNX9 77 clones and NMuMg shSNX9 78 clones) along with a cell line expressing a non-targeting short hairpin sequence (NMuMg shNT clones). NIH3T3 is an immortalized mouse fibroblast cell line that undergoes mild proliferation and morphological transformation upon TGF β treatment (Daniels 2004). WI38 is an immortalized human lung fibroblast that morphologically transforms into a myofibroblast, proliferates and deposits extracellular matrix upon TGF β stimulation (Fukasawa 2004). Eph4 cells are an epithelial cell line derived from mice that undergo growth arrest in response to TGF β . When transformed with H-ras, TGF β also induced an EMT-like phenotype as seen in NMuMg cells (Gal 2008).

Cells were obtained and cultured as specified (Table 3.2) using standard mammalian cell culture techniques (see Chapter 3) and grown to confluence (unless otherwise stated) prior to stimulation with TGF β 1 to a final concentration of 10 ng/ml in the appropriate growth media (Table 3.2). Stock TGF β was stored in 4mM HCl with 0.1% Bovine Serum Albumin (BSA) and stored at -20 °C. Cells were incubated in the presence of TGF β for various times (as indicated) at 37 °C with 5 % CO₂.

4.2.2 Gene silencing and expression of mutant SNX9 constructs

Protein expression was knocked down by infection of cells with lentivirus expressing shRNA to either SNX9, Importin8 or Importin β as described in Chapter 3 (Table 3.1). Lentivirus was generated as indicated in Chapter 3 and clones with the shRNA sequences stably incorporated into the genome in a position resulting significant protein knockdown were selected and maintained with antibiotic (puromycin) selection. In cells expressing endogenous wild type SNX9 it is challenging to examine the influence of introduced mutant SNX9 on TGF β signalling. To overcome this difficulty, we re-introduced mutant (and WT as a control) SNX9 into cell lines with SNX9 expression knocked down (AKR-2B shSNX9 77) via transient transfection of plasmids carrying the SNX9 constructs as described in Chapter 3 (Table 3.1). Because SNX9 genes (either endogenous or recombinant) present in any cell expressing short hairpin RNA against the SNX9 gene sequence is unable to be transcribed/translated into

SNX9 protein, we introduced conserved mutations (changes in the DNA sequence that results in codons that still encode the same amino acid after translation) into the DNA sequence of our SNX9 mutants within the region of the cDNA that is hybridized by the shRNA. In this way, the resulting cDNA will still encode a SNX9 protein with identical amino acid sequence but will escape silencing by the shRNA: we termed these “escape constructs” (Fig 4.2).

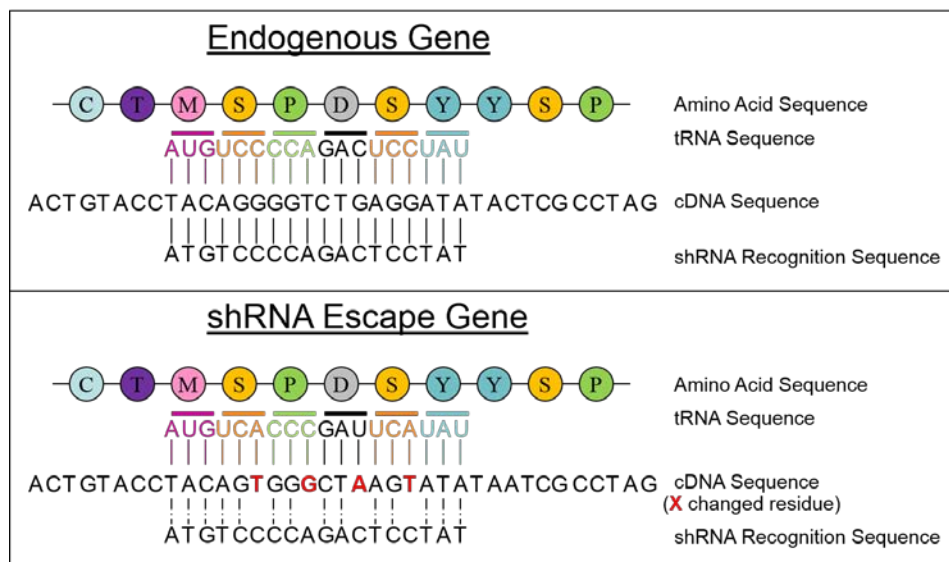


Figure 4.2 Design of SNX9 escape constructs to evade SNX9 shRNA. Top panel indicates the cDNA sequence of the endogenous gene with the translational RNA and amino acid sequence above. Note the sequence is broken into codons (indicated by different colours) that correspond to amino acids on the ribosome. shRNA hybridizes with mRNA but only a short stretch of residues, which is represented below the cDNA sequence. Bottom panel is represented in the same way, however the recombinant sequence has been modified (changed residues are marked in red) and while these changes result in codons that encode for the same amino acids (as can be seen above the cDNA sequence), the mRNA sequence has changed significantly from the optimal shRNA recognition sequence and no longer supports high affinity shRNA hybridization which allows it to escape shRNA-mediated degradation.

4.2.3 Role of SNX9 in TGFβ-induced anchorage-independent growth in fibroblasts

The ability to support anchorage-independent growth of fibroblasts which are normally restricted to growth when attached to a supportive substrate was the first documented response to TGFβ stimulation and is the defining characteristic of *in vitro* cell transformation (Moses 1981, Roberts 1981). The ability to grow in anchorage-independent conditions was assessed through the ability of individual cells that were embedded in a three dimensional soft agar matrix to form colonies and was performed as described in Chapter 3. Four clones derived from AKR-2B cells stably expressing

shRNA against one region of SNX9 mRNA sequence (AKR shSNX9 77 clones) and four clones stably expressing shRNA against an entirely different sequence in SNX9 mRNA (AKR-2B shSNX9 78 clones) were assessed for their ability to form colonies in soft agar after 10 days in the absence or presence of TGF β . Two clones stably expressing a non-targeting shRNA were assessed concurrently (AKR-2B shNT clones) as a control. Cell colonies were counted using a Gel Count[®] cell colony counter (Oxford Optronix, Oxford, UK) with 100 μ m set as the minimal diameter to define a colony with each experiment repeated a minimum of three times with the four shSNX9 77 clones and shSNX9 78 clones pooled separately.

4.2.4 Role of SNX9 in TGF β induced growth arrest in epithelial cells

While TGF β induces anchorage-independent growth in a number of fibroblast cell lines, in many cells (including epithelial cells), it causes normally dividing cells in log phase growth to undergo an abrupt growth arrest (Howe 1991). Standard methods for detecting [³H] thymidine incorporation into DNA (described in Chapter 3) were utilized as a surrogate readout of cell division and growth. Three clones derived from NMuMg cells stably expressing shRNA against one region of SNX9 mRNA sequence (NMuMg shSNX9 77 clones) and two clones stably expressing shRNA against an alternative sequence in SNX9 (NMuMg shSNX9 78 clones) were assessed for cell growth after being cultured in the absence or presence of TGF β for two hours. Results presented are from a minimum of three independent experiments, each done in duplicate wells.

4.2.5 Role of SNX9 in the TGF β -induced transcriptional regulation of Smad2 and Smad3 responsive Genes

TGF β induces and represses a large number of genes (Koinuma 2009) and while Smad2 and Smad3 both bind SBEs with the same affinity (Yagi 1999) a subset of TGF β -induced genes appear to be exclusively regulated by Smad2 and another subset by Smad3 (Chen 1996). Goosecoid, MixL1 and Furin are three genes recognized as Smad2-dependent genes while Serpine (or PAI-1), Smad7 and CTGF are Smad3-dependent genes (Miyazono 2000). AKR-2B were grown in the absence or presence of TGF β for six hours before cell lysis and qRT-PCR analysis as described in Chapter 3 with primers listed in Appendix V. To further validate qRT-PCR data, AKR-2B cells expressing either endogenous or shRNA silenced levels of SNX9 were transiently transfected with one of three plasmids encoding the luciferin gene (described in Table

3.1). As well as a minimal promoter sequence, the promoters on these plasmids contained either; 1) the promoter sequence of the ARE gene (ARE-luc), 2) a major regulatory component of the Serpine (PAI-1) promoter (3TP-luc), or 3) six repeats of the Smad Binding Element (SBE-luc). While all 3 promoters contain Smad Binding Elements (and therefore have *in vitro* affinity for both Smad2 and Smad3), other elements within the promoters ensure ARE-luc is predominantly Smad2-dependent while 3TP-luc and SBE-luc are predominantly Smad3-dependent. Each well was also co-transfected with 0.5 μ g of pCMV- β -galactosidase for normalization of transfection efficiency. Following serum starvation (24 hr) cells were either left untreated (-) or stimulated (+) with 5 ng/ml TGF β for 24 hr and normalized luciferase activity determined by luciferase reporter assay, performed as described in Chapter 3. Results shown represent data pooled from a minimum of three independent experiments.

4.2.6 Western blotting and immunoprecipitation

Western blotting and co-immunoprecipitation was used extensively in this study and were performed as described in Chapter 3. Antibodies used and working dilutions are listed in Table 3.3 and antibody validation is documented in Appendix VI. Observed bands were referenced against known protein standard markers for size and, where possible, both positive and negative controls were run alongside experimental samples to ensure the correct interpretations were made. All experiments were performed in triplicate with representative blots included at an optimal exposure for qualitative assessment.

4.2.7 Isolation of SNX9/Smad protein complexes using GST-pull-down

In conjunction with co-immunoprecipitations, GST pull-downs were utilized to examine the association of SNX9 with Smads. Pull downs were performed as per standard procedure (Cold Spring Harbor Protocols) and outlined in Chapter 3. In preparation to perform experiments comparing the binding affinity of SNX9 to phosphorylated and non-phosphorylated Smads, purified Smad2 and Smad3 were phosphorylated *in vitro* (detailed in Chapter 3). Smads were incubated in conditions supportive of kinase activity in the presence of [γ -³²P]ATP, MgCl₂ and immunopurified myc-TGF β R1 (from transfected Cos7 cells that had been either unstimulated or stimulated with TGF β for 30 minutes –see Chapter 3 for details). After 30 minutes incubation, detection of Smad phosphorylation was determined by autoradiography. The ability of phosphorylated and

unphosphorylated GST-Smad proteins to bind to SNX9 in pulldown assays was then compared.

4.2.8 Isolating nuclear compartments to determine the role of SNX9 in trafficking of Smads into the nucleus

Smads are believed to traffic into the nucleus through the nuclear pore (Koopmann 2000, Xiao 2000, Xu 2002, Kurisaki 2006, Xu 2007, Yao 2008) although a role for the nuclear membrane has not been investigated. Unphosphorylated Smads remain soluble while phosphorylated Smads bind to DNA (Inman 2002, Xu 2002, Schmierer 2005). Nuclear fractions were obtained using using NE-PER™ Nuclear and Cytoplasmic Extraction Reagents (Pierce Biotechnology, Rockford, Illinois) as per manufacturer instructions. Crude nuclear pore complexes were isolated as described in Chapter 3, based on a protocol described by Aaronson and Blobel (Aaronson 1975, Aaronson and Blobel 1975). Nuclear membrane, nuclear soluble and chromatin-associated fractions were generated as per manufacturers' instructions utilizing NE-PER™ (Pierce Biotechnology, Rockford, Illinois) and Subcellular Protein Fractionation Kit for Cultured Cells (Thermo Fisher Scientific, Waltham, Massachusetts) with modifications described in Chapter 3.

4.2.9 Visualization of SNX9 and Smads using immunofluorescence microscopy

Standard Immunofluorescence staining and microscopy techniques were used as outlined in Chapter 3 to examine SNX9 and Smad co-localization and the role of SNX9 in Smad localization. Images were acquired using the LSM510 confocal microscope (Zeiss, Heidenheim, Germany) and quantification of fluorescent intensity and pixellation was achieved using MetaMorph® (Molecular Devices, Sunnyvale, California). Antibodies used and the working dilutions are reported in Table 2.3.

4.2.10 Generation of TAT-Smad fusion proteins

The transducing Trans-Activator of Transcription (TAT) domain from the Human Immunodeficiency Virus (HIV) is an 11 amino acid sequence (YGRKKRRQRRR) that enables proteins to cross bilayer membranes and enter cells when it is expressed at the carboxy terminus (Becker-Hapak 2001). In this way, protein (not plasmids or

viruses encoding protein) can be directly added to cells. The concentration of protein within the cells is directly quantifiable and isn't dependent on the transfection and/or expression efficiency of DNA-based methods of protein expression. Furthermore by knowing the exact concentration of protein introduced into cells, a comparison between more than one protein on a cellular effect is possible, as each protein can be added to the cells at a desired concentration. Dose response curves are straightforward as increases in the amount of protein added to cells are directly proportional to the concentration present within the cells. Modifications in DNA/viral expression vector amounts may lead to a complex and relatively inaccurate correlation with the observed protein concentrations within the cells (Becker-Hapak 2001).

One of the difficulties in drawing comparisons between unphosphorylated and phosphorylated Smads *in vivo* is that it is impossible to determine the percentage of unphosphorylated Smads that are phosphorylated by TGF β R1 after ligand addition. At no point are 100% of Smads phosphorylated so localization and association studies are difficult to interpret due to an unknown proportion of the two pools of Smads and how that influences the interpretation of data obtained. We sought to utilize the TAT system to bypass ligand and receptor phosphorylation of Smads, and instead introduce 100% unphosphorylated or 100% phosphorylated Smad3 at the same concentrations to cells, however a number of complications required addressing between protein purification and application to the cells. To facilitate immunoprecipitation of TAT-Smad3 and TAT-SNX9 fusion proteins from cell lysates, Smad3 or SNX9 were inserted into the MCS of pHA-TAT (Table 3.1). This plasmid also contains a His6 tag for use in metal affinity purification.

The high protein yielding BL21 (DE3) pLysS strain of *E.coli* (Promega, Madison, Wisconsin) was transformed with pSmad3-HA-TAT or pSNX9-HA-TAT and grown to an OD₆₀₀ of 0.4 before the addition of IPTG to a final concentration of 0.5 mM (to induce expression of the TAT protein) for a further 4 hours incubating at 37°C with agitation. After the 4 hour TAT protein induction, bacteria were collected, washed, and suspended in 15 ml 50 mM sodium phosphate buffer, pH 7.4, containing 300 mM NaCl and 20 mM imidazole. The cell suspension was sonicated and the lysate cleared by 12000 x g centrifugation at 4°C for 20 min. The supernatant was then poured into a TALON Metal Affinity Resin column (Clontech, Mountain View, California), washed with

50 mM sodium phosphate buffer containing 40 mM imidazole, and eluted with 150 mM imidazole for further processing before protein quantification and addition to cells.

4.2.11 Isotope labelling of unphosphorylated and phosphorylated TAT-Smad proteins

Before nuclear entry and retention rates of phosphorylated versus unphosphorylated Smad3 could be compared, purified TAT-fused Smad3 proteins required a number of modifications prior to addition to cells. Firstly, because cells have endogenous Smads, we needed to introduce Smads that could be distinguished from the endogenous pool, and secondly, because TAT-fused Smads were generated in bacteria (with no TGF β receptors) obtaining phosphorylated Smads required a process of *in vitro* phosphorylation of the specific residues targeted by activated TGF β R1 after purification.

To distinguish the TAT-fused Smads from endogenous Smads, we radio-labelled 100 μ g of TAT-Smad proteins with 125 Iodine (Perkin Elmer, Waltham, Massachusetts) by Bolton-Hunter reaction. In this way, the levels of recombinant (and not endogenous) Smad3 in whole cell and nuclear lysates could be assessed with high precision by gamma counter (125 Iodine decays by gamma decay with a half-life of 59.43 days).

To generate traceable phosphorylated TAT-Smad3, 50 μ g of 125 I-labeled TAT-Smad3 was incubated in kinase buffer containing 5 μ M ATP, 20 μ Ci [γ - 32 P]ATP per μ l and activated myc-TGF β R1 (purified from TGF β stimulated Cos7 cells transfected with plasmids carrying myc-TGF β R1 and HA-TGF β R2 as described in Chapter 3). Removal of free [γ - 32 P]ATP was achieved by dialysis in phosphate buffered saline (PBS) containing 1mM EDTA and DTT for 4-6 hours at 4°C with two rounds of buffer exchange.

4.2.12 Determining Smad3/pSmad3 nuclear entry kinetics using TAT-Smad3

Having generated 125 I-labelled TAT-Smad3 and phosphorylated TAT-Smad3 proteins that could be distinguished from endogeneous Smads, we next sought to compare the kinetics of nuclear entry of the phosphorylated and unphosphorylated forms of Smad3 and determine if SNX9 is involved in any aspect of the process.

Confluent AKR-2B cells in 24-well plates were exposed to 0.8 μ M TAT-Smad3 or TAT-pSmad3 at time 0. At interspersed time-points, cells were washed twice with binding buffer (0.2M HEPES, 2.5% BSA in DMEM pH7.4) containing 75% horse serum and twice with PBS before normalizing for cell number and split into two samples. Total intracellular TAT-protein was determined by cell lysis (0.2 M NaOH, 40 mg/ml salmon sperm DNA), while nuclear TAT-protein was determined from nuclear fractions obtained using NE-PERTM Nuclear extraction kit (Pierce Biotechnologies, Rockford, Illinois) prior to nuclear lysis in 0.2 M NaOH, 40 mg/ml salmon sperm DNA (Life Technologies, Grand Island, New York). Both ¹²⁵I (indicating the presence of TAT-Smad3 in whole cell and nuclear lysates) and ³²P (indicating phosphorylated TAT-Smad3) counts were obtained by gamma or beta scintillation counters respectively. Nuclear Smad values were normalized against the level of TAT-Smad3 entering the whole cell lysate, to compensate for possible differences in TAT-Smad3 cellular and nuclear rates into the cell.

4.2.13 SNX9/pSmad3 binding to lipid membranes

SNX9 dimers bind to phosphoinositides-2-phosphates (PIP2) at the plasma membrane and early endosomes during endocytosis of receptors such as transferrin and EGFR (Childress 2006, Lundmark 2009). To determine if SNX9 complexes containing Smads, similarly bind to lipid membranes containing PIP2 in TGF β signalling, we modified an assay described by Song *et al* (Song 2004, Yazar 2004). Essentially microsomes are generated that contain PIP2 (or control microsomes without PIP2) and these are incubated with whole cell lysates in the presence of ³²P-labelled pSmad3. Because SNX9/Smad3 complexes (and not SNX9 alone) were of interest (neither pSmad3 nor SNX9 bind nuclear membranes alone), we indirectly measured the binding of SNX9/pSmad3 to liposomes by tracking the ability of ³²P-pSmad3 to bind the artificial liposomes in the presence or absence of SNX9, or SNX9 mutants bearing mutations (Mut^{PIP2} and Δ 13C).

Microsomes were generated by taking 76 μ l of a 10 mg/ml stock of egg yolk phosphatidyl choline (Calbiochem, San Diego, California) in chloroform and mixing with or without 110 μ l of the specific PIP2, porcine brain PI4,5P2 (1 mg/ml; Avanti Polar Lipids, Alabaster, Alabama) with gentle agitation for 2 minutes. The chloroform was

evaporated under nitrogen and the lipids suspended in 2.5 ml Lipid Suspension Buffer (50 mM HEPES (pH 7.5), 150 mM KCl).

Cell lysates (AKR-2B with endogenous SNX9 silenced, alone or with escape WT, Mut^{PIP2}, or Δ 13C mutants transfected) were obtained by French Press Lysis (2X) operated at 16,000 lb/in², chilling the cell suspension to 4°C after each pass, and collecting in a HEPES Liposome Buffer (Appendix IV). 3 μ g of ³²P-Smad3-GST was incubated in 250 μ l of liposome solution and for 10 min with lysates, prior to fractionation of the liposomes by discontinuous sucrose density gradient centrifugation. The gradient was formed with a base of 700 μ l liposome suspension mixed with 1.3 ml of 64% (w/w) sucrose (final liposome suspension ~40% sucrose) was generated and the suspension was layered with 37.0, 32.5, 29.5, 25.1, 21.0, 17.2, 13.4, and 9.0% (w/w) sucrose solutions. Following ultracentrifugation for 3 hours at 160000 x *g* at 4°C, the opaque fractions were collected (liposomes) and the amount of TAT-pSmad3 associated with the liposomes was determined by ³²P counts obtained by beta counter scintillation.

4.2.14 Determination of Dynamin GTPase activity

During endocytosis at the plasma membrane, SNX9 recognizes the curvature of forming endocytic vesicles (Cullen 2008, Lundmark 2009). However the formation of endocytic vesicles requires scission of the encapsulating vesicle membrane from the parental membrane and this scission is performed by the pinchase, Dynamin (Childress 2006). Dynamin itself cannot bind membranes, and is recruited to forming vesicles via SNX9, and in the absence of SNX9 the GTPase activity required for vesicle scission in Dynamin is not activated (Cullen 2008, Lundmark 2009). In order to compare and contrast the effects of SNX9 mutations on both endocytosis (i.e. Dynamin-mediated) effects and Smad3 nuclear translocation effects we sought to first determine the impacts of SNX9 mutations in Dynamin GTPase activity. Cells were lysed and incubated with SNX9 antibody (See Table 3.3 for antibody details and working dilution) overnight at 4°C. Immune complexes were precipitated by addition of Agarose G beads for 1 hr at 4°C, washed 3X with cold PBS, and bound proteins eluted with 50 mM Glycine (pH 2.7). Dynamin GTPase activity was performed as described by Leonard et al. (Leonard 2005) with some modifications. Briefly, 4 μ l eluted protein was incubated in 192 μ l GTPase assay buffer (20 mM HEPES-KOH, pH 7.5, 150 mM

KCl, 2 mM MgCl₂, 1 mM DTT) to which 4 µl GTP stock solution (100 mM GTP, 20 mM Hepes, pH 7.4) was added. Dynamin activity results in GTP hydrolysis and production of free inorganic phosphate which can be detected with a Malachite Green Assay. This assay relies on the complex that forms between malachite green molybdate and free inorganic phosphate in acidic conditions. Malachite green molybdate in solution is yellow, but in the presence of free inorganic phosphate, the solution turns to a green colour (Childress 2006) Following 10 min at room temperature, 100 µl was transferred to a 96 well microtiter plate containing 5 µl 0.5M EDTA (pH 8.0) to stop the reaction. An equal volume (100 µl) of Malachite Green stock solution (1 mM Malachite Green, 10 mM ammonium molybdate in 1 N HCl) was added to each well and GTPase activity measured by absorbance at 650 nm using a microplate reader.

4.3 RESULTS

4.3.1 Sorting Nexin 9 Specifically Regulates Smad3-dependent TGFβ Signalling

TGFβ was isolated and characterized by its ability to stimulate anchorage-independent growth (AIG) of anchorage-dependent fibroblasts (Moses 1981, Roberts 1981). As an *in vitro* correlate of transformation, AIG remains unmatched and is accessed by the ability of cells to divide and form extensive colonies while suspended in a gelatinous, soft agar. As shown in Figure 4.3A, when soft agar colony formation was assessed in multiple AKR-2B clones expressing two distinct SNX9 shRNAs although basal growth was unaffected by either treatment, ligand-induced AIG was reduced to control (i.e. unstimulated) levels. Knockdown of SNX9 expression in AKR-2B fibroblasts using these two different shRNAs is shown in Fig 4.4A. Identical findings were observed using stable NMuMg epithelial cell lines expressing wild-type (WT)-SNX9 and dominant negative (DN)-SNX9 constructs (Fig 4.4A).

In contrast to promoting mesenchymal cell proliferation, a number of epithelial cell types have been reported to undergo a late G1 phase growth arrest upon TGFβ treatment (Howe 1991). In these studies actively dividing cells in the presence of multiple mitogens (including serum) are over-ridden by TGFβ with growth rates inhibited in excess of 80-90% relative to non-TGFβ stimulated cultures. Similar to our observations in fibroblast AIG assays, DNA synthesis in the NMuMg mammary

epithelial cell line was inhibited ~80% by TGF β in the non-targeting (NT) shRNA clones while SNX9 KD significantly abrogated the growth inhibitory response (Figs 4.3B).

Anchorage independent growth and the failure of cells to recognize growth arrest cues are phenotypes associated with cellular transformation and are the two primary TGF β phenotypes modulated in fibroproliferative and carcinoma progression (Shi and Massagué 2003, Attisano and Wrana 2002) Because both were dependent upon SNX9 we next investigated whether Smad transcriptional responses displayed a similar SNX9 requirement. qPCR evaluation of three endogenous Smad2- or Smad3-responsive genes was undertaken in AKR-2B control or lines expressing SNX9 shRNA and while none of the Smad2-responsive genes were inhibited, a marked reduction in each of the Smad3-responsive genes was observed (Fig 4.3C). In fact, for two of the three Smad2-responsive genes there was a statistically significant increase with reduced SNX9; likely reflecting positive and negative actions of Smad2 and Smad3 respectively (Labbe 1998). Since this was quite surprising, the response of the aforementioned AKR-2B lines expressing SNX9 shRNA or DN vectors to a transiently transfected Smad3 (3TP or SBE) or Smad2 (ARE) luciferase construct (Figs 4.4C and 3.4D) was examined. As seen with the qPCR studies, these studies showed an approximate 50-70% reduction from both Smad3-dependent reporters, yet no effect on Smad2-regulated ARE signalling.

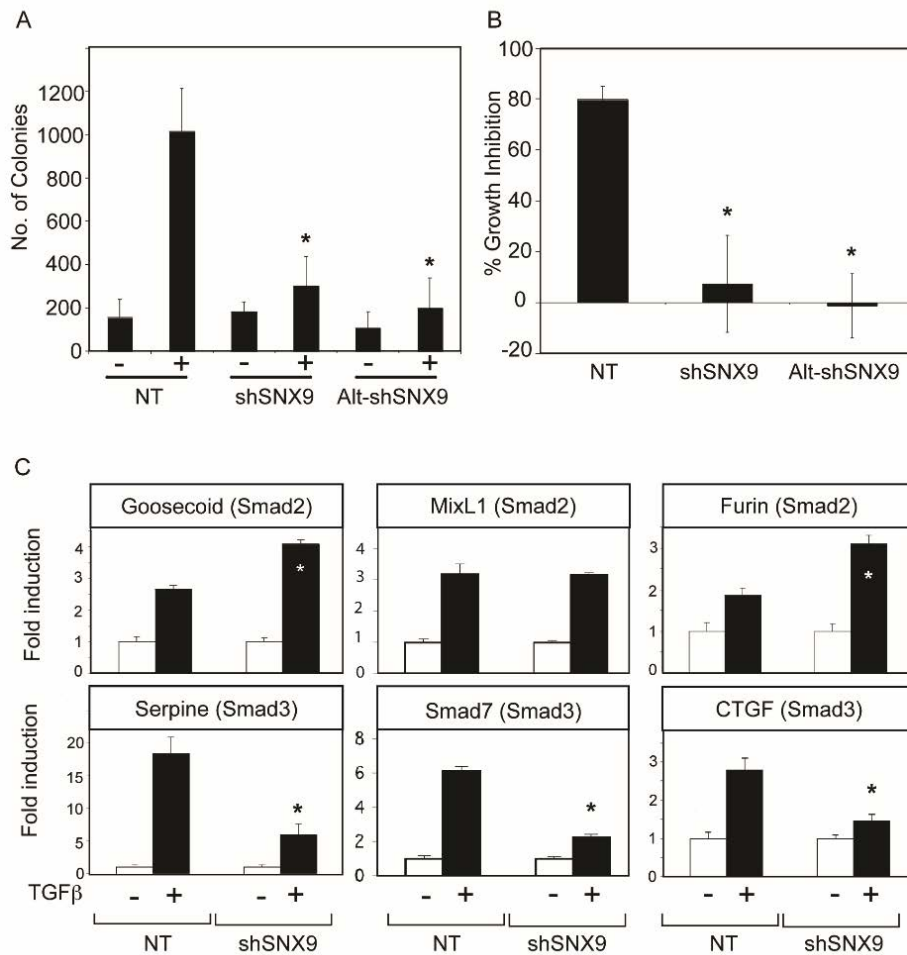


Figure 4.3 SNX9 regulates soft agar colony formation, growth inhibition, and Smad3-dependent transcriptional activity. (A) AKR-2B cells stably integrated with non-targeting (NT) or SNX9 shRNA were seeded in soft agar in the absence (-) or presence (+) of 10 ng/ml of TGFβ. Data depict the number of colonies >100 μm ± SD on day 10 from 2 pooled NT (A-NT.8 and A-NT.10), 4 pooled SNX9 shRNA1 (shSNX9; A-77.1, A-77.2, A-77.7, and A-77.11), and 4 pooled SNX9 shRNA2 (Alt-shSNX9; A-78.1, A-78.2, A-78.5, and A-78.6) clones. * indicates significant difference (defined as p<0.05 for all studies) from NT+. SNX9 knockdown is shown in Figure 3.4A and Appendix VIII provide statistical analysis for Chapter 4. (B) The growth inhibitory response to TGFβ in NMuMg cells infected with non-targeting or SNX9 shRNA lentiviruses was determined as described in Chapter 3. Data reflect the pooled % growth inhibition from 3 independent experiments ± SD of 2 pooled NT (M-NT.8 and M-NT.10), 3 pooled SNX9 shRNA1 (shSNX9; M-77.1, M-77.8, and M-77.9), and 2 pooled SNX9 shRNA2 (Alt-shSNX9; M-78.2 and M-78.6) clones. Negative numbers reflect proliferation and * indicates significant difference from NT. (C) A-77.7 cells stably expressing shRNA for SNX9 were arrested and treated (+) for 6 hr with TGFβ. Total RNA was prepared and processed for qPCR analysis using primers for Goosecoid, MixL1, Furin (Smad2-dependent) or Serpine (PAI1), Smad7, CTGF (Smad3-dependent). GAPDH was used as a negative control and total RNA from AKR-2B cells expressing non-targeting (A-NT.8) shRNA similarly treated with TGFβ used as a positive control. * denotes significant difference from NT+. Data reflect the fold induction (normalized to GAPDH) above unstimulated NT controls ± SD.

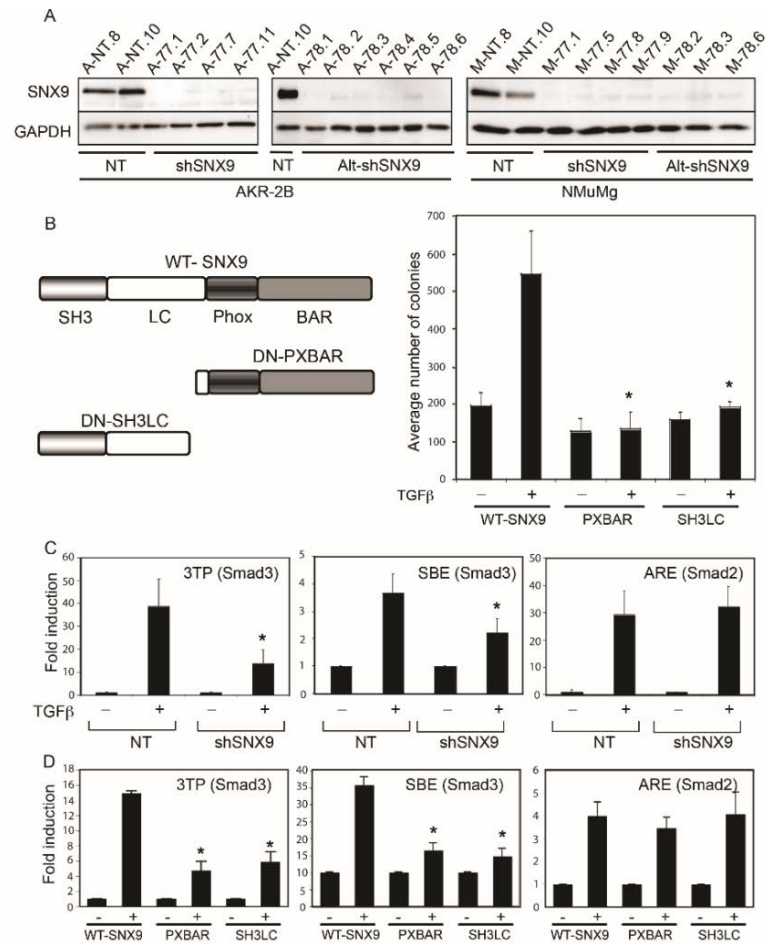


Figure 4.4 SNX9 knockdown and dominant negatives distinguish Smad3 from Smad2 responses. (A) AKR-2B cells were infected with non-targeting (NT), SNX9 shRNA1 (shSNX9), or SNX9 shRNA2 (Alt-shSNX9) lentiviruses. Following stable clone selection knockdown level was analyzed by Western blotting for SNX9 and loading verified with GAPDH. The specific clones used are stated in each figure legend. (B) Left panel: Cartoon depicting the domain structure of wild-type (WT) and dominant negative (DN) SNX9 constructs. SNX9 consists of a SH3 domain (known to bind proline rich sequences such as in dynamin2, WASp, and Cdc42-associated kinase 2), a low complexity region (LC; binds clathrin and AP2), a Phox homology domain (PX; binds phosphatidylinositol-3-phosphate), and a Bin/Amphiphysin/Rvs domain (BAR; dimerization and membrane binding module able to sense membrane curvature) (Worby and Dixon 2002, Carlton, Bujny 2005). Right panel: Wild-type (WT-SNX9, clone SNX9.1) and dominant negative SNX9 (SH3LC, clone SH3LC.2; and PXBAR, clone PXBAR.6) expressing A105 cells (AKR-2B cells with chimeric and native TGFβ receptors; (Anders and Leof 1996) were seeded for soft agar in the absence (-) or presence (+) of 10 ng/ml of TGFβ. Each bar represents the mean number of colonies >100 μm ± SD on day 10 from three independent experiments. * denotes statistical significance (defined as p<0.05) between stimulated WT and PXBAR and SH3LC clones. Appendix VIII contains statistical analysis. (C) NT or SNX9 knockdown AKR-2B cultures were transiently transfected with the indicated Smad3 (3TP and SBE) or Smad2 (ARE) regulated luciferase reporters. Each well was also co-transfected with 0.5 μg of CMV-β-galactosidase for normalization of transfection efficiency. Following serum starvation (24 hr) cells were either left untreated (-) or stimulated (+) with 5 ng/ml TGFβ for 24 hr and normalized luciferase activity determined. Data are from three independent experiments for each cell type (A-NT.8 and pooled data from A-77.7 and A-77.11 clones) and represent the mean fold induction ± SD relative to untreated. * indicates statistical significance between stimulated NT and KD cultures. (D) A105 cells stably expressing WT or the indicated DN SNX9 constructs were transiently transfected with Smad3 (3TP or SBE, left or middle panels) or Smad2 (ARE, right panel) regulated luciferase reporters along with 0.5 μg of CMV-β-galactosidase. Cultures were serum starved for 24 hr and either left untreated (-) or stimulated (+) with 5 ng/ml TGFβ for 24 hours and normalized luciferase activity determined. Each bar represents the mean fold induction relative to untreated ± SD of three clones (WT-SNX9.1, WT-SNX9.4, WT-SNX9.6; DN-PXBAR.6, DN-PXBAR.28, DN-PXBAR.22; DN-SH3LC.2, DN-SH3LC.24, DN-SH3LC.34) from two independent experiments.

4.3.2 SNX9 required for Smad3 but not Smad2 nuclear translocation

SNX9 is essential for clathrin-dependent (as well as fluid phase) endocytosis of various cargo (Lundmark 2009). Since TGF β -stimulated Smad2/3 phosphorylation occurs downstream of dynamin action (Hayes 2002, Di Guglielmo 2003), it seemed reasonable that SNX9 might modulate TGF β signalling through specific inhibition of Smad3 phosphorylation. Contrary to our expectations, no statistically significant difference in either the kinetics or extent of R-Smad phosphorylation was observed in SNX9 KD or DN clones relative to control (Figs 4.5A, 4.5B, and 4.6A). As the current model for Smad signalling proposes that R-Smad phosphorylation enhances their nuclear accumulation (Feng 2005, Schmierer 2007, Hill 2009), we next investigated whether SNX9 was required for Smad3 nuclear translocation.

As shown in Figure 4.5C, while SNX9 loss significantly reduced nuclear pSmad3 levels at all time-points, nuclear pSmad2 was unaffected. Quantitation of this response demonstrated an approximate 70% decrease in the nuclear accumulation of pSmad3 with no appreciable effect on pSmad2 or basal nuclear R-Smads (Fig 4.5D). Suggesting a sorting nexin plays a role in the nuclear translocation of a protein is a significant deviation from our current understanding of the role of sorting nexin proteins. To further strengthen our conclusions using SNX9 KD cells, we examined the ability DN-SNX9 constructs to impact Smad3 nuclear delivery. Consistent with that observed in the KD cells, each DN-SNX9 construct specifically prevented ligand stimulated Smad3 nuclear delivery but not Smad2 (Fig 4.6B and Fig 4.6C).

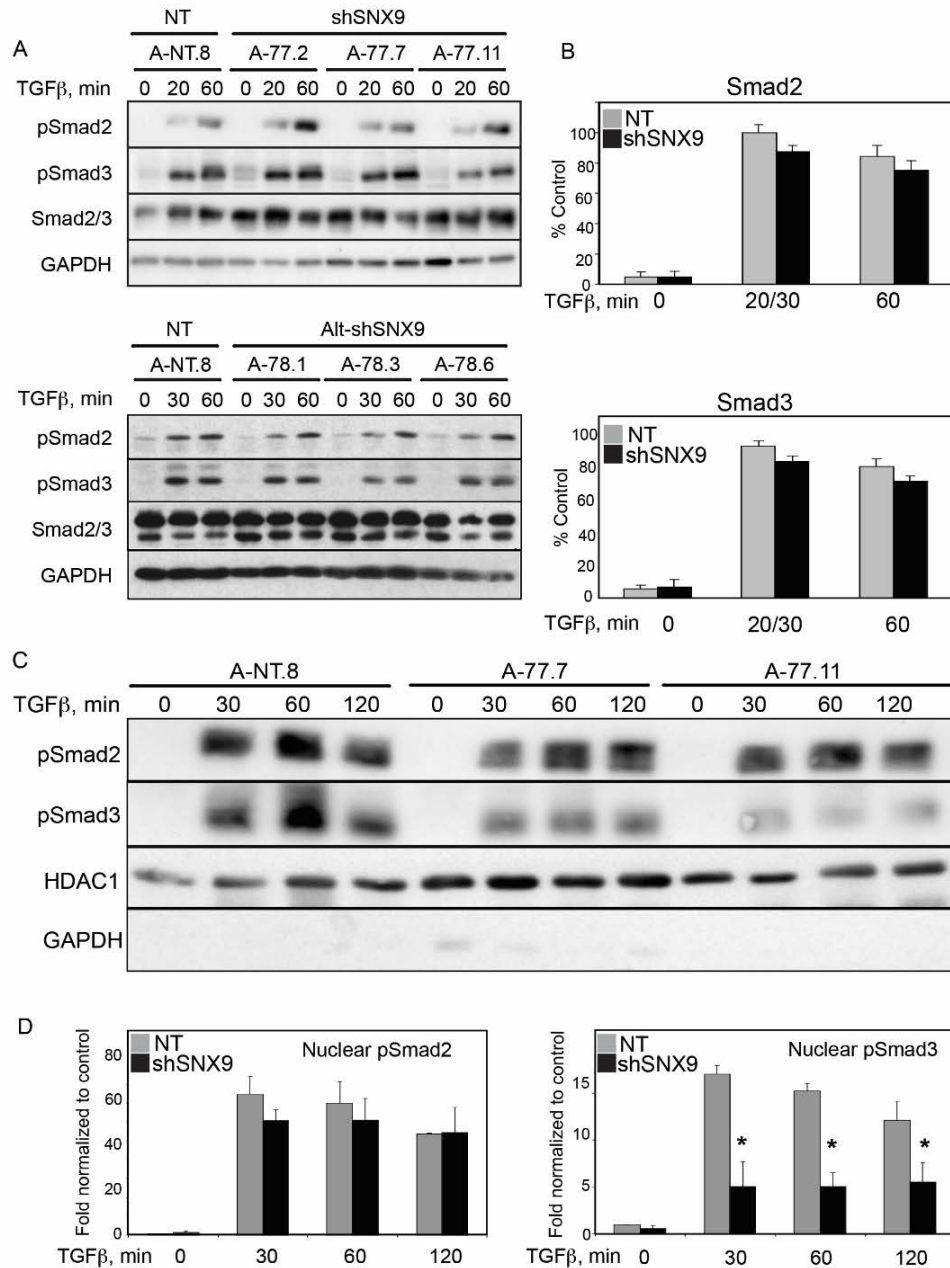


Figure 4.5 SNX9 functions downstream of R-Smad phosphorylation. (A) AKR-2B clones expressing non-targeting (NT) or the indicated SNX9 shRNA were left untreated (0) or stimulated with 5 ng/ml TGFβ for 20 (top), 30 (bottom) or 60 (both) min.. Western analysis was performed on 50 μg cell lysate for the indicated phospho (pSmad2, pSmad3) or total (Smad2/3, GAPDH) protein. (B) Quantitation of pSmad2 or pSmad3 at each time compared to NT and normalized to GAPDH. The 20 and 30 min time points shown in (A) for the 2 shRNAs were pooled and are presented as 20/30. (C) AKR-2B clones expressing non-targeting (A-NT.8) or SNX9 shRNA (A-77.7 and A-77.11) were either left untreated (0) or stimulated for the indicated times with 5 ng/ml TGFβ. Nuclear extracts were prepared and 30 μg Western blotted for pSmad2, pSmad3, HDAC1 (nuclear marker) or GAPDH (cytoplasmic marker). (D) Quantitation of nuclear R-Smad. Results are presented as the fold increase (normalized to the corresponding HDAC1 intensity) in nuclear Smad2 or Smad3 phosphorylation at the indicated times. The pSmad signal observed at time 0 in A-NT.8 cells represents 1.0. Data are the mean ± SD on each cell line and the SNX9 knockdown results are presented as the pooled response from A-77.7 and A-77.11. * denotes significant deviation from NT at same time point. See also Appendix 3.5.

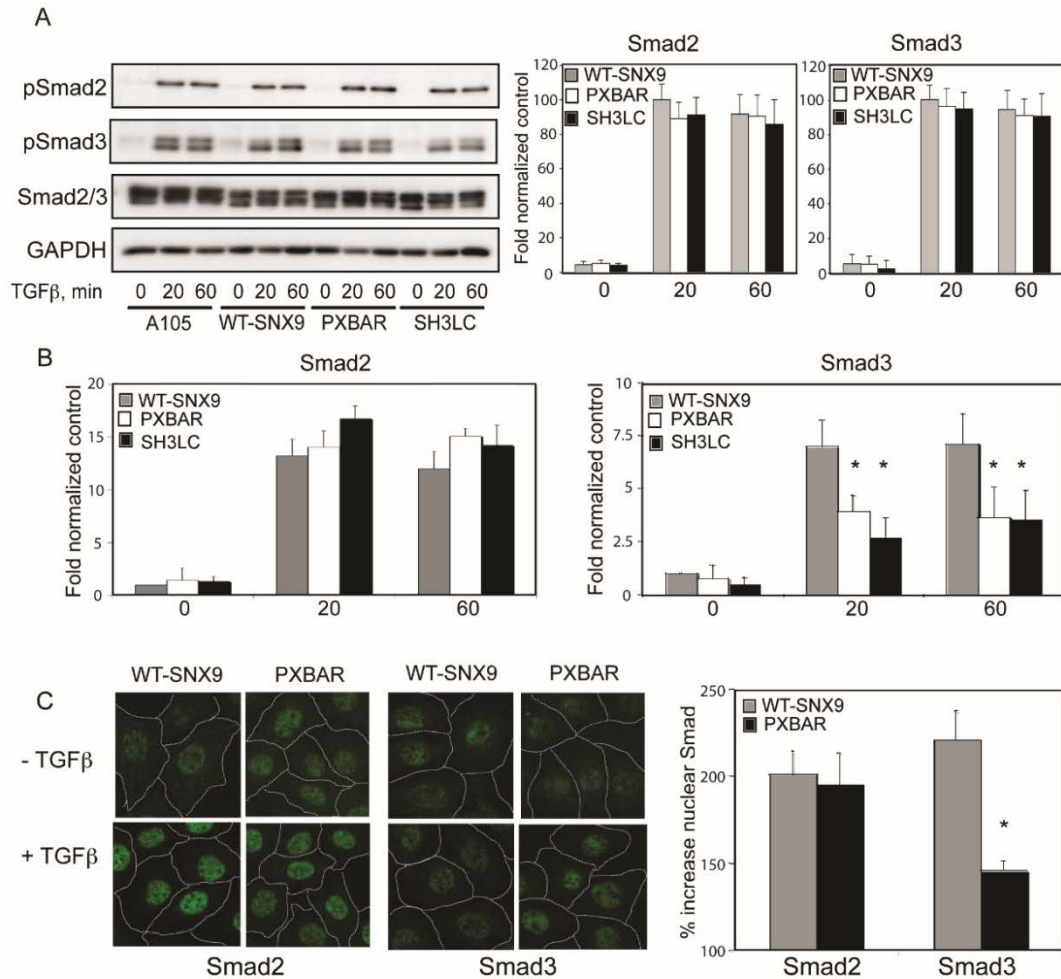


Figure 4.6 Smad2 and Smad3 phosphorylation is unaffected by dominant negative SNX9. (A; left panel) Parental A105 cells or A105 clones stably transfected with wild-type (WT-SNX9.1) or dominant negative (DN-PXBAR.6 and DN-SH3LC.2) SNX9 were left untreated (0) or stimulated with 5 ng/ml TGFβ for 20 or 60 min. Western analysis was performed on 50 μg cell lysate for the indicated phospho (pSmad2, pSmad3) or total (Smad2/3, GAPDH) protein. (A; right panels) Quantitation of pSmad2 or pSmad3 levels normalized to GAPDH. No statistically significant effect on R-Smad phosphorylation was observed with either DN-SNX9 construct. (B) Wild-type (WT-SNX9.1) and dominant negative (DN-PXBAR.6 and DN-SH3LC.2) SNX9 expressing A105 clones were processed for nuclear Smad3 and Smad2, respectively, as described in Figure 3.5. Data reflect the mean ± sd from 3 separate studies and * denotes statistical significant difference between WT- and DN-SNX9 for Smad3 at each time point. (C; left panels) Wild-type (WT-SNX9.1) or dominant negative (DN-PXBAR.6) SNX9 clones were grown to confluence on coverslips and either left untreated or stimulated for 45 minutes with 5 ng/ml TGFβ. Cells were fixed and stained with primary antibody to total Smad2 or phospho-Smad3 and AF488-conjugated goat anti-rabbit secondary antibody. (C; right panel) Each bar represents the mean fold increase in nuclear fluorescent intensity stimulated by TGFβ ± SD from three independent experiments using Metamorph in WT-SNX9.1 or DN-PXBAR.6 cells. * denotes statistical significance of Smad3 nuclear inhibition for DN-PXBAR compared to WT-SNX9. Analogous results were observed with DN-SH3LC (not shown).

4.3.3 SNX9 specifically impacts phosphorylated Smad3 nuclear entry

In both the absence and presence of TGF β , Smad proteins shuttle between the cytoplasm and nucleus (Inman 2002, Xu 2002, Schmierer 2005). While it has been suggested that R-Smad nuclear accumulation is due primarily to retention of phosphorylated over non-phosphorylated R-Smads (Schmierer 2007, Varelas 2008), other studies have also observed increased rates of R-Smad nuclear trafficking in stimulated versus unstimulated cells (Kurisaki 2001, Schmierer 2008).

To address these issues *in vivo* without the complication of unknown ratios of unphosphorylated to phosphorylated Smad3 produced after ligand stimulation, we generated a Smad3 construct fused to the cell transducing Trans-Activator of Transcription (TAT) domain from the Human Immunodeficiency Virus (HIV) (Becker-Hapak 2001), labeled the purified protein with ¹²⁵I, and phosphorylated half with the immunopurified/activated type I TGF β receptor (T β RI). After normalizing for initial cellular uptake (Fig 4.8, we observed clear differences in both the kinetics of nuclear import as well as retention between TAT-pSmad3 and TAT-Smad3 (Fig 4.7; top panel). For instance, while half maximal nuclear translocation of pSmad3 occurred within ~20 min, unphosphorylated Smad3 was ~3.5 times slower. Furthermore, consistent with a role for Smad phosphorylation in also enhancing nuclear retention, the rate of pSmad3 and Smad3 nuclear loss was 28.6 counts per minute (cpm) and 235.7 cpm, respectively, which was unaffected by SNX9 KD (i.e., corresponding rates of 26.6 cpm and 211.8 cpm). Of particular relevance and consistent with the western blot/immunofluorescent analyses shown in Figures 4.4C, 4.4D, 4.5B, and 4.5C, while SNX9 loss had no appreciable effect on unphosphorylated TAT-Smad3 (i.e., basal shuttling), it significantly inhibited TAT-pSmad3 nuclear accumulation (Fig 4.6A; middle and bottom panels, respectively).

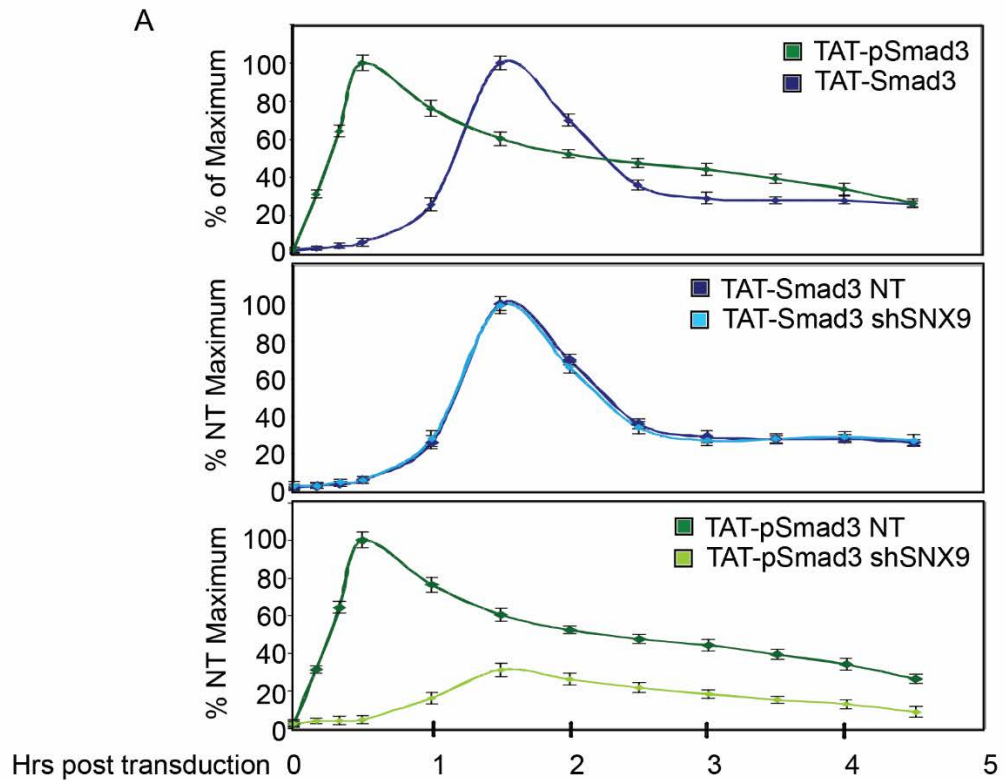


Figure 4.7 SNX9 is required for enhanced pSmad3 nuclear entry. (A) ^{125}I labeled TAT-Smad3 and TAT-pSmad3 proteins were generated as described in Chapter 3. AKR-2B cells expressing non targeting (NT) shRNA (A-NT.8) or shRNA against SNX9 (shSNX9; A-77.7) were transduced with the indicated TAT peptides and ^{125}I counts in total cell and nuclear lysates obtained from 10-270 min. Nuclear counts were normalized to total cell counts (i.e., to account for the time delay in TAT-protein transduction; Fig. 3.8) and maximal counts in NT cells were defined as 100%. Top panel. Kinetics of nuclear entry and retention of TAT-Smad3 (i.e., basal shuttling) and phosphorylated (p) TAT-pSmad3 (i.e., ligand activated) in A-NT.8 cells. Middle panel. Effect of shSNX9 on the kinetics of unphosphorylated TAT-Smad3 nuclear import and retention in A-NT.8 and A-77.7 cells. Bottom panel. Effect of shSNX9 on the kinetics of phosphorylated TAT-Smad3 nuclear import and retention in A-NT.8 and A-77.7 cells. Data reflect the mean \pm SD from 3 experiments for the 30-240 min time points and 2 experiments for the 10, 20, and 270 min time points. Raw and normalized ^{125}I and ^{32}P TAT-Smad3 cell transduction counts are provided in Fig 3.8.

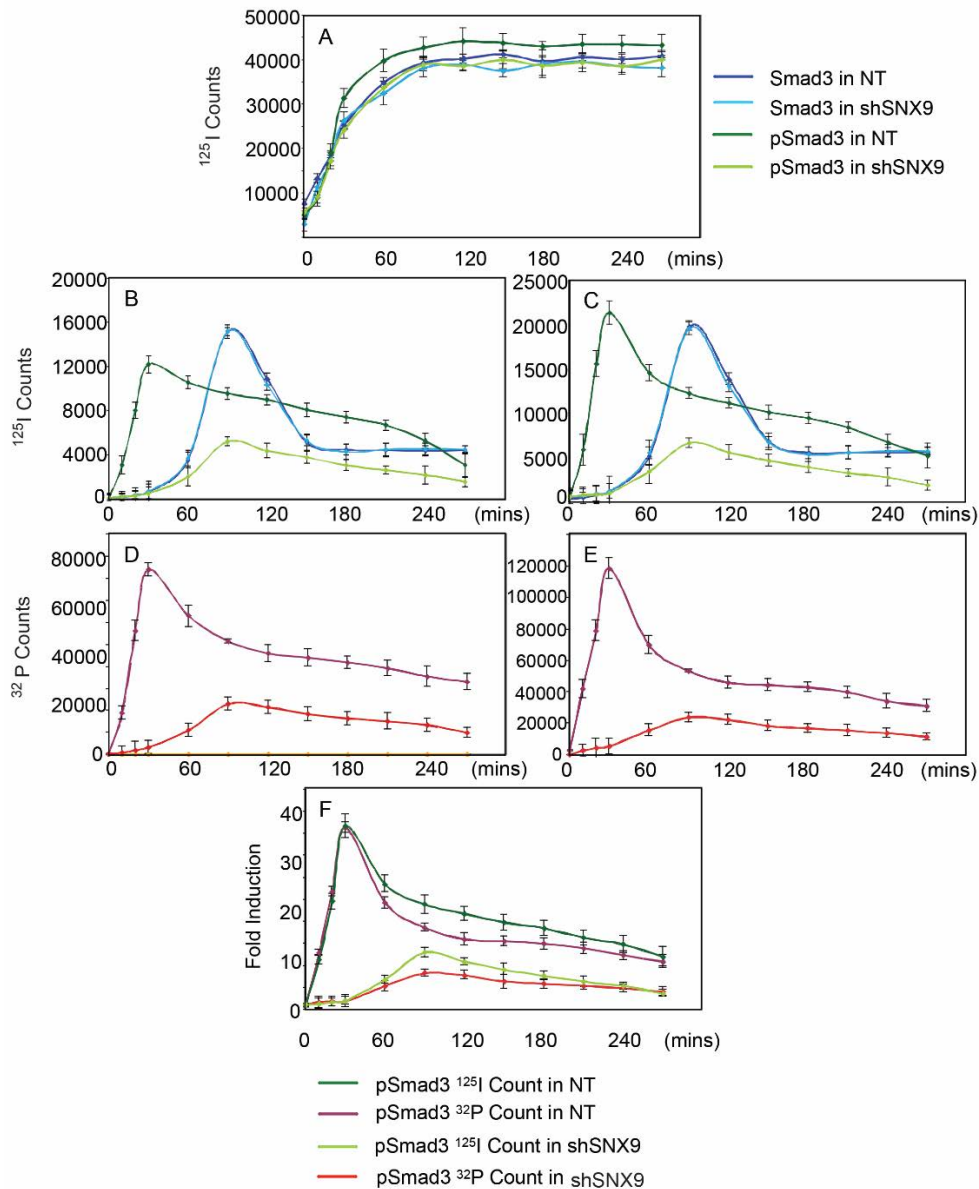


Figure 4.8 Differing kinetics of nuclear entry between phosphorylated and unphosphorylated Smad3. ^{125}I labeled TAT-Smad3 and phosphorylated (^{32}P) TAT-Smad3 proteins were generated as described in Chapter 3. (A) AKR-2B cells expressing non-targeting shRNA (NT; A-NT.8) or shRNA against SNX9 (shSNX9; A-77.7) were transduced and ^{125}I incorporation in total cell lysates determined at the indicated times. (B) ^{125}I incorporation in nuclear lysates from cultures as in (A). (C) Nuclear counts in (B) at each time point normalized to maximal cell transduction observed in (A). (D) Nuclear ^{32}P counts from NT and shSNX9 cells transduced with TAT-pSmad3. (E) Normalized nuclear ^{32}P incorporation to maximal cell transduction observed in (A). (F) To document that ^{125}I and ^{32}P were assessing the same populations of TAT-Smad3 peptides (i.e., the delayed nuclear uptake of ^{125}I pSmad3 in shSNX9 cells observed in (B) was not due to a sub-population of nonphosphorylated TAT-pSmad3 molecules), the ^{125}I and ^{32}P counts shown in (C) and (E), respectively, were normalized to their fold induction to allow direct comparison. Data reflect the mean \pm SD from 3 experiments for the 30-240 min timepoints and 2 experiments for the 10, 20, and 270 timepoints.

4.3.4 SNX9 preferentially binds phosphorylated Smad3

As our data define a role for SNX9 in mediating Smad3 nuclear transport, we addressed the following mechanistic questions. *Firstly*, does SNX9 show differential R-Smad binding, is this regulated by ligand, and is there any identifiable role for Smad4; *secondly*, is SNX9 required for karyopherin and/or nucleoporin binding to Smad3 and; *thirdly*, how does SNX9 function to promote pSmad3 nuclear import?

To investigate the first of these issues, AKR-2B cells were stimulated with TGF β and the ability of SNX9 to co-immunoprecipitate (co-IP) Smad2 or Smad3 determined. While a slight basal association with Smad3 was observed consistent with the phospho-Smad3 levels at time 0, addition of ligand significantly enhanced the interaction (Fig 4.9A). In contrast, no binding of SNX9 and Smad2 could be detected basally or following TGF β treatment. Although these findings clearly show that a SNX9/Smad2 association cannot be observed in cultured cells, they do not address the alternative possibility that Smad2 has a role in promoting and/or enhancing SNX9/Smad3 binding. Evidence that this is not the case is provided by the data presented in Figure 4.10A where the association of SNX9 with Smad3 was assessed in both Smad2 as well as Smad3 null cultures. In the absence of Smad2 there was similar ligand-dependent SNX9/Smad3 binding as that seen in AKR-2B cells, regardless of the order by which the immunoprecipitation/Western blotting analysis was performed.

Since the association of SNX9 with pSmad3 is unexpected, we further documented this result by: (i) determining whether similar findings were observed with Glutathione S-transferase (GST)-Smad proteins; (ii) assessing the SNX9/pSmad3 relationship in multiple cell types and; (iii) addressing the role (if any) of Smad4. GST-Smad2 or – Smad3 fusion proteins were either used directly or following *in vitro* phosphorylation by the TGF β activated TGF β R1 in pull-down assays for SNX9. Analogous to what we observed by co-IP (Fig 4.9A and Fig 4.10A), significant SNX9/R-Smad binding was only observed with phosphorylated GST-Smad3 (Fig 4.9B top panel, lane 5). This association was further documented in 4 additional cell lines (i.e., 2 mesenchymal and 2 epithelial) using GST-SNX9 in pull-down assays for Smad3. As shown in Figure 4.9C, TGF β enhanced GST-SNX9/Smad3 binding in all cell lines coincident with increased Smad3 phosphorylation.

Since the canonical model of R-Smad nuclear translocation has Smad4 present to generate the most energetically favorable heterotrimer (Wu 2001, Chacko 2004), we next investigated the relation and/or requirement for Smad4 in the formation of the pSmad3/SNX9 complex following TGF β stimulation (Fig 4.10B and Fig 4.10C, respectively). In agreement with earlier publications showing that Smad4 is dispensable for R-Smad nuclear accumulation in response to TGF β (Wu 2001, Chacko 2004, Massagué 2005, Schmierer 2007, Hill 2009), no identifiable role for Smad4 was observed.

While Figures 4.3-10 clearly show a pSmad3/SNX9 interaction, this was further confirmed using immunofluorescent microscopy in multiple murine and human cell lines (Fig 4.11A, and 4.11B, and Fig 4.12). The increased co-localization ranged from 2.6 fold (NIH3T3) to 8.5 fold (NMuMg) with a significant increase observed in all lines. Thus, using multiple cell lines and various independent approaches, these findings document that: (i) SNX9 primarily binds phosphorylated Smad3; (ii) binding is independent of and unaffected by either the presence or absence of Smad2 or Smad4 and; (iii) SNX9 is required for Smad3-dependent (not Smad2) transcriptional responses and phenotypes.

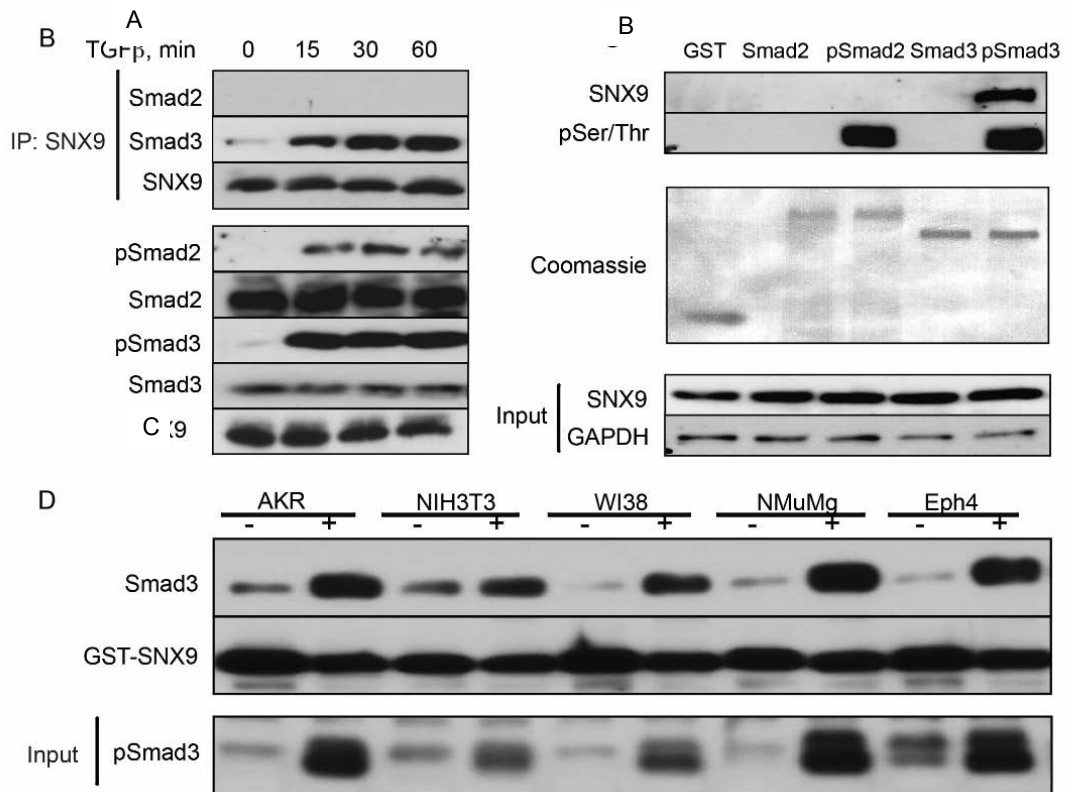


Figure 4.9 SNX9 specifically binds pSmad3 but not pSmad2. (A) AKR-2B cells were stimulated with 5 ng/ml TGF β and harvested at the indicated times. Following cell lysis and SNX9 immunoprecipitation (IP; top 3 panels), the indicated co-precipitating proteins were detected by Western blotting. Bottom 5 panels: total lysate was Western blotted for the indicated proteins. (B). AKR-2B lysates were incubated with GST or GST-Smad fusion protein untreated or *in vitro* phosphorylated by TGF β RI as described in Chapter 3. Bound SNX9 (top panel) and the phosphorylated R-Smad (2nd panel) used in the pull-down were detected by Western blotting using SNX9 and phospho-Ser/Thr antibodies, respectively. The middle panel shows a Coomassie stain (1.5 μ g) of the various GST proteins while the lower panels depict expression of SNX9 and GAPDH from 30 μ g of AKR-2B lysate. (C) The indicated cell lines were stimulated in the absence (-) or presence (+) of 5 ng/ml TGF β for 60 min. Following cell lysis, equivalent protein (500 μ g) was used for GST-SNX9 (10 μ g) pull-down and Western blotting (top 2 panels). Bottom panel depicts pSmad3 expression in 20 μ g total cell lysate.

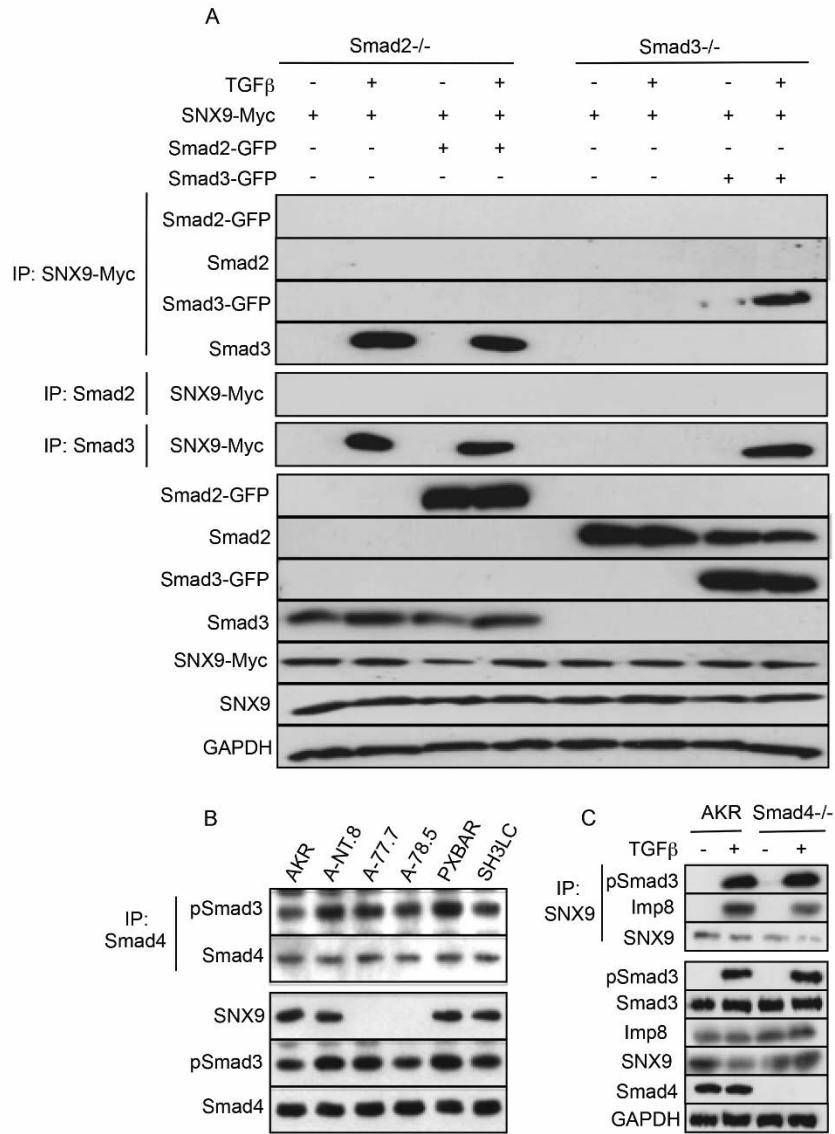


Figure 4.10 pSmad3/SNX9 binding is independent of Smad2 or Smad4. (A) Smad2^{-/-} and Smad3^{-/-} null MEFs were transfected (+) with SNX9-Myc, Smad2-GFP and/or Smad3-GFP, as indicated. The cells were serum-starved for 24 hr and either left untreated (-) or stimulated (+) with 5 ng/ml TGFβ for 30 min. Co-immunoprecipitations (top 6 panels) were performed using antisera to the Myc epitope tag (panels 1-4), Smad2 (panel 5) or Smad3 (panel 6) and the samples Western blotted for GFP (panels 1 and 3), Smad2 (panel 2), Smad3 (panel 4) or Myc (panels 5 and 6). Bottom 7 panels: Western analysis was performed as described for panel A except that the Smad and SNX9 fusion proteins were detected with antisera to GFP or Myc, respectively. (B) Parental AKR-2B cells (AKR) and clones stably expressing non-targeting (A-NT.8) or SNX9 shRNA1 (A-77.7) or shRNA2 (A-78.5) as well as two SNX9 dominant negative stable lines (DN-PXBAR.6 and DN-SH3LC.2) were grown to confluence, serum starved overnight, and stimulated with 5 ng/ml TGFβ for 30 min. Lysates were prepared and immunoprecipitated (600 μg) with antisera to Smad4 (top 2 panels). Following Western transfer the membrane was probed with antibodies to pSmad3 (panel 1) and Smad4 (panel 2). For the bottom three panels, expression of the indicated proteins in 30 μg of lysate was determined. (C) AKR-2B fibroblasts (AKR) and Smad4^{-/-} MEFs were left untreated (-) or stimulated (+) with 5 ng/ml TGFβ for 30 min. Cultures were harvested, lysed, and co-immunoprecipitation performed (350 μg) with SNX9 (top 3 panels). Following Western blotting, the membrane was probed for pSmad3 (panel 1), Imp8 (panel 2), and SNX9 (panel 3). The remaining six panels depict expression of the indicated proteins in 40 μg lysate.

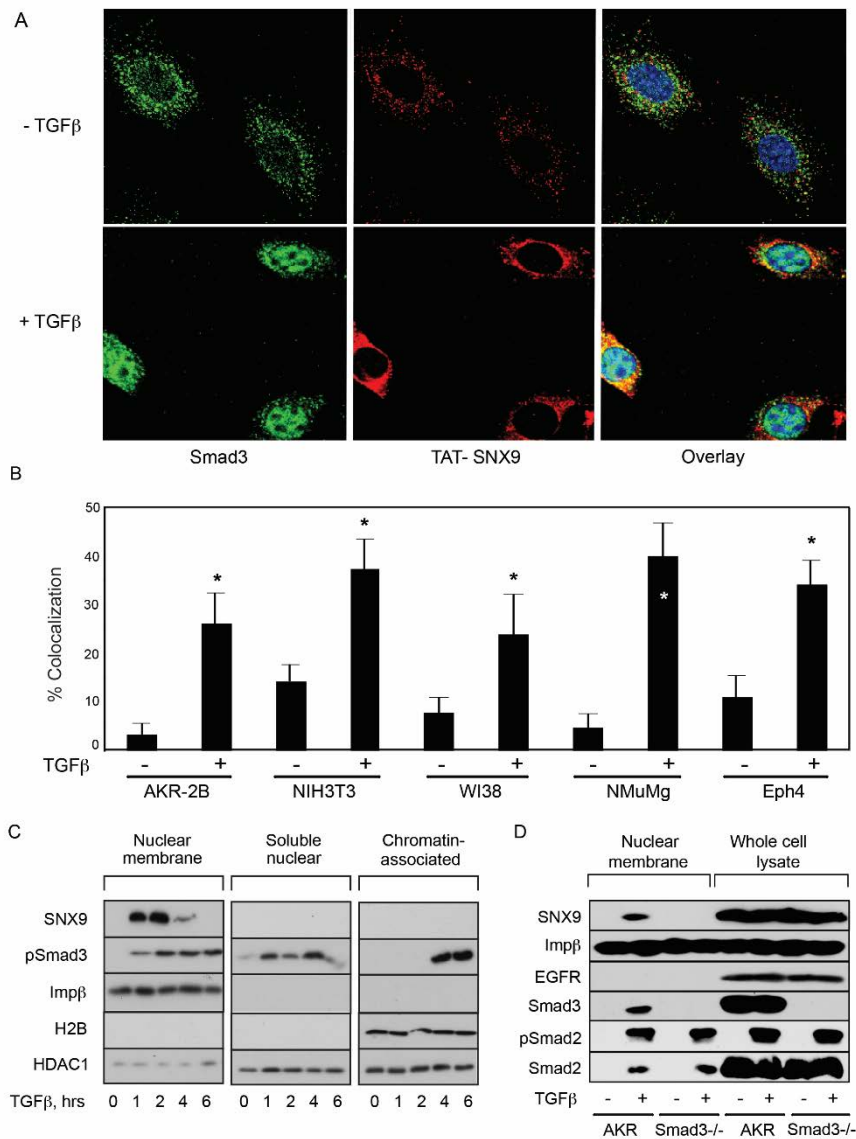


Figure 4.11 TGF β induces perinuclear/nuclear SNX9/pSmad3 localization. (A) AKR-2B cells were grown on glass coverslips and transduced with HA-TAT-SNX9 protein (0.8 μ M) for 90 min. After transduction and treatment with 5 ng/ml TGF β for 60 min, cells were incubated with anti-mouse HA or anti-rabbit Smad3 and detected by immunofluorescence analysis using anti-mouse Alexa Fluor 594 (red) or anti-rabbit Alexa Fluor 488 (green) coupled secondary antibody. Nuclei were stained with DAPI. (B) AKR-2B, NIH3T3, WI38, NMuMg, and Eph4 cells were treated as above except stimulation with TGF β was for 45 minutes for all lines other than AKR-2B. Co-localization of TAT-SNX9 and Smad3 was determined by Metamorph analysis from 3 experiments \pm SD. * denotes significant difference from unstimulated of the same cell type. See also Fig. S5. (C) Quiescent AKR-2B cells were left untreated (0) or stimulated with 5 ng/ml TGF β . At the indicated times equivalent cell numbers from 4 x 100 mm plates were processed for nuclear membrane, soluble nuclear, or chromatin-associated proteins as described in Chapter 3. Expression of SNX9, pSmad3, importin- β (Imp β ; nuclear membrane marker), histone 2B (H2B; chromatin-associated marker), and histone deacetylase 1 (HDAC1; soluble nuclear marker) in each of the fractions was determined by Western blotting. (D) Analogous study as in (C) was performed on nuclear membrane fractions and RIPA buffer lysates (Whole cell lysate) prepared from quiescent (-) and 30 min TGF β treated (+; 5 ng/ml) AKR-2B (AKR) cells and Smad3 null MEFs (Smad3 $^{-/-}$). EGFR (epidermal growth factor receptor) controls for plasma membrane contamination.

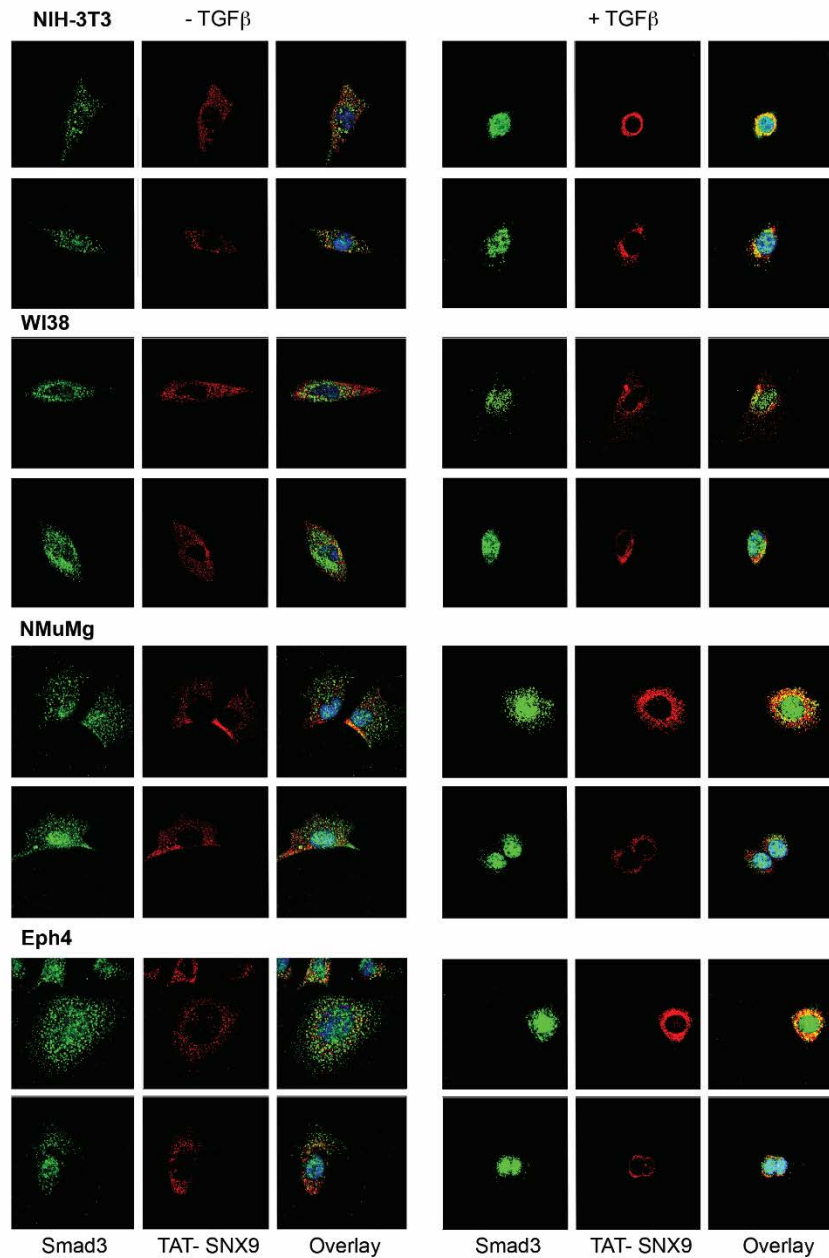


Figure 4.12 Increased co-localization of SNX9 and Smad3 upon TGF β stimulation in different cell types. NIH3T3, WI38, NMuMg, and Eph4 cells were grown on glass coverslips and transduced with TAT-SNX9 protein (0.8 μ M) for 90 min. After transduction cells were left untreated (left 3 panels) or stimulated with 5 ng/ml TGF β for 60 min (right 3 panels). Cells were then fixed/permeabilized and incubated with anti-mouse-HA (to visualize TAT-HA-SNX9 peptide) or anti-rabbit Smad3. TAT-SNX9 and Smad3 were detected by immunofluorescence analysis using anti-mouse Alexa Fluor 594 or anti-rabbitAlexa Fluor 488 coupled secondary antibody, whereas nuclei of cells were stained with DAPI. Two fields of each cell type are shown.

4.3.5 SNX9 requirements for nuclear membrane association

We have shown that SNX9 has an obligate role in pSmad3 nuclear import (Fig 4.5C and 3.5D, 3.6B and 3.6C, and 3.7A). We next investigated: (i) whether SNX9 bound and/or traversed the nuclear membrane similar to pSmad3 and; (ii) the individual *cis* and *trans* requirements for the SNX9/pSmad3 complex to bind and/or translocate the nuclear membrane. As can be seen in Figures 4.11C and 4.11D, while TGF β similarly stimulated the association of SNX9 and pSmad3 with the nuclear membrane, only pSmad3 entered the nucleus and bound chromatin. Since SNX9 shows minimal basal nuclear membrane binding in the absence of TGF β treatment (Fig 4.11C and 4.11D), yet is necessary for pSmad3 nuclear trafficking (Fig 4.5C, 4.5D, 4.6B, 4.6C, and 4.7A), suggests that in the absence of Smad3 negligible SNX9 would associate with the nuclear membrane following addition of TGF β . This was directly confirmed using Smad3 null MEFs (Fig 4.11D).

4.3.6 SNX9 is required for Smad3/Importin 8 complex formation

Prior studies have reported roles for the importins (Imp7, Imp8, and Imp β) and/or nucleoporins (Nup153 and Nup214) in pSmad3 nuclear translocation (Koopmann 2000, Xiao 2000, Xu 2002, Kurisaki 2006, Xu 2007, Yao 2008). Because we had identified a similar function for SNX9 we next considered whether these findings might be related. AKR-2B cells were treated with TGF β and the association of the aforementioned importins with SNX9 determined by co-IP/Western analysis. As shown in Figure 4.13A, ligand-dependent binding of Imp8 and SNX9 was observed with essentially identical kinetics to that observed for the SNX9/Smad3 association (Fig 4.9A). In contrast, no significant basal or ligand-stimulated binding of Imp7 or Imp β with SNX9 could be detected at any time point (Fig 4.13A). Due to difficulties immunoprecipitating endogenous nucleoporins, we transiently transfected HA-tagged Nup153 and Nup214 and examined the ability of these to co-IP with SNX9. No binding between SNX9 and either Nup153 or Nup214 was observed (Figs 4.14A and 4.14B).

The TGF β -induced association of SNX9 with Imp8 and pSmad3 indicates that Smad3 nucleocytoplasmic shuttling is even more complex than previously thought. These findings, however, do not address whether these various interactions occur via dependent or independent mechanisms. To address that issue, the Smad3, SNX9 and/or Imp8 requirement to generate SNX9/Imp8, Smad3/Imp8 or SNX9/Smad3

complexes was investigated. Surprisingly, while the absence of Smad3 prevented the association of SNX9 with Imp8 (Fig 4.13B, compare lanes 2 and 6 in panel 1), and loss of SNX9 significantly diminished the formation of Smad3/Imp8 complexes (Fig 4.13B, compare lanes 2 and 4 in panel 3), knockdown of Imp8 had minimal impact on SNX9/Smad3 association (Fig 4.13C, compare lanes 2 or 4 with 6 in panel 1). Consistent with a model whereby SNX9 is required to “bridge” pSmad3 and Imp8, a full length GST-SNX9 was shown to bind both pSmad3 and Imp8 (Fig 4.12D). This is contrasted by the SNX9 amino and carboxyl terminal SH3LC and PXBAR fragments which selectively bound pSmad3 and Imp8, respectively (Fig 4.13D). These findings not only indicate why both SNX9 SH3LC and PXBAR constructs act in a dominant negative fashion (Figs 4.4 and 4.6), but emphasize the cooperative role(s) of SNX9 and Imp8 in pSmad3 nuclear binding and translocation.

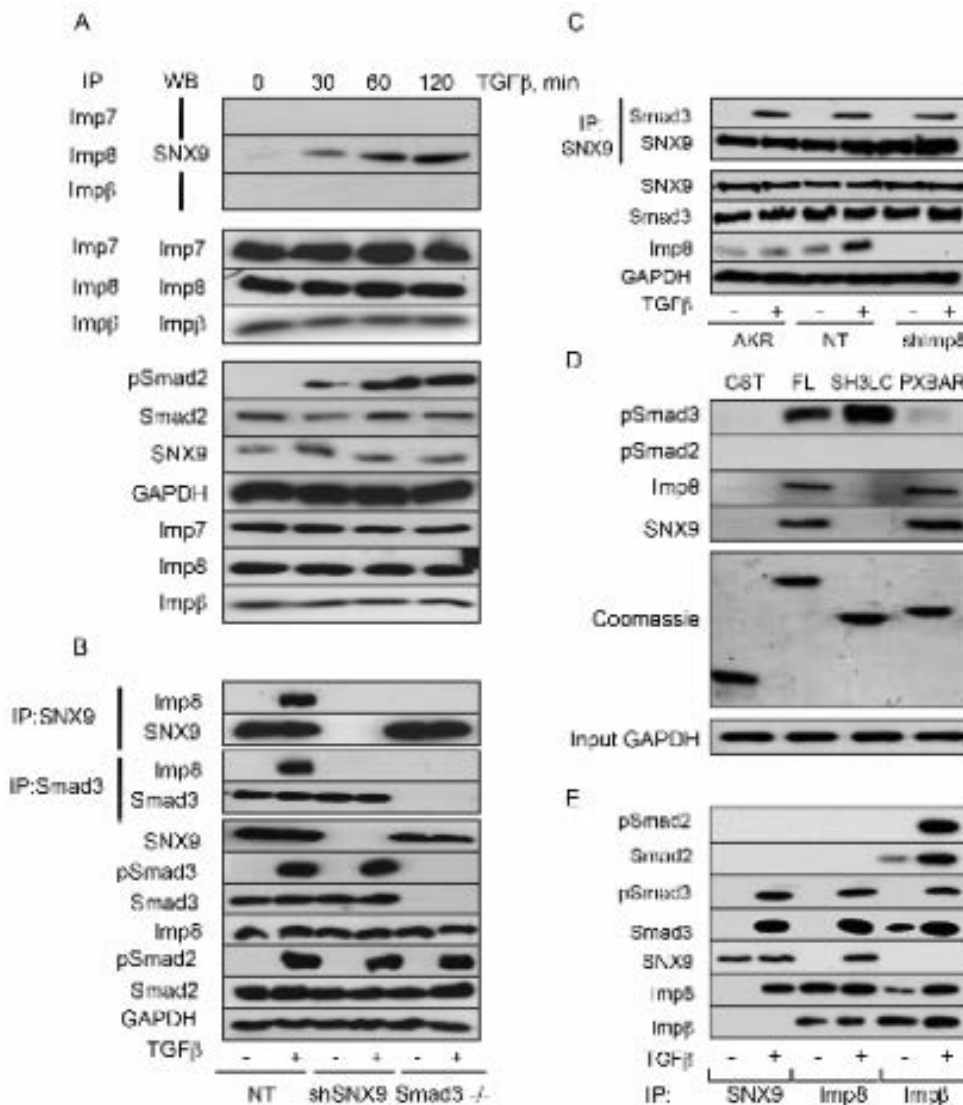


Figure 4.13 SNX9 is required for pSmad3/Imp8 Binding but SNX9/pSmad3 association is independent of Imp8. (A) AKR-2B cells were stimulated with 5 ng/ml TGF β and harvested from 0-120 min. Cultures were lysed and immunoprecipitated (IP) (600 μ g) with the indicated Imporin (Imp) antibodies. Following Western transfer (WB) the membrane was probed for associated SNX9 (first 3 panels) or the IP protein (panels 4-6). In the bottom 7 panels 60 μ g total cell lysate was immunoblotted for the indicated targets. (B) AKR-2B cells stably expressing non-targeting (NT; A-NT.8) or SNX9 shRNA (shSNX9; A-77.7) as well as Smad3 null MEFs (Smad3^{-/-}) were left untreated (-) or stimulated with 5 ng/ml TGF β for 30 min. Cultures were lysed and immunoprecipitated (IP; 350 μ g) for SNX9 (panels 1 and 2) or Smad3 (panels 3 and 4) prior to Western analysis for bound Imp8 (1st and 3rd panels), SNX9 (2nd panel) or Smad3 (4th panel). Remaining panels show expression of the indicated phosphorylated (p) or total protein in 30 μ g of total cell lysate. (C) Parental AKR-2B cells (AKR) or clones stably expressing non-targeting (NT; A-NT.8) or Imp8 (shImp8; A-89.4) shRNA were left untreated (-) or stimulated (+) with 5 ng/ml TGF β for 30 min. Lysates were prepared and immunoprecipitated (IP; 400 μ g) with antisera to SNX9 (top 2 panels) and co-precipitating Smad3 or SNX9 detected by Western blotting. Remaining panels depict expression of the indicated proteins in 40 μ g total cell lysate. (D) Lysates prepared from AKR-2B cells treated for 30 min with 10 ng/ml TGF β were incubated with GST or GST-SNX9 fusion proteins (FL [full length], SH3LC, and PXBAR). Bound pSmad3, pSmad2, Imp8 and SNX9 were detected by Western blotting. The Coomassie stain (1.0 μ g) shows expression of the various GST proteins while the lower panel depicts expression of GAPDH from 50 μ g of TGF β treated AKR-2B lysate. Figure 3.2B pictorially presents the SNX9 constructs. (E) AKR-2B cells were left untreated (-) or stimulated (+) with 5 ng/ml TGF β for 30 min. Cultures were lysed and immunoprecipitated (IP; 600 μ g) with SNX9, Imp8, or Imp β antibodies. Following Western transfer the membrane was probed for indicated targets.

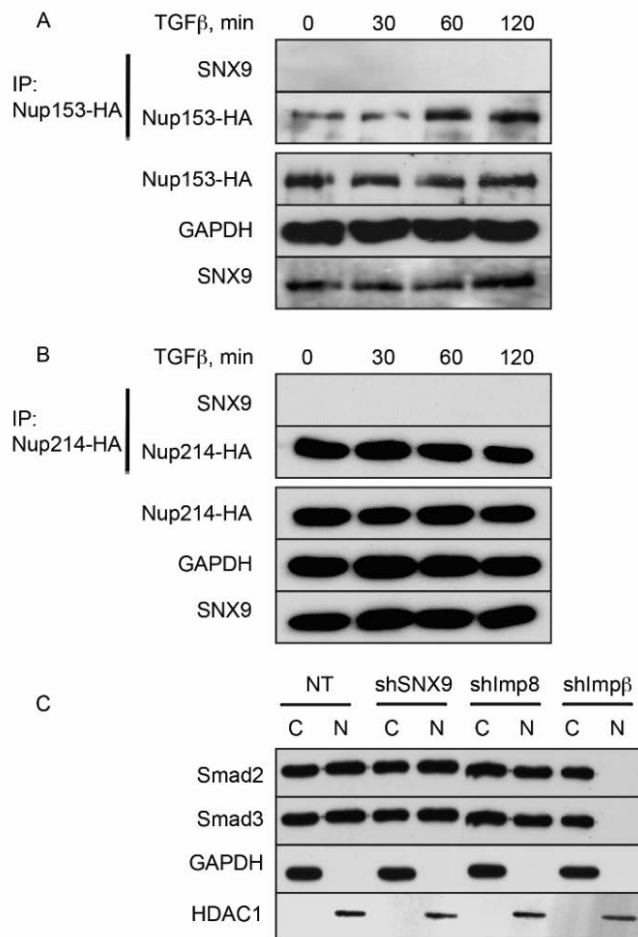


Figure 4.14 Nucleoporins and Impβ have distinct roles in R-Smad nuclear accumulation. (A) AKR-2B cells were transiently transfected with HA epitope tagged Nucleoporin153 (Nup153-HA), stimulated with 5 ng/ml TGFβ, and lysates (260 μg) prepared as in figure 5A. Following HA immunoprecipitation (IP), associated SNX9 (top panel) or transfected Nup153-HA (2nd panel) were detected by Western blotting. The bottom 3 panels reflect expression of Nup153-HA, GAPDH, and SNX9, respectively, in 40 μg total cell lysate. HA-tagged Nup153 was used as we were unable to find a commercially available antibody which reproducibly immunoprecipitated endogenous Nup153 (not shown). (B) Same as (A) except HA-epitope tagged Nup214 was used for the same reason. (C) AKR-2B cells stably expressing non-targeting shRNA (NT; A-NT.8) or shRNA to SNX9 (shSNX9; A-77.7), Imp8 (shImp8; A-89.4) or Impβ (shImpβ; non-clonal population) were fractionated into cytoplasmic (C) and nuclear (N) pools. The indicated proteins within each fraction were detected by Western blotting. GAPDH (cytoplasmic marker) and HDAC1 (nuclear marker) reflect fraction purity.

4.3.7 Importin 8 links pSmad3 to Importin- β for nuclear entry

We investigated the role of Imp β in R-Smad nuclear import as evidence for its requirement in this process is contradictory (Xiao 2000, Kurisaki 2001). Cultures were treated in the absence or presence of TGF β and the relationships between R-Smads, SNX9, Imp8, and/or Imp β determined. While SNX9, Smad3, and Imp8 showed the TGF β -dependent interactions depicted in Figures 4.9-3.13, and previously documented (Strom 2001) Imp8/Imp β heteromers were readily observed (Fig 4.13E), Imp β bound both Smad2 and Smad3 with ligand increasing the association (Fig 4.13E). The functional significance of this interaction was investigated using immunofluorescence and immunoblot analyses. As shown in Figures 4.15A-C and 4.14C, Imp β knockdown abrogated both basal and TGF β -stimulated nuclear import of Smad2 and Smad3. In contrast, SNX9 or Imp8 knockdown specifically prevented ligand-induced Smad3 nuclear accumulation further documenting that basal and stimulated R-Smad import are differentially regulated (Figs 4.7, 4.13, 4.15A, and 4.15B).

The preceding data demonstrated a requirement for SNX9, Imp8, and/or Imp β in pSmad3 nuclear entry. It does not, however, address whether each component blocks pSmad3 trafficking at defined sites. To investigate this further, SNX9, Imp8 or Imp β KD cells were treated with TGF β and purified nuclei fractionated into a nuclear membrane fraction, a crude nuclear pore fraction (contains pore and lamina components), and a soluble nuclear fraction. As expected, pSmad2 was unaffected by SNX9 or Imp8 KD (i.e. pSmad2 was found in all fractions) and only excluded from the soluble nuclear fraction by the absence of Imp β (Fig 4.15D). This is consistent with pSmad2 activity/trafficking being independent of SNX9 or Imp8 (Figs 4.3, 4.4, 4.6, 4.7, 4.12A, 4.12D, 4.12E, 4.15A, and 4.15B), yet requiring Imp β for translocation through the nuclear pore (Figs 4.15A, 4.15B, and 4.15D). While a similar block was observed for pSmad3 in Imp β KD cells, loss of SNX9 or Imp8 had distinct phenotypes. For instance, although SNX9 was never detected in the nuclear soluble fraction (Figs 4.11C and 4.16A), SNX9 KD prevented pSmad3 association with the nuclear membrane (Figs 4.15D and 4.16). This is contrasted by the absence of Imp8, which had no effect on pSmad3 nuclear membrane binding, but abrogated entry into the nuclear pore and subsequent translocation (Figs 4.15D and 4.16).

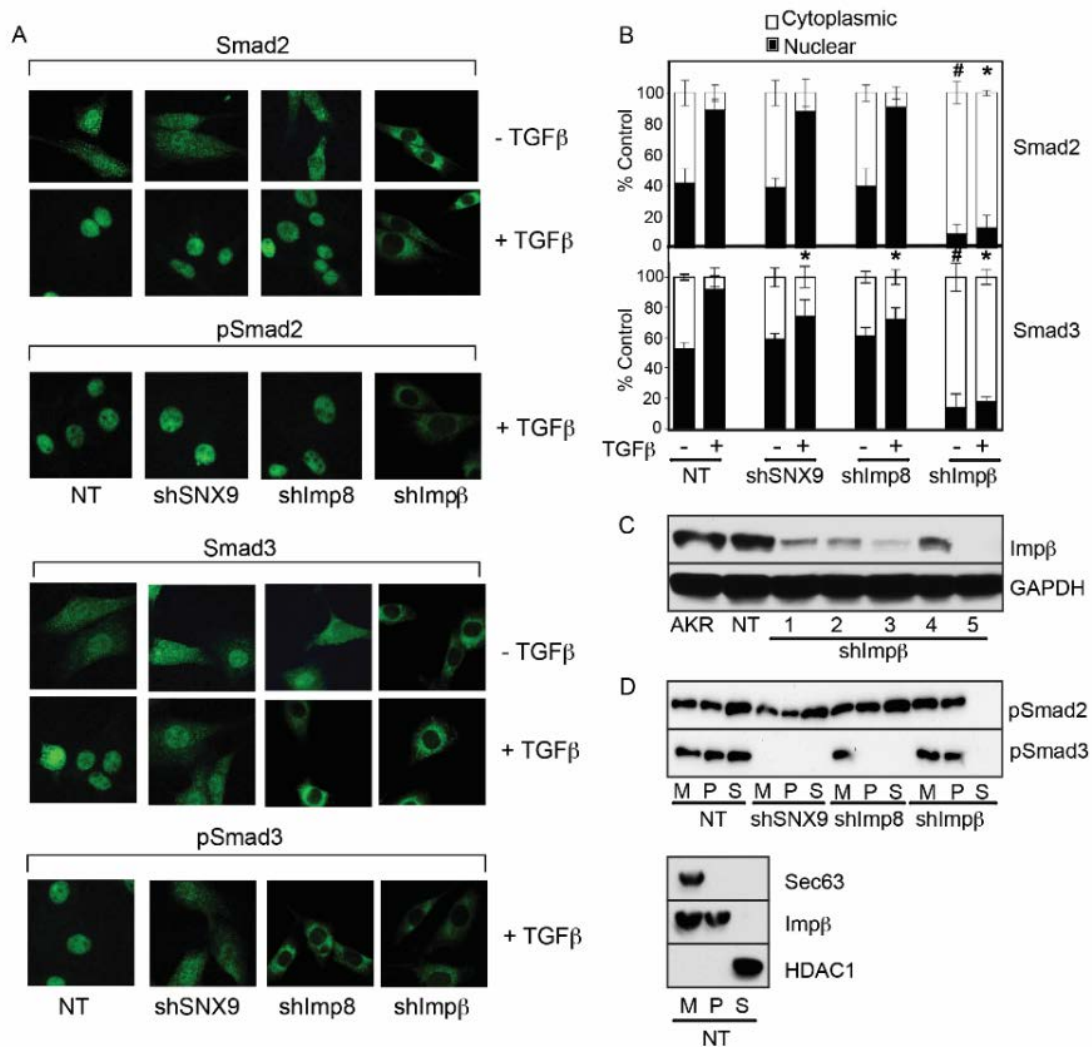


Figure 4.15 SNX9 and Imp8 differentially regulate pSmad3 association with the nuclear membrane and pore. (A) AKR-2B cells stably expressing non targeting shRNA (NT; A-NT.8) or shRNA to SNX9 (shSNX9; A-77.7), Imp8 (shImp8; A-89.4), or Imp β (shImp β ; non-clonal population) were grown to ~35% confluence on coverslips and either left untreated or stimulated for 30 min with 5 ng/ml TGF β . Cells were fixed and stained with primary antibody to Smad2, Smad3, pSmad2 or pSmad3 and AF488-conjugated goat anti-rabbit secondary antibody. (B) Quantification of nuclear and cytoplasmic Smad2, pSmad2, Smad3, and pSmad3 by Metamorph analysis from 2 experiments \pm SD. (C) AKR-2B cells were infected with lentivirus expressing non-targeting (NT) or 5 distinct shRNAs (1-5) to Imp β . Following 2 weeks selection in puromycin, lysates were prepared and 50 μ g processed for Western blotting. Cultures expressing Imp β shRNA 5 were used for all studies where shImp β is indicated. (D) Upper Panel: Confluent AKR-2B cells expressing non-targeting shRNA (NT; A-NT.8) or shRNA to SNX9 (shSNX9; A-77.7), Imp8 (shImp8; A-89.4), or Imp β (shImp β ; non-clonal population) were stimulated with 5 ng/ml TGF β for 30 min. Nuclear membrane (M), crude nuclear pore (P), and nuclear soluble (S) fractions were prepared as described in Experimental Procedures and pSmad2 and pSmad3 assessed by Western analysis. Lower panel: Fraction purity was determined by examining sec63 (rough endoplasmic reticulum/outer nuclear membrane marker), Imp β (nuclear pore marker), and HDAC1 (soluble nuclear protein marker) from NT control cells.

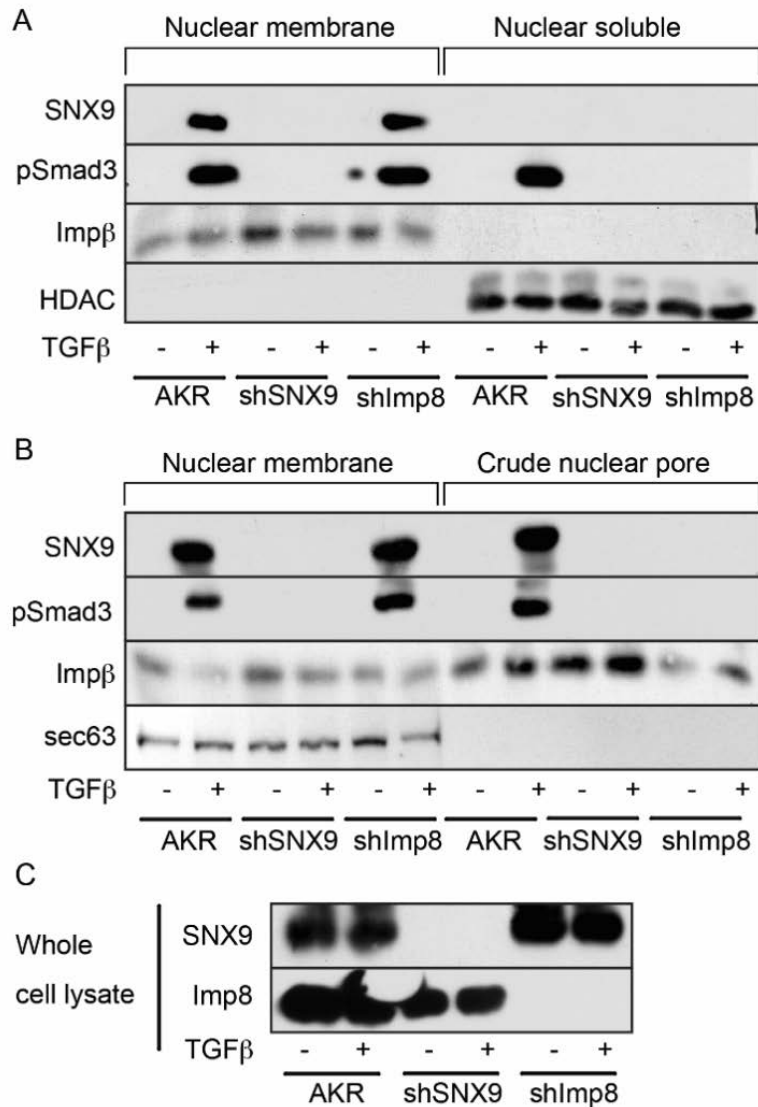


Figure 4.16 SNX9 does not enter the soluble nuclear fraction but does co-purify with the nuclear pore in an Imp8-dependent manner. (A) AKR-2B (AKR), SNX9 KD (shSNX9; A-77.7) or Imp8 KD (shImp8; A-89.4) cell lines were left untreated (-) or stimulated (+) for 30 min with 5 ng/ml TGFβ. Nuclear membrane (lanes 1-6) and soluble (lanes 7-12) fractions were prepared as in Experimental Procedures and expression of the indicated proteins assessed by Western analysis. (B) Analogous to (A) except that a crude nuclear pore fraction (lanes 7-12) was isolated as described in Experimental Procedures. Sec63 represents a rough endoplasmic reticulum/outer nuclear membrane marker. (C) Documentation of SNX9 and Imp8 knockdown in cells used for (A) and (B).

4.3.8 pSmad3/SNX9 is recruited to nuclear membrane by SNX9 PIP2 binding domain

While the plasma membrane and endocytic role(s) of SNX9 has been extensively examined (Cullen 2008, Lundmark 2009), SNX9 function at the nuclear membrane is

uncharacterized. As previous trafficking functions of the sorting nexins have been shown to be dependent upon phosphoinositide binding and homodimerization (Childress 2006), we investigated whether SNX9 action at the nucleus was controlled in an analogous manner. SNX9 KD cells were reconstituted with shRNA resistant WT-SNX9 or analogous escape constructs harbouring either point mutations in both the PX and BAR domain motifs required for high avidity PIP2 binding or a truncation of the carboxyl-terminal 13 amino acids required for homodimerization (Childress 2006). As shown in Figure 4.17A, re-expression of wild-type ($_{esc}WT$) or truncated ($_{esc}\Delta13C$) SNX9 bound pSmad3 (Left; 5th panel, lanes 4 and 8) and reconstituted both pSmad3 and SNX9 nuclear membrane binding following TGF β stimulation (Right; panels 1, 2, and 5, lanes 4 and 8). In contrast, although the PX/BAR mutant ($_{esc}Mut^{PIP2}$) was capable of binding pSmad3 (Left; 5th panel, lane 6), it was unable to couple the SNX9/pSmad3 complex with the nuclear membrane (Right; panels 1, 2, and 5, lane 6). Furthermore, while $_{esc}WT$ - and $_{esc}\Delta13C$ -SNX9 reconstituted Smad3-dependent 3TP-luciferase activity in SNX9 KD cells, this was not observed with the PX/BAR mutant (Fig 4.17B).

To further confirm the SNX9 PIP2 binding domain, *per se*, was recruiting pSmad3 to the nuclear membrane (Figs 4.15D, 4.16, and 4.17A), the incorporation of exogenously added ^{32}P -Smad3 was assessed in synthetic liposomes generated in the presence or absence of PIP2 and incubated with lysate from NT control, SNX9 KD, or SNX9 KD cells reconstituted with the escape wild-type, homodimerization defective, or PIP2 binding SNX9 mutant. Consistent with the findings of Figure 4.17A, in the absence of SNX9 pSmad3 was unable to associate with the liposome membrane (Fig 4.17C, compare lanes 2 and 4). Moreover, while reconstitution of SNX9 rescued pSmad3 binding, this was dependent upon both membrane PIP2 (Fig 4.17C, compare lanes 3 and 4) and the PIP2 binding PX/BAR domains in SNX9 (Fig 4.17C, compare lanes 4 and 6), but independent of SNX9 dimerization (Fig 4.17C, compare lanes 4 and 8).

SNX9 homodimerization (in conjunction with phosphoinositide binding) has been reported to be essential for correct plasma membrane/early endosome targeting, dynamin binding, and cargo endocytosis (Childress 2006, Lundmark 2009). While we similarly observed this requirement for dynamin binding (Fig 4.17A Left, panel 6 compare lanes 3 and 4 with 7 and 8), dynamin GTPase activity (Fig. 4.17D), and SNX9 association with the plasma membrane (Fig 4.17E, panel 1 compare lanes 5 and 6 with 7 and 8), that SNX9-dependent Smad3 signalling (Figs 4.16A-C) and nuclear

membrane binding (Figs 4.17A and 4.17E) similarly occur with a dimerization defective SNX9 escape construct would suggest that SNX9 associated with pSmad3 at the nuclear membrane is monomeric. This was directly tested by co-expressing myc- and YFP-tagged SNX9 constructs and determining whether a SNX9 complex containing both tags could be co-immunoprecipitated. While such a complex was readily observed with plasma membrane-associated SNX9, no analogous complex was detected in nuclear membranes (Fig 4.17F).

The results show that: (i) both phosphorylated and unphosphorylated forms of Smad2 and Smad3 require Imp β to enter the nucleus; (ii) unphosphorylated and phosphorylated Smad3 have differing kinetics of nuclear entry and retention; (iii) SNX9 specifically recognizes pSmad3 from pSmad2, Smad2, or Smad3; (iv) SNX9 in cooperation with Imp8 facilitates rapid delivery of pSmad3 to the nuclear pore; (v) SNX9 dissociates from the pSmad3/Imp8/Imp β complex before nuclear delivery; (vi) nuclear membrane SNX9/pSmad3 association and Smad3-regulated signalling are dependent upon SNX9's phosphoinositide binding motifs yet independent of SNX9 dimerization; and most importantly (vii) SNX9 has an obligate role in TGF β action, differentiates Smad3- from Smad2-dependent biology, and defines a SNX9 activity distinct from its canonical functions. This is shown diagrammatically in Figure 4.18.

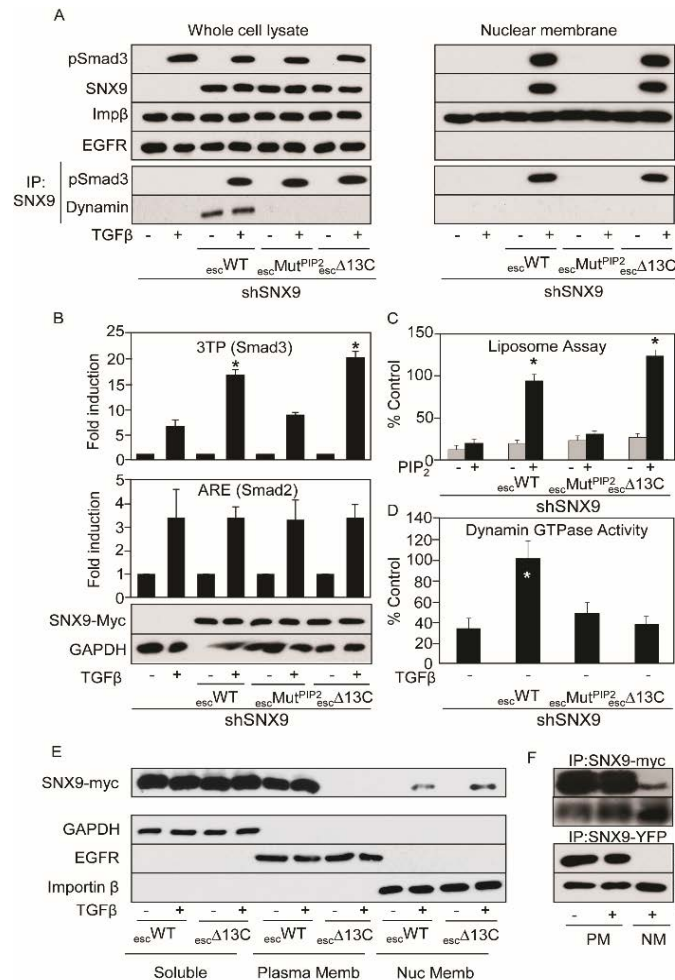


Figure 4.17 Nuclear membrane association of pSmad3/SNX9 is dependent upon phosphoinositide binding motifs in SNX9 and independent of SNX9 homodimerization. (A) Whole cell lysate (left) or nuclear membrane fractions (right) were prepared from SNX9 KD A-77.7 cells (lanes 1 and 2) or following transient transfection with a wild-type (esc^{WT}; lanes 3 and 4), phosphoinositide binding mutant (esc^{Mut^{PIP2}}; lanes 5 and 6), or homodimerization deficient mutant (esc^{Δ13C}; lanes 7 and 8) SNX9 escape construct resistant to the shRNA (shown in left; 2nd panel, lanes 3-8). Cultures were left untreated (-) or stimulated (+) for 30 min with 5 ng/ml TGFβ prior to fractionation and Western blotting for the indicated proteins. In panels 5 and 6 lysates were first immunoprecipitated (IP) for SNX9 before pSmad3 or dynamin Western analysis. (B) SNX9 KD A-77.7 cells (shSNX9) were transiently transfected with the indicated Smad3- (3TP, top panel) or Smad2-specific (ARE, middle panel) regulated luciferase reporters alone (lanes 1 and 2) or in conjunction with either Myc-tagged wild-type (esc^{WT}; lanes 3 and 4), phosphoinositide binding mutant (esc^{Mut^{PIP2}}; lanes 5 and 6), or homodimerization deficient mutant (esc^{Δ13C}; lanes 7 and 8) SNX9 escape construct as in (A). Following serum starvation (24 hr), cells were either left untreated (-) or stimulated (+) with 5 ng/ml TGFβ for 24 hr and normalized luciferase activity determined. Data represent the mean fold induction ± sd relative to untreated from 3 experiments. Bottom two panels reflect Western analysis (20 μg) of the Myc-tagged SNX9 escape construct or GAPDH from the first assay. * denotes statistical difference from TGFβ treated shSNX9 cells. (C) Liposomes and ³²P-labeled GST-Smad3 were incubated (30 min) with the indicated cell lysates as described in Experimental Procedures. The incorporated ³²P was determined with that obtained in the NT/PIP₂ from 3 experiments defined as 100%. * denotes statistical difference from PIP₂ containing shSNX9 liposomes. (D) Dynamin GTPase assay was performed as described (Leonard, Song 2005) on SNX9 KD A-77.7 cells (shSNX9) transfected with the indicated constructs. Data reflect relative GTPase activity from 3 experiments with the wild-type escape plasmid defined as 100%. * denotes statistical difference from shSNX9 cultures. (E) Soluble (lanes 1-4), plasma membrane (lanes 5-8), and nuclear membrane fractions (lanes 9-12) were prepared from SNX9 KD A-77.7 cells following transient transfection with a wild-type (esc^{WT}; lanes 1, 2, 5, 6, 9, and 10) or homodimerization mutant (esc^{Δ13C}; lanes 3, 4, 7, 8, 11, and 12) SNX9 escape construct. Cultures were left untreated (-) or stimulated (+) for 30 min with 5 ng/ml TGFβ prior to fractionation and Western blotting for the indicated proteins. (F) SNX9 KD A-77.7 cells were transiently co-transfected with SNX9-myc plus SNX9-YFP and left untreated (-) or stimulated (+) for 30 min with 5 ng/ml TGFβ prior to plasma (PM) or nuclear (NM) membrane fractionation. After normalization to SNX9 levels (~9 fold more NM protein), SNX9-myc (top 2 panels) or SNX9-YFP (bottom 2 panels) were immunoprecipitated before Western blotting for the indicated tagged SNX9 construct.

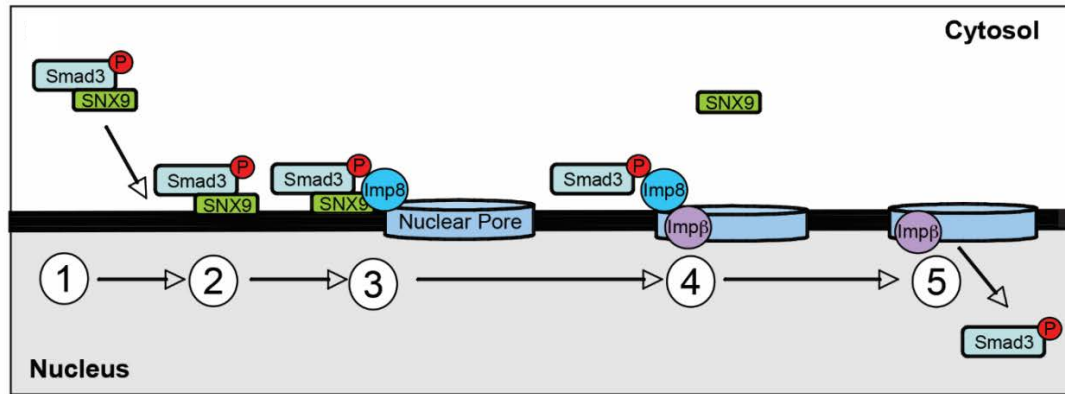


Figure 4.18 Schematic representations of SNX9/pSmad3 interaction and mechanism of nuclear entry. (1) TGF β -stimulated Smad3 phosphorylation results in the binding of pSmad3 (but not pSmad2) with SNX9 independent of Smad4; (2) phosphoinositide binding motifs in SNX9 mediate pSmad3/SNX9 complex association with the nuclear membrane; (3) nuclear membrane associated Imp8 targets pSmad3 and SNX9 to the nuclear pore complex where (4) SNX9 is released back to the cytosol, while pSmad3 undergoes Imp β -nuclear translocation to modulate gene expression (5).

4.4 DISCUSSION

As the majority of TGF β -regulated R-Smad transcriptional activity and biological action is associated with Smad3 (Feng 2005), that mechanisms exist which distinguish Smad3 from Smad2 nuclear trafficking would seem likely. The importance of that question is best exemplified for kidney fibrosis and skin cancer where it has been documented that while Smad3 signalling is profibrotic/procarcinogenic, Smad2 is antifibrotic/anticarcinogenic (Hoot 2008, Meng 2010). Thus, rather than designing studies to simply “inhibit TGF β signalling”, more appropriate strategies would impact specific targets. In the current study we directly address that issue and provide data supporting a cooperative role for SNX9 and Imp8 in that process.

TGF β -stimulated Smad activity is dependent upon the integrated action of the trafficking and signalling machinery (Hayes 2002). One family of proteins involved in various aspects of endocytic control and protein trafficking are the sorting nexins (Worby 2002, Carlton 2005, Cullen 2008). While earlier work documented an association of SNXs 2, 4, and 6 with type I and type II TGF β R (Parks 2001), these results have not been significantly extended in the ensuing years. As SNX9 is known to function at both the plasma membrane as well as early endosome (Lundmark 2009), cellular locations where Smad signalling is regulated (Hayes 2002, Di Guglielmo 2003), studies were initiated to determine whether there is a link between SNX9 and TGF β

signalling. Surprisingly, while loss of SNX9 activity had no effect on R-Smad phosphorylation or protein stability (Figs 4.5A, 4.5B, and 4.6A), specific inhibition of Smad3-dependent responses was observed (Figs 4.3 and 4.4). Subsequent studies showed this was through an inhibition of Smad3 nuclear translocation (Figs 4.5C, 4.5D, 4.6B, and 4.6C).

R-Smad proteins are known to continuously shuttle between the cytoplasm and nucleus in unstimulated cells as well as in the presence of TGF β (Inman 2002, Xu 2002, Schmierer 2005), however, upon TGF β stimulation the ratio of cytoplasmic to nuclear R-Smads decreases dramatically. Mechanisms of increased nuclear trafficking (Kurisaki 2001, Chen 2005, Schmierer 2007), increased nuclear retention (Inman 2002, Nicolas 2004, Schmierer 2005), or a combination thereof could all account for this and evidence exists supporting each (Schmierer 2008). The preceding data not only strongly indicates ligand addition both increases R-Smad nuclear import and nuclear retention but that increased nuclear localization is through the action of SNX9. More importantly, the role of SNX9 in accelerating nuclear translocation is restricted to pSmad3 and plays no role in pSmad2 nuclear translocation. These significant insights into how cells differentially regulate between the two R-Smads and a new mechanism to regulate the efficiency and ratio of R-Smad nuclear delivery, provides a basis for further unravelling how TGF β is recognized and signals in cells as the progress from healthy to transformed or fibrotic cells.

SNX9 was found to preferentially bind phosphorylated Smad3 *in vivo* by co-IP as well as *in vitro* using GST pull-down in a number of cell types (Figs 4.9, 4.10A, 4.10C, 4.13C, and 4.13D) however the two proteins could not bind one another *in vitro* in the absence of other cytoplasmic factors (unpublished observations). As these findings indicated the requirement for a multi-protein complex, we investigated two relevant possibilities: firstly would SNX9/pSmad3 binding only occur in the context of a heteromeric R-Smad interaction (i.e., also require Smad2 and/or Smad4); and secondly, might this reflect a need for a previously identified karyopherin or nucleoporin implicated in R-Smad nuclear import?

To address the first question, studies were performed in Smad2, Smad3, as well as Smad4 null MEFs (Fig 4.10). While an obligate requirement for Smad3 was observed,

neither the presence nor absence of Smad2 or Smad4 had any detectable impact on the co-precipitation of SNX9 and Smad3 following TGF β treatment. While this supports the hypothesis that SNX9 can regulate homomeric pSmad3 complexes, heteromeric complexes containing pSmad3 and Smad4 (but not pSmad2) are just as likely to be regulated by SNX9 as the heterotrimer (consisting of two pSmad3 and a single Smad4 molecule) represents the most energetically favorable structure (Chacko 2004).

Investigating the second possibility, however, was somewhat more problematic as published evidence supports a role(s) for Imp7, Imp8, Imp β , Nup153, and/or Nup214 in R-Smad nuclear entry (Xu 2002, Moustakas 2008, Yao 2008, Hill 2009). As our findings documented a need for SNX9 in TGF β stimulated proliferative phenotypes dependent upon Smad3 (Figs 4.3 and 4.4), we first determined whether any of the aforementioned karyopherins and nucleoporins could be co-precipitated with SNX9 following addition of TGF β . Such an interaction was only observed with Imp8 (Figs 4.13A, 4.13B, 4.13D, 4.14A, and 4.14B), supporting previous work suggesting that Imp8 is required for nuclear import of Smad3 in stimulated cells (Xu 2007). Of particular note was that in the absence of SNX9 we were not only unable to co-IP Imp8 with pSmad3 (Fig 4.13B), but pSmad3 was not associated with the nuclear membrane (Figs 4.15 and 4.16). This is contrasted by studies using Imp8 KD cells where no detectable impact on SNX9/pSmad3 binding (Fig 4.13C) or association with the nuclear membrane was observed (Figs 4.15 and 4.16). These findings suggest that SNX9 functions to promote the interaction of pSmad3 with Imp8 by recruiting it to the nuclear membrane. However, while Imp8 can associate with SNX9 and Imp β (Figs 4.13A, 4.13B, and 4.13E), SNX9 is never found with Imp β (Figs 4.13A and 4.13E), indicating that the formation of pSmad3/SNX9 and pSmad3/Imp β complexes may be mutually exclusive. Collectively, these data suggest nuclear delivery of pSmad3 occurs sequentially whereby initially SNX9 is necessary for pSmad3 nuclear membrane binding and presentation to Imp8 and subsequently Imp8 promotes pSmad3 complexing with the nuclear pore machinery and finally Imp β is required for pSmad3 translocation through the nuclear pore (Fig 4.18).

As mentioned earlier, there is both supporting (Xiao 2000, Kurisaki 2001) and contradictory (Xu 2003, Xu L 2007) evidence for Imp β involvement in R-Smad nuclear entry. Each of these studies however was based upon *in vitro* import assays or Dpp

stimulation of *Drosophila* S2 cells. These studies are of limited value in determining how R-Smad nuclear translocation operates in the context of intact mammalian cells. Since we were able to co-IP an Imp β /R-Smad complex (Fig 4.13E), the significance of this association was assessed in Imp β KD cells by western blot analysis (Figs 4.14C, 4.15 and 4.16). While the data support a role for Imp β in Smad2 and Smad3 nuclear import, as this was observed for both phosphorylated and non-phosphorylated R-Smads, it raises the question as to why pSmad3 also requires SNX9 and/or Imp8? One possibility is that because pSmad3 nuclear delivery occurs ~3.5X faster than Smad3 (Fig 4.7), it provides a more efficient/effective mechanism to respond to external cues (i.e., the biological significance of nuclear non-phosphorylated R-Smads is unknown). Alternatively, it may simply be that the higher order Smad complexes formed following phosphorylation have additional requirements for nuclear pore entry.

SNX9, like other SNX family members, has high specificity to specific membranes (Worby 2002). In the case of SNX9, PIP2 binding domains and the specific curvature of the homomeric dimer allow it to bind plasma membrane and early endosomes (Shin 2008). These findings prompted us to test whether pSmad3/SNX9 nuclear membrane recruitment similarly required the PIP2 binding domain and/or homodimerization activity of SNX9. When reconstituted into SNX9 KD cells (Fig 4.17), we were unable to co-purify a SNX9 escape construct mutated at residues required for PIP2 binding with the nuclear membrane fraction following TGF β treatment. As the model predicts (Fig 4.18), pSmad3 was also not detected at the nuclear membrane and Smad3-dependent luciferase activity was not reconstituted (Figs 4.17A and 4.17B). In contrast, a homodimerization-deficient SNX9 construct (_{esc} Δ 13C) reconstituted pSmad3 association with the nuclear membrane as well as pSmad3-dependent luciferase activity to a similar degree as WT-SNX9 (Figs 4.17A, 4.17B, and 4.17E). Of note, although pSmad3-regulated TGF β signalling is independent of SNX9 homodimerization, dimerization was necessary for SNX9 association with the plasma membrane (Figs 4.16E and 4.16F) and dynamin binding/GTPase activation (Figs 4.17A and 4.17D).

In summary, we provide evidence that SNX9 is involved in Smad3, but not Smad2, signalling following TGF β treatment and acts as an adaptor for the nuclear translocation of pSmad3 via its recruitment to the nuclear membrane and subsequent binding Imp8. This reflects an activity distinct from the canonical trafficking role of SNX9 at the plasma

membrane as it occurs independently of SNX9 dimerization and dynamin binding/activation. As the majority of TGF β -regulated transcriptional activity and biological action is associated with Smad3, the ability to specifically impact Smad3-dependent phenotypes would provide a previously unavailable degree of specificity to modulate and/or treat various TGF β -dependent pathologies.

CHAPTER 5

ROLE OF p21-ACTIVATED KINASE 2 (PAK2) IN DEPHOSPHORYLATION OF SMAD2 IN TGF β SIGNALLING

CHAPTER 5: ROLE OF p21-ACTIVATED KINASE 2 (PAK2) IN DEPHOSPHORYLATION OF SMAD2 IN TGF β SIGNALLING

5.1 BACKGROUND

TGF β signalling is a cascade of ligand binding TGF β R2, which then phosphorylates TGF β R1, which can then phosphorylate Smad2 and Smad3, allowing the formation of Smad trimers with Smad4, which can bind promoter sequences within the DNA (Wrana, 2013). Apart from the kinase cascade through the receptors and Smads, the cell can also regulate the TGF β signalling response by less direct mechanisms, that don't involve modifications of the key receptor and Smad proteins directly, but rather impact accessory proteins that influence the localization and availability of the core proteins during signalling. The regulation of mechanisms that control nuclear import and export of the Smads is one example of indirect control of TGF β signalling. In Chapter 4 we demonstrated a role for SNX9 in nuclear import, but not nuclear export of Smad3 following TGF β stimulation. This suggests that there is more than one mechanism regulating this critical checkpoint in the TGF β signal. However, both increased nuclear import and reduced nuclear export of Smad2 and Smad3 were dependent on the phosphorylation of the Smads by the TGF β receptors.

Smad proteins contain no recognized structural motifs, however they do possess amino and carboxy terminal regions termed MH1 and MH2 domains that share high conservation across species (Attisano 1996) with these domains connected by a proline-rich linker (Matsuura 2005). Receptor interacting-Smads (R-Smads) interact with and are phosphorylated by the TGF β family receptors. Of these, Smad2 and Smad3 are the R-Smads that are phosphorylated when cells are stimulated by TGF β and Activin, while Smad1 and Smad5 are the R-Smads phosphorylated after BMP stimulation (Attisano 1998). While the receptors mediating TGF β , activin and BMP responses are different, each of them phosphorylates a SSxS motif found at the far C-terminus on all of the R-Smads (Massagué 1998). Once phosphorylated, the R-Smads bind the common mediator Smad4 and accumulate in the nucleus where they form complexes with other transcription factors including P300 (Pouponnot 1998, Topper 1998), ATF/CREB family members (Topper 1998, Kang 2003, Warner 2004), AP1 (Zhang 1998, Sundqvist 2013), FAST1 (Chen 1996) and E2F family members (Chen

2002). Transcriptional activity ends upon dephosphorylation by PPM1A and export of Smads back into the cytoplasm (Lin 2006).

Cell type specific responses to TGF β are varied and the mechanisms behind these different responses remains poorly defined. Once activated, TGF β binds the single-pass transmembrane TGF β R2, which recruits and phosphorylates the transmembrane receptor, TGF β R1 (Wrana 1994). Phosphorylation activates TGF β R1 serine/threonine kinase activity (Marcías-Silva 1996) and once internalized (Hayes 2002) TGF β R1 phosphorylates Smad2 (Baker 1996, Marcías-Silva 1996) and Smad3 (Liu 1997). TGF β receptor and Smad phosphorylation rates and expression levels are virtually indistinguishable between all cell types (Rahimi 2007) which raises many questions in regard to how different cell types respond so differently to TGF β . The differential expression of Smad interacting transcription factors (Mullen 2011), as well as differences at the epigenetic level such as promoter methylation (Suzuki 2005, Matsumura 2011) and histone acetylation (Juan 2013) have all been suggested as mechanisms to account for the cell type differences. Substantial evidence also supports a role for cell-type specific activation of accessory signalling molecules following TGF β stimulation that may contribute to the pleiotropic effects of this cytokine. Ras (Mulder 2000, Suzuki 2007), TAK1 (Kim 2009), p38 (Yu 2002), JNK (Hocevar 1999), ERK (Mulder 2000, Suzuki 2007), PKC (Lim 2005), PI3K (Bakin 2000, Wilkes 2005), PAK2 (Wilkes 2003, Wang 2005, Wilkes 2005, Wilkes 2006, Wilkes 2009), c-Abl (Daniels 2004, Wilkes 2006, Wang 2006, Wang 2009) have all been reported as having a cell type dependent activation in response to TGF β . Many of these factors, along with others such as GSK3 β (Wang 2009) and CDK8/9 (Alarcón 2009) have been implicated in phosphorylating R-Smads in the linker region between the MH1 and MH2 domains to either reduce (Kretzschmar 1997, Grimm and Gurdon 2002, Matsuura 2005), or enhance (Blanachette 2001, Alarcón 2009, Hough 2012) nuclear entry/activity of C-terminally phosphorylated Smads.

While TGF β causes a myriad of different cellular responses in different cell types with activation of cell-type specific accessory factors reported in virtually every cell type, in the present study we have focused on TGF β signalling in fibroblast and epithelial cells. Due to the high degree of characterization of their responses to TGF β , AKR-2B fibroblasts and Mv1Lu epithelial cells were chosen as representatives of each cell type. While actively dividing epithelial cells undergo a robust growth arrest in response to

TGF β (Wrana 2013), fibroblasts transform into myofibroblasts that proliferate, divide and form colonies in anchorage-independent conditions, deposit large volumes of extracellular matrix, and undergo gross morphological alterations (Wilkes 2003, Daniels 2004, Wilkes 2005). Interestingly, the response of fibroblasts to TGF β is very similar to that of advanced carcinoma lines. Indeed, during disease progression, most carcinomas mature from being growth inhibited initially, to refractile, before finally proliferating and becoming metastatic in response to TGF β in advanced stages of the disease (Wrana 2013).

In fibroblasts, but not epithelial cells, TGF β activates PAK2 (Wilkes 2003) and c-Abl (Roig 2001, Daniels 2004, Wilkes 2006) contributing to TGF β driven fibrosis of the lung (Daniels 2004) and kidney (Wang 2005, Wilkes 2006, Wang 2009), scleroderma (Bhattacharyya 2009, Hinchcliff 2012) and hepatoma cell migration (Sato 2013)(Fig 5.1). PAK2 kinase activity can be induced in a number of ways (Roig 2001) however TGF β induced activation is mediated by cdc42/Rac (Roig 2000, Wilkes 2009), PI3K (Wilkes 2005, Wilkes 2009), ROS (Sato 2013) and likely α -PAK Interacting and Exchange Factor (PIX) (Barrios-Rodiles 2005). Activated PAK2 recognizes a consensus sequence of **(K/R)RX(S/T)** in substrates for subsequent phosphorylation (Tuazon 1997). There are many well characterized PAK2 substrates in diverse cell types and cellular contexts (Roig 2001).

Central to the current study are two reported findings. Firstly, in response to TGF β , PAK2 is activated in fibroblast and not epithelial cells (Wilkes 2003), and secondly, phosphorylation of Smad2 and Smad3 at serines 465/67 is greatly prolonged in duration in fibroblasts relative to epithelial cells (Rahimi 2007, Wilkes 2009, Andrianifahanana 2013). The core question addressed in the current study is whether these two events are linked and whether this can explain differential responses of cells to TGF β stimulation.

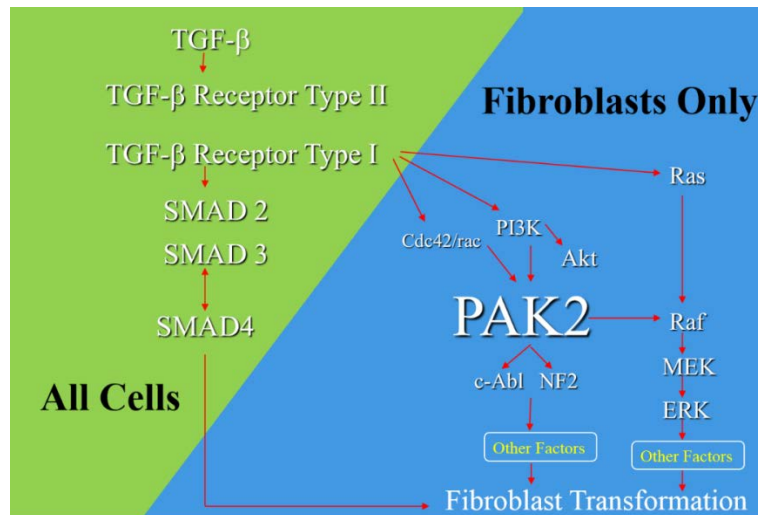


Figure 5.1 Fibroblast specific signalling in response to TGF β . While all cells expressing TGF β receptors activate the Smad cascade, a much more restricted number of cell types activate the PAK2 pathway (including fibroblasts and high grade glioblastomas). While the PAK2 pathway is required for the fibroblast-specific response to TGF β , it is not sufficient, as both inhibition of Smads and PAK2 activation alone, fails to support the fibroblastic response to TGF β

The extent of Smad2 and Smad3 phosphorylation at the far carboxy terminal (SSXS motif) at serines 465/67 by TGF β R1 is virtually identical between fibroblast and epithelial cells and not impacted by PAK2 (Wilkes 2003). However dephosphorylation of Smad2 and Smad3 at these residues differs significantly between these two cell types (Rahimi 2007, Wilkes 2009, Andrianifahanana 2013) and while PAK2 is known to be activated in fibroblasts only, a link between PAK2 activation and differences in R-Smad dephosphorylation kinetics has not been investigated.

Objectives

The only known differences in TGF β signalling between fibroblast and epithelial cells is the activation of PAK2 kinase in fibroblasts, and more rapid dephosphorylation of R-Smads at serines 465/67 in epithelial cells. In order to explain the differences in Smad dephosphorylation kinetics between fibroblast and epithelial cells at S465/67 we sought to determine if there was a link between PAK2 activation and the kinetics of dephosphorylation at serines 465/67. To address this objective we investigated the following aims:

1. To determine if active PAK2 can phosphorylate R-Smads *in vitro* and *in vivo*, with a PAK2 binding consensus sequence.
2. To determine if PAK2 inhibition in fibroblasts reduces R-Smad phosphorylation at the TGF β Receptor-mediated sites (S465/467) to a similar extent as that found in epithelial cells.
3. Using point mutants at PAK2 site (T430) and TGF β Receptor sites (S465/467), to determine if the phosphorylation status of these sites were independent or influenced one another in either the extent or duration of phosphorylation.
4. To examine the relationship between PAK2 site and TGF β Receptors site phosphorylation in Smad nuclear translocation, ligand sensitivity, Smad4 hetero-oligomerization and phosphatase binding.

Here we document that PAK2-mediated phosphorylation of Smad2 at threonine 430 occurs in fibroblast and not epithelial cells. When phosphorylated at T430, binding of the phosphatase PPM1 is inhibited, leaving Smad2 insensitive to dephosphorylation at S465/67. In this way Smad2 S465/67 phosphorylation is prolonged in fibroblasts relative to epithelial cells in response to TGF β . These results may contribute to our understanding of the pleiotropic effects of TGF β in different cell types.

5.2 MATERIALS AND METHODS

5.2.1 Cell culture and stimulation

AKR-2B is an immortalized mouse fibroblast line with a robust signalling and morphologic response to TGF β . Mv1Lu is an epithelial cell of mink origin with a well characterized TGF β response and is an immortalized, untransformed line. Smad2 $-/-$ mouse embryo fibroblasts (MEFs) have been characterized previously for Smad (Roberts 2003) and PAK2 responses (Wilkes 2003) to TGF β . Cells were obtained and cultured as specified (Table 3.2) using standard mammalian cell culture techniques (Chapter 3) and grown to confluence prior to stimulation with TGF β 1 to a final concentration of 10 ng/ml in the appropriate growth media (Table 3.2). Stock TGF β was stored in 4mM HCl with 0.1% Bovine Serum Albumin (BSA) and stored at -20 °C. Cells were incubated in the presence of TGF β for various times (0 to 24 hours) at 37 °C with 5 % CO₂.

5.2.2 Phosphorylation of Smads by activated PAK2

Kinase assays were performed essentially as described in Chapter 3. Smads 1,2,3,4 and 5 were purified as recommended by the manufacturer using the Catch and Release®v2.0 protein purification system (Merck Millipore, Darmstadt, Germany). Smads were obtained from AKR-2B fibroblasts cultured in 10mm² plates. Antibodies utilized to capture the Smads are listed in Table 3.3 and confirmation that the appropriate Smads were highly enriched was achieved through Western blotting (Appendix IX) prior to protein quantitation to ensure Smads were equally represented in subsequent reactions. Purified Smads were utilized as potential PAK2 substrates in kinase reactions performed as stated in Chapter 3 and Wilkes 2003.

5.2.3 Detection of Smad phosphorylation by western blotting

Because Smad2 can be phosphorylated on a number of different residues we sought to analyze the phosphorylation status of distinct residues within the protein. We used antibodies specifically recognizing Smad2 with certain residues phosphorylated in Western blot analysis (See Chapter 3 for details). Antibody recognizing Smad2 phosphorylated at serines 465/467 (TGFβ receptor site) was purchased from Millipore while an antibody raised against Smad2 phosphorylated at the threonine 430 (PAK2 site) was generously supplied by Dr Jinhua Li (Table 3.3). Validation of these antibodies has been determined previously (Wilkes 2003, Wilkes 2004, Wilkes 2005, Wilkes 2006, Wilkes 2009, Wilkes 2015 and Qu 2014 respectively). To ensure failure to detect phosphorylated forms of Smad2 were not due to the absence of Smad2 from the samples, concurrent examination for the presence of total Smad2 was determined with a minimum of three independent experiments.

5.2.4 p21-Activated Kinase-2 (PAK2) expressing adenovirus production and infection

Wild Type and Dominant negative PAK2 constructs were supplied by Rolf Jakobi (University of Wisconsin, Milwaukee) and were subcloned into a pAd.CMV shuttle vector and generation of adenovirus was performed as described in Chapter 3. Because PAK2 serves dual roles as both a kinase and scaffolding molecule we chose to utilize a kinase-deficient PAK2 bearing a K298R point mutation. In this way any scaffolding role PAK2 may serve would remain intact, with only the kinase activity of the protein inhibited.

5.2.5 Smad mutant construction and validation

Constructs were generated using standard molecular biology techniques as stated in Chapter 3. Point mutants were generated by site directed mutagenesis using Quikchange® II XL (Agilent Technologies, Santa Clara, California) and mutants were confirmed by sequencing prior to transfection into Smad2^{-/-} MEFs and Western blot analysis to determine expression. Smad2 mutants were generated in the backbone of pHA-Smad2-myc and pHA-Smad2-GFP with specific mutants outlined in Figure 5.2. The rationale behind generating both a myc- and GFP-tagged Smad2 constructs was that the presence of the myc epitope tag adds negligible length to the construct (Smad2 is approximately 60kDa), whereas GFP domain is approximately 30kDa generating a Smad2-GFP fusion product of close to 90kDa. This size difference allows the expression of both a GFP- and myc-tagged Smad2 in the same cells, each carrying a different mutation, but within the same experimental conditions.

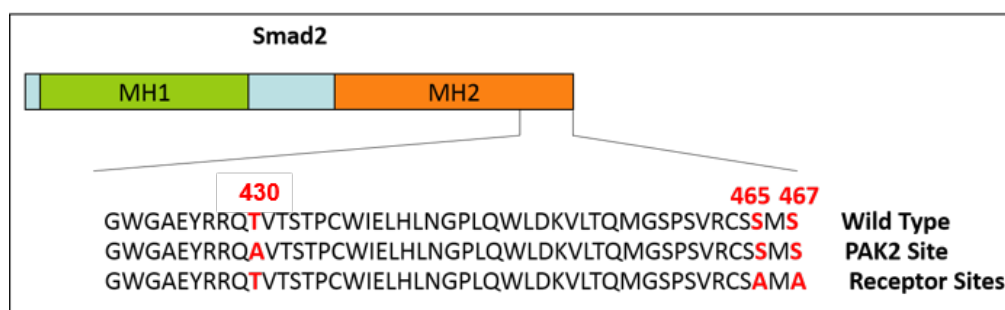


Figure 5.2 Smad2 constructs. Threonine 430 or Serines 465 and 467 were mutated to Alanines in both Smad2-myc and Smad2-GFP constructs. All constructs carried epitope tags (either myc or GFP) at the NH-terminus.

5.2.6 Smad Co-Immunoprecipitations

Co-Immunoprecipitation experiments were performed as outlined in Chapter 3 with specific antibodies outlined in Table 3.3. As with all immunoblotting results, observed bands were referenced against known protein standard markers for size and, where possible, both positive and negative controls were run alongside experimental samples. All experiments were performed in triplicate with representative blots included at an optimal exposure for qualitative assessment.

5.2.7 Nuclear fractionations

Nuclear fractionation experiments were performed as outlined in General Materials and Methods using NE-PER™ Nuclear and Cytoplasmic Extraction Reagents (Pierce Biotechnology, Rockford, Illinois) supplemented with Complete® protease inhibitor.

5.3 RESULTS

5.3.1 TGFβ-induced R-Smads contain conserved PAK2 phosphorylation consensus sequences and can be phosphorylated by activated PAK2 *in vitro* and *in vivo*

Active PAK2 recognizes substrates that contain the consensus sequence **(K/R)RX(S/T)** and phosphorylate the serine or threonine residues (Tuazon 1997). Alignment of the carboxy-termini of Smads 1 to 5 revealed putative PAK2 consensus sequences in both Smad2 and Smad3 but not Smads1,4 or 5 (Fig 5.3A). In both Smad2 and Smad3, the potential residue phosphorylated by PAK2 within the consensus sequence is a threonine (Thr430 in Smad2 and Thr388 in Smad3) which is separated by 34 residues from the C terminus serines 465/67 phosphorylated by TGFβR1 (Fig 5.2). Although protein folding determines the proximity of one residue to another *in vivo*, the separation of T430 from S465/67 does not exclude the potential influence that phosphorylation at one of these sites may influence phosphorylation at the other. Indeed, phosphorylated residues separated by much larger distance have been reported to influence one another (Bornancin 1996).

To determine if any Smads could act as substrates for activated PAK2 *in vitro*, we immunopurified Smads 1-5, inactive PAK2 (from unstimulated cells), and activated PAK2 (from TGFβ-stimulated cells). Inactive or activated PAK2 was co-incubated in the presence of ATP and MgCl₂ (enzyme cofactor) with immunopurified Smads and Smad phosphorylation determined by autoradiography. Both Smad2 and Smad3 were robust *in vitro* substrates of TGFβ-activated PAK2, while Smads1, 4 and 5 remain unphosphorylated (Fig 5.3B). Although Smad2 and Smad3 served as substrates, we chose to focus our studies on Smad2 due to the availability of more robust reagents and amenable cell lines.

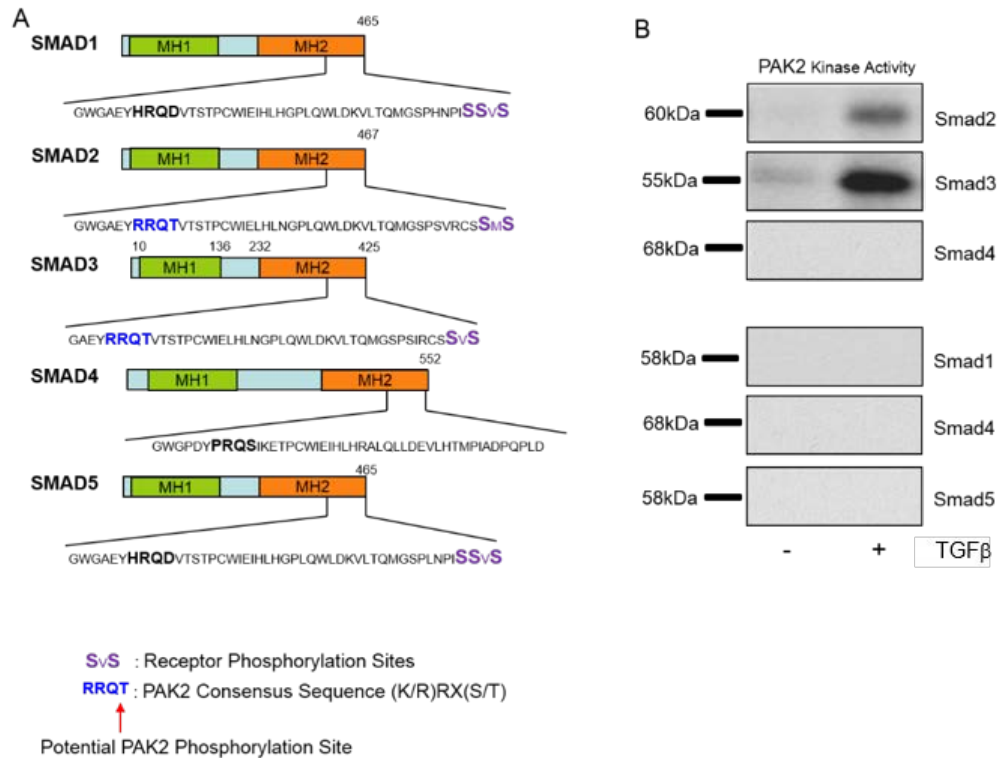


Figure 5.3 Smad2 and Smad3 can be phosphorylated by PAK2 *in vitro* and possess PAK2 phosphorylation consensus sequences. (A) Alignment of C-termini of Smads 1-5 reveals putative PAK2 sequences, (shown in blue) in both Smad2 and Smad3 but not Smads1, 4 or 5. (B) Immunopurified Smad1-5 were subjected to *in vitro* kinase assay to determine if any could function as targets for activated PAK2. PAK2 was immunopurified from TGFβ stimulated (+) or unstimulated cells (-).

5.3.2 Phosphorylation of Smad2 at Threonine 430 only occurs in fibroblasts

We have previously documented that PAK2 is activated in fibroblasts and not epithelial cells in response to TGFβ (Wilkes 2003) so we sought to determine if Smad2 was phosphorylated at T430 by PAK2 *in vivo* and if PAK2 activity had an impact on S465/67 dephosphorylation kinetics. In both AKR-2B fibroblasts and Mv1Lu epithelial cells, phosphorylation of Smad2 at the S465/467 (TGFβR1 sites) occurred within 15 minutes (Fig 5.4). However phosphorylation at T430 (predicted PAK2 site) was only observed in AKR-2B cells and occurred concurrently, or was slightly delayed relative to reported PAK2 activation (Wilkes 2003) with robust detection at 30 minutes after TGFβ stimulation and peaking between 1 and 2 hours, before returning to basal levels by 8 hours.

When PAK2 activity was inhibited through the adenoviral infection of a dominant negative PAK2 (K298R), no Smad2 phosphorylation could be observed at the potential PAK2 site (Fig 5.4). Parallel cultures infected with adenovirus expressing Green Fluorescent Protein (GFP) showed the same T430 phosphorylation profile as uninfected AKR-2B cells (data not shown). Although initiation of TGF β 1-mediated phosphorylation was essentially identical in Mv1Lu and both PAK2-inhibited and untreated AKR-2B cultures, the dephosphorylation at S465/467 was significantly faster in both Mv1Lu and PAK2-inhibited AKR-2B cultures relative to normal AKR-2B cells (Fig 5.4), suggesting PAK2 is required for both Smad2 phosphorylation at T430 and the increased duration of phosphorylation at S465/67.

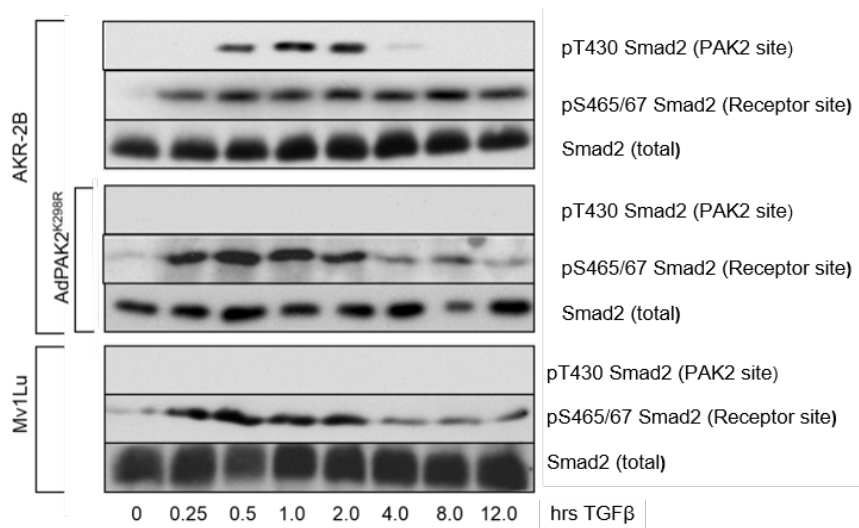


Figure 5.4 Smad2 phosphorylation at Threonine 430 is induced by TGF β when PAK2 activation occurs and correlates with extended duration of phosphorylation at Serines 465/467. AKR-2B fibroblasts alone (top 3 panels) or infected with adenovirus expressing dominant-negative PAK2 (middle 3 panels), along with Mv1Lu epithelial cells (bottom 3 panels) were treated with TGF β 1 at 10ng/ml for the indicated times. Cells were lysed, protein levels normalized and subjected to SDS-PAGE before Western analysis for Smad2 phosphorylated at Threonine 430, Smad2 phosphorylated at Serines 465/467, or total Smad2.

5.3.3 Phosphorylation at Threonine 430 decreases the susceptibility of Smad2 to dephosphorylation at Serines 465/467

While Figure 5.4 determined PAK2 activity is required for both T430 phosphorylation and the slower dephosphorylation of S465/65 of Smad2, it was unclear if they were independent events or if one event was causal to the other. To address this, GFP was cloned upstream of Wild type Smad2 (GFP-Smad2 WT) while myc amino terminal tags

were fused to Smad2 constructs with either a T430A mutation (myc-Smad2 T430A) or S465/67A mutations (myc-Smad2 S465/67A). While the myc tag adds negligible size to the Smad2 mutant proteins, addition of GFP increases the size of Smad2 by ~30kDa. After the generation of these three constructs two pools of cells were generated (Fig 5.5A). Smad2 null mouse embryonic fibroblasts (Smad2^{-/-} MEFs) were transfected with two Smad2 constructs, a GFP-tagged wild type Smad2 (GFP Smad2 WT) and one of the myc-tagged Smad2 mutants (myc-Smad2 T430A or myc-Smad2 S465/67A). Because the wild type and mutant Smad2 constructs were fused with significantly different sized tags, the two Smad2 forms could be distinguished based on differential migration following SDS-PAGE, facilitating comparison between wild type (WT) and mutant forms of Smad2 in the same cells, under the same conditions.

As expected, in cells expressing WT GFP-Smad2 and myc-Smad2 with serine 465 and 467 mutated to alanine (myc-Smad2 C-sites) C-terminal phosphorylation only occurred in wild type GFP-Smad2. However, despite the difference in receptor-mediated phosphorylation, virtually identical phosphorylation at the PAK2-mediated T430 site occurred (Fig 5.5B). While apparent mild differences in phosphorylation between WT and C-sites Smad2 can be seen in individual blots (as appears in Fig 5.5B), no observable difference in T430 phosphorylation between the two Smad2 forms could be observed after normalization for total expression levels of the two Smad2 forms.

Although phosphorylation of C-sites has no impact on T430 phosphorylation, the phosphorylation status of the receptor site of Smad2 is influenced by the PAK2 site phosphorylation status. For instance, when expressing both GFP-Smad2 WT and myc-Smad2 with threonine 430 mutated to an alanine (myc-Smad2 T430A), as expected no phosphorylation at the PAK2 site could be detected in myc-Smad2 T430A while GFP-Smad2 WT showed the same kinetics observed for endogenous Smad2. In contrast, the rate of dephosphorylation (but not the phosphorylation) at S465/67 of Smad2 was significantly increased in the myc-Smad2 T430A mutant compared to the GFP Smad2 WT (Fig 5.5C). In Smad2 T430A, phosphorylation at S465/67 was virtually reduced to background by 8 hours while Smad2 WT retained significant phosphorylation at least 12 hours after ligand challenge (Fig 5.5C). Indeed the increase in dephosphorylation of TGF β R1-mediated sites of Smad2 by mutating T430 was strikingly similar to the observations using a dominant-negative PAK2 (Compare Fig 5.4 with Fig 5.5C).

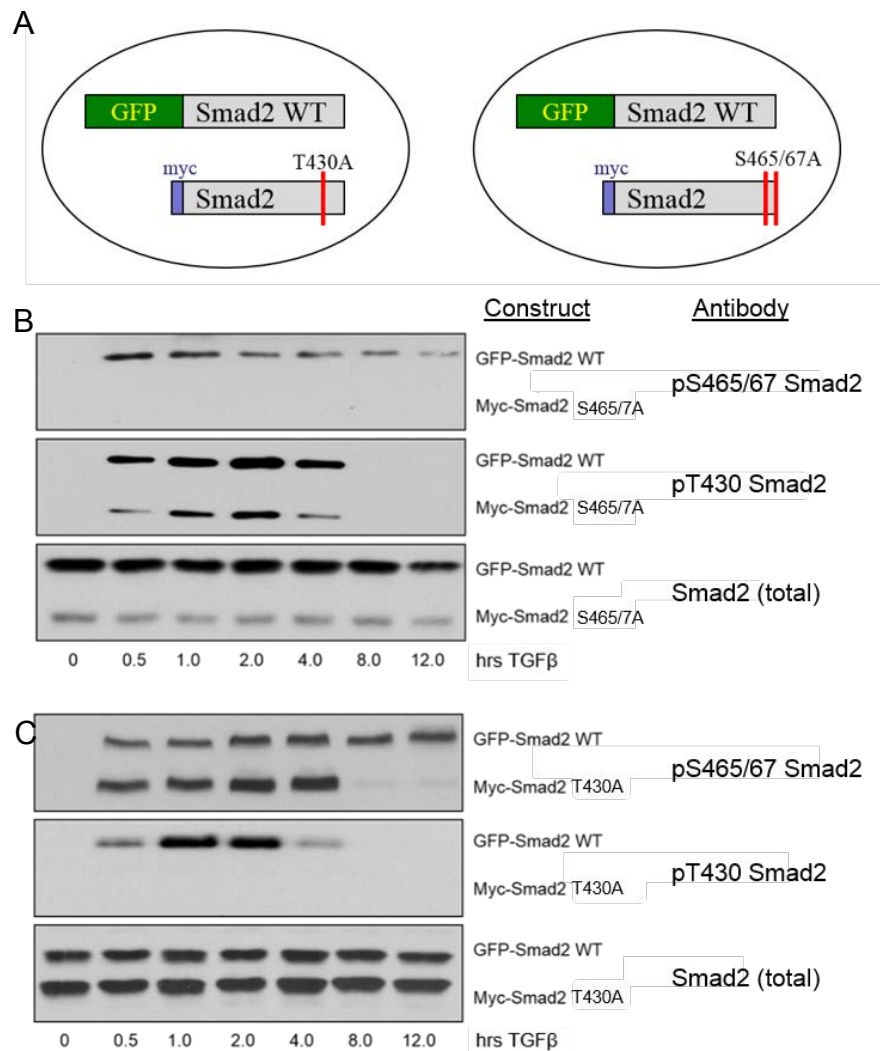


Figure 5.5 Receptor site phosphorylation is not required for PAK2 site phosphorylation whereas PAK2 phosphorylation extends duration of receptor site phosphorylation. (A) Diagrammatic representation of the two pools of cells used in this study. Smad2^{-/-} MEFs were transiently transfected with both wild type Smad2 tagged with GFP (GFP-Smad2 WT) and a Smad2 tagged with myc and serines 465/467 mutated to alanines (myc-Smad2 Csites). (B) Cells were stimulated with 10ng/ml TGFβ for indicated times before subjection to SDS-PAGE and Western analysis for (top panel) Smad2 phosphorylation at S465/467, (middle panel) Smad2 phosphorylation at T430, (bottom panel) Total Smad2. (C) Cells were treated as above except transfection with Smad2 WT GFP and Smad2 tagged with myc bearing a mutation of threonine 430 to alanine (myc-Smad2 T430A).

5.3.4 Smad2 phosphorylation at Threonine 430 has no impact on nuclear translocation, heterodimerization with Smad4, or sensitivity to ligand

Receptor-mediated phosphorylation of R-Smads initiates nuclear translocation and accumulation (Attisano 1998). Unphosphorylated Smad2 exists as a monomer but

upon receptor-mediated phosphorylation forms higher order complexes with other Smad2 molecules and/or Smad4 (Shi 2001) and it is these complexes that enter the nucleus to bind DNA (Attisano 1998). Having documented PAK2 phosphorylation of Smad2 has an impact on the duration of TGF β R1-mediated phosphorylation (Fig 5.5), we sought to determine the impact on downstream events. No differences in nuclear accumulation (Fig 5.6) or the affinity with Smad4 after TGF β challenge (Fig 5.7) were observed between WT and Smad2 T430A mutant. Analysis of nuclear fractions yielded high nuclear enrichment with very limited cytoplasmic contamination (Fig 5.6).

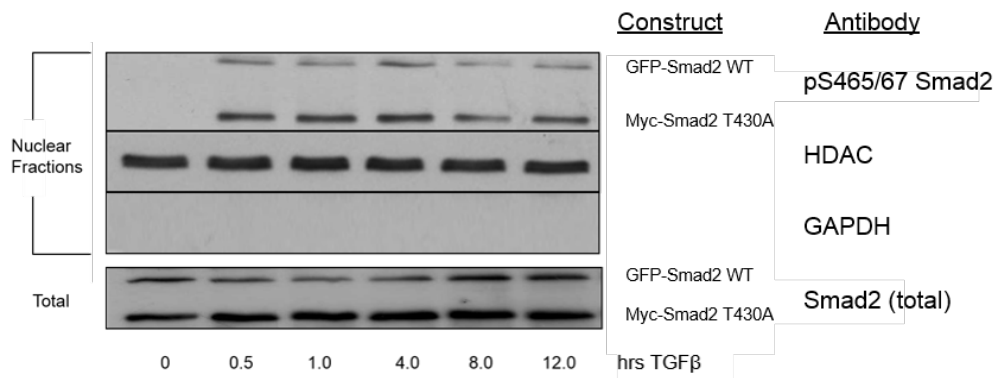


Figure 5.6 Phosphorylation of Smad2 at Thr430 has no impact on TGF β induced nuclear translocation of Smad2. After transient transfection of Smad2^{-/-} MEFs with both GFP-Smad2 WT and myc-Smad2 T430A constructs and TGF β stimulation at 10ng/ml for indicated times, nuclear fractionation was performed. Fractions were assayed by SDS-PAGE and Western analysis for receptor site phosphorylation of Smad2. Purity of the fractions was confirmed by probing for HDAC and GAPDH. Parallel samples were prepared and total cellular levels of Smad2 determined.

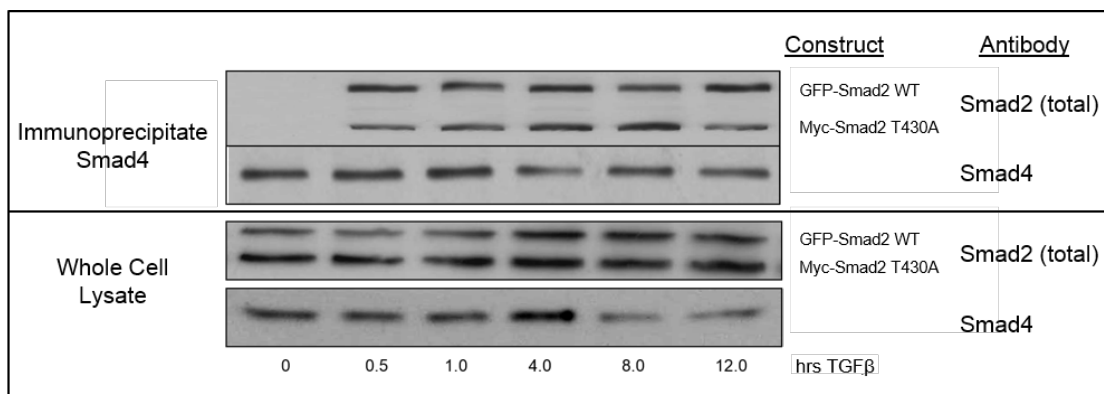


Figure 5.7 Smad2 wild type and those unable to be phosphorylated by PAK2 have the same ability to form heterodimers with Smad4 upon TGF β stimulation. Smad2^{-/-} MEFs cells transiently transfected with both a wild type Smad2 tagged with GFP and mutant T430A Smad2 tagged with myc, were stimulated with 10 ng/ml TGF β for indicated times. Cells were lysed, protein levels normalized across samples, lysates were immunoprecipitated with antibodies to Smad4 prior to Western analysis for Smad2 and Smad4. Parallel samples were subjected to Western analysis against total Smad2 and Smad4 to ensure equal loading.

In previous experiments, cells were treated with 10 ng/ml of TGF β , which exposes cells to concentrations well in excess of physiological conditions. To address if phosphorylation at T430 impacts the TGF β R1-mediated sensitivity of Smad2 in non-saturating concentrations of ligand, cells expressing WT and T430A Smad2 were stimulated with TGF β concentrations ranging from 0.001-10 ng/ml. No differences were observed between the two Smads at any ligand concentration, with robust receptor-mediated phosphorylation at even the lowest ligand concentration (Fig 5.8) in both Smad2 constructs.

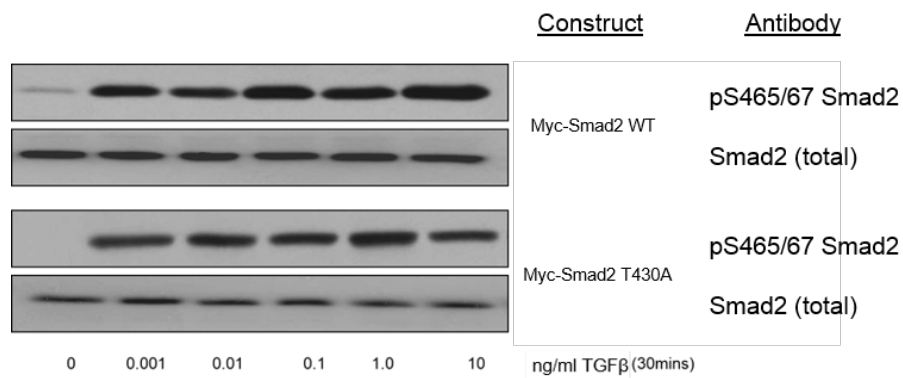


Figure 5.8 Phosphorylation of Smad2 at Threonine 430 has no impact on ligand sensitivity to TGF β . Smad2^{-/-} MEFs were transiently transfected with either myc-Smad2 WT (top panels) or myc-Smad2 T430A (bottom panels). Cells were challenged with the indicated concentration of TGF β for 30 mins, lysed and processed by SDS-PAGE and Western analysis examining receptor site phosphorylation or total Smad2.

5.3.5 Phosphorylation at Threonine 430 prevents the phosphatase PPM1A from binding Smad2 and dephosphorylating Serines 465/467

Upon entering the nucleus R-Smads are dephosphorylated prior to export back into the cytoplasm, which is regulated by the PPM1A phosphatase (Lin 2006). PPM1A did not robustly co-immunoprecipitate with WT Smad2 until 12 hours after TGF β challenge. In contrast PPM1A co-immunoprecipitated with Smad2 T430A after 1 hour and remained strongly associated until 8 hours post stimulation (Fig 5.9). Evidently this increased association with PPM1A precedes detectable dephosphorylation at the receptor-mediated sites in both WT and T430A Smad2. However, the association of PPM1A with Smad2 only occurs in the absence of T430 phosphorylation, strongly implying that presence of phosphorylated T430 prevents the association of Smad2 with PPM1A, and therefore the dephosphorylation of the receptor-mediated phosphorylation sites. In the

absence of T430 phosphorylation (in epithelial cells of fibroblasts expressing Smad2 T430A), PPM1A binds to pS465/67-Smad2 robustly, apparently facilitating dephosphorylation. When phosphorylation of T430 occurs (in fibroblasts expressing WT Smad2), binding of PPM1A to Smad2 does not occur until T430 is first dephosphorylated, effectively delaying PPM1A-mediated dephosphorylation of S465/67 (Fig 5.9).

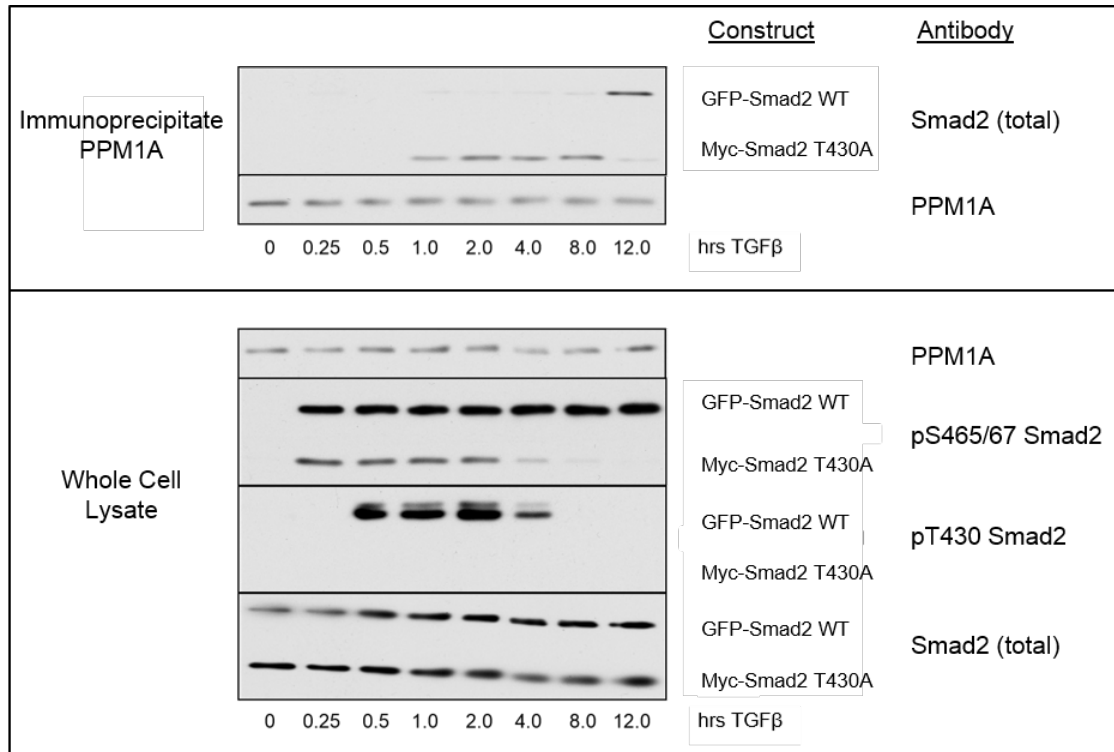


Figure 5.9 Smad2 mutants are unable to be phosphorylated at Threonine 430 and have increased association with phosphatase PPM1A which correlates with dephosphorylation at receptor sites. Smad2^{-/-} MEFs were transiently transfected with both Smad2 WT GFP and Smad2 T430A myc and treated with 10 ng/ml TGFβ1 for indicated times. Following lysis and protein normalization samples were split into two aliquots. The first aliquot was subjected to immunoprecipitation for PPM1A before SDS-PAGE and Western analysis against Smad2 and PPM1A. The remaining aliquots (Whole Cell Lysate) were, after SDS-PAGE, probed for levels of PPM1A, Smad2 phosphorylation at S465/467, Smad2 phosphorylation at T430, and total Smad2.

5.4 DISCUSSION

Evidence of a role for PAK2 in TGFβ driven disease processes was first suggested when inhibition of the PAK2 and downstream factors significantly attenuated pulmonary (Daniels 2004, Wilkes 2006) and renal (Wang 2005, Wang 2009) fibrosis and scleroderma (Bhattacharyya 2009, Hinchcliff 2012). In TGFβ induced hepatoma cell migration the knockdown of PAK2 resulted in increased focal adhesion formation

and dramatically reduced migration (Sato 2013). Furthermore, examination of 62 hepatocellular carcinoma (HCC) patient samples showed PAK2 activation closely associated with tumor progression, metastasis, and early recurrence of HCC (Sato 2013).

We determined that in fibroblasts stimulated by TGF β , PAK2 phosphorylated Smad2 and Smad3 but did not phosphorylate Smad1, 4 or 5. PAK2 phosphorylation occurs on residue 430 which is a threonine (Fig 5.4) and corresponds with a PAK2 consensus sequence of (K/R)RX(S/T), in this case RRQT (Fig 5.3). The corresponding residue is T388 in Smad3 which is similarly contained within a RRQT motif (Fig 5.3). In Smad2, when T430 was mutated to an alanine, it could no longer be phosphorylated and while T430 phosphorylation had no impact on the rate of Smad nuclear translocation, Smad hetero-oligomerization or cell sensitivity to ligand, the duration of TGF β -induced phosphorylation at nearby S465/67 was impacted.

Because PAK2 activity was not required for the initiation of Smad2/3 phosphorylation after TGF β stimulation and the Smads were not required for PAK2 activation (Wilkes 2003), PAK2 and other members of the signalling cascade were deemed to be “Smad-independent”. Here we document a direct association between PAK2 and the Smads with specific residues of Smad2 (and presumably Smad3) phosphorylated by PAK2 when it is activated by TGF β in fibroblasts (Figs 5.4, 5.5, 5.9) suggesting the term “Smad-independent” is somewhat of a misnomer. The phosphorylation of Smad2 at serines 465 and 467 by the TGF β receptors is critical in propagating the TGF β signal as this facilitates accelerated entry to the nucleus, increased nuclear retention and DNA binding (Attisano 1998). PAK2 phosphorylation at T430 does not inhibit phosphorylation at S465/67 but instead leads to a prolonged phosphorylation at these sites (Figs 5.4 and 5.5). In this way, PAK2 does not directly impact the phosphorylation of Smad2 at S465/67 but instead *inhibits the dephosphorylation*. The duration of Smad2 phosphorylation at S465/67 was reduced from around 12 hours in wild type Smad2 in fibroblast cells, to approximately 4 hours in Smad2 with a T430A mutation (Fig 5.5). This 4 hour duration corresponds closely with that observed in epithelial cells in which PAK2 is not activated by TGF β (Fig 5.4). Further evidence that PAK2 phosphorylation of T430 is causally linked to the delayed dephosphorylation at S465/67 is presented when inhibition of PAK2 kinase activity (by expression of a dominant-negative PAK2) resulted in virtual identical kinetics of S465/67 dephosphorylation between epithelial cells and fibroblasts with PAK2 inhibited (Fig

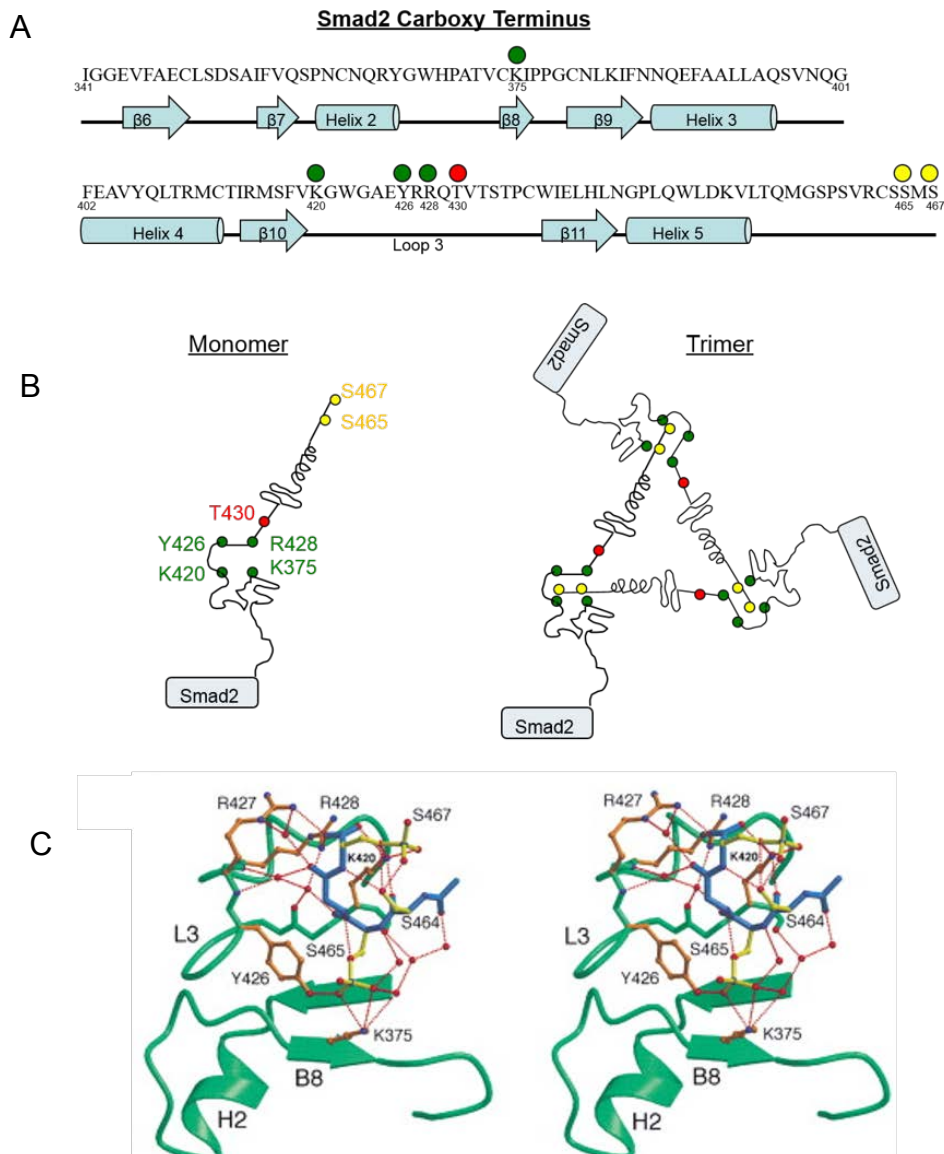
5.4). Collectively, a strong case can be made that T430 phosphorylation directly impacts S465/67 dephosphorylation while having no impact on the initiating events of S465/67 phosphorylation.

Smad2 (and other R-Smads) are dephosphorylated at S465/67 by the nuclear localized phosphatase PPM1A (Lin 2006). Co-immunoprecipitation experiments demonstrate that in fibroblasts in which Smad2 is phosphorylated at T430, PPM1A does not associate with Smad2 until between 8 and 12 hours. This contrasts with Smad2 with a T430A mutation, where PPM1A association is detected at between 1 and 2 hours post TGF β stimulation (Fig 5.9). Our data suggests PAK2 phosphorylation at T430 inhibits binding of PPM1A to Smad2 and therefore prevents dephosphorylation of S465/67 (Fig 5.9).

The phosphorylation of Smad2 at T430 occurs only 34 residues away from the S465/67 sites that are phosphorylated by the TGF β receptors (Fig 5.2) but this tells us little in terms of the distance between the residues in the native, 3-dimensional conformation. The crystal structure of Smad2 has been solved (Wu 2001) and sheds insight into how T430 phosphorylation may inhibit phosphatase action. In the unphosphorylated form Smad2 exists as a monomer with the carboxy terminal 15 residues flexible, but when phosphorylated at S465/67 trimers form and the carboxy terminal becomes rigid and well ordered (Wu 2001). The negatively charged phosphorylated carboxy terminus binds a neighbouring pSmad2 at a positively charged surface pocket formed by the L3 loop and β 8 strand, referred to as the loop-strand pocket (Fig 5.10).

The interactions between the phosphorylated carboxy terminus of one pSmad2 and the loop-strand pocket of another “receiving” pSmad2 is dominated by a large network of hydrogen bonds, with the phosphate groups serving as nucleating centers (Wu 2001). Four residues on the “receiving” Smad coordinate these hydrogen bonds, and are K375 on the β strand of β 8 and K420, Y426 and R428 on the L3 loop, with R427 contributing an additional hydrogen bond with pS467 (Fig 5.10). These residues are found on all R-Smads and Smad4 suggesting a critical role in heteroligomerization. Threonine 430 is within the L3 loop but just adjacent (two amino acids) to the critical residues forming hydrogen bonds with incoming pSmad2 proteins. Considering the

close proximity of T430 to the phosphorylated S465/67 of a bound neighbouring pSmad2 it is likely phosphorylation at T430 does not prevent phosphatase action with S465/67 on the same Smad2 molecule, but rather inhibits phosphatase action of the phosphorylated S465/67 of the bound Smad2.



Adapted from "Crystal Structure of a Phosphorylated Smad2" by J-W Wu et al, 2001, Molecular Cell, Vol 8, p1277-89 Copyright ©2001 Cell Press. Adapted with Permission

Figure 5.10 Structural analysis of the carboxy terminus of Smad2. (A) Residues 341 to 467 of Smad2 with the corresponding secondary structure represented below. Serines 465/67 are indicated with yellow circles, Threonine 430 with a red circle and the critical residues of the loop-strand pocket indicated with green circles. (B) A diagrammatic representation of a monomeric form of Smad2 (left) and trimer (right) of Smad2 molecules with the phosphorylated S465/67 residues inserted into the loop-strand pocket of the neighbouring Smad2. (C) A stereo view of the hydrogen bond network between two pSmad2 molecules. One pSmad2 is green while the other is blue with their side chains coloured in orange and yellow. Hydrogen bonds among oxygen (red) and nitrogen (blue) atoms and water molecules (red) are indicated by red dotted lines. On one side of the interface Y426 and K375 donate 3 hydrogen bonds to the phosphate of S465 and are buttressed by several additional water-mediated hydrogen bonds. On the other side, K420 and R428 hydrogen bond to the carboxylate of S464 and R427 and R428 hydrogen bond to the carboxylate of S467.

However, while this model of trans-protection is appealing, it does not preclude the event that T430 phosphorylation may sterically hinder (or otherwise physically influence), phosphatase binding and action on S465/67 on the same Smad molecule. Indeed such an interaction has been observed in PKC α , where phosphorylation at T638 greatly influenced the phosphatase sensitivity of T497 in the catalytic domain of the protein (Bornancin 1996) with the two sites separated by 141 amino acids. Whether T430 phosphorylation inhibits dephosphorylation in a *cis*- or *trans*- manner remains to be determined.

In a TGF β driven model of renal fibrosis, examination of normal and fibrotic kidneys revealed a significant increase in the degree of Smad3 phosphorylation at threonine 388, which is the corresponding PAK2 site of threonine 430 of Smad2 (Qu 2014). Further characterization demonstrated phosphorylation at this site was required for TGF β induced collagen production and extracellular matrix deposition (Qu 2014). Although the study found no evidence of Smad2 phosphorylation at threonine 430, fibrosis results from an imbalance of Smad3 signalling overwhelming Smad2 (Feng 2005), perhaps explaining an absence of Smad2 phosphorylation at the PAK2 site. Although Qu and colleagues did not determine the kinase responsible for threonine 388 phosphorylation, PAK2 would be a likely candidate. Furthermore, as fibrosis is often considered the failing of the normal TGF β -mediated wound healing response to recognize stop cues (Hinchcliff 2012), the prolonged Smad signal induced by PAK2 activation may well be a contributing factor.

It has been reported that activated ERK can phosphorylate R-Smads in the linker region between the MH1 and MH2 domains in many cell types, with conflicting reports as to whether this increases/decreases nuclear entry/activity (Hough 2012). Although ERK activation can have many stimuli, ERK activation by TGF β in fibroblasts is mediated largely by PAK2 phosphorylation of cRaf (Suzuki K 2007, Hough 2012). In fibroblasts, PAK2-mediated ERK activation, and subsequent Smad2 linker phosphorylation, did not impact Smad2 entry to the nucleus yet sustained pSmad2 signalling by increasing protein stability (Hough 2012). This established the possibility of PAK2 activation increasing the duration of TGF β induced signalling in the nucleus in

two ways; increasing protein stability and as we report here preventing dephosphorylation of the receptor-mediated site by PPM1A.

Further support that PAK2 and R-Smad cross-talk may be linked to cell type-specific outcomes involves the expression levels of Erbin. High levels of Erbin inhibit both PAK2 activity (Wilkes 2009) and R-Smad signalling (Dai 2007, Sflomos 2011) with Erbin expression low in mesenchymal but high in epithelial cultures (Wilkes 2009). PAK2 activation has been shown to be elevated in ovarian cancer and others (Siu 2009), however the link between PAK2 activity, TGF β and Smads in cancer is provocative but remains to be explored.

Why PAK2 is not activated in all cell types by TGF β is not understood. However, when PAK2 mutants bearing constitutive kinase activity were expressed in NMuMg epithelial cells in conjunction with TGF β cells, the cells underwent catastrophic death (Wilkes 2009). PAK2 activation in MDCK epithelial cells inhibited R-Smad signalling through phosphorylation at yet another site (serine 417 of Smad2) antagonizing R-Smad interaction with TGF β receptors and preventing receptor-mediated phosphorylation – but no cell death (Yan 2012). Although MDCK and NmuMg are both of epithelial lineage, their normal response to TGF β differs (growth arrest and epithelial to mesenchymal transition (EMT) respectively) which may explain why PAK2 activation caused different cellular outcomes. The characterization of serine 417 phosphorylation has not been examined beyond MDCK cells.

In summary, we document the presence of potential PAK2 phosphorylation sites in Smad2 and Smad3 that are indeed phosphorylated by PAK2 in response to TGF β in fibroblasts and not epithelial cells. Phosphorylation at the PAK2 site does not impact the ability of the receptor to phosphorylate R-Smads at the C-terminal, nor the ability of the R-Smads to enter the nucleus. However, phosphorylation at the PAK2 site prevents receptor-mediated dephosphorylation by preventing R-Smad association with the phosphatase PPM1A in the nucleus (See Fig 5.11). Considering PAK2 activation occurs in a number of fibroblast cell lines and not epithelial cells, it will be interesting to uncover how the differential phosphorylation of the PAK2 site in Smad2 and Smad3 influences the impact of Smad signalling on the biological response to TGF β between the two cell types.

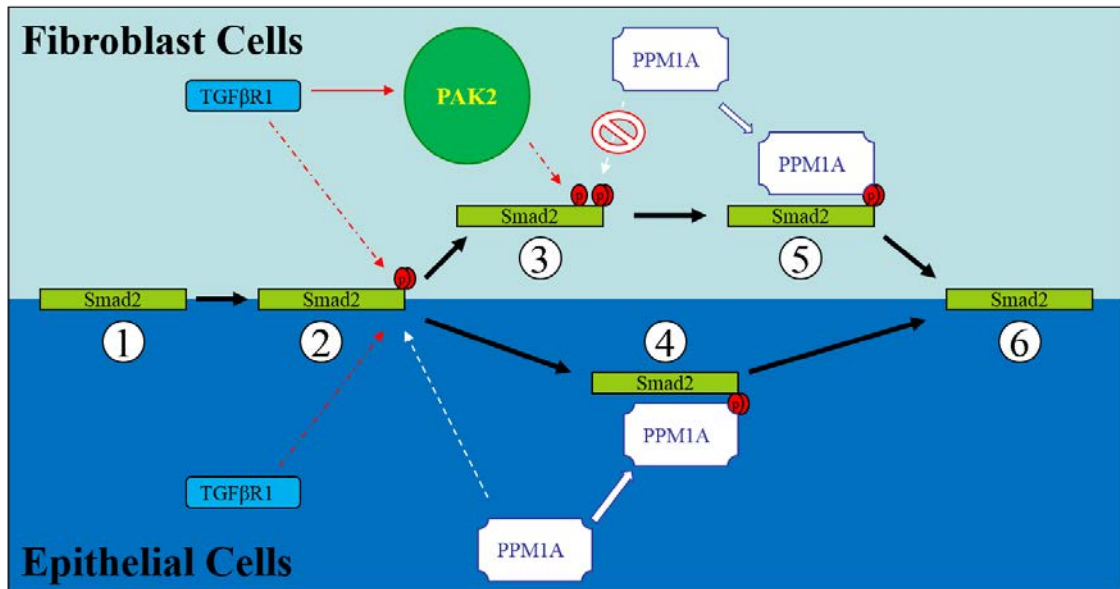


Figure 5.11 Differences in Smad2 phosphorylation and dephosphorylation in fibroblast and epithelial cells. Black arrows indicate the progression of Smad2 molecules as they respond to TGF β stimulation over time in both fibroblast (Top) and epithelial (Bottom) cells. Prior to stimulation (1) Smad2 is unphosphorylated before being recognized as a substrate for activated TGF β R1, resulting in phosphorylation at serines 465/67 (2). This occurs in both cell types. In fibroblasts TGF β also activates PAK2 which adds an additional phosphate group to threonine 430 (3). While Smad2 phosphorylated at serines 465/67 is recognized by the phosphatase PPM1A in both epithelial (4) and fibroblast (5) cells, the presence of a phosphate at threonine 430 prevents PPM1A binding and subsequent dephosphorylation until such time as threonine 430 is dephosphorylated. In both cell types, Smad2 is ultimately dephosphorylated (6) however the duration of phosphorylation of Smad2 at serines 465/67 is significantly extended by the disruption of PPM1A binding by threonine 430 phosphorylation.

CHAPTER 6

RETROGRADE TRAFFICKING OF TGF β RECEPTOR POOL TO THE NUCLEUS UPON TGF β STIMULATION

CHAPTER 6: RETROGRADE TRAFFICKING OF TGF β RECEPTOR POOL TO THE NUCLEUS UPON TGF β STIMULATION

6.1 BACKGROUND

TGF β is a multifunctional cytokine with a wide range of pathological and physiological roles (Massagué 1998). Pleiotropic effects are via ligand-induced heteromeric complex formation of two serine/threonine kinase receptors, TGF β R1 and TGF β R2, with sequential activation in which TGF β R1 acts as a substrate for ligand-bound TGF β 2 (Wrana 1994). Although both are serine/threonine kinases, only a complex of both TGF β R1 and TGF β R2 in a cooperative heterotetrameric complex, mitigates TGF β signalling (Anders 1996). This contrasts with tyrosine kinase receptors that propagate their signal as simple homodimers upon ligand binding (Carpenter 2009). Furthermore, while many receptors signal from the cell surface (Carpenter 2009), phosphorylation of Smad2/3 by TGF β R1 occurs only after clathrin-coated vesicles containing TGF β receptors are severed from the plasma membrane to undergo endocytosis (Hayes 2002, Panopoulou 2002, Penheiter 2002). TGF β receptors recycle constitutively and the rate of recycling is not altered upon TGF β insult (Mitchell 2004), however virtually all receptors are very rapidly removed from the cell surface (Anders 1997, Doré 2001, Garamszegi 2001) after ligand addition. It is widely accepted these down-regulated receptors are destined for degradation, yet observed degradation is substantially slower and less dramatic than down-regulation (Di Guglielmo 2003) perhaps suggesting an alternate fate for a pool of down-regulated receptors.

Intracellular trafficking studies have been inhibited by the lack of high quality antibodies to the native receptors, however, since 2000 (Zwaagstra 2000) there have been reports of TGF β R1 within the nucleus. It was shown that TGF β R1 was redistributed from being largely excluded from, to densely concentrated within the nucleus after prolonged TGF β treatment in both A549 lung adenocarcinoma and Mv1Lu normal epithelial cells. It was also reported that TGF β R1 localized to the nucleus in transformed but not normal breast epithelia (Chandra 2012) however as both Zwaagstra's and Chandra's studies documented the total (intracellular and surface) receptor pool, it was unclear if ligand-induced activation directly targeted surface receptors to the nucleus, or a downstream signalling event redirected intracellular/inactive receptors to the nucleus.

While the nuclear translocation of a number of receptors after ligand induced proteolytic cleavage, such as Notch and Growth Hormone Receptor, is well characterized, it has also been observed in a number of tyrosine kinase receptors including ErbB4, Vascular Endothelial Growth Factor Receptor 1 (VEGFR1) and Insulin-like Growth Factor Receptor 1 (IGFR-1) (Carpenter 2009). The sequential process begins with most of the extracellular domain being cleaved by enzymes such as α -secretase in the case of Notch, or TNF α -converting enzyme (TACE) for ErbB4, followed by recognition and subsequent intracellular cleavage by the γ -secretase complex.

In prostate, lung and breast carcinoma lines (but not primary cells), Landström and colleagues (Mu 2011, Gudey 2014) observed the truncated intracellular domain of TGF β R1 present in the nucleus after TGF β treatment. Similar to other receptors, in carcinoma cell lines expressing high levels of TRAF6, they observed TGF β R1 was first cleaved in its extracellular domain, by TACE (Mu 2011) prior to intracellular cleavage by the γ -secretase catalytic subunit Presenilin 1 (Gudey 2014). However, nuclear receptors were also observed in non-transformed lines (Zwaagsta 2000) with low TRAF6 levels. The question arises: is there another mechanism driving nuclear translocation in these cells?

Retrograde trafficking to the nucleus of full-length receptors has also been observed. EGFR (ErbB1-3), Met, Fibroblast Growth Factor Receptors 1 and 2 (FGF-R1/R2), Tropomyosin receptor kinase A (TrkA), VEGFR1, and others (see Carpenter and Liao, 2009 for review) utilize much of the same retrograde trafficking machinery as many bacterial toxins (e.g. Shiga and cholera toxins, ricin and *Pseudomonas* exotoxin) (Carpenter 2009). Receptors contained in vesicles are endocytosed through clathrin-mediated endocytosis (Brand 2011) traffic to the Golgi and undergo retrograde transport to the ER in COPI-coated vesicles (Wang 2010).

Classically, cargo exiting the ER undergoes anterograde transport during synthesis and maturation (Koenig 2014), with retrograde trafficking largely limited to degradation of mis-folded proteins through the Endoplasmic-Reticulum Associated protein Degradation (ERAD) pathway (Ruggiano 2014). Mis-folded proteins exiting the

retrotranslocon, are immediately ubiquitinated and targeted to the 26S proteasome that is either closely affiliated with or directly associated with the retrotranslocon pore (Nakatsukasa 2008). However degradation isn't the only fate of retrotranslocon cargo. SV40 virus (Marsh 2006), Ricin (Matlack 1998), *Pseudomonas* exotoxin (Koopmann 2000) and cholera toxin (Schmitz 2000) avoid degradation and a number surface-derived receptor kinases, not only avoid degradation, but require transport through the retrotranslocon *en route* to the nucleus (Liao 2007, Wang 2010). How these proteins avoid degradation is not yet apparent.

Removal of the hydrophobic transmembrane domain by proteolytic cleavage most easily explains the problems associated with getting an insoluble protein to solubilize in the nucleus. How full length-receptors achieve this is more difficult to understand with two models proposed for EGFR. In both models, EGFR exits the ER through the retrotranslocon (Liao 2007, Wang 2010) and enters the nucleus through direct association with components of the nuclear pore complex (Liao 2007, Wang 2010) however, in one model the receptor enters in a soluble form (Liao 2007) while the other doesn't solubilize until after nuclear entry (Wang 2010). Liao and Carpenter suggest physical interaction with the retrotranslocon extracts EGFR from the lipid bilayer where chaperones escort receptors in a soluble conformation through the cytoplasm to the nuclear pore for nuclear entry (Liao 2007). In contrast, Min Chi Hung and colleagues (Wang 2010) suggest receptors exit the retrotranslocon and remain in the membranous environment, traversing the contiguous ER / outer nuclear membrane to the nuclear pore. Upon nuclear entry, EGFR remains embedded in the inner nuclear membrane awaiting an unknown mechanism for solubilization (Wang 2010).

Objectives

The objective of this study was to examine processes regulating TGF β receptors in the nucleus. It has been reported the abundance of TGF β receptors in nuclei is much higher in cancerous than normal tissue (Mu 2011, Chandra 2012, Gudey 2014) but how this is regulated is undefined. A number of contradictions have developed due to discrepancies in the data observed by the various groups examining the presence of nuclear receptors, diverse cell/tissue types, the role/s for nuclear receptors and how the nuclear pool of receptors differs from those undergoing the classically defined

downregulation/degradation route. Specifically we have sought to experimentally address the following aims:

1. To determine if there is increased nuclear trafficking of TGF β receptors (TGF β R1 and/or TGF β R2) from the cell surface after ligand stimulation, to define the kinetics of any observed nuclear trafficking from the cells surface to the nucleus, and determine if nuclear trafficking of TGF β receptors is increased in transformed/cancerous cells relative to untransformed, immortalized control cells.
2. To define the trafficking route of the TGF β receptor/s and determine the solubility in the nucleus. As the EGFR nuclear trafficking route is well characterized, initial studies will determine if TGF β and EGF receptors shared any trafficking machinery *en route* to the nucleus.
3. To define elements within TGF β receptor/s that regulate nuclear trafficking.

Here we present data documenting how TGF β stimulation leads to rapid internalization of surface bound receptors and while many are degraded, a significant proportion traffic to the nucleus. This occurs in numerous cell types and both TGF β R1 and TGF β R2 travel together. TGF β R2 is required for the complex to enter the Golgi, while TGF β R1 facilitates entry into COPI vesicles for delivery to the ER. Receptors exit the ER via the retrotranslocon, sliding along the contiguous ER/outer nuclear membrane, through the nuclear pore into the inner nuclear membrane. The receptors never truly solubilize but instead enter PML nuclear bodies derived from the inner nuclear membrane.

6.2 MATERIALS AND METHODS

6.2.1 Cell culture and stimulation

A range of immortalized cells from different tissues and species as well as normal and disease states were utilized in this study (Table 3.2). AKR-2B mouse fibroblasts were used throughout. Mv1Lu (epithelial cell of mink origin with well characterized TGF β response), MDCK (canine epithelial cells that establish polarity in culture models) and Cos7 (green monkey fibroblast line with high transfection efficiency), as well as human lung fibroblast (IMR90) and breast (MCF10A) provide a broad spectrum of lines to

determine if diversity exists in nuclear trafficking across different cell types and species. A number of immortalized and transformed human cancer cells were also analysed (A549, PC3, MCF10A/Neu and MDA MB231) being derived from lung, prostate, and two different stages of progression in breast cancer tissue respectively. Cells were obtained and cultured as specified (Table 3.2) using standard mammalian cell culture techniques (Chapter 3) and grown to confluence (unless otherwise stated) prior to stimulation with TGF β 1 to a final concentration of 10 ng/ml in the appropriate growth media (see Table 3.2). Stock TGF β was stored in 4mM HCl with 0.1% Bovine Serum Albumin (BSA) and stored at -20 °C. Cells were incubated in the presence of TGF β for various times (0 to 10 hours) at 37 °C with 5 % CO₂.

6.2.2 Visualization of surface receptors and intracellular compartments using immunofluorescence confocal microscopy

All images were obtained using a 100 \times objective (1.3 NA oil lens) on a Zeiss LSM 510 confocal system in accordance with standard confocal microscopy and cell preparation methods (Chapter 3). Confocal microscopy was utilized in order to confidently conclude any receptors detected in the nucleus, or other compartments, were indeed contained within that thin X/Y slice, rather than on top or below the organelle as can occur using standard immunofluorescence microscopy. A list of antibodies and dilutions used and fluorophore-conjugated secondary antibodies is provided (Table 3.3). Quantification of receptors in the nucleus and other compartments, relative to total cellular levels was determined by fluorescence intensity measurements using MetaMorph® quantitation (Molecular Devices, Sunnyvale, California).

Because our experimental questions focused only on the cellular fate of TGF β receptors that originated from the cell surface at the time of initial TGF β stimulation (as opposed to total receptor population that would also include receptors being delivered to, recycled from, and *en route* to degradation) we modified the standard staining protocol. A diagrammatic representation of the technique is shown in Figure 6.1. Essentially, cells were cooled to a temperature in which receptor internalization is blocked (Mitchell 2004) and incubated in the presence of primary antibody recognizing an extracellular domain epitope of the receptor. After a mild wash to remove excess antibody, cells were warmed to allow internalization and exposed to experimental manipulation, prior to fixation and permeabilization and conventional staining.

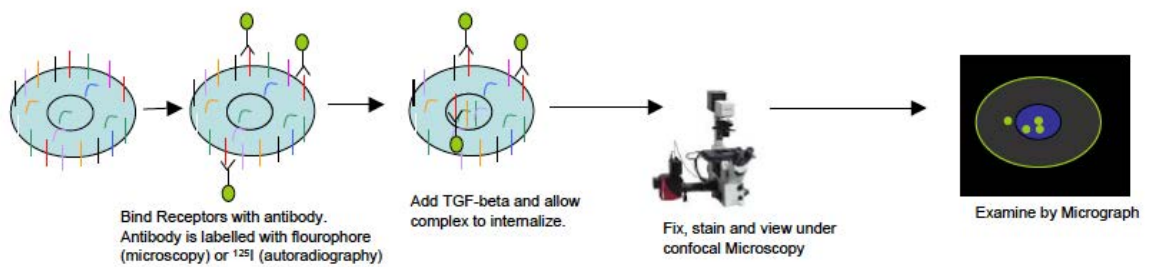


Figure 6.1 Diagrammatic representation of tracking surface-derived TGFβ receptors after ligand stimulation. At endocytosis non-permissive temperatures, surface receptors are bound and cross-linked to primary antibodies. Cells are returned to normal temperatures and stimulated with TGFβ for various times. Cells are fixed, permeabilized and mounted before visualizing with a confocal microscope.

Cells were seeded on coverslips and allowed 24 hours to attach prior to cooling to 12°C and washing with ice-cold antibody buffer (DME + 50 mM HEPES [pH7.2]) 3 times. Cells were then incubated in 1 ml of antibody buffer containing antibody to specified receptor (Table 3.3) for 1h. After 3 washes in cold antibody buffer cells were incubated at 37°C in 0.1% FBS-DME in the absence or presence of 10 ng/ml TGFβ1 for various times. At the conclusion of the experiment, cells were washed twice in DME pH2.0, twice in DME pH7.0 and twice in cold PBS before fixation with 4% paraformaldehyde at 27°C for 20 min and permeabilization for 3 min with 0.1% Triton X100. After 60 min blocking (0.05% Saponin (Sigma-Aldrich, St Louis, Missouri) / 2% FBS in PBS) cells were incubated with antibodies recognizing compartment-specific proteins (listed in Table 3.3), followed by fluorophore-conjugated secondary antibodies and 3 minute incubation with DAPI. Slides were mounted using Vectashield (Vector Laboratories, Cambridgeshire, UK) and confocal images were acquired. No three-dimensional reconstructions, surface or volume rendering, or gamma adjustments were performed and only results are included that could be validated by a minimum of three repeats with the majority of cells on the slide sharing the reported phenotype. Where possible, multiple cells showing the observed phenotype are displayed in each field. The specificity of this technique was validated using cell lines lacking TGFβ receptors where no cellular or nuclear staining could be observed (data not shown).

6.2.3 Isolation of intracellular compartments via fractionation

6.2.3.1 Nuclear fractions

A number of techniques were employed depending on the required nuclei purity. Nuclear extracts (soluble nuclear components with only limited nuclear membrane and chromatin-associated components) were obtained using NE-PER™ Nuclear and Cytoplasmic Extraction Reagents (Pierce Biotechnology, Rockford, Illinois) supplemented with Complete® protease inhibitor. For some assays purer nuclear fractions were required (Figs 6.6, 6.8, 6.11, 6.12B and 6.14). To obtain purer, intact nuclei, pelleted cells were allowed to swell in hypotonic buffer prior to gentle homogenization with a dounce homogenizer and brief centrifugation (Chapter 3). Purity of the nuclear fractions was determined by the enrichment of the nuclear protein marker HDAC, and exclusion of the cytosolic protein GAPDH by immunoblotting (Fig 3.4A).

6.2.3.2 Inner nuclear membrane fractions

Inner nuclear membrane fractions were purified as outlined in Chapter 3. While emerin expression was not limited to this fraction (indicating limited inner nuclear membrane recovery), the presence of the outer nuclear membrane/rough endoplasmic reticulum (ONM/RER) Sec64 was virtually undetectable, suggesting high purity inner nuclear membrane fraction (see Fig 3.4D). Isolated nuclei were suspended in INM Buffer A and subjected to centrifugation at 10000 x g for 2 hours prior to ultracentrifugation at 100000 x g for 20 minutes on a sucrose gradient.

6.2.3.3 COPI vesicle fractions

COPI vesicle fractionation was performed as outlined in Chapter 3 and adapted (from Sönnichsen 1996). Because COPI vesicles and clathrin-coated vesicles are similar in size, the purity of these fractions was assessed by the absence of clathrin heavy chain and enrichment of Copα (See Fig 3.4).

6.2.3.4 Golgi and Endoplasmic Reticulum fractions

Purification of the Golgi was adapted for cell lysates using the Golgi Isolation Kit (Sigma-Aldrich, St Louis, Missouri) which yielded a high purity fraction. A high purity endoplasmic reticulum (ER) enrichment fraction was obtained by performing as per the manufacturer instructions using the Endoplasmic Reticulum Isolation Kit (Sigma-

Aldrich, St Louis, Missouri). Purity was determined by Western blot analysis for the enrichment or depletion of GM130 or giantin (restricted localization to Golgi), calnexin (restricted localization to ER), cytochrome C (restricted localization to mitochondria), GAPDH (restricted localization to cytoplasm), and histone or HDAC (restricted localization to nucleus). See Chapter 3 and Figure 3.4E for details.

6.2.3.5 Nuclear membrane, soluble nuclear and chromatin associated fractions

The nuclear soluble and chromatin-bound fractions were prepared using the Subcellular Protein Fractionation Kit for Cultured Cells (Thermo Fisher Scientific, Waltham, Massachusetts) as per manufacturer instructions while the nuclear membrane fraction came from a membrane prep (as per the manufacturer recommendations) on purified nuclei. Nuclei were purified using NE-PER™ Nuclear and Cytoplasmic Extraction Reagents (Pierce Biotechnology, Rockford, Illinois) followed by membrane extraction using the Subcellular Protein Fractionation Kit for Cultured Cells (See General Materials and Methods for details). Purity was determined by Western blot analysis for the enrichment or depletion of Sec64 (restricted localization to ER and outer nuclear membrane), HDAC (largely soluble with some chromatin association), and Histone 1 (restricted localization to chromatin) (Fig 3.4G).

6.2.4 Generation of TGFβ receptor constructs for receptor trafficking analysis

In a non-permeabilized cell only the extracellular domain of receptors at the plasma membrane are available for antibody binding. The experimental questions we have attempted to address focus only on this cell-surface localized pool of receptors, so binding an antibody in these conditions would be an ideal way to exclusively track this pool of receptors. However, no antibodies are available that specifically recognize the extracellular domain of native TGFβ receptors. In an effort to compensate for this, a number of alternative approaches were developed including generation of receptors with both extracellular and intracellular epitope tags (e.g. HA, myc and FLAG), generation of chimeric receptors (fusion of GM-CSF and TGFβ receptors) and the generation of mutant and truncated receptors (e.g. di-Lysine mutant TGFβR1).

6.2.4.1 TGFβ receptors expressing extracellular epitope for use in immunofluorescence confocal microscopy imaging

The simplest of these involved introducing a common epitope tag into the extracellular domain of the receptors. Expression of tags at the extreme N-terminal impaired the

affinity of the receptor for the ligand (Di Guglielmo 2005), but insertion of small tags a small distance inside the N-terminal resulted in biologically functional receptors with an exposed epitope for antibody binding (Di Guglielmo 2005; Yin 2013). Receptor constructs were generated using standard molecular biology techniques (see Chapter 3) and confirmed by DNA sequencing. Myc-TGF β R1 and HA-TGF β R2 expression and functionality were validated by western blotting and gene regulation assays (Di Guglielmo 2005; Yin 2013).

6.2.4.2 TGF β receptors expressing intracellular FLAG epitope

TGF β R1 and TGF β R2 receptors expressing C-terminally tagged FLAG epitopes are biologically functional (Wilkes 2003) and plasmids were kindly provided by Jeff Wrana (University of Toronto) or generated using standard cloning techniques as described in Chapter 3. These were expressed on a CMV promoter ensuring abundant expression and antibodies are available to FLAG epitopes providing increased specificity and affinity.

6.2.4.3 GM-CSF/TGF β chimeric receptors

As an alternative to native or extracellularly tagged TGF β receptors, chimeric receptors expressing the extracellular ligand-binding domain of the GM-CSF α or β receptor coupled to the transmembrane and cytoplasmic domain of the TGF- β type I and type II receptors, respectively (Anders 1996) were utilized (see Fig 3.2 for advantages of chimeric receptors over tagged native receptors) to determine the requirement and regions of TGF β R2 required for nuclear trafficking of the receptors (Figs 6.8 and 6.9). Previous work documented that chimeric and native TGF β receptors have analogous signalling and trafficking activity regardless of the culture conditions or cell type tested (Anders 1996, Anders 1997, Yao 2002, Mitchell 2004, Murphy 2004, Wilkes 2009).

6.2.4.4 TGF β R1 expressing di-Lysine mutations

Two pairs of lysines are found in TGF β R1 at residues 342, 343 and 489, 490. Using standard molecular biology techniques (Chapter 3) point mutants were generated within TGF β R1 by site directed mutagenesis using Quikchange® II XL (Agilent Technologies, Santa Clara, California). Mutants were confirmed by sequencing prior to transfection into TGF β R1-deficient Mv1Lu cells and Western blot analysis to determine

expression. Specific mutants are outlined in Figure 6.11 with lysines at residues 342 and 343 and/or residues 489 and 490 mutated to alanines.

6.2.4.5 TGF β R2 truncations, Δ 484-498 deletion, K488Q mutant and DUB fusion mutants

Truncations were generated in TGF β R2 after residues 474, 484, 498 and 517 through the introduction of three consecutive stop codons after the corresponding residue using standard molecular biology techniques (Chapter 3). TGF β R2 lacking amino acids 485-498 and a point mutant (K488Q) were generated using Quikchange® II XL (Agilent Technologies, Santa Clara, California) while TGF β R2 with a deubiquitination domain fused to the carboxy terminal of the receptor was generously provided by Dr David Katzmann.

6.2.5 Biotinylation of surface proteins for detection of Activin and TGF β receptors in subcellular compartments

In order to accommodate our need to focus on TGF β receptors that were at the cell surface and available for ligand binding, we used a surface-restricted biotinylation method that offers high affinity and specificity during purification to differentiate between surface-derived receptors and those that are newly synthesized or part of another cellular compartment. Because biotin can bind a number of different amino acids and is a cell permeable protein we used sulfo-N-hydroxysuccinimide (NHS) biotin which is cell permeable and can therefore bind both cell surface and intracellular proteins. However, Sulfo-NHS-biotin has the added property of being unable to cross cell membranes and therefore only labels the extracellular lysines of transmembrane and secreted proteins. Being small (MW=244.31 g/mol), biotin usually has very little modification of protein activity or trafficking. Therefore, by binding biotin (specifically sulfo-NHS-SS biotin/HBSS) to the lysine residues of extracellular components of transmembrane proteins at time we can trace the cellular fates of these proteins over time.

To label cell surface proteins (including TGF β receptors), cells were pre-chilled to 12°C and washed 3 times in ice-cold Hank's balanced salt solution (HBSS; Mediatech, Manassas, Virginia) before incubation in 1 mg/ml freshly prepared sulfo-NHS-SS biotin/HBSS (Thermo Scientific, Waltham, Massachusetts) for 60 min. Cells were then washed 3 times in 0.1% FBS-DME to remove free biotin that could bind intracellular

proteins after cell lysis and the temperature raised to 37°C prior to TGFβ treatment for various times. Upon conclusion of experiments, cells were subjected to fractionation before either whole cell lysates, or the various organelle fractions were rocked for 1 hour at 4°C before washing with ice-cold 5 mM Tris/HBSS and lysis in 500 µl of modified radioimmunoprecipitation assay (RIPA) buffer (50 mM Tris pH7.4, 1% Triton X100, 0.25% deoxycholate, 150 mM NaCl, 1 mM EDTA, 10 mM NaF) supplemented with Complete® protease inhibitor at 4°C for 1 hour. Streptavidin–agarose (Thermo Scientific, Waltham, Massachusetts) was mixed with 1-3 mg protein in 2 ml total volume for 2 hours at 4°C. The agarose was washed twice with lysis buffer and biotin-bound proteins eluted by boiling for 10 min in 2× Laemmli buffer. Samples were resolved on 10% SDS–PAGE and Activin Receptor 2a (ActIIa), TGFβR1 and TGFβR2 detected by western blotting. The process is summarized below in Figure 6.2.

• Biotin

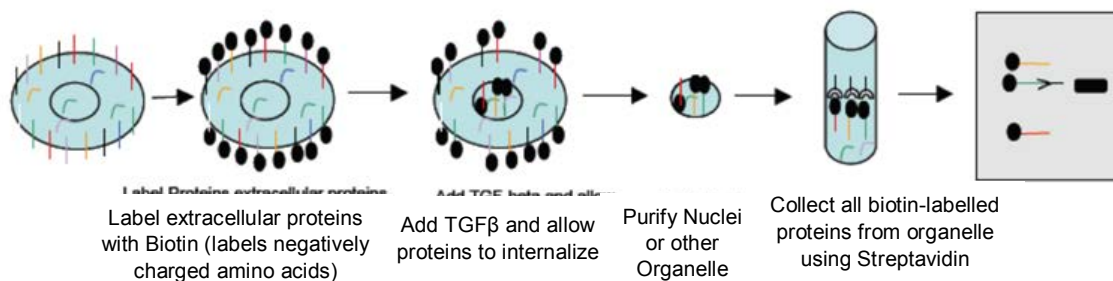


Figure 6.2 Detection of cell surface derived receptors in nuclear fractions using sulfo-NHS-SS-biotin. Surface receptors have exposed primary amine residues that can be covalently bound to sulfo-NHS-SS-biotin which occurs at non-internalization permissive temperatures. Upon raising the temperature, surface proteins traffic to other cellular compartments (including the nucleus) and upon fractionation, the surface-derived biotinylated proteins can be purified due to their affinity for streptavidin-conjugated agarose beads. Detection of specific surface-derived proteins is via western blot detection of SDS-PAGE separated samples.

Both endogenous and recombinant receptors were amenable to this technique, allowing us to examine nuclear trafficking in various cell types. All immunoblotting was performed using standard techniques (Chapter 3) with antibody details provided in Table 3.3 and all results shown are representative of a minimum of three experiments completed using the same experimental conditions.

6.2.6 Disruption of retrograde trafficking components

The biological function of a number of trafficking organelles/compartments can be disrupted by pharmacological treatment or gene silencing of key genes encoding

proteins associated with the compartments. For example, without the sec61 protein, the retrotranslocon (and translocon) pore complex is not functional (Rapoport 2008). Similarly, in the absence of Vps35 the retromer complex fails to assemble and function is lost (Yin 2013) and coatamer vesicles cannot be generated in the absence of Cop α (Ostermann 1993). While nuclear pores still assemble in the absence of importin- β , the ATP-dependent trafficking of cargo through the pore is severely hampered (Ström and Weis 2001) functionally disrupting biological activity. A diagrammatic representation of the proposed retrograde trafficking route of TGF β receptors is presented in Figure 6.3 with a list of the specific processes, genes that were silenced, method of blocking activity (e.g. pharmacological, siRNA or shorthairpin RNA) and where the components function within the proposed trafficking pathway.

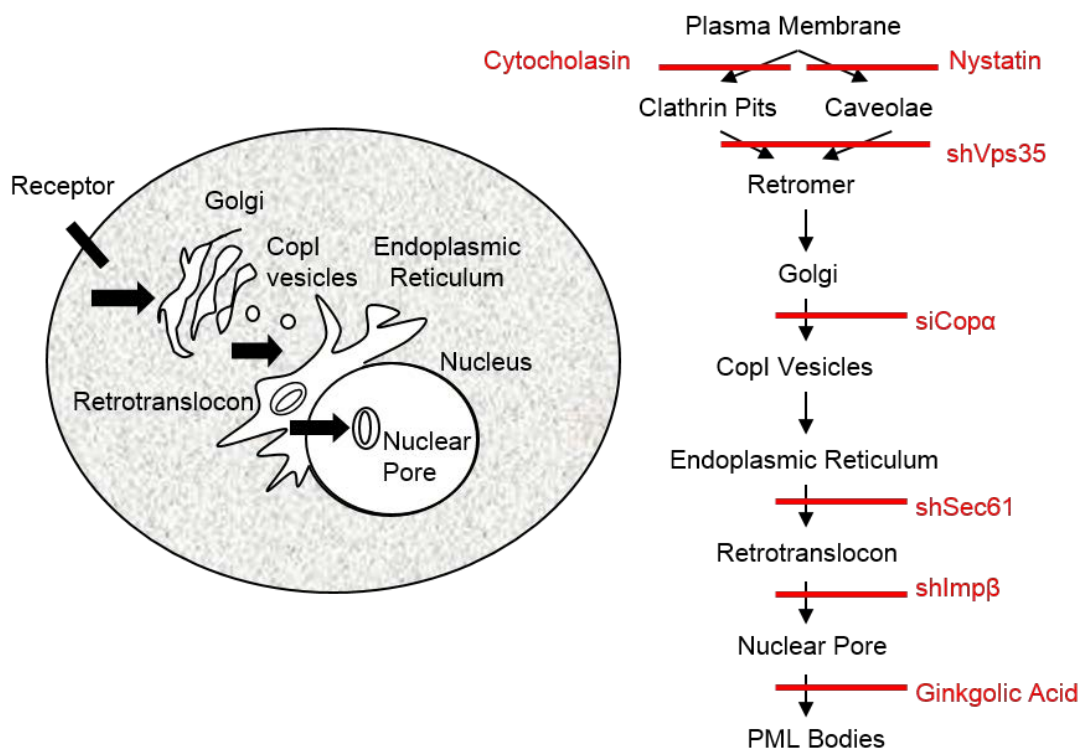


Figure 6.3 Retrograde trafficking pathway and gene silencing and pharmacological inhibitors designed to disrupt specific compartments along the trafficking route. Clathrin mediated endocytosis can be disrupted by cytocholasin treatment while caveolae mediated endocytosis is inhibited by nystatin. The retromer complex consists of two SNX proteins together with Vps35, Vps26 and Vps29. Targeted disruption of any of the Vps proteins (including Vps35) prevents complex formation. COPI vesicles deliver cargo from the Golgi to the ER and the coatmer components are essential for vesicle formation and loss of any (in this case Cop α) prevents vesicle formation. Exit from the ER is through energy-dependent transport through the retrotranslocon pore. This pore is made up of a number of proteins, with a central role for Sec61. In the absence of Sec61 the pore and associated retrotranslocon does not form. Entry into the nucleus is through the nuclear pore. While Importin β is not a component of the nuclear pore, it serves to shuttle cargo through it. Loss of Importin β does not prevent nuclear pore formation, but prevents cargo passage into the nucleus. The formation of PML bodies requires extensive sumoylation which can be inhibited through Ginkgolic acid treatment.

6.2.6.1 Gene silencing of retrograde trafficking components

To examine the roles of these complexes in nuclear trafficking of TGF β receptor trafficking we generated stable cell lines (see Chapter 3 for details) in which the expression of these proteins was dramatically reduced. Where possible (Vps35, sec61, importin- β) we utilized lentiviral infection of short-hairpin RNA sequences to stably integrate in the genomes of the desired cell lines. Depending on where in the genome these sequences integrated, different levels of gene suppression were observed, so clones were screened for the extent of “knockdown” on the protein of interest (by western blotting) with clones expressing the least protein selected for further validation. To control for non-specific effects introduced by viral infection or assembly of short-hairpin RNA complexes, cell lines expressing a non-targeting sequence were generated in parallel. To ensure the level of knockdown was sufficient to functionally impair the complex of interest, assays were conducted analyzing documented controls. Specifically, retromer function was determined by ensuring Mannose-6-phosphate (M6PR) receptor trafficking was disrupted (Yin 2013), retrotranslocon function was determined by ensuring EGFR nuclear translocation was disrupted and nuclear pore import machinery function determined by ensuring Smad2/3 and EGFR nuclear translocation was disrupted. See Appendix X for validation of efficient gene knockdown and loss-of-function of the targeted compartment.

Despite repeated attempts generating clones with various coatamer proteins knocked down using lentiviral delivery of short-hairpin RNA sequences, no clones were viable. As an alternative we opted to transiently transfect small interfering RNA sequences to initiate the RNA interference (RNAi) pathway in cells to suppress Cop α . For this reason a highly transfectable cell line was required and we chose the Cos7 line as it is well characterized for TGF β signalling. Validation was by western blot analysis of Cop α protein expression (Appendix X) and the functional disruption of coatmer formation demonstrated through the blockage of EGFR in the Golgi via confocal microscopy (Appendix X). All shRNA and siRNA sequences are listed in Appendix I and transfection/infection and cell culturing details are found in Chapter 3.

6.2.6.2 Pharmacological disruption of clathrin and caveolar endocytosis and polymyeloid leukemia (PML) body formation

Both clathrin- and caveolar-mediated endocytosis have been linked to TGF β receptor endocytosis, particularly regarding degradation (Di Guglielmo 2005). The pharmacological disruption of both methods of endocytosis is widely accepted using chlorpromazine to inhibit clathrin-mediated endocytosis, and nystatin to inhibit caveolar-mediated internalization (Giri 2005, Bryant and Stow 2005). While both agents have severe detrimental impacts on cells at high concentrations, conditions were optimized to minimize off-target impacts while retaining endocytic disruption in our cell types of interest (Mitchell 2004). Optimizing the effective drug concentration of nystatin was particularly crucial as higher concentrations impacted both clathrin and caveolar events (Mitchell 2004). Validation of effective doses was achieved through visualization of endocytosis of transferrin receptor (clathrin-mediated endocytosis) and low density lipoprotein (LDL) receptor (caveolar-mediated endocytosis)(Wilkes 2006).

The formation of polymyeloid leukemia (PML) bodies requires sumoylation which can be disrupted in the presence of Ginkgolic acid (Perusina 2013). An effective concentration to block PML body formation (and maintain cell integrity) was determined using fluorescence microscopy screening for the presence of visible bodies contained within the nuclei (Appendix X).

For all three agents, thirty (30) minutes prior to TGF β stimulation, culture media was removed and replaced with new media with the specified drug added at the desired concentration (see Appendix XI). TGF β was added directly to this media in the concentration desired and for the required duration.

6.2.7 Activin and TGF β receptor co-immunoprecipitation with retromer subunits

The core of the retromer complex is very stable and consists of three proteins along with one of a number of sorting nexins (SNXs) that localizes the complex to specific endosomes (see Fig 2.14). The core proteins consist of Vacuolar Protein Sorting Vps26, Vps29 and Vps35 and the absence of one component disrupts the stability of the complex and substantially reduces the half-life of the remaining two components (Yin 2013). Vps35 is the primary cargo binding unit (Burd and Cullen 2014) however evidence suggests TGF β R2 binding is through Vps26 (Yin 2013). Antibody limitations prevented consistent co-precipitation of all retromer components with the exception of

Vps26, which was immunoprecipitated using 2 µg/ml rabbit polyclonal anti-Vps26 antibody (Abcam, Cambridge, UK) in modified RIPA buffer (Table 3.3) overnight, followed by standard immunoprecipitation and western blotting against Activin Receptor 2a (Act11a) and TGFβ1 and TGFβR2 (Chapter 3). Efficient immunoprecipitation was confirmed by western blot of Vps26 each time other proteins were co-immunoprecipitated and each result was confirmed by repeating the experiment a minimum of three times with a representative image presented at an exposure best depicting the experimental result (Figs 6.12 and 6.13).

6.3 RESULTS

The presence of TGFβ receptors in the nucleus upon ligand stimulation has been reported previously (Zwaagstra 2000, Mu 2011, Chandra 2012, Gudey 2014) but precisely how the TGFβ receptors get to the nucleus has not been determined. For a more comprehensive understanding we employed two techniques, limiting our studies to receptors that were at the cell surface and exposed to ligand upon TGFβ challenge. Firstly, surface receptors were labelled with non-cell-permeable biotin prior to treatments, consequently biotinylated proteins/receptors present in isolated intracellular fractions were assumed to be cell surface derived. The second approach utilized antibody labelling the extracellular domains of the receptors of live (non-permeabilized) cells prior to treatment and subsequent re-localization. Utilizing these two independent approaches we are confident receptors detected in intracellular compartments were indeed present at the cell surface when cells were stimulated with TGFβ.

6.3.1 Upon TGFβ stimulation, a subset of surface receptors traffic to the nucleus through the golgi and endoplasmic reticulum

6.3.1.1 TGFβR1 and TGFβR2 translocate from the cell surface to the nucleus after TGFβ stimulation in different cell types, from different species and in transformed and non-transformed lines as full-length proteins

Due to the lack of high quality antibodies to the external domain of endogenous TGFβ receptors, we expressed receptors with high affinity/specificity epitope tags engineered into a region of the extracellular domain (as outlined in 5.2.3.1) that did not impact ligand binding or receptor activation (Di Guglielmo 2003, Hong 2011). Binding was performed at internalization non-permissive temperature (by cooling cultures to 12°C) (Penheiter 2002, Mitchell 2004, Yin 2013) and transfected Cos7 cells were returned to

normal conditions before TGF β stimulation. Within 4 hours of TGF β insult, both myc-TGF β R1 (green) and HA-TGF β R2 (red) had significant perinuclear localization. While not present in every cell, within 8 hours most of the receptors were contained within the nucleus (Fig 6.4A) as visualized with DAPI.

Endogenous receptor nuclear trafficking was examined using biotinylated AKR-2B cells. Similar to immunofluorescence results, both TGF β receptors began to appear in a nuclear fraction between 2-4 hours but peaked after around 8-10 hours (Fig 6.4B). As seen by others (Anders 1997, Doré 2001, Garamszegi 2001, Di Guglielmo 2003, Luga 2009, Huang 2012) approximately 60% of surface-derived receptors were lost by 8 hours (Fig 6.4B). However, during this period of surface-receptor degradation, there was an accumulation of both TGF β R1 and TGF β R2 in nuclear fractions (Fig 6.4B). Indeed, at later time points, almost the only receptors detected were contained in the nucleus. While nuclear receptors constituted nearly all the surface-derived receptors in the cell at later time-points, the percentage of receptors escaping degradation and getting to the nucleus was approximately 15-30% (20-35% by MetaMorph® quantification using immunofluorescence; 10-20% by densitometry analysis after nuclear fractionation and western blotting) of what was at the cell surface at time 0 (Fig 6.4B). The phenomenon of nuclear trafficking of TGF β receptors appeared to be widespread. Accumulation of surface-derived receptors after TGF β stimulation was detected in all cell lines examined including non-transformed and transformed lines and from species including human, mouse, green monkey, dog and mink (Fig 6.4C). Furthermore, the kinetics of nuclear accumulation and percentage of surface-derived receptors that entered the nucleus were remarkably similar (Fig 6.4C).

A number of receptor tyrosine kinases have been shown to require cleavage of the extracellular domain prior to nuclear delivery, while others traffic as full length proteins (Carpenter 2009). While antibodies bound to the extracellular domain of TGF β receptors entering the nucleus after TGF β stimulation suggests nuclear receptors are indeed full length, the possibility of a mix of full length TGF β R1 and cleaved receptors could not be ruled out. To address this possibility, Cos7 cells expressing both a carboxy-(intracellular) FLAG epitope tagged, and amino-(extracellular) myc epitope tagged TGF β R1 were stimulated with TGF β and the nuclear fractions probed for detection of both myc and FLAG by western blotting (see Fig 6.5 – left panel, for clarification). Both myc- and FLAG-tagged forms were observed with a band readily

detected at a size corresponding with full length TGF β R1. Additionally, no truncated forms could be detected with either antibody (Fig 6.5 – middle panels). Examination of TGF β R2 using the same approach also failed to yield any evidence of a truncated form of receptor (Fig 6.5 – right panels).

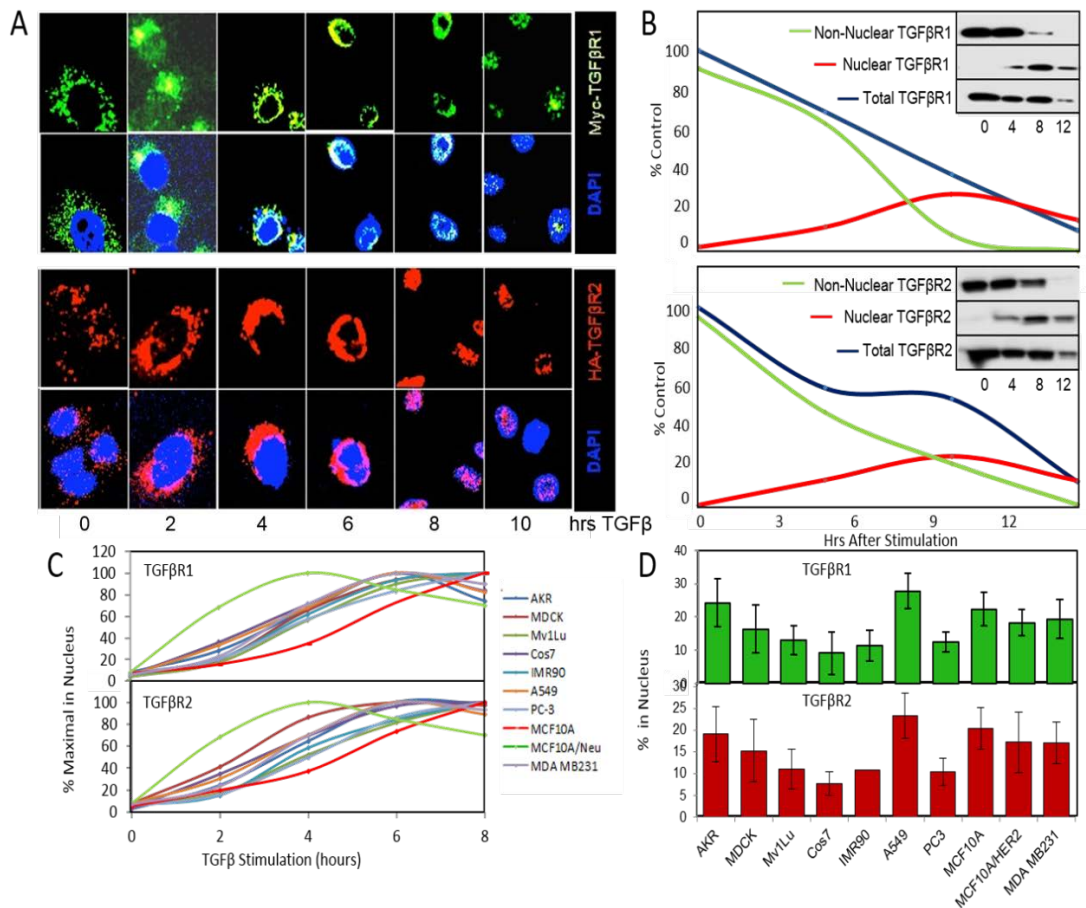


Figure 6.4 A subset of surface receptors translocate to the nucleus in cells derived from different species, tissues and healthy or diseased organs. (A) Receptors with extracellular epitope tags were transiently expressed in Cos7 cells. After binding antibodies recognizing the epitopes Myc-TGF β R1 (top panels) and HA-TGF β R2 (bottom panels) at 12°C cells were warmed to 37°C and treated with TGF β for indicated times, fixed and visualized. (B) To examine endogenous receptors, AKR-2B cell surface proteins were labelled with non-permeable biotin at 12°C before warming back to 37°C and TGF β stimulation for the indicated times. Whole cell lysates, nuclear, or non-nuclear fractions, were lysed and biotinylated proteins immunopurified with streptavidin and subjected to SDS-PAGE and western analysis for TGF β R1 (top panel, right corner) and TGF β R2 (bottom panel, right corner) and quantified relative to receptors at the surface at time 0 (TGF β R1-top and TGF β R2-bottom panel respectively). (C) Normal, immortalized lines from human, mouse, green monkey, dog, or mink (IMR-90, MCF10A, AKR-2B, Cos7, MDCK and Mv1Lu respectively) or human transformed lines from lung, prostate and breast (A549, PC3, MCF10/Neu and MDA MB231 respectively) were treated as above, with the exception of Cos7 cells that were transiently transfected with epitope-tagged receptors due to low endogenous receptor levels, prior to treatment and extent of kinetics of nuclear accumulation of TGF β R1 (top) and TGF β R2 (bottom) was determined by western analysis and plotted as a percentage of maximal levels. (D) The level of surface-derived TGF β R1 (top) and TGF β R2 (bottom) in the nucleus at the maximal time point was plotted as a percentage of the levels of receptors after initial surface labelling.

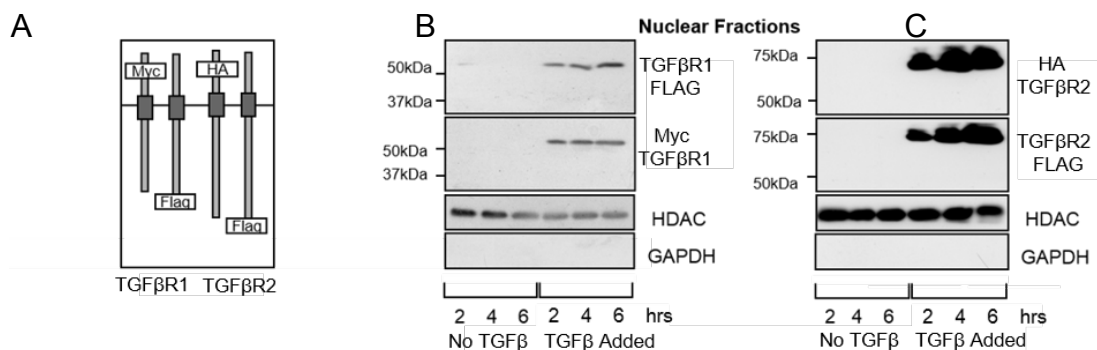


Figure 6.5 Receptors in the nucleus are full length and not cleaved fragments. (A) Diagrammatic representation of TGF β receptor combinations used. Epitope tags were cloned at either the carboxy terminal C epitope tag) or close to the amino terminal (N epitope tag) of both receptors with the tagged pairs expressed together. If cleavage of the extracellular region occurs, no extracellular epitope tag would be detectable in nuclear fractions. (B - C) AKR-2B cells expressing both C and N epitope tagged TGF β R1 (B) or TGF β R2 (C) were incubated in the presence (+) or absence (-) of TGF β for indicated times after pre-labelling surface proteins with biotin. Nuclear fractions were prepared and subjected to western analysis for N- and C-terminally tagged receptors. Fraction purity was determined by HDAC enrichment and GAPDH exclusion.

6.3.1.2 Nuclear TGF β Receptors enter the cell via clathrin-mediated endocytosis

As endocytosis of surface receptors is the first step of any trafficking journey, the endocytic mechanism responsible for receptors destined for nuclear delivery was investigated. Roles for both clathrin-mediated (Di Guglielmo 2003, Mitchell 2004) and caveolae-mediated endocytosis (Di Guglielmo 2003) have been proposed with the contribution of each to signalling and degradation somewhat unresolved. Using chemical inhibitors of clathrin-mediated (chlorpromazine) and caveolae-mediated (nystatin) only inhibition of clathrin-mediated endocytosis had the ability to prevent receptors (both TGF β R1 and TGF β R2) entering the nucleus (Fig 6.6).

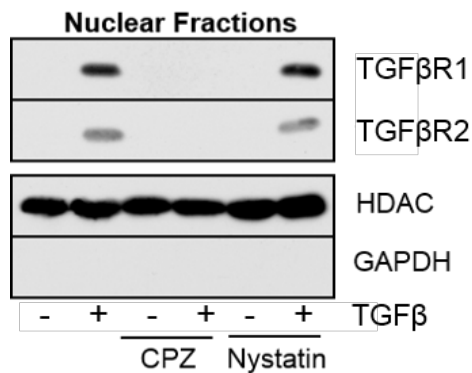


Figure 6.6 TGFβ receptors enter the nucleus through clathrin-mediated endocytosis. AKR-2B cells were biotinylated at 12°C before switching to 37°C. Cultures were pretreated alone or in the presence of 10 μg/ml of chlorpromazine (CPZ) or 25 μg/ml of nystatin for 30 minutes before stimulation (+) with 10 ng/ml TGFβ or untreated (-) for 6 hours. After nuclear fractionation, biotinylated proteins were immunopurified using streptavidin and subjected to western analysis for the presence of TGFβR1 or TGFβR2. Nuclear fraction purity was determined by characterizing the extent of GAPDH exclusion and HDAC enrichment.

6.3.1.3 TGFβ Receptors translocate to the nucleus via the Golgi and Endoplasmic Reticulum

TGFβ receptors traffic to the nucleus as full length proteins (Fig 6.4), similar to EGFR (Liao 2007). EGFR nuclear delivery requires intact Golgi apparatus (Wang YN 2010) and ER (Liao 2007, Wang 2010) so we sought to investigate whether the Golgi and ER were required for TGFβ receptor trafficking. Purification of both Golgi and ER (Fig 6.7A) fractions yielded surface-derived TGFβ receptors only after TGFβ stimulation. Levels of receptors were plotted relative to maximal detection (Fig 6.7 - bottom) indicating flow of receptors through Golgi preceded ER which preceded the nucleus. While Golgi and ER presence decreased significantly after the peak, receptors were largely retained in the nucleus (Fig 6.7 - bottom). Observing surface-derived receptors in Golgi and ER compartments in steady-state conditions was problematic, probably due to such low levels of receptors at any given moment in time.

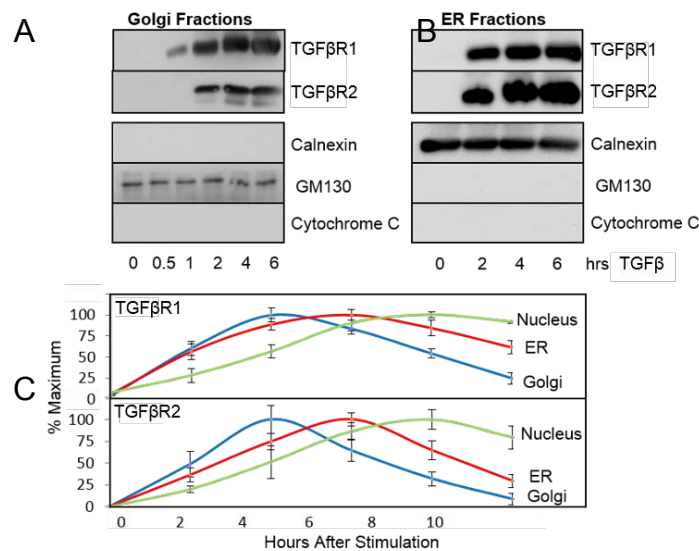


Figure 6.7 TGFβ receptors travel from cell surface to nucleus through Golgi and ER. (A) AKR-2B cells were grown to confluence and surface proteins labelled with biotin before incubation with TGFβ for indicated times. Golgi, ER and nuclear fractions were prepared and biotinylated proteins immunopurified with streptavidin before probing for TGFβR1 and TGFβR2. To ensure appropriate enrichment fractions were probed for Calnexin, GM130 and Cytochrome C as markers specific to ER, Golgi and mitochondria respectively. (B) Similar as described in A except that an ER fraction was prepared. (C) Graphical representation of 3 independent experiments normalized to percentage of maximal level for each fraction. Note; data does not allow comparison between levels in each compartment. Nuclear contribution is superimposed from data displayed in Fig 6.4C to facilitate comparison between Golgi, ER and nuclear kinetics.

6.3.2 TGFβ receptors traffic to nucleus together: TGFβR2 facilitates Golgi entry, while TGFβR1 is required for COPI vesicle entry and subsequent nuclear delivery

Both TGFβR1 and TGFβR2 enter the nucleus, both can be found in Golgi and ER fractions, both require clathrin-mediated endocytosis, and the kinetics through these compartments is almost identical (Figs 6.4, 6.5, 6.7), but this does not provide any information as to whether the receptors are travelling together or separately. The first step in determining if the receptors travelled to the nucleus independently or together involved expressing HA-TGFβR2 alone in the virtually TGFβ receptor-deficient Cos7 cells. TGFβR2 from unstimulated cells were retained in distinct punctate structures reminiscent of endosomes, while even in the absence of TGFβR1, TGFβR2 travelled to a distinct perinuclear compartment upon TGFβ stimulation (Fig 6.8A). Introducing TGFβR1 with TGFβR2 shifted the receptors from the perinuclear structure into the nucleus, suggesting the perinuclear observation in cells expressing only TGFβR2 was not due to a cell type/clonal difference (Fig 6.8A), but instead occurs only when both receptors are present. The perinuclear compartment was confirmed to be the Golgi

through strong colocalization of TGF β R2 (when expressed alone and TGF β stimulated) with the Golgi marker giantin (Fig 6.8B).

Examination of TGF β R1 in the absence of TGF β R2 presents a more difficult problem. TGF β R1 alone does not bind ligand with strong affinity and its activation requires direct phosphorylation by TGF β R2 (Attisano 1998, Shi Y 2003). A mutation at residue 204 of TGF β R1 from a threonine to an aspartic acid (T204D) results in a partially constitutively active receptor (Willis SA 1997), however “activation” is at least in part due to an increased ligand-independent affinity for TGF β R2. Furthermore, the homodimerization of TGF β R1 T204D mutants could form dimers with endogenous inactive receptors making assessment of the data problematic. To circumvent these potential problems, cells stably expressing chimeric receptors consisting of Granulocyte/Macrophage Colony Stimulating Factor Receptor (GM-CSFR) extracellular domains fused to TGF β R intracellular domains were utilized (Fig 6.9A and Fig 3.2). Both TGF β (type 1 and 2) and GM-CSF (α and β) receptors require heterodimerization after ligand binding to mitigate signalling. Whilst TGF β receptors signal through Smads, GM-CSF initiates the Jak/Stat pathway. Fusing the extracellular domain of GM-CSF receptors with the transmembrane and intracellular domains of TGF β receptors generates a system whereby TGF β /Smad signalling can be induced with GM-CSF. Most importantly, cell type expression of endogenous GM-CSF receptors is extremely limited and no cross reactivity occurs between chimeric and endogenous receptors.

Neither chimeric wild type nor “activated” (i.e. T204D mutant) TGF β R1 when expressed alone (Fig 6.9B) entered the Golgi, ER or nucleus in the absence of ligand. However, when expressed with the partnering chimeric TGF β R2, some nuclear trafficking was observed for the “activated” mutant but significantly less than upon ligand stimulation (Fig 6.9B). Collectively, data suggests neither receptor can enter the nucleus independently, however TGF β R2 enters the Golgi by an unknown mechanism, but is retained there in the absence of TGF β R1.

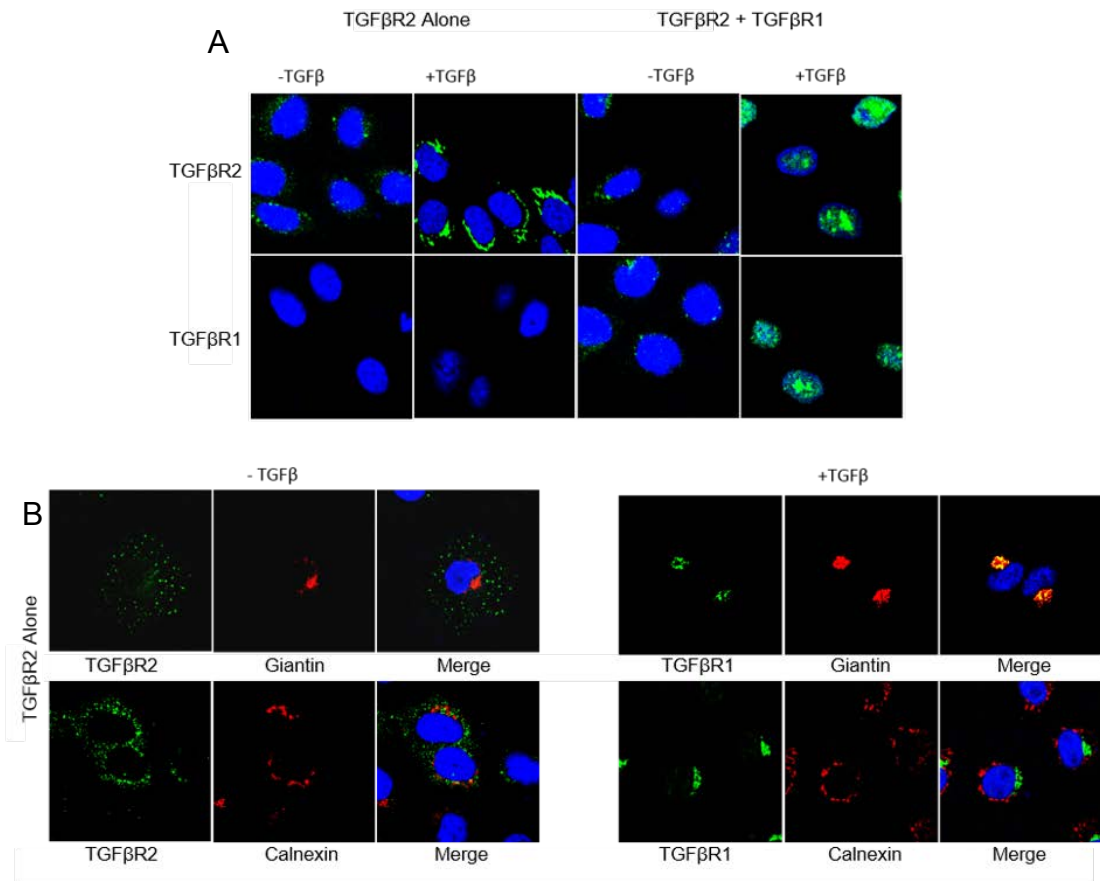


Figure 6.8 TGFβR2 can enter the Golgi after TGFβ stimulation in the absence of TGFβR1. (A) Cos7 cells expressing either HA-TGFβR2 alone (left) or together with myc-TGFβR1 (right). After incubating with antibody at 12°C, cultures were warmed and left unstimulated (-TGFβ) or stimulated (+TGFβ) with 10 ng/ml TGFβ for 6 hours. (B) Cos7 cells expressing only HA-tagged TGFβR2 were incubated in the presence of HA antibody prior to addition (+TGFβ – right panels) or absence (-TGFβ – left panels) for 6 hours. Upon fixation and permeabilization, co-staining with giantin or calnexin resolved Golgi and ER respectively.

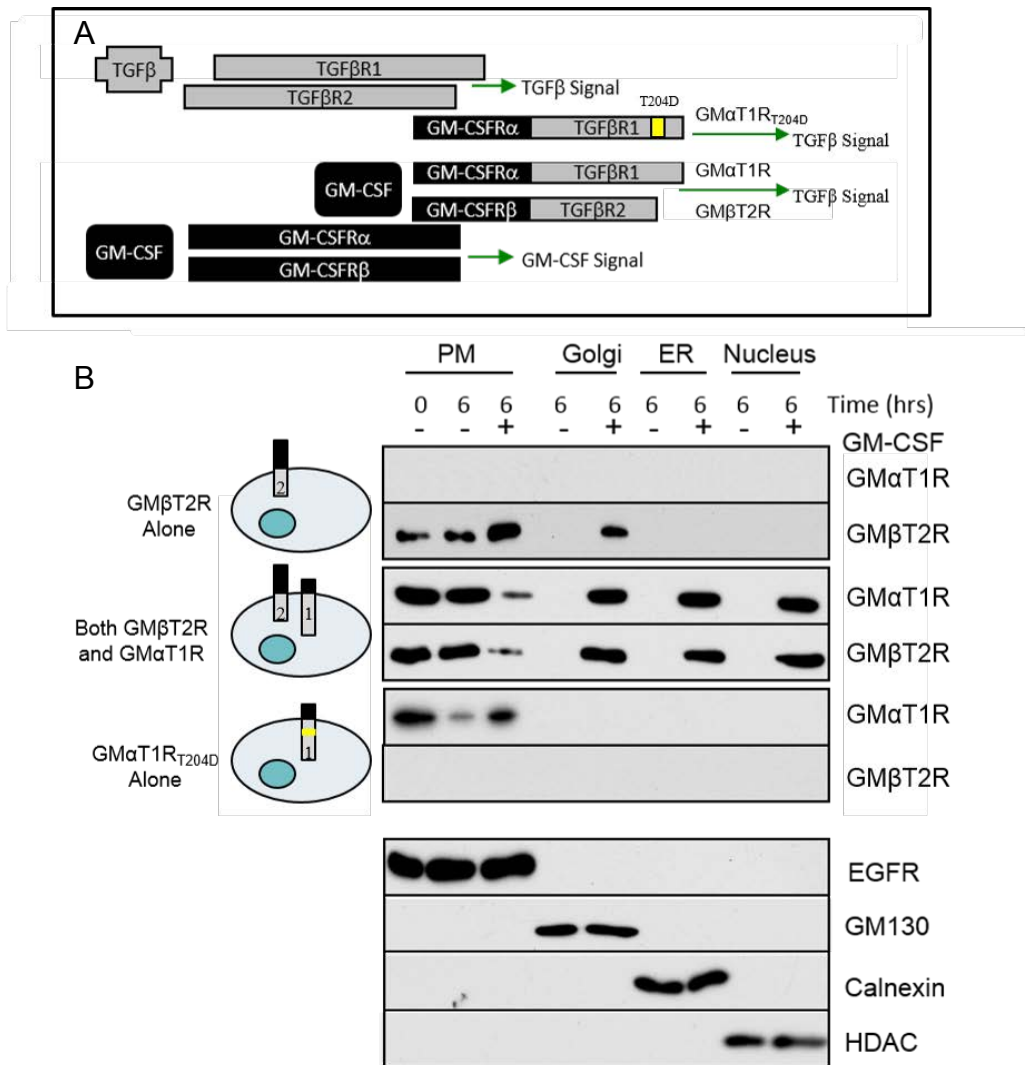


Figure 6.9 While TGFβR2 can enter the Golgi alone, both TGFβ receptors are required to enter the ER and nucleus. (A) Diagrammatic representation of GM-CSF/TGFβ chimeric receptor system. The chimeric fusion of GM-CSFRα with TGFβR1 is referred to as GMαT1R, while the fusion of GM-CSFRβ and TGFβR2 is referred to as GMβT2R. The GMαT1R_{T204D} does not require ligand to initiate Smad signalling. (B) Antibodies recognizing the extracellular domains of GM-CSFRs were used to detect the presence of surface-derived chimeric (GMαT1R and/or GMβT2R) in plasma membrane (PM), Golgi, endoplasmic reticulum (ER) and nuclear fractions of cells 6 hours after surface labelling in the absence (-) or presence (+) of GM-CSF. To determine the level of receptors at the cell surface immediately after labelling, a plasma membrane sample was also collected at time 0. Three cell lines were examined; (1) expressing only GMβT2R (top two panels), (2) expressing both GMβT2R and GMαT1R (panels three and four), and (3) expressing only GMαT1R (panels five and six). Because GMαT1R cannot bind ligand and requires a complementary GMβT2R to phosphorylate/activate it, to determine if GMβT2R had a role (independent of activation) in nuclear trafficking of GMαT1R we introduced a GMβT2R bearing a mutation at residue 204 rendering the receptor constitutively active (T204D). The purity of the fractions was determined by the enrichment or absence of PM (EGFR), Golgi (GM130), ER (Calnexin) and nuclear (HDAC) markers (bottom four panels). The level of receptors in each compartment six hours after ligand stimulation is vastly different. To standardize samples to all be within the linear range for visual detection after western blotting, samples were loaded at a ratio of 1-plasma membrane:20-nuclear:200-ER:800-Golgi.

6.3.3. Golgi sorting requires TGF β R2 domain interacting with retromer complex

While TGF β R1 is phosphorylated and kinase activity induced upon ligand binding, there are no recognized changes in the state of TGF β R2. With no specific residue modification to target as a potential cue for nuclear targeting, we utilized cell lines expressing truncated forms of TGF β R2 (Fig 6.10A) to determine the region of the receptor required for nuclear entry. Presumably the region required for association with TGF β R1 would be required for full nuclear delivery, so our initial experiments focused only on the ability of chimeric GM β T2R (expressed alone) to enter the Golgi upon TGF β insult. Truncations upstream of residue 498, along with GM β T2R with residues 485-498 deleted, prevented Golgi entry (Fig 6.10B and 6.10D). Expression of truncated forms was documented by western analysis (Fig 6.10B – bottom panels) and they could localize to the cell surface (as they became biotinylated). Furthermore these truncated receptors underwent degradation after ligand treatment (Fig 6.10B – middle panels), indicating the truncated receptors were fully functional other than a deficit in nuclear entry. Confirmation that this region was required for subsequent ER and nuclear delivery came when transient co-expression of TGF β R2 with residues 485-498 deleted with the corresponding chimeric TGF β R1 was unable to enter the ER or nucleus (Fig 6.10C).

Because the region 485-498 has been documented to bind the retromer complex (unpublished results Leof Lab) we examined the ability of TGF β receptors to enter the nucleus when Vps35 (a component of the retromer) was knocked down. As indicated, (Fig 6.10D) receptors fail to enter the Golgi, ER or nucleus upon ligand stimulation in the absence of a functional retromer. Further confirmation of the role of the residues 485-498 of TGF β R2 in nuclear trafficking is seen by the absence of receptors colocalizing with giantin or calnexin (Fig 6.10E). Indeed the receptors remain in small punctate structures reminiscent of endosomes (Fig 6.10E) seen in unstimulated cells.

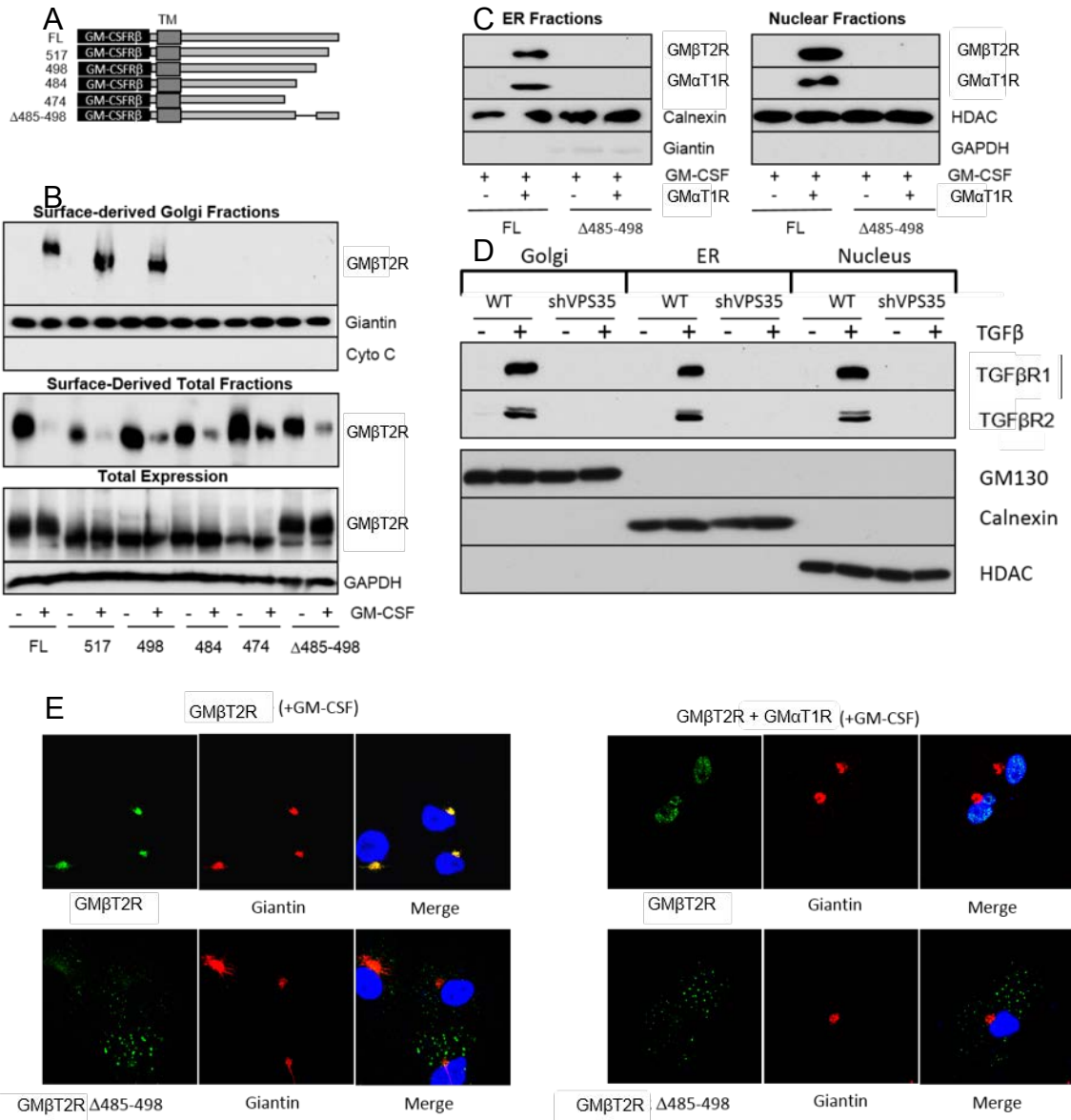


Figure 6.10 Residues 485-498 in TGFβR2 are required for Golgi and subsequent nuclear delivery. (A) Diagrammatic representation of chimeric receptor truncations and deletion mutants used in the study. (B) Due to their distinct cellular compartments, MDCK cells stably expressing either full length or truncated/deletion mutant chimeric receptors were biotinylated and treated with (+) or without (-) GM-CSF for 8 hours. Golgi (upper 3 panels) fractions were prepared and probed for the presence of surface-derived GMβT2R, giantin and cytochrome C (cyto C), while whole cell lysates were examined expression of surface-derived and total GMβT2R as well as GAPDH. (C) MDCK cells stably expressing GMα/T1R was transiently transfected with full length GMβT2R or a mutant with residues 485-498 deleted. Following biotinylation, ER (top) and nuclear (bottom) fractions were probed for surface-derived chimeric receptors. Purity of the fractions was determined by determining ER (calnexin), Golgi (Giantin), nuclear (HDAC) and cytoplasmic (GAPDH) protein marker enrichment/absence. (D) AKR-2B lines stably expressing shRNA to efficiently silence the retromer subunit Vps35 and a non-targetting sequence were biotinylated before 6 hours in the presence (+) or absence (-) of TGFβ. Golgi, ER and nuclear fractions were probed for surface-derived TGFβR1 and TGFβR2 as well as GM130, calnexin and HDAC to ensure fraction purity. (E - left) Cos7 cells transiently expressing GMβT2R full length (top) or the 485-498 deletion mutant (bottom) were incubated in the presence of antibody to the extracellular domain of GMβT2R, before stimulation with 50 ng/ml GM-CSF for 8 hours before visualization of GMβT2R and the Golgi marker giantin. (E - right) Cells were treated as above except GMαT1R was expressed in addition to GMβT2R.

6.3.4 TGFβ Type II receptor superfamily share retromer binding but Lys488 confers nuclear targeting in TGFβR2 but not other superfamily members

Having defined the region of TGFβR2 that is required for Golgi (and subsequent nuclear) trafficking to a 14 amino acid sequence (residues 485-498), we sought to refine our search to individual residues within the 14 amino acid sequence. Furthermore, the sequence shares significant sequence homology with other TGFβ Type II superfamily receptors (Fig 6.11) allowing us to examine; (1) if retromer binding is conserved across the TGFβ receptor superfamily and; (2) if other superfamily receptors traffic to the nucleus upon activation.

Alignment of TGFβR2, Activin type II receptors and BMP type II receptor with a Swiss Secondary Structure Prediction Model indicated a striking feature. A large proportion of the required region is predicted to be an alpha helix, meaning every three to four residues will line up on a face of the 3-dimensional structure (Fig 6.11). When comparing homology across the superfamily Type II receptors, the sequences are virtually identical every three to four residues with little conservation of the residues between. Supporting the theory of an important conserved 3-dimensional structure, both proline residues in the sequence are conserved ensuring a rigid conserved shape (Fig 6.11).

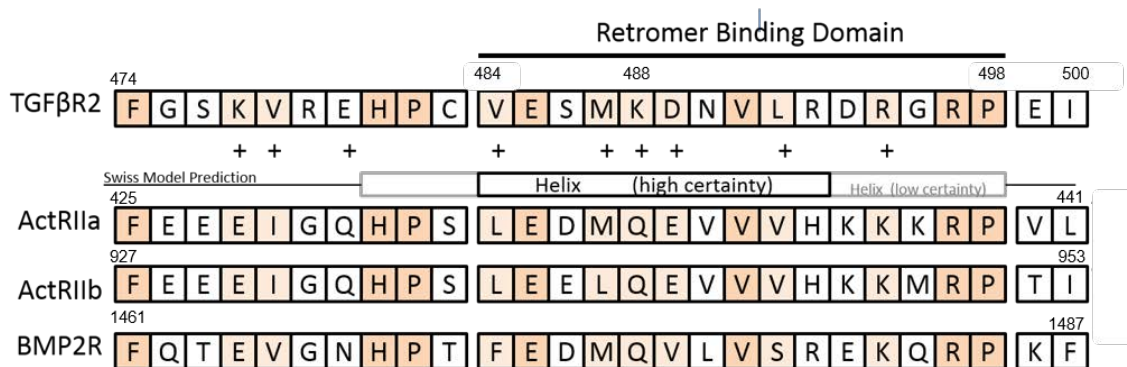


Figure 6.11 Alignment of TGFβ superfamily Type II receptors and predicted secondary structure at retromer binding region. Comparison of TGFβR2, Activin receptor Type IIa and b, as well as BMP Type II receptor region corresponding with residues 474 to 500 of TGFβR2. Swiss model secondary structure prediction is indicated with conserved residues shaded.

6.3.4.1 Retromer binds TGFβR2 and Activin Type II receptor

Considering the degree of sequence conservation within the alpha helical region of all the receptors, it wasn't surprising to see that Activin Type II Receptor and TGFβR2 could bind retromer in both stimulated and unstimulated conditions (Fig 6.12A), probably interacting with the retromer at the conserved interface.

6.3.4.2 Activin Type II Receptor does not traffic to the nucleus after Activin stimulation

Despite the high degree of sequence homology and shared retromer binding, Activin Type II receptor was unable to traffic to the nucleus when stimulated with Activin (Fig 6.12B) allowing us to speculate there is something about the 14 amino acid sequence in TGFβR2 that supports nuclear delivery that is not present in other family members.

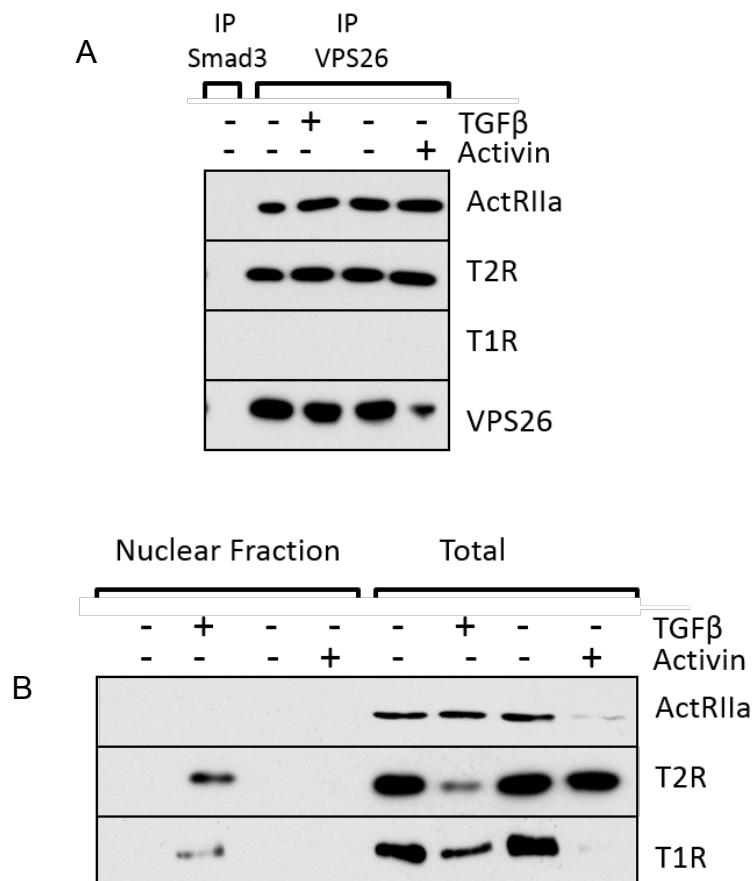


Figure 6.12 Activin Type II receptor and TGFβR2 can bind retromer but only TGFβR2 can traffic to the nucleus upon stimulation. (A) AKR-2B cells were unstimulated or stimulated with TGFβ or Activin for 30 minutes as indicated, prior to lysis and immunoprecipitation against the retromer subunit VPS26. Immunoprecipitates were then subjected to SDS-PAGE and western blotting for Activin receptor Type IIa (ActRIIa) TGFβR2 (T2R) or TGFβR1 (T1R). Western blotting of VPS26 confirmed successful immunoprecipitation of VPS26. Antibodies against Smad3 served as a negative control for retromer binding. (B) Cells were treated as above and fractionated into nuclear (left) and total (right) fractions and probed for the presence of the indicated receptors by western blotting,

6.3.4.3 Lysine 488 in TGF β R2 confers Golgi targeting, possibly via ubiquitination

Lysine 488 in TGF β R2 caught our attention for two reasons. Firstly, Lys488 was the only residue in the middle of one of the exposed turns of the alpha helix that was not conserved in other Type II receptor superfamily members (Fig 6.10). Secondly, lysines are commonly ubiquitinated in internalization and degradation processes.

To determine if lysine at residue 488 was required for nuclear trafficking after ligand stimulation, we generated a point mutation in TGF β R2 where the lysine at 488 was changed to glutamine. While lysines are frequently mutated to arginines in ubiquitination studies, we chose to substitute lysine 488 with a glutamine, to mimic Activin and BMP receptors (K488Q). To begin to address the potential of ubiquitination at lysine 488 having a role in the nuclear trafficking of TGF β receptors a deubiquitination domain (DUB) was fused to TGF β R2 thereby immediately deubiquitinating any ubiquitination event on (or in close proximity to) TGF β R2. While both the K488Q mutant and DUB fusion receptors could bind retromer (Fig 6.13A), neither was able to facilitate the nuclear trafficking of either TGF β receptor (Fig 6.13B).

This data supports the model of ubiquitination at lysine 488 being crucial for nuclear translocation, but western blot analysis of the total levels of TGF β R2 under different conditions indicates a compounding problem potentially impacting our interpretation of the data. As can be seen in wild type (WT) samples (Fig 6.13B) total TGF β R2 levels should decrease substantially after 6 hours of stimulation (due to degradation). While degradation occurs normally in the K488Q mutant, no degradation is observed with receptors fused to a deubiquitination domain. Similar complications were observed when the receptor construct were viewed by immunofluorescence microscopy. Expressed alone a wild type TGF β R2 could enter the Golgi upon ligand stimulation, whereas K488Q mutant was excluded (Fig 6.13C). Cells expressing TGF β R2-DUB displayed gross morphological alterations making comparisons problematic, even in the absence of ligand (data not shown).

Lysine at residue 488 is important for nuclear delivery, but whether ubiquitination at this site is required to “mark” receptors for nuclear trafficking cannot be confirmed. The retromer is not required for receptor degradation (Yin 2013) and receptors lacking the entire retromer binding motif (Δ 485-498) still degrade in the presence of ligand (Fig

To definitively determine if ubiquitination of lysine 488 is involved in nuclear delivery would require an alternative approach. The first step would be to determine if TGF β R2 is indeed ubiquitinated (by co-immunoprecipitation) followed by determining which residues are ubiquitinated and if the ubiquitin bound at each residue is mono, or one of the various poly linked forms. Such a comprehensive mapping of TGF β R2 would require individually (and in combination) mutating each of the lysine residues of the intracellular region of TGF β R2, prior to attempting to determine how ubiquitination of each residue impacts various aspects of TGF β R2 trafficking, recycling and degradation.

6.3.5 Di-Lysines in TGF β R1 required for COPI vesicle sorting of both TGF β receptors

While TGF β R2 gets the receptor complex to the Golgi, evidence indicates TGF β R1 is required for subsequent delivery to the ER and onwards (Figs 6.4 - 6.13). Retrograde trafficking of cargo from Golgi to ER generally occurs through coatamer vesicles known as COPI vesicles (Lanoix J 2001). Indeed when COPI vesicle formation was reduced by expressing short inhibitor RNA to the coatamer component Cop α , both TGF β R1 and TGF β R2 were unable to enter the ER and nucleus, remaining trapped in the Golgi (Fig 6.14). Although not universal, many proteins are sorted into COPI vesicles by direct interactions with Di-lysine motifs (KKXX) (Lanoix J 2001) and interestingly, TGF β R1 has two such motifs while TGF β R2 has none (Fig 6.15A). While mutation of either of these motifs alone had limited effect on nuclear localization (data not shown), virtually no nuclear localization of either TGF β R1 or TGF β R2 could be detected when both motifs on TGF β R1 were mutated, with TGF β R1 and TGF β R2 retained in Golgi fractions, as observed by western blot (Fig 6.15B) and by immunofluorescence (Fig 6.15D). Isolation of COPI vesicles indicated both wild type TGF β receptors were present only after TGF β stimulation while mutation of both Di-lysine motifs in TGF β R1 prevented this and mutation of either motif alone was incomplete (Fig 6.15C).

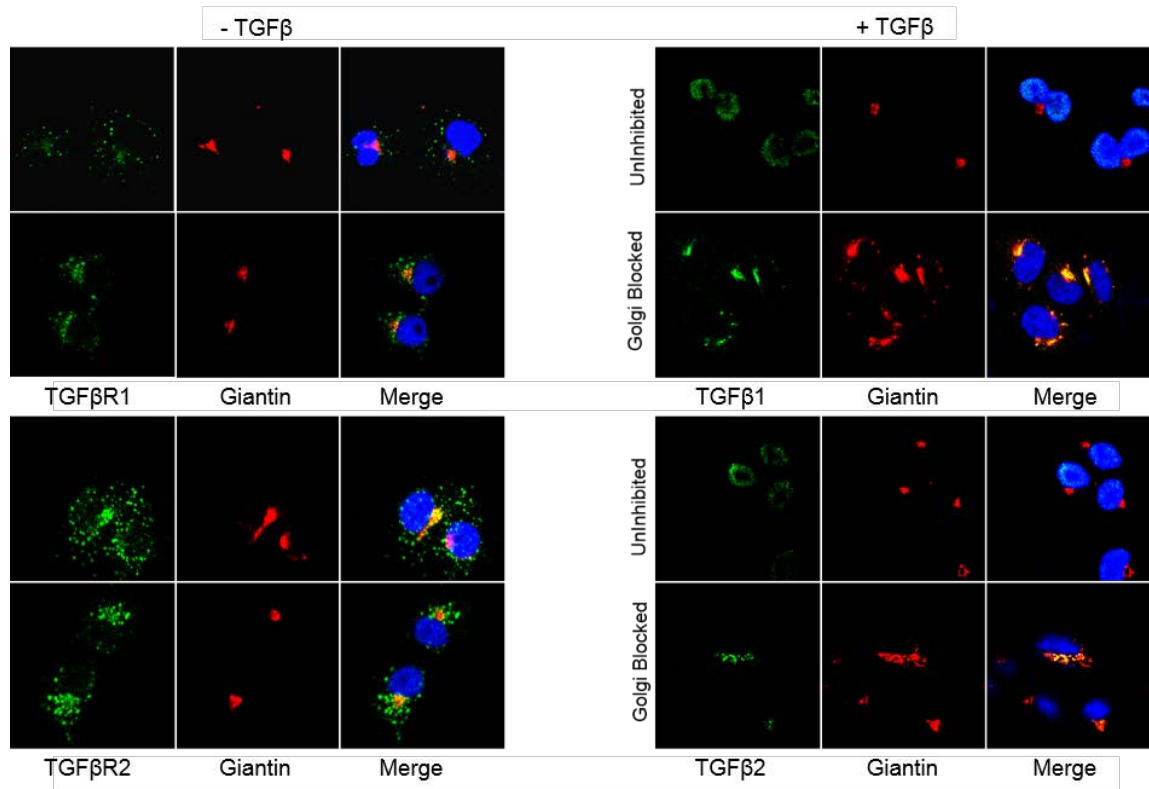


Figure 6.14 COPI vesicle transport required for receptors to exit Golgi and reach ER and nucleus. Cos7 cells transiently expressing epitope-tagged forms of both TGFβ receptors (Myc-TGFβR1 and HA-TGFβR2) and siRNA to Copα were stimulated (+TGFβ – right panels) or not (-TGFβ – left panels) for 8 hours after pre-labelling receptors with respective antibodies (Top panels TGFβR1 and bottom panels TGFβR2). Fixed cells were co-stained with giantin to compare receptor distribution relative to the Golgi. It should be noted, Golgi morphology appeared somewhat altered with siRNA to Copα expressed.

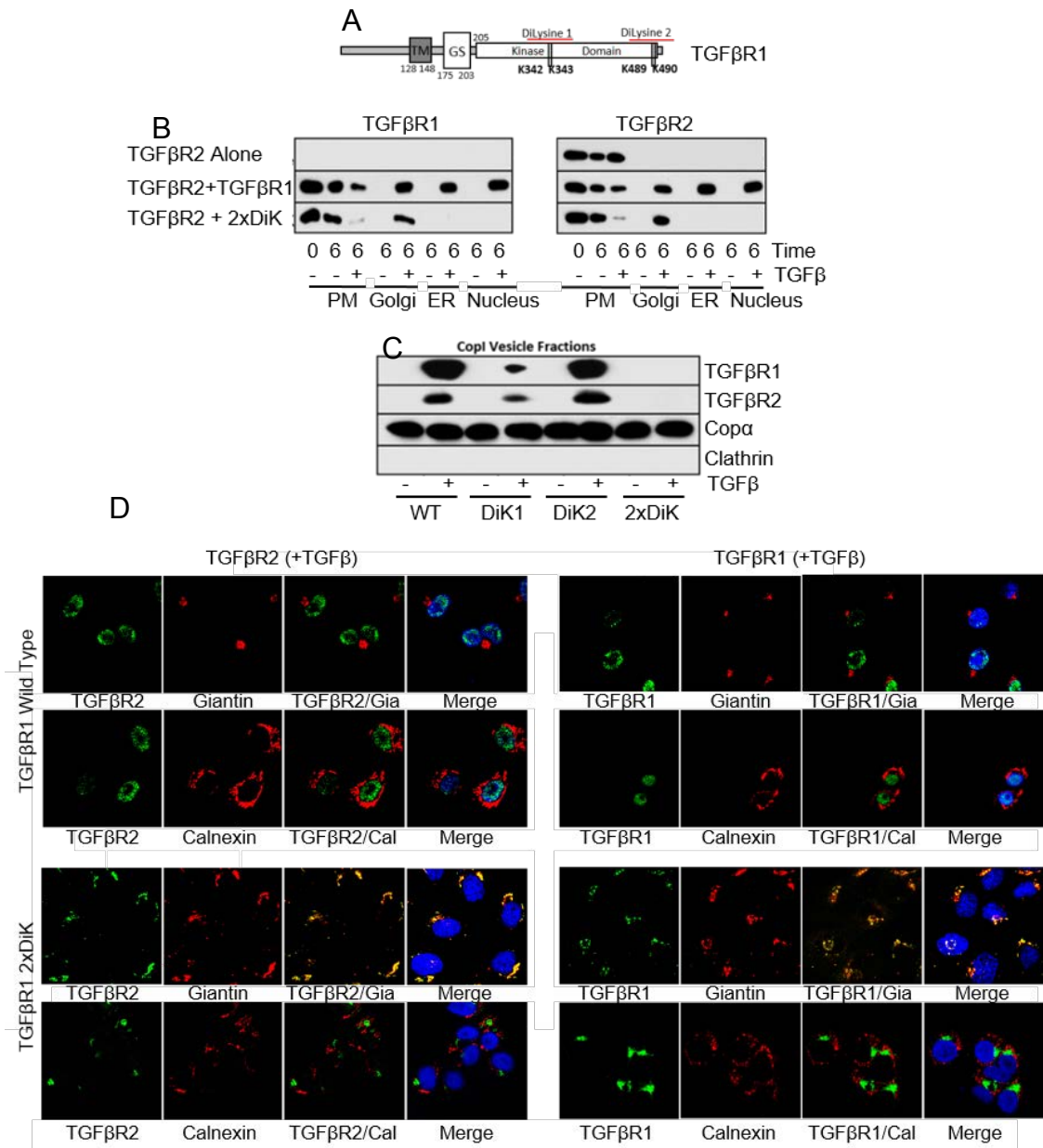


Figure 6.15 TGFβR1 facilitates receptor pair moving from Golgi to ER through sorting into COPI vesicles. (A) Diagrammatic representation of TGFβR1 incorporating the transmembrane domain (TM), G/S-rich domain (GS), kinase domain and Di-Lysine motifs present in the receptor. (B) Plasma membrane, Golgi, ER and nuclear fractions were isolated from Mv1Lu cells expressing TGFβR2 alone (top panels) or with a wild type TGFβR1 (middle panels) or TGFβR1 with lysines 342,343,489 and 490 mutated to isoleucines (bottom panels). Cells were biotinylated at 12°C and before raising to 37°C for 8 hours in the presence (+) or absence (-) of TGFβ prior to compartmental fractionation. Biotinylated proteins were immunopurified with streptavidin before western analysis for presence of TGFβR1 (left) and TGFβR2 (right). As in Fig. 4.3.6, compartmental fractions were loaded unevenly by protein with a ratio of 1-PM:20-Nuc:200-ER:800-Golgi for optimal visualization. (C) Mv1Lu cells expressing TGFβR2 were transiently transfected with either wild type TGFβR1 (WT), or TGFβR1 with lysines 342/343 mutated to isoleucines (DiK1), TGFβR1 with lysines 489/490 mutated to alanines (DiK2) or TGFβR1 with all 4 lysines mutated (2xDiK). After biotinylation and 8 hour incubation in the presence (+) or absence (-) of TGFβ COPI vesicle fractions were prepared and assayed for the presence of surface-derived TGFβR1 and TGFβR2 as well as the COPI vesicle component Copα, and potential contaminate, clathrin. (D) Cos7 cells expressing both HA-tagged TGFβR2 and either myc-tagged wild type (TGFβR1 WT – top panels) or the double Di-Lysine mutant (TGFβR1 2xDiK – bottom panels) were incubated with antibody to either HA (TGFβR2 – left panels) or myc (TGFβR1 – right panels) prior to stimulation with TGFβ for 8 hours. Cells were co-stained for giantin and calnexin after fixation and permeabilization to aid visualization of Golgi and ER compartments respectively.

6.3.6 Receptors are delivered to the inner nuclear membrane through the retrotranslocon and nuclear pore

Anterior-grade transport from the ER is through COPII vesicles while cargoes designated for degradation and retrograde transport utilize the enigmatic retrotranslocon (Nakatsukasa K 2008). Supporting a role for the retrotranslocon in TGF β receptor nuclear transport, we found that both TGF β R1 and TGF β R2 associated with the retrotranslocon component sec61 after TGF β stimulation with kinetics corresponding to nuclear entry (Fig 6.16A – left). Likewise, retrotranslocon disruption (through expression of shRNA to sec61) prevented nuclear delivery of both TGF β receptors as seen by western blot (Fig 6.16B –middle panels) and by immunofluorescence (Fig 6.18 – middle panels). Retrotranslocon disruption caused both TGF β R1 and TGF β R2 (Fig 6.18 – middle panels) to be retained within the ER as determined by strong overlap of TGF β receptor and the ER marker, calnexin signals.

Nuclear entry of TGF β receptors requires an intact nuclear pore as targeted disruption of the essential nuclear pore component importin- β prevents both TGF β R1 and TGF β R2 from appearing in the nucleus (Fig 6.17B – right panels) after TGF β treatment. Both receptors are also found associated with importin- β after ligand stimulation (Fig 6.16 - right). Microscopy imaging reveals receptors appear at least partially backed up in the ER in the absence of importin- β as revealed by the overlap with calnexin staining (Fig 6.17 – lower panels).

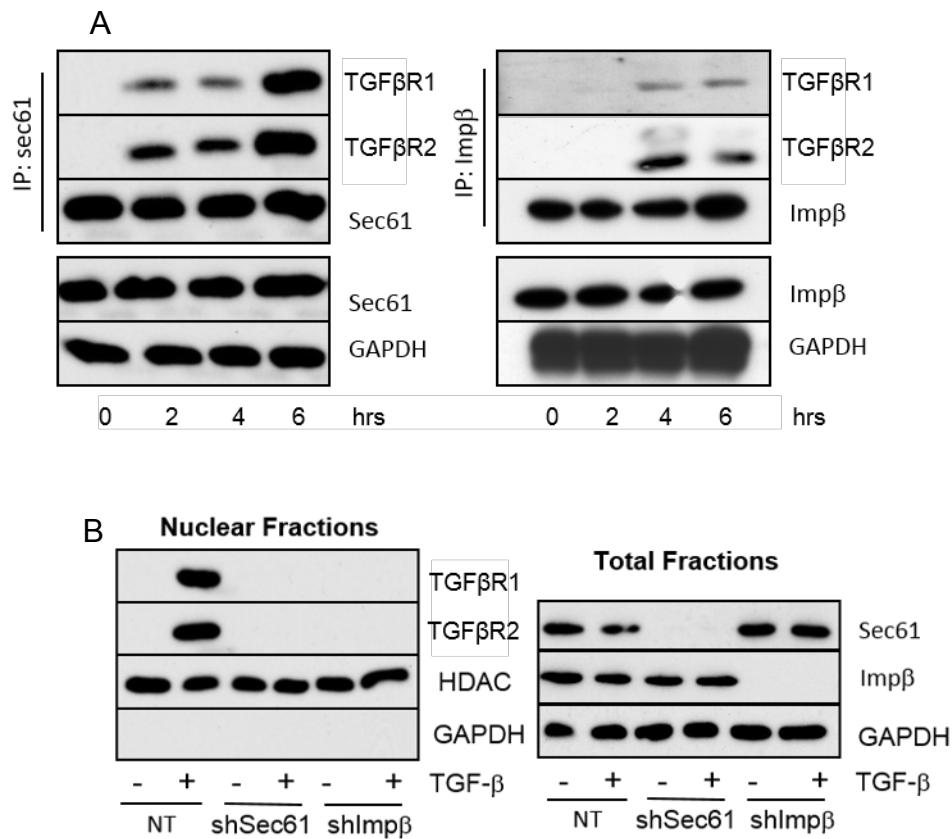


Figure 6.16 TGFβ Receptors bind to and require retrotranslocon and nuclear pore factors for nuclear entry. (A) AKR-2B cells were grown to confluence, serum starved overnight, and stimulated with 5 ng/ml TGFβ for indicated times. Lysates were prepared and immunoprecipitated (800 μg) with antisera to Sec61 (left panels) or Impβ (right panels). Following western transfer the membrane was probed with antibodies to TGFβR1 (top panels) and TGFβR2 (second panels). For the bottom three panels, expression of the indicated proteins in 15 μg of lysate was determined. (B) AKR-2B lines stably expressing shRNA to efficiently silence Sec61 and Importin-β and a non-targetting sequence were biotinylated before 6 hours in the presence (+) or absence (-) of TGFβ. Nuclear (left) fractions were probed for surface-derived TGFβR1 and TGFβR2 while whole cell lysates (total fractions right) were probed for Sec61 and Impβ to document effective knockdown, GAPDH documenting equal protein loading and the purity of nuclear fraction determined by enrichment of HDAC and lack of GAPDH.

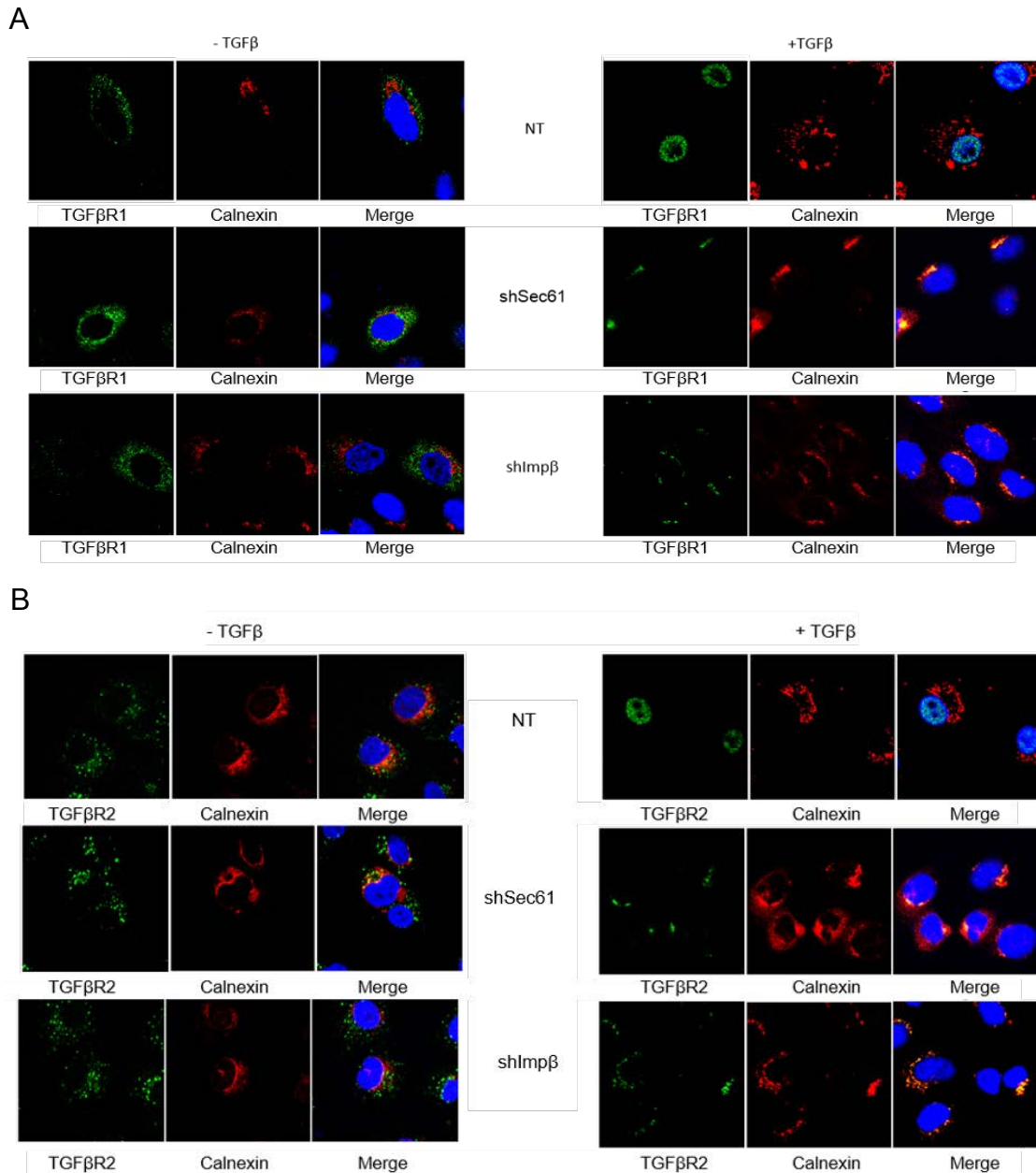


Figure 6.17 Receptors require intact retrotranslocon and nuclear pore complex for nuclear delivery to the inner nuclear membrane. AKR-2B cells stably expressing shRNA to non-targeting (NT), Sec61 (shSec61) or importin-β (shImpβ) along with myc-TGFβR1 and HA-TGFβR2 were incubated in the presence of (A) myc (TGFβR1) or (B) HA (TGFβR2) antibody at 12°C before raising the temperature to 37°C and the addition (Right panels) or absence (Left panels) of TGFβ for 8 hours. Co-staining with the ER marker calnexin was permitted after fixation and permeabilization.

Determining if nuclear TGF β receptors are soluble or within the membranous inner nuclear membrane has important implications on our understanding of how a protein with a hydrophobic transmembrane domain can enter the nucleus. Upon TGF β stimulation both TGF β R1 and TGF β R2 were readily observed in inner nuclear membrane fractions (Fig 6.18A) and, as expected, in cells with disrupted nuclear pores (shImp- β) no receptors could be detected in the inner nuclear membrane fractions (NB: receptors weren't present in total nuclear fractions either – Figs 6.16, 6.17 and 6.18A). Interestingly, treatment with the sumoylation inhibitor Ginkgolic acid resulted in a dramatic increase in both TGF β R1 and TGF β R2 in the inner nuclear membrane fraction (Fig 6.18A).

6.3.7 TGF β receptors enter PML bodies from the inner nuclear membrane

To determine just where TGF β receptors were localized inside the nucleus sub-fractionation into nuclear membrane, nuclear soluble and chromatin-bound fractions was performed. After TGF β insult, receptors were found in both a nuclear membrane and nuclear soluble fractions, but not bound to chromatin (Fig 6.18B). Smad3 constitutively recycles through the nucleus as a soluble protein, however after TGF β stimulation and resulting phosphorylation, there is an increase in nuclear abundance and newly acquired DNA binding. In conjunction with enrichment profiles of known membrane, soluble and chromatin-bound markers, this ensures the absence of receptors in the chromatin-bound fraction was not due to poor preparations. As Ginkgolic acid treatment induced a dramatic increase of receptors in the inner nuclear membrane fraction (Fig 6.18A) we sought to determine where the net influx was coming from. While treating cells with Ginkgolic acid had no appreciable impact on either TGF β R1 or TGF β R2 in the nuclear membrane fraction, virtually no receptor could be detected in the nuclear soluble fraction (Fig 6.18B).

Ginkgolic acid is a potent inhibitor of the formation of PML bodies in the nucleus, suggesting nuclear TGF β receptors might not be free-floating and soluble, but instead contained in these small nuclear bodies. Colocalization between both TGF β R1 (Fig 6.19A) and TGF β R2 (Fig 6.19B) with PML show a striking overlap 8 hours after TGF β treatment that is completely lost in the presence of Ginkgolic acid. Indeed culturing cells in Ginkgolic acid leads receptors from TGF β stimulated cells to re-localize from being largely punctate within the nucleus (in cells without Ginkgolic acid) to encircling

the nuclear perimeter (with Ginkgolic acid). Co-staining with the inner nuclear membrane marker emerin implies these receptors are trapped in the inner nuclear membrane (Fig 6.19A and B – bottom right).

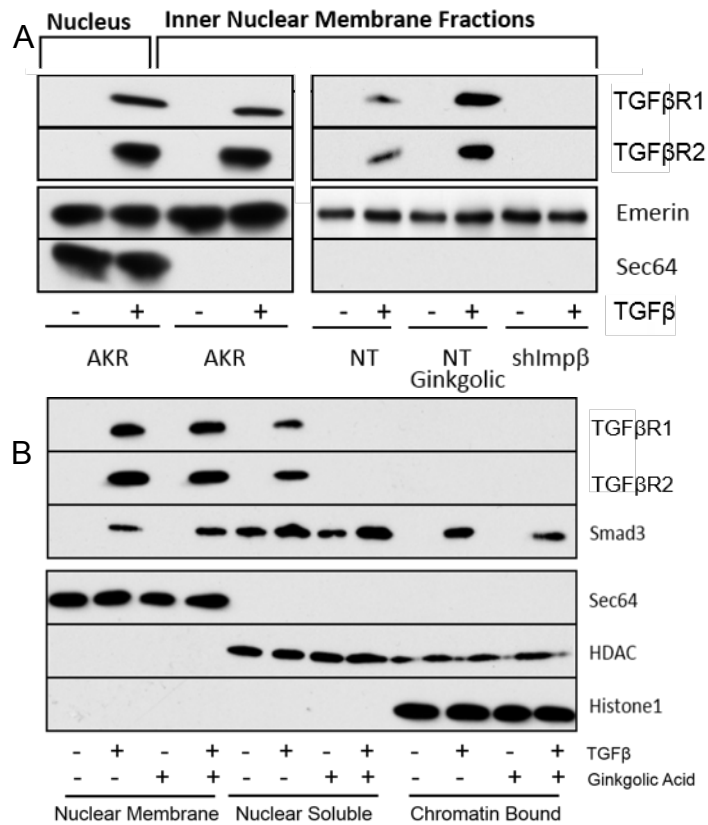


Figure 6.18 TGFβ Receptors are present in inner nuclear membrane and PML nuclear bodies. (A) Cell lines stably expressing shRNA to non-targetting or Importin-β were biotinylated and incubated in the presence (+) or absence (-) of TGFβ and Ginkgolic acid. Nuclear and Inner nuclear membrane fractions were purified and probed for surface-derived TGFβR1 and TGFβR2 as well as the inner nuclear membrane marker emerin and rough ER/outer nuclear membrane marker Sec64. (B) AKR-2B cells were grown to confluence and treated with 5ng/ml TGFβ for 6 hours in the presence or absence of Ginkgolic Acid. Nuclear membrane, nuclear soluble, and chromatin-bound fractions were prepared and subjected to SDS-PAGE prior to blotting for TGFβR1 and TGFβR2 as well as Smad3, Sec64, HDAC and Histone 1.

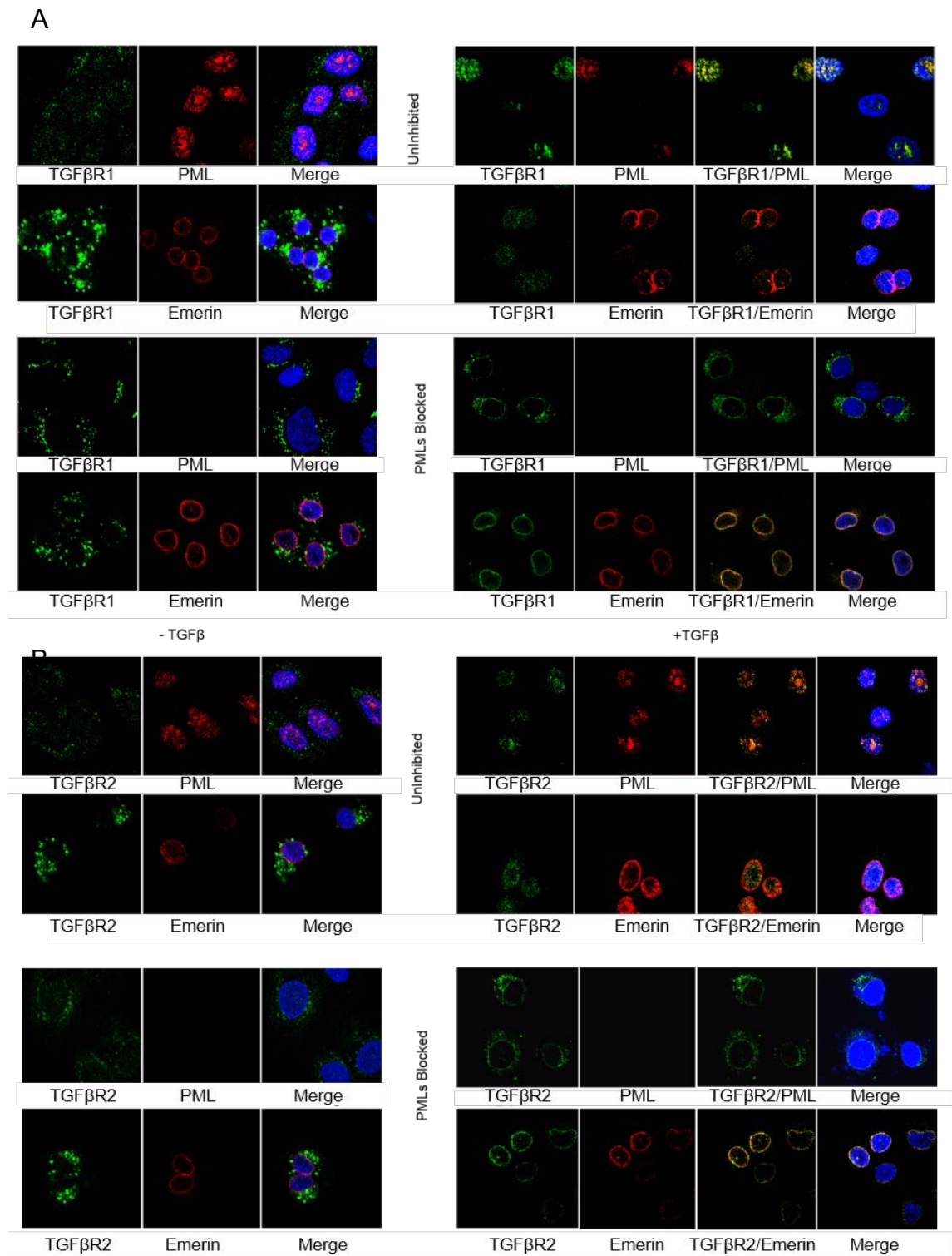


Figure 6.19 TGF β Receptors enter PML bodies from the inner nuclear membrane. Cos7 cells transiently expressing myc-TGF β R1 and HA-TGF β R2 were incubated in the presence of (A) myc (TGF β R1) or (B) HA (TGF β R2) antibody before an 8 hour treatment with (+) or without (-) TGF β and/or Ginkgolic acid (i.e. uninhibited (without Ginkgolic acid) or PML blocked (+ Ginkgolic acid)). After fixation cells were co-stained with PML (to visualize PML nuclear bodies) or emerlin (to visualize inner nuclear membrane).

The preceding data documents nuclear delivery of full length versions of both TGF β R1 and TGF β R2 from the cell surface after TGF β challenge. This occurs in all cell types examined with transit through the Golgi, COPI vesicles, ER, retrotranslocon and nuclear pore. The receptors travel together with TGF β R2 supporting Golgi entry, while Di-Lysine motifs on TGF β R1 facilitates entry into COPI vesicles for ER, and subsequent nuclear delivery. Upon nuclear entry the receptors reside in the inner nuclear membrane before incorporating into PML nuclear bodies.

6.4 DISCUSSION

Reports of receptor kinases trafficking from the cell surface to the nucleus are not new (see Carpenter and Liao for review). Reports of TGF β receptors translocating to the nucleus after stimulation were reported as early as 2000 (Zwaagstra 2000). Defining the role of nuclear receptors in mitigating TGF β signalling in physiological and pathological processes and defining the route of delivery has the potential to greatly improve our understanding of TGF β function and provide potential targets to address clinically undesired manifestations while retaining the homeostatic functions of TGF β .

In all cell types examined, full length TGF β R1 and TGF β R2 entered the nucleus after TGF β stimulation (Figs 6.4 – 6.20) and no evidence of truncated forms were observed in epitope-tagged, chimeric or endogenous receptors (Figs 6.4 – 6.20). Receptors expressing epitope tags on both extracellular and intracellular domains were present in the nucleus after stimulation and only at a size corresponding to a full length protein (Fig. 6.5). It has been suggested TGF β R1 enters the nucleus as a fragment after cleavage of the extracellular and transmembrane domains (Mu 2011 and Gudey 2014) following TGF β treatment. These conclusions relied heavily on immunofluorescence microscopy studies using antibodies to endogenous receptors that notoriously provide difficult to interpret results.

To circumvent these issues, and to focus only on surface-derived receptors, our immunofluorescence microscopy studies utilized TGF β receptors with engineered extracellular epitope tags as well as chimeric receptors comprising the extracellular and transmembrane domains of GM-CSF receptors fused to the intracellular domains of TGF β receptors. Chimeric receptors faithfully reproduce a full TGF β signalling response with GM-CSF (Anders 1996, Anders 1997, Yao 2002, Mitchell 2004, Murphy

2004, Wilkes 2009), do not cross react with endogenous TGF β receptors and, most importantly, high quality antibodies to the extracellular domain are available. All immunofluorescence studies were corroborated with fractionation and western blotting examining endogenous receptors. Why we didn't observe truncated forms in the same cell types observed by others (Mu 2011, Gudey 2014) is difficult to explain, however western blot detection of intracellular domain fragments is known to be problematic, as these fragments are produced in substoichiometric amounts and are metabolically labile (Carpenter and Liao, 2009)

Comparison of both the percentage of surface-derived receptors entering the nucleus and the rate of nuclear entry across a wide range of transformed and untransformed cell types revealed surprisingly limited differences (Fig 6.4C and 6.4D). It has been reported (Mu 2011, Chandra 2012) that levels of TGF β R1 in the nucleus are substantially higher in transformed versus normal cells. While our study addresses only nuclear entry of surface-derived receptors after an acute TGF β treatment, observations of increased nuclear receptors in transformed cells and carcinoma tissue were reported in conditions of extended TGF β treatment (Mu 2011). Perhaps elevated levels of nuclear TGF β R1 in transformed cells is not due to increased trafficking TO the nucleus, but rather accumulation due to defects of degradation/removal of nuclear receptors FROM the nucleus. Such differences would be amplified in the state of chronic TGF β stimulation observed in tumours constantly bathed in a TGF β -rich environment. Alternatively, pools of receptors in the nucleus in transformed cells may not be derived from the surface, as differentiation between intracellular and cell-surface pools is not possible in those studies, which would not have been detected by the techniques employed in our study.

However, as reported by others (Chandra 2012) TGF β R1 was found in the nuclei of HER-transformed MCF10A cells and not untransformed MCF10A cells after shorter (up to 120 min) duration of TGF β (Fig 6.4C and 6.4D). As stated by the authors, this likely reflects the accelerated nuclear delivery due to significantly higher activity of nuclear import molecules (such as Ran) in HER-transformed cells (Chandra 2012), accelerating passage through the nuclear pore. Extending these findings to include later timepoints, indicated that indeed both cell types DO traffic TGF β receptors to the nucleus and while a clear difference in levels of receptors in the nucleus is observed at early timepoints (due to faster nuclear import), at later timepoints the levels become

increasingly similar as the slower rate of import of the untransformed cells “catches up” with the transformed line. By 6-10 hours no significant differences could be observed between the two cell lines (Fig 6.4 C and 6.4D).

Previous observations of TGF β receptors in the nucleus have been restricted to TGF β R1 (Zwaagstra 2000, Mu 2011, Chandra 2012, Gudey 2014). We observed both TGF β R1 and TGF β R2 traffic to the nucleus (Fig 6.4) Indeed, nuclear translocation of TGF β R1 was observed only in the presence of TGF β R2 (Figs. 6.8-6.12 and 6.19) leading us to conclude the nuclear trafficking of TGF β R1 is dependent on TGF β R2. This observation contrasts with interpretations drawn by others stating TGF β R1 traffics to the nucleus independently from TGF β R2 (Mu 2011).

Experiments documenting TGF β R1 with an “activating” mutation (T204D) trafficking to the nucleus in the absence of TGF β is offered to support the concept of no role for TGF β R2 in nuclear trafficking of TGF β R1 (Mu 2011). Two conceptual issues arise in this interpretation. Firstly, the T204D mutation does not increase the kinase activity of the receptor *per se* as is the case for many other “constitutively active” kinase mutants. Instead this mutation mainly works by increases affinity of TGF β R1 for TGF β R2, which facilitates the increased rate of interaction, phosphorylation (and subsequent activation) of TGF β R1 by TGF β R2 (unpublished data). In a cell expressing endogenous TGF β R2, introduced TGF β R1 mutants will be able to interact with endogenous TGF β R2, so while a ligand-independent signalling event will be initiated, it would be inconclusive to assume TGF β R2 is not involved. Secondly, TGF β R1 exist as homodimers. Introducing a mutant TGF β R1 into a cell with endogenous receptors will result in a mixed population of dimers with pairs consisting of none, one, or both receptors carrying the mutation, making interpretation problematic. Our introduction of the T204D mutation into a GM-CSFR α /TGF β R1 chimera circumvented the compounding issues arising from introducing the same mutation into TGF β R1 (i.e. the chimeric receptor does not interact with endogenous TGF β R1 or TGF β R2), allowing our approach to more robustly test the ability to TGF β R1 to traffic to the nucleus independently from TGF β R2.

Recognition of a short sequence of TGF β R2 after TGF β stimulation allows TGF β R2 alone, or coupled to TGF β R1, entry to the Golgi (Figs. 6.8 – 6.13). TGF β R2 is not

known to undergo any post-translational modifications following TGF β stimulation so it is hard to know how the retromer could discriminate between ligand bound and free TGF β R2. Our data supports the model that ubiquitination at lysine 488 is required for retromer delivery of TGF β R2 to the Golgi, but a number of potential caveats remain. The incorporation of a deubiquitination domain on TGF β R2 did prevent nuclear delivery of the receptors (Fig 6.13B – top Panel) but likewise prevented degradation (Fig 6.13B – bottom panel). Such a large domain could deubiquitinate other proteins in the vicinity, including TGF β R1 or multiple sites along TGF β R2. It is possible lysine 488 is required for nuclear delivery while another lysine residue is required for degradation and the deubiquitination domain removed both. Perhaps it is the nature of the ubiquitin itself that determines the receptors fate? Interestingly, while retromer binds TGF β R2 along with ActivinR2 and BMPR2, only TGF β R2 was able to traffic to the nucleus (Fig 6.12). Comparison of the amino acid sequence of the retromer binding region revealed only TGF β R2 possesses a lysine residue at position 488, further supporting a possible role for ubiquitination in delivery to the nucleus.

Passage of the receptor complex into COPI vesicles is then bestowed by a pair of di-lysine motifs in TGF β R1 which facilitate entry to the ER. Whether receptors remain complexed in the nucleus is not known, however both are present in inner nuclear membrane and PML nuclear body fractions (Figs. 6.18 and 6.19). We report nuclear receptors are localized to the inner nuclear membrane and PML bodies. Indeed, the truncated form of TGF β R1 has been observed in PML bodies previously (Mu 2011). It is unclear if receptor signalling in the nucleus requires entry into PML bodies or if signalling can occur from the inner nuclear membrane. A role for PML bodies may well prove essential for other nuclear functions of either TGF β R1 or TGF β R2. Another possibility is PML bodies may prove to be involved in the degradation of nuclear receptors. Indeed, after approximately 8 h of TGF β stimulation, nuclear receptor levels decrease markedly coinciding with a decrease in co-staining of receptors and PML bodies (Fig. 6.4A) however this remains an area of ongoing research.

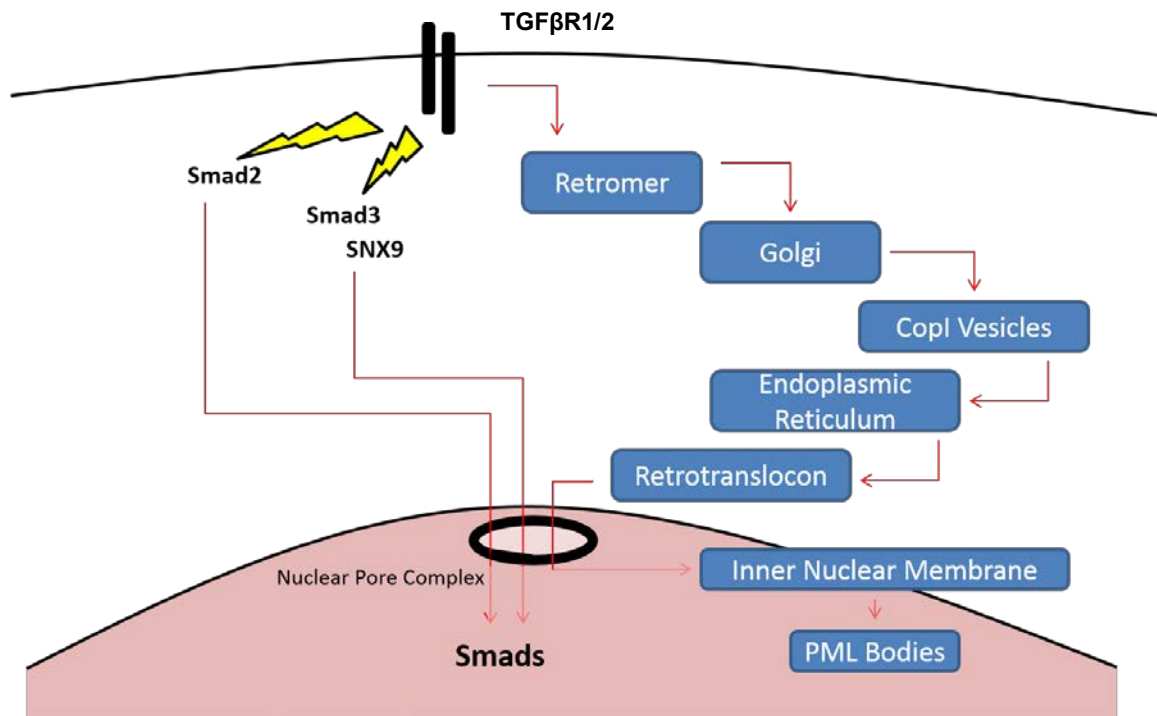


Figure 6.20 Diagrammatic representation of route of nuclear trafficking of TGF β receptors after ligand stimulation. Firstly, the receptor subset for nuclear delivery is sorted by the retromer for Golgi transport due to a motif on TGF β R2. Secondly, di-lysine motifs on TGF β R1 sort receptors into COPI vesicles for delivery to the ER. Receptors exit ER through the retrotranslocon pore and enter the nucleus through the nuclear pore and reside in the inner nuclear membrane (INM). From INM PML bodies containing receptors are formed. While Smads have long been recognized as the main TGF β signalling molecules trafficking to the nucleus, the observation that TGF β receptors themselves localize to the nucleus establishes yet another regulatory checkpoint a cell can use to fine tune the TGF β signal.

The role of TGF β receptors in the nucleus is an emerging area, shedding new light on how TGF β exerts its action in both normal and disease states. Translocation of an activated kinase to different locales not only removes it from substrate pools in one location, but exposes it to new pools of potential substrates. At the plasma membrane TGF β receptors are exposed to and activated by ligand, priming them for subsequent Smad phosphorylation. The rapid removal of the receptors from the cell surface effectively ends Smad phosphorylation but while most receptors are degraded, some go on to be exposed to substrates in the nucleus (summarized in Fig 6.20). Defining what these substrates are, the impact of their phosphorylation and determining ways to prevent it, may prove fruitful in developing therapeutic strategies to target dysregulated aspects of TGF β signalling.

CHAPTER 7

ROLE OF NUCLEAR TGF β RECEPTORS IN THE REGULATION OF TGF β -RESPONSIVE GENES

CHAPTER 7: ROLE OF NUCLEAR TGF β RECEPTORS IN REGULATION OF TGF β -RESPONSIVE GENES

7.1 BACKGROUND

After ligand binding at the cell surface, phosphorylation activates the kinase activity of TGF β R1 resulting in phosphorylation and nuclear accumulation of Smad2 and Smad3 (Marcías-Silva 1996) where they serve as transcription factors after DNA binding. Cellular responses induced by TGF β do not occur in the absence of Smads (Attisano 1998), however non-Smad signalling molecules have been described including Ras, PAK2 and c-Abl, often in cell type specific contexts (Mulder 1992, Wilkes 2003, Daniels 2004). Smad DNA binding alone is undetectable *in vivo* (Shi Y 1998) and full biological induction/repression requires recruitment of other transcription factors, including P300 (Pouponnot 1998, Topper 1998), ATF/CREB family members (Topper 1998, Kang 2003, Warner 2004), AP1 (Zhang 1998, Sundqvist 2013), FAST1 (Chen 1996) and E2F family members (Chen 2002).

Data presented in Chapter 6 documents the nuclear delivery of TGF β receptors from the cell surface after ligand stimulation, however the subsequent functions and downstream events of nuclear TGF β receptors remains undefined. While it has been reported full length nuclear TGF β receptors do not associate with chromatin (Chandra 2012), a cleaved form of TGF β R1 was found to bind the TGF β R1 promoter, (Gudey 2014). Although unable to bind DNA, full length nuclear TGF β R1 could recognise and bind a consensus sequence in RNA (Chandra 2012). Both TGF β R1 and TGF β R2 are functional kinases (at least at the plasma membrane) and the kinase activity of TGF β R1 is modulated by the presence of ligand. In Chapter 6 we reported the nuclear trafficking of both receptors into the nucleus, a location where a vast array of potential new substrates become available. Transcriptional and translational regulation within the nucleus is significantly impacted by phosphorylation and dephosphorylation (Bannister 1996) and the role of TGF β receptors as kinases within the nucleus is completely unexplored.

As mentioned above, even promoters with multiple Smad Binding Elements (SBEs) require other cooperating factors for high affinity DNA binding and transcriptional

changes (Seoane 2004). This apparent paradox ensures that while Smads are absolutely required for TGF β -induced transcriptional changes, they are not sufficient alone, requiring the co-operation of other factors that may, or may not be, further influenced by TGF β stimulation. Focusing on recognized transcription factors that cooperate with Smads at the promoters of TGF β -influenced genes we sought to investigate a potential role for nuclear TGF β receptors as kinases that may regulate these interactions. Of particular interest were the nuclear transcription factors ATF2, CREB and sp1 that have been reported to both; 1) play a role in the TGF β induction of a subset of genes and, 2) be phosphorylated in response to TGF β by unknown kinases (Topper 1998, Kang 2003, Warner 2004, Zhang 1998, Sundqvist 2013).

Objectives

1. To determine if nuclear TGF β receptors retain kinase activity and if kinase activity is required for nuclear trafficking.
2. To determine if blocking nuclear receptor trafficking influences TGF β -modulated genes.
3. To determine if nuclear TGF β receptors can phosphorylate recognized TGF β -associated transcription factors *in vitro* and *in vivo*.
4. To determine if phosphorylation of transcription factors by nuclear TGF β receptors modulates activity and/or chromatin binding *in vitro* and *in vivo*.
5. To uncover the mechanism of cooperation between Smads and nuclear receptor-phosphorylated transcription factors at the gene promoter level.

While the receptors do not interact with chromatin directly, we report here that TGF β R1 retains kinase activity and phosphorylates a number of transcription factors, the activation of which is required for induction of various TGF β -responsive genes. Transcription factor phosphorylation increases the histone acetyltransferase activity leading to increased chromatin binding and unfolding. This chromatin unfolding exposes Smad Binding Elements in some promoters which then become available to nuclear-localized pSmads, that consequently bind and initiate full transcriptional induction of these TGF β -responsive genes.

7.2 MATERIALS AND METHODS

7.2.1 Cell culture and stimulation

Mv1Lu are an epithelial cell of mink origin with a well characterized TGF β response that transfect readily and are amenable to standard culturing techniques. The R1B cell line is derived from Mv1Lu and lacks TGF β R1. As the majority of data presented in this study involves comparisons between Wild type TGF β R1 (WT) and TGF β R1 carrying mutations in the two di-Lysine motifs (2xDiK), R1B cells transfected with the two TGF β R1 constructs in parallel provided an ideal model. Cos7 cells were utilized because of their high transfection efficiency and high recombinant protein expression to ensure high yields of immunopurified HA-TGF β R2 and myc-TGF β R1 that were transfected into these cultures. Cells were obtained and cultured as specified (Table 3.2) using standard mammalian cell culture techniques (see Chapter 3) and grown to confluence prior to stimulation with TGF β 1 to a final concentration of 10 ng/ml in the appropriate growth media (see Table 3.2). Cells were stimulated for various times with TGF β , with 20-30 minutes optimal for initial activation of receptors and Smads at the plasma membrane (Marcías-Silva 1996), 6-8 hours for subsequent delivery of receptors to the nucleus (Chapter 6), and 24 hours to examine downstream transcriptional responses (Wilkes 2007). When Ginkgolic Acid was used to prevent PML body formation (Fig 7.5B), it was added concurrently with TGF β and used at 10 μ M.

As well as constructs contained in Table 3.1, we transfected Cos7 cells with plasmids expressing constitutively active forms of the transcription factors CREB and ATF2 (Fig 7.5B) that contained mutations (S133D in CREB and S155D in ATF2) to mimic phosphorylation at sites reported to result in increased transcriptional activity (Kang 2010, Fell 2012). We thank Jin Chen (Emory University) and Caroline Schild-Poulter (University of Western Ontario) for the CREB_{S133D} and ATF2_{S155D} constructs respectively.

7.2.2 Transcription Factor phosphorylation by TGF β Receptors

Kinase Assays to determine the ability of TGF β receptors to phosphorylate potential transcription factor substrates were performed essentially as described in Chapter 3. Myc-epitope tagged receptors were transiently transfected into Cos7 cells and either unstimulated or stimulated with TGF β for 30 minutes. Whole cell lysates, or purified

Golgi, ER or nuclear fractions (see Chapter 3 for details on preparation), were subjected to standard immunoprecipitation methods. Purified receptor kinases were incubated in the presence of potential substrates in kinase buffer containing 5 μ M ATP and 5 μ Ci [γ - 32 P]ATP per reaction for 30 minutes at 37°C. Transcription factors with the potential to be kinase substrates of TGF β R1 were purchased from Sigma-Aldrich (St Louis, Missouri)(GST-CREB, GST-ATF2, GST-Fos and GST-Elk1) or were purified as GST-fusion proteins from BL21 *E.coli* bacteria (intracellular domain of TGF β R1, (termed Δ T1R), and Smad3)(See Chapter 3 for details). Native transcription factors including sp1, Stat6, NF κ B and P300, were purified from AKR-2B cells using Catch and Release[®]v2.0 protein purification system (Upstate Biotechnology, Lake Placid, New York). Purified receptors and transcription factors were incubated together in kinase permissive conditions (see Chapter 3 for details) prior to SDS-PAGE and analysis by autoradiography.

7.2.3 Comparison of kinase activity between plasma membrane and nuclear TGF β R1

The specific kinase activity of plasma membrane or nuclear TGF β R1 utilizing both Smad3 and ATF2 as substrates was determined using ADP-Glo[™] Activity Assay (Promega, Madison, Wisconsin) Protocol. As the kinase utilized available ATP to phosphorylate ATF2 or Smad3 it generated ADP. Addition of the ADP-Glo[™] reagent terminated the kinase reaction and depleted remaining ATP. Addition of the supplied kinase detection reagent facilitated the reconversion of ADP back to ATP, which was converted to light using a luciferase/luciferin reaction and detected using a Lumat 9501 luminometer (Berthold Technologies, Bad Wildbad, Germany). An ATP to ADP conversion curve was generated through serial dilutions of purified TGF β R1 and specific kinase activity was determined by calculating the following values:

$$\frac{\text{ADP production in the presence of substrate} - \text{ADP production in the absence of substrate}}{(\text{reaction time}) \times (\text{enzyme amount at maximal catalytic activity})}$$
(see Fig 7.3B)

7.2.4 The role of kinase activity in nuclear trafficking of TGF β Receptors

The advantages of using chimeric TGF β receptors have been discussed previously (Chapters 3, 4 and 6) and consist of the extracellular domain of the GM-CSFR α fused to the intracellular and transmembrane domains of TGF β R1 (designated **GM α T1R**),

and the extracellular domain of GM-CSFR β fused to the intracellular and transmembrane domains of TGF β R2 (designated **GM β T2R**). Chimeric receptors maintain TGF β signaling but the signal is initiated by stimulating with GM-CSF (Anders 1996). In this way, mutants can be introduced into chimeric receptors and the impact on TGF β signaling can be compared between mutant (by stimulating with GM-CSF) and native (by stimulating with TGF β) in the same cells side by side. AKR2B cells stably expressing both wild type chimeric receptors, Wild Type GM α T1R and kinase-deficient GM β T2R (GM β T2R_{K277R}), and kinase-deficient GM α T1R (GM α T1R_{K232R}) and Wild Type GM β T2R (see Table 3.2 for cell details) were stimulated with TGF β for 6 hours prior to nuclear, Golgi and ER fractionation as outlined in Chapter 3. As determined in Chapter 6, six 6 hours of TGF β stimulation is enough time for a large amount of receptors to have entered the nucleus, but not so long that all the receptors have passed through the Golgi and ER compartments (Fig 6.7). Nuclear, Golgi and ER fraction purity was confirmed by Western blot analysis using the relative absence, or abundance of the markers HDAC (nuclear protein), GM130 (Golgi protein) and Calnexin (ER protein) as described previously.

7.2.5 Effect of TGF β R1 mediated phosphorylation on histone acetyltransferase (HAT) activity of Transcription Factors

Histone acetylation is an important process in chromatin rearrangement, whereby acetylated histones facilitate loosened chromatin and expose promoter regions of DNA to transcription factors for modulation of gene expression. Histone Acetyltransferase Assays were performed as recommended by the manufacturer using supplied reagents in the Histone Acetyltransferase Activity Assay Colorometric Kit (EPI001 Sigma-Aldrich, St Louis, Missouri) with the exception of the potential transcription factor acetyltransferases which were purchased from Sigma-Aldrich (St Louis, Missouri)(GST-CREB, GST-ATF2, GST-Fos and GST-Elk1), purified as GST-fusion proteins from BL21 *E.coli* bacteria (Δ T1R and Smad3)(See Chapter 3 for details) or purified from AKR-2B cells using Catch and Release[®]v2.0 protein purification system (Upstate Biotechnology, Lake Placid, New York)(sp1, Stat6, NF κ B, P300). Prior to HAT assay analysis, purified proteins were exposed to immune purified myc-TGF β R1 or HA-TGF β R2 from transfected Cos7 cells that had been either unstimulated or stimulated with TGF β for 30 minutes in kinase reaction conditions (see Chapter 3 for details) as above. Positive and negative controls were supplied with the kit and compared with experimental samples. All samples were analysed in triplicate.

7.2.6 Determination of the role of di-Lysine motifs in TGF β R1-mediated Smad phosphorylation, nuclear translocation and binding to Smad Binding Elements

In order to determine the role of nuclear receptors, it was imperative to be able differentiate events initiated by the receptors close to the cell surface from those that occur after entering the nucleus. It was observed that there are two di-lysine motifs within TGF β R1 at K342/K343 and K489/K490. Collectively they facilitate loading of nuclear-bound TGF β R1 and TGF β R2 into COPI vesicles (Fig 6.15) and the mutation of both pairs of lysines is required to inhibit COPI vesicle loading. However the impacts of these mutations on receptor kinase activity and cell surface functions have not been analysed but because TGF β R1 phosphorylation of Smad2 and Smad3 occurs prior to COPI vesicle loading (in a very early endosome just after endocytosis (Di Guglielmo 2003)), mutations that impact COPI vesicle loading should not influence Smad phosphorylation and activation. Comparisons between Wild Type TGF β R1 and TGF β R1 carrying mutations at both di-lysine motifs (2xDiK) in their ability to phosphorylate and activate Smads was performed in four ways.

7.2.6.1. Comparison of TGF β R1 WT and 2xDiK Smad3 phosphorylation *in vitro*

R1B cells were transfected with pBabe-myc-TGF β R1 WT or pBabe-myc-TGF β R1 2xDiK (Table 3.1) and stimulated with TGF β for 30 minutes prior to lysis in histone lysis buffer (see Chapter 3 for details). TGF β R1 was immunoprecipitated (see Table 3.3 for conditions) and incubated in the presence of GST-Smad3 in conditions facilitating kinase activity (see Chapter 3) under standard kinase assay conditions (see Chapter 3).

7.2.6.2. Comparison of TGF β R1 WT and 2xDiK Smad2 and Smad3 phosphorylation *in vivo*

R1B cells were transfected with pBabe-myc-TGF β R1 WT or pBabe-myc-TGF β R1 2xDiK (Table 3.1) and stimulated with TGF β for 30 minutes prior to lysis. Detection of phosphorylated forms of Smad2 and Smad3 was achieved by standard Western blotting procedures (see Chapter 3) and compared with total Smad2/3 levels. Antibodies and the blotting conditions are found in Table 3.3.

7.2.6.3. Comparison of TGF β R1 WT- and 2xDiK-mediated Smad2 and Smad3 nuclear translocation

R1B cells were transfected with WT or 2xDiK TGF β R1 and stimulated with TGF β for 30 minutes prior to nuclear fractionation using NE-PER™ Nuclear and Cytoplasmic

Extraction Kit (Pierce Biotechnology, Rockford, Illinois) and as per the manufacturers instructions, followed by Western blotting using standard procedures (see Chapter 3) with antibodies raised against Smad2 and Smad3 (see Table 3.3).

7.2.6.4. Comparison of TGF β R1 WT- and 2xDiK-mediated Smad2 and Smad3 binding to SBEs

When phosphorylated and inside the nucleus, Smads bind sequences within the DNA recognized as Smad Binding Elements (SBEs). Because Smads are not efficient transcription modulators (require additional input from other transcription factors to induce significant genetic changes) a single SBE inserted in the promoter region of a gene has a negligible impact (Seoane 2004). However, if a string of 6-12 SBEs are inserted adjacent to a minimal promoter driving expression of a luciferase gene, a moderate (2-4 fold induction) can be observed in response to TGF β stimulation. Unlike endogenous promoters that are influenced by TGF β (where Smads cooperate with other transcription factors) the SBE-luciferase readout is unique in that induction is entirely due to pSmad binding and independent of other transcription factors that may, or may not, be influenced by Smad-independent elements of TGF β signalling (See Fig 7.1).

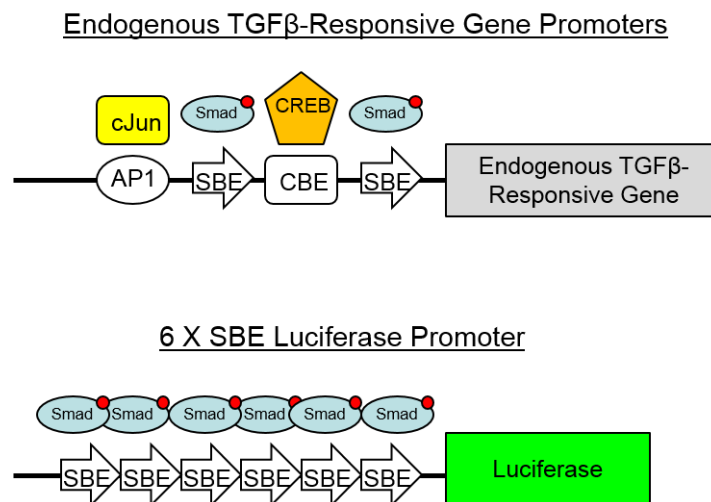


Figure 7.1 Comparison between the promoters of endogenous TGF β -responsive genes and the 6xSBE responsive Luciferase reporter gene. (Top) Endogenous Gene Promoters consist of both SBEs and other Binding Elements (eg Creb- Binding Elements and AP1 elements) that recruit other transcription factors (eg cJun and Creb) to cooperate with the Smads to facilitate full gene modulation. (Bottom) The 6xSBE Luciferase Reporter consists only of a minimal promoter with six consecutive SBEs to drive expression of the Luciferase gene, thereby making luciferase expression entirely dependent on phosphorylated Smads binding to SBEs without a contribution of other transcription factors.

R1B cells (Mv1Lu devoid of TGF β R1) were plated in six-well dishes at 2.5×10^5 per 6-well dish and allowed to divide overnight prior to co-transfection with two reporter constructs, pCMV5-cytomegalovirus- β -galactosidase (β -gal) and pCMV5-6xSBE Luciferase (SBE-Luc). Accurate determination of the impacts of di-Lysine receptor

mutations on 6xSBE Luciferase induction required normalization of samples for both protein concentration and transfection efficiency. While protein normalization was achieved using a Bradford Assay (standard techniques), determination of transfection efficiency was assessed by determining the β -galactosidase activity of the cell lysates (directly correlates to the expression of cytomegalovirus- β -galactosidase). 2 μ g of 2xSBE luciferase reporter and 0.5 μ g of cytomegalovirus- β -galactosidase reporter were co-transfected with Lipofectamine® 2000 (see Chapter 3 for details) along with 1.0 μ g of either pBabe-myc-TGF β R1 WT or 2xDiK. Cultures were unstimulated or stimulated with TGF β for 24 hours to allow for the accumulation of luciferase protein before being harvested in 200 μ l of reporter lysis buffer (Promega, Madison, Wisconsin). Luciferase activity was determined in a Lumat 9501 luminometer (Berthold Technologies, Bad Wildbad, Germany) after normalization for protein and transfection efficiency using β -galactosidase activity as a readout. Results presented are pooled from three independent experiments, each performed in duplicate with standard deviation as a measure of variability across experiments.

7.2.7 Effect of diLysine mutations in TGF β R1 on pSmad3 promoter binding using Chromatin Immunoprecipitation (ChIP)

In order to determine if the presence of TGF β receptors in the nucleus had any impact on the binding of Smad3 to TGF β -induced genes, we performed chromatin immunoprecipitation assays. Confluent R1B cells were transfected with pBabe-myc-TGF β R1 WT or pBabe-myc-TGF β R1 2xDiK (Table 3.1) to cells in 10mm² dishes prior to stimulation with TGF β for 24 hours. Formaldehyde was added to a final concentration of 0.75% at 27°C for 20 minutes to cross-link the chromatin-associated proteins to the DNA. The cross-linking reaction was terminated by the addition of glycine to 125 mM. Sonication for 10 minutes yielded DNA fragment sizes between 200-500 base pairs. A small aliquot was separated to determine DNA concentration by absorbance, measured from 230 to 320 nm. DNA concentration reliability was maximized by first removing RNA and protein (by RNase A and proteinase K treatment respectively) from the aliquot, prior to measuring absorbance.

After determining DNA concentration, 25 μ g Chromatin was diluted 10 fold into RIPA buffer (see Appendix IV) and mixed with 3 μ g anti-Smad3 antibody before incubation for 60 minutes at 4°C. Chromatin/Smad3/antibody complexes were pulled down with

60 μ l of blocked protein A-agarose beads with overnight incubation at 4°C. Chromatin/Smad3 was eluted in 120 μ l of elution buffer (see Appendix IV) and treated with RNase A, (to degrade associated RNA) and proteinase K (to cleave peptide bonds of aliphatic and aromatic amino acids and the cross-links between the proteins and DNA) to produce DNA of high enough quality for PCR. Prior to pulling down DNA/Smad3/antibody complexes, Protein A-agarose beads were blocked in 75 μ l salmon sperm and 0.1 μ g of BSA per μ l of beads to prevent non-specific DNA and protein binding respectively.

7.2.8 qRT-PCR of TGF β -induced genes

Quantitative reverse-transcriptase polymerase chain reaction (qRT-PCR) was performed essentially as stated in Chapter 3. Total RNA was extracted using the RNeasy Plus Mini Kit with gDNA eliminator spin columns to remove genomic DNA (QIAGEN, Velno, The Netherlands) from the R1B cells transfected with either pBabe-myc-TGF β R1 WT or 2xDiK that had been treated with TGF β for 24 hours. RNA was converted to cDNA for quantitative PCR using Superscript III Reverse Transcriptase (Life Technologies, Grand Island, New York). While a significant number of genes were assessed, we limited our studies to genes reported to be TGF β -responsive and have a requirement for CREB (PAI-1, CTGF, eNOS), ATF2 (CRP, TGF β 3 and ATF3) or ETF4A (CDC25A, MYB and TP53). A selection of genes that are not induced by TGF β but reported to be influenced by CREB (MDM2, Bcl2 and Akt1) or ATF2 (IL-8, E-Selectin and uPA) were also assessed (see Table 7.1). For clarification, CREB associated genes will be demarked in pink, ATF2 associated genes will be in green and ETF4A associated genes will remain in black.

Quantitative real-time PCR was performed using the CFX96 Real-Time PCR detection system (Bio-Rad, Hercules, California). The cDNA samples were diluted 1:5 with water and 2% used as template. The amplified nucleic acids were quantified using the SYBR® Green PCR Master Mix (Life Technologies, Grand Island, New York). The conditions for the PCR reactions were as follows: 50°C for 2 minutes, 95°C for 2 minutes, and 40 cycles of 95°C for 15 seconds, 60°C for 30 seconds, and 72°C for 30 seconds and SYBR® quantification. Primers (0.2 μ M final concentration) are listed in Appendix V. To determine the relative expression levels of TGF β -regulated genes, the mRNA levels were normalized to the level of GAPDH mRNA using the comparative threshold cycle (CT) method, in which the fold difference is $2^{-\Delta CT}$ of target gene -

Δ CT of reference gene). Data is compiled from three separate repeats of each experiment.

Table 7.1 Genes examined and grouped by association with transcription factor

Transcription Factor	Gene	TGF β Responsive
CREB	PAI-1 CTGF eNOS	YES
	MDM2 Bcl2 Akt1	NO
ATF2	CRP TGF β 3 ATF3	YES
	IL-8 E-Selectin uPA	NO
ETF4A	CDC25A MYB TP53	YES

7.2.9 Analysis of gene and chromatin array data

CREB and phosphor-CREB promoter binding analysis was performed as described by Zhang and colleagues (Zhang 2005). Genome sequences and annotations were obtained from the UCSC Genome Bioinformatics Site (<http://genome.ucsc.edu>). A whole genome search of full cAMP-response element (CRE) (TGACGTCA), half CRE (TGACG/CGTCA) and SBE (CAGA) sites was performed as published (Zhang 2005, Koinuma 2009) using Affymetrix® GeneChip (Affymetrix, Santa Clara, CA) All CRE hits were mapped to promoter, exonic, intronic, and intergenic regions according to the locations of RefSeq genes. Promoters were defined as 3 kb upstream to 300 bp downstream of the annotated transcription start sites. For all CREs located in the promoter regions, a search of downstream (within 300 bp) TATA boxes was performed by using a weight matrix and CREs located within 50 bp of each other were considered to form clusters of CREs. Profile hidden Markov models (pHMMs) for full CRE and half CRE sites were built based on known CREB target genes and were used to search for positional conserved sites. Images were generated using DCHIP software

(<http://www.hsph.harvard.edu/cli/complab/dchip/manual.htm>) and the expression data are available at <http://natural.salk.edu/CREB>.

The TGF β -induced Smad CHIP-chip and TGF β gene expression microarray raw data were re-analysed and converted into the same format as CREB promoter binding data using DCHIP software (<http://www.hsph.harvard.edu/cli/complab/dchip>). CHIP and control input DNA samples were amplified by two cycles of in vitro transcription and hybridized on separate Affymetrix human promoter 1.0 oligonucleotide tiling arrays and relative fluorescence signal intensity data for Smad CHIP and TGF β gene microarray have been deposited in the NCBI Gene Expression Omnibus and are accessible at (<http://www.ncbi.nlm.nih.gov/geo/query/acc.cgi?acc=GSE11710>) through GEO series accession number GSE11710 .

7.3 RESULTS

TGF β receptors function as kinases at the cell surface. To determine if receptors in the nucleus maintain kinase activity and if kinase activity has any role in the trafficking or function of the receptors within the nucleus is one of the objectives of this Chapter. A number of transcription factors involved in TGF β signalling have been reported to be phosphorylated by unknown kinases in the nucleus. Determining if nuclear TGF β receptors are the kinases responsible for any of these phosphorylation events was a further objective of this study.

7.3.1 Kinase activity of TGF β R2 (but not TGF β R1) is required for nuclear entry

The kinase activity of TGF β R2 is required for internalization and subsequent endocytosis (Anders 1998) which is also the first step in nuclear trafficking (Fig 6.6) and therefore, as expected, cells expressing chimeric receptors yielding a kinase-deficient TGF β R2 were unable to enter Golgi, ER or nuclear fractions. In contrast, when a kinase-deficient TGF β R1 was expressed both the mutant TGF β R1 and TGF β R2 trafficked to the nucleus (Fig 7.2).

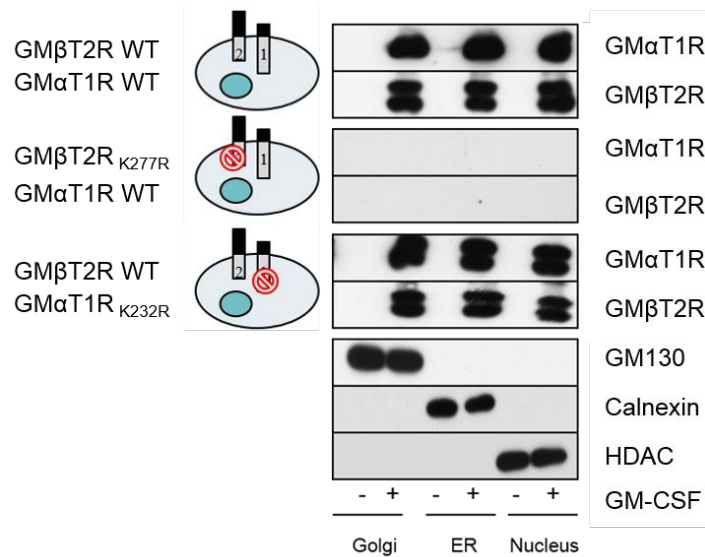


Figure 7.2 Kinase activity of TGFβR2 required for nuclear delivery of receptors, while TGFβR1 kinase is irrelevant. AKR-2B cells stably expressing both wild type chimeric receptors, wild type GMβT2R with the kinase-deficient GMαT1R_{K232R}, or the kinase-deficient GMβT2R_{K277R} with the wild type GMαT1R were biotinylated and treated with GM-CSF for 6 hours before Golgi, ER and nuclear fractions were generated. Streptavidin-purified cell-surface derived proteins were assessed for the presence of both chimeric receptors by Western analysis, while fraction purity was determined by enrichment and exclusion of Golgi (GM130), ER (Calnexin) and nuclear (HDAC), markers.

7.3.2 TGFβR1 kinase activity is maintained after trafficking to the nucleus

We previously demonstrated no direct chromatin association with TGFβR1 (Fig 6.18B), however the kinase activity of TGFβ receptors may play a role in TGFβ signalling by phosphorylating substrates not available prior to localization in the nucleus. TGFβR1 kinase activity is dispensable for nuclear translocation but is maintained after trafficking to the nucleus. The specific activity of TGFβR1 isolated from the plasma membrane in both unstimulated and stimulated conditions was compared with TGFβR1 isolated from the nucleus after stimulation. There was no observable difference in the ability of plasma membrane- or nuclear-obtained TGFβR1 from stimulated cells to phosphorylate GST-Smad3 (Fig 7.3) suggesting no gross stoichiometric changes of the intracellular domain occur during nuclear trafficking.

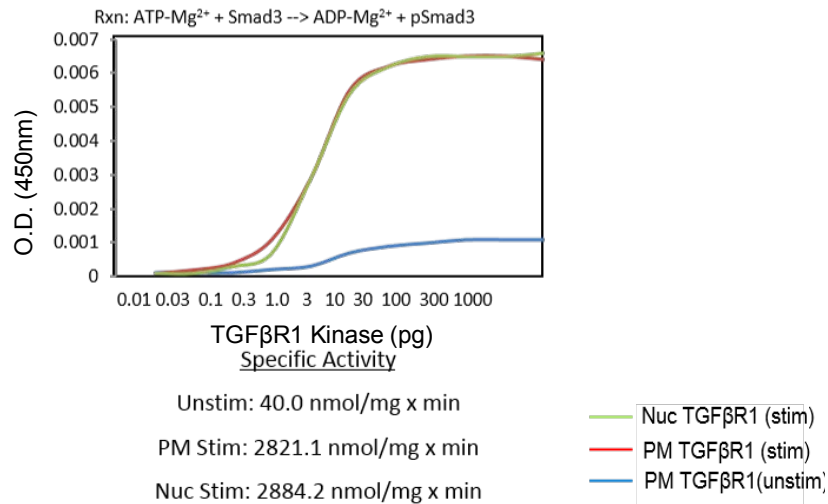


Figure 7.3 TGFβ1 kinase activity is intact in the nucleus. Cos7 cells transiently expressing both HA-TGFβR2 and Myc-TGFβR1 were stimulated (Stim) or unstimulated (UnStim) with TGFβ for 20 minutes prior to purification of plasma membrane fractions and isolation of non-denatured TGFβR1. Parallel samples were stimulated with TGFβ for 6 hours and nuclear extracts isolated and non-denatured TGFβR1 purified. (NB: no TGFβR1 could be detected in nuclear fraction without TGFβ stimulation). Specific activity of the various TGFβR1 samples was determined for Smad3 as described with no significant difference between stimulated receptors from the nucleus (2884.2 nmol/mg x min) or plasma membrane (2821.1 nmol/mg x min) compared to unstimulated receptors (40.0 nmol/mg x min) for Smad3.

7.3.3 TGFβ1 phosphorylates ATF-CREB Transcription Factors *in vitro*

Because both ATF2 and CREB have documented roles in propagating the TGFβ signal, are localized in the nucleus, and are reported to be phosphorylated by unknown kinases in response to TGFβ, we sought to determine if either of the TGFβ receptors play any role in the phosphorylation of any recognized transcription factors implicated in TGFβ signaling using *in vitro* kinase assays. We confirmed that TGFβR1 (and not TGFβR2) could phosphorylate ATF2 and CREB while no phosphorylation of Elk1 or c-Fos (two other transcription factors recognized as important in TGFβ signalling) was observed (Fig 7.4A). A Di-lysine mutant TGFβR1, although unable to be trafficked to the nucleus *in vivo* (Fig 5.15) maintained the ability to phosphorylate CREB and ATF2 when incubated together *in vitro* (Fig 7.4A). Furthermore, just as was observed with Smad3 as a substrate (Fig 7.3) TGFβR1 derived from the plasma membrane or the nucleus from stimulated cells showed comparable specific activity for phosphorylating ATF2 (Fig 7.4B). TGFβR2 did not lose kinase activity during purification as it was able to phosphorylate a GST-bound intracellular domain of TGFβR1 (ΔT1R).

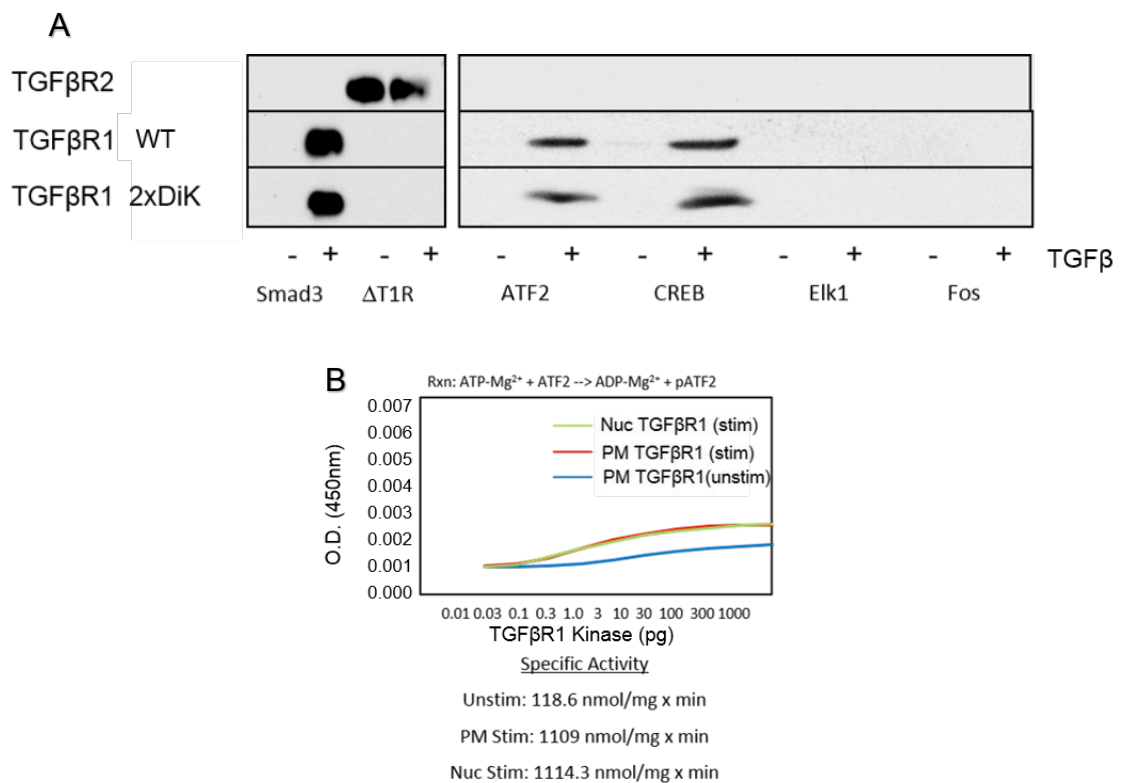


Figure 7.4 TGFβR1 kinase activity is intact in the nucleus and is able to phosphorylate ATF/CREB family member transcription factors. (A) Immunopurified TGFβR2, wild type TGFβR1 (TGFβR1_{WT}), or TGFβR1 double di-Lysine mutant (TGFβR1_{2xDiK}) from either unstimulated (-) or TGFβ stimulated (+) transfected Cos7 cells, were incubated in the presence of 5 μM ATP, 0.5 μCi γATP [³²P], MgCl₂ and GST-Smad3, -ΔT1R (intracellular domain of TGFβR1), ATF2, CREB, Elk1 or Fos for 30 minutes at 37°C, and visualized by autoradiography for incorporation of ³²P into the substrate. (B) Cos7 cells transiently expressing both TGFβ receptors were stimulated (Stim) or unstimulated (UnStim) with TGFβ for 20 minutes prior to purification of plasma membrane fractions and isolation of non-denatured TGFβR1. Parallel samples were stimulated with TGFβ for 6 hours and nuclear extracts isolated and non-denatured TGFβR1 purified. (NB: no TGFβR1 could be detected in nuclear fraction without TGFβ stimulation). Specific activity of the various TGFβR1 samples was determined for ATF2 with no significant difference between stimulated receptors from the nucleus (1114.3 nmol/mg x min) or plasma membrane (1109 nmol/mg x min) compared to unstimulated receptors (118.6 nmol/mg x min).

7.3.4 Nuclear delivery of activated TGFβR1 is required for the phosphorylation and increased P300 binding of ATF-CREB Transcription Factors in response to TGFβ

P300 association with CREB, ATF2 and other transcription factors correlates with increased gene transcription by recruitment of the transcription machinery, and is regularly associated with an increase in transcription factor phosphorylation (Rogge 2010). As published (Topper 1998, Kang 2003, Warner 2004), TGFβ stimulation resulted in marked increase in phosphorylation of ATF2 and CREB that corresponded with an increased association with P300 (Fig 7.5A - Left 2 lanes). Yet despite having the ability to phosphorylate ATF2 and CREB when combined *in vitro* (Fig 7.4A), cells

expressing the nuclear-trafficking mutant (2xDiK) TGF β R1 showed no increase in ATF2 or CREB phosphorylation or P300 binding upon TGF β stimulation (Fig 7.5A - Right 2 lanes). At least two possible explanations exist. Firstly, 2xDiK receptors, while being able to be activated at the cell surface, may not be able to endocytose and stimulate signalling of any downstream factors *in vivo*. Secondly, the receptors are functional and simply unable to traffic into the nucleus to access the potential nuclear substrates. A blockage of 2xDiK receptors was observed (Fig 6.15) supporting the hypothesis that nuclear exclusion of TGF β R1 was responsible for the lack of increased phosphorylation of ATF2 and CREB and P300 association. Furthermore, no differences in the ability of TGF β to phosphorylate Smad2 or Smad3 (Fig. 7.5B), the ability of pSmad2/3 to enter the nucleus (Fig 7.5C) or bind Smad-Binding Elements in DNA (Fig 7.5D) was observed with the 2xDiK mutant, arguing against 2xDiK receptors having a general signalling defect. No changes in phosphorylation, or P300 association, were observed in other transcription factors Elk1, E2F4 or c-Fos (Fig 7.5A).

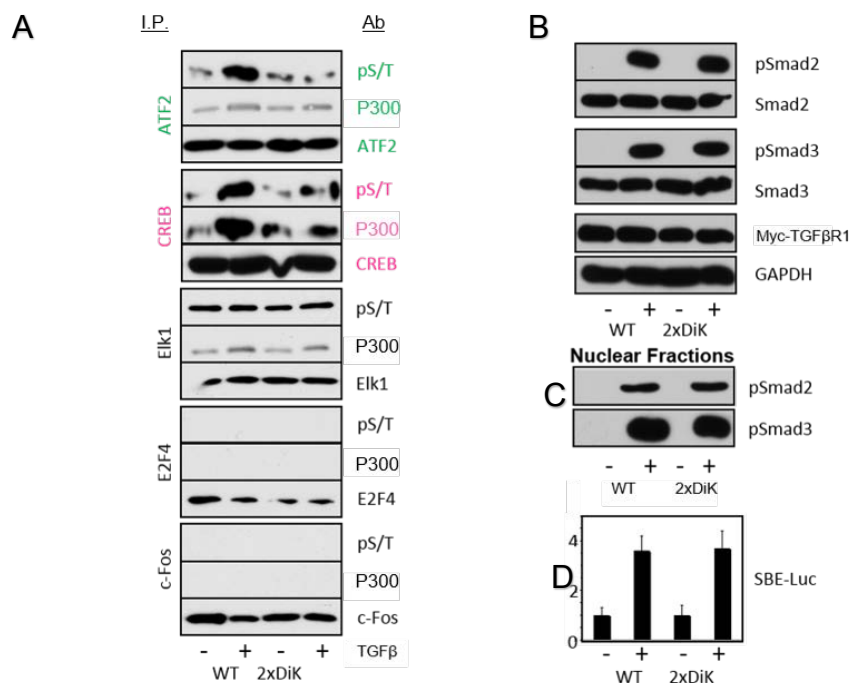


Figure 7.5 Nuclear TGF β R1 is required for phosphorylation of ATF/CREB but not Smad2 signalling in vivo. (A) Mv1Lu cells expressing TGF β R2 plus wild type myc-TGF β R1 or double Di-Lysine mutant myc-TGF β R1 were stimulated for 8 hours in the presence (+) or absence (-) of TGF β . Lysed cells were immunoprecipitated for ATF2, CREB, Elk1, E2F4 or c-Fos with each subjected to Western analysis for pS/T (pan-phospho-serine/threonine), P300 association, and the corresponding transcription factor to ensure robust immunoprecipitation. (B) Concurrently, cells were treated for only 30 minutes and accessed for TGF β -induced phosphorylation of Smad2 and Smad3 as well as total expression levels of Smad2, Smad3, myc-TGF β R1 and GAPDH. (C) Simultaneous with whole cell lysates being examined, nuclear fractions were prepared and examined for the presence of pSmad2 and pSmad3. (D) Cells were treated as above, with additional expression of a plasmid carrying 7 copies of the Smad-Binding element (SBE) driving luciferase expression. After 24 hours stimulation with TGF β , cells were normalized for protein and transfection efficiency and luciferase activity determined.

7.3.5 Nuclear delivery of active TGF β R1 is required for activation of a subset of TGF β responsive genes

A role for ATF2 and CREB is recognized in a number of TGF β regulated genes (Topper 1998, Kang 2003, Warner 2004), suggesting they play an accessory role with the Smads. Cells expressing a nuclear-trafficking deficient 2xDiK TGF β R1 were compared to those expressing the wild type TGF β R1 in regards to three Smad/CREB genes (PAI-1, CTGF and eNos), three Smad/ATF2 genes (CRP2, TGF β 3 and ATF3) and three Smad/E2F4 genes (CDC25A, Myb and TP53). In each of the Smad/CREB and Smad/ATF2 genes the induction by TGF β was significantly reduced when the TGF β R1 nuclear-trafficking mutant was expressed (Fig 7.6A). No difference in the response to TGF β could be observed between wild type and mutant receptors in any of the Smad/E2F4 genes (Fig 7.6A).

Smad/CREB and Smad/ATF2 induction in cells expressing a nuclear-trafficking deficient TGF β R1 was restored by co-expressing constitutively active mutants of CREB (CREB_{S133D}) and ATF2 (ATF2_{S155D}) that bare serine to aspartate mutations that mimic phosphorylation at serine residues reported to regulate transcriptional activity (Kang 2010, Fell 2012) while there was no observable impact on Smad/E2F4 genes (Fig 7.6B). The importance of regulating ATF2/CREB phosphorylation is evidenced by significant increases in basal induction in both TGF β stimulated and unstimulated cultures. Interestingly, treating these cells with Ginkgolic acid (which allows TGF β receptor nuclear entry but prevents formation of PML bodies, see Fig 6.18) had only a mild impact (Fig 7.6B), suggesting receptor aggregation into PML bodies may not be necessary for transcription factor phosphorylation and subsequent gene induction.

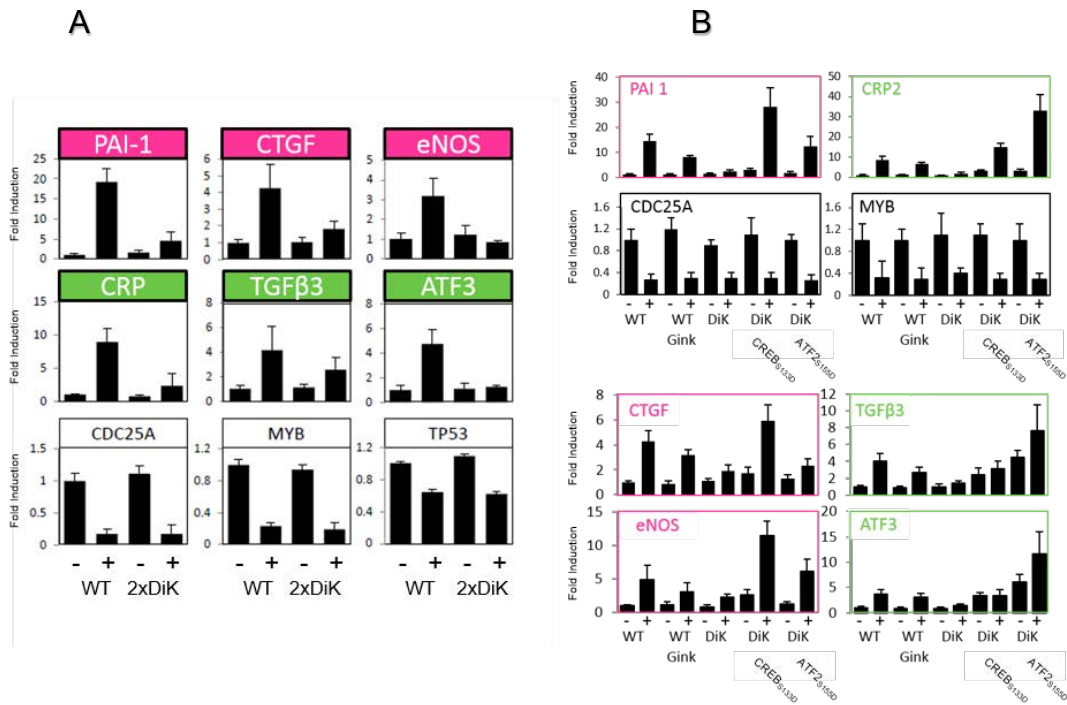


Figure 7.6 Nuclear TGFβR1 phosphorylation of ATF/CREB is required for full induction of subset of TGFβ regulated genes. (A) Mv1Lu cells expressing TGFβR2 and either wild type myc-TGFβR1 (TGFβR1_{WT}) or myc-TGFβR1 double Di-Lysine mutant (TGFβR1_{2xDiK}) were stimulated in the presence of TGFβ for 16-24 hours and RNA collected. Reverse transcribed cDNA was processed by qRT-PCR examining gene products for three TGFβ induced genes with known CREB contributions (PAI1, CTGF and eNOS), three TGFβ induced genes with known ATF2 contributions (CRP2, TGFβ3 and ATF3) and three TGFβ repressed genes with known E2F4 contributions (CDC25, MYB and TP53). (B) Wild type or double Di-Lysine mutant of TGFβR1 (TGFβR1_{WT} or TGFβR1_{2xDiK} respectively) and/or CREBS_{133D} or ATF2_{S155D}, were introduced into Mv1Lu cells expressing TGFβR2. Cells were cultured in the presence or absence of TGFβ and/or Ginkgolic acid for 16-24 hours and PAI1, CTGF, eNOS, CRP2, TGFβ3, ATF3, CDC25 and MYB gene induction determined by qRT-PCR.

7.3.6 Cross talk between nuclear receptors and Smads in gene regulation

While there is clearly a requirement for nuclear receptor kinase activity in the induction of these genes, it has long been established that Smad binding to these promoters is also essential (Massagué 2005), suggesting cross talk between Smads and nuclear TGFβR1-phosphorylated transcription factors. One possible mechanism of cross talk centres around the enzymatic function of phosphorylated ATF-CREB; histone acetylation. ATF-CREB transcription factors can be phosphorylated at numerous residues and only some have been shown to induce histone acetyltransferase (HAT) activity (Kang 2010, Fell 2012). To investigate if TGFβR1-mediated phosphorylation caused an increase in HAT activity we first purified activated TGFβR1 and mixed a number of known TGFβ associated transcription factors in conditions that would

promote phosphorylation. As seen in Figure 7.4 we again saw ATF2 and CREB were phosphorylated but also SP1 (Fig 7.7A). After exposure to activated TGF β R1 the *in vitro* HAT activity of these transcription factors was determined with a marked increase in HAT activity of those transcription factors that were phosphorylated (Fig 7.7B).

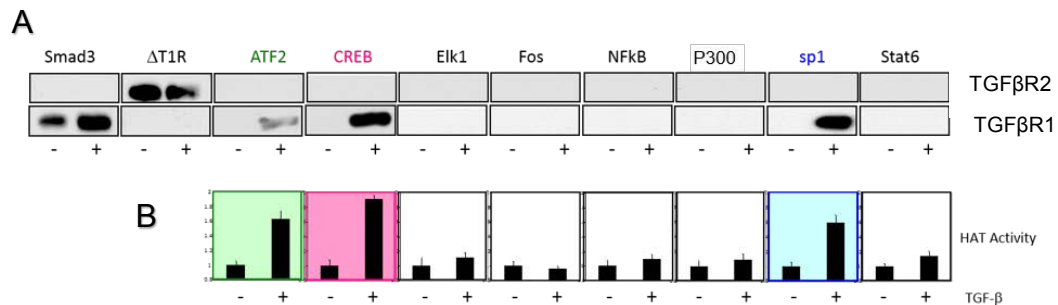


Figure 7.7 Activated TGF β R1 phosphorylates and increases Histone Acetyltransferase (HAT) activity of ATF2, CREB and AP1. (A) Type I and Type II receptors were purified from unstimulated or stimulated cos7 cells that had been transfected with TGF β receptors and mixed with indicated potential substrates in kinase-permissive conditions in the presence of 32 P-labelled ATP. (B) After being subjected to *in vitro* kinase assay, substrates were purified and *in vitro* Histone Acetyltransferase activity of the indicated substrates was assessed.

Regulation of chromatin between heterochromatin and euchromatin is mediated in part by acetylation of the histones themselves. Acetyltransferases add acetyl groups which loosen heterochromatin to euchromatin, and deacetylases (HDACs) remove them to tightly pack things up again (Hayashi 2014). Many transcription factors possess their own intrinsic histone acetyltransferase activity that can be increased by phosphorylation or other post-translational modifications, including ATF2 and CREB (Hayashi 2014).

We report that nuclear TGF β R1 phosphorylates ATF2 and CREB (Figs 7.4, 7.5 and 7.7A) that causes an increase in HAT activity (Fig 7.7B), but ATF-CREB transcription factors bind a diverse subset of all promoters with as many as a third of promoters targeted by an active CREB that binds chromatin only when phosphorylated (Rogge 2010). While we suggest nuclear receptors can mediate this phosphorylation (see Fig 7.4-5), TGF β stimulation does not cause upregulation of all the genes of which phosphorylated ATF-CREB transcription factors bind to the promoters (Fig 7.8). When CREB/pCREB chromatin immunoprecipitation array data (Rogge 2010) is aligned with gene array data examining TGF β -mediated gene modulation (Koinuma 2009) it

becomes clear the vast majority of CREB bound genes are not impacted by TGF β (Fig 7.8). Interestingly, CREB only binds DNA when phosphorylated (Fig 7.8). This raises the question of why some genes with ATF-CREB elements in their promoter are modulated, and some are not. Alignment of chromatin immunoprecipitation array data examining Smad binding (Koinuma 2009) with array data examining ATF-CREB binding (Rogge 2010) and TGF β gene induction (Koinuma 2009) reveals that of all the gene promoters ATF-CREB bind, only those that are also bound by Smads are modulated in response to TGF β , without exception (see Fig 7.8).

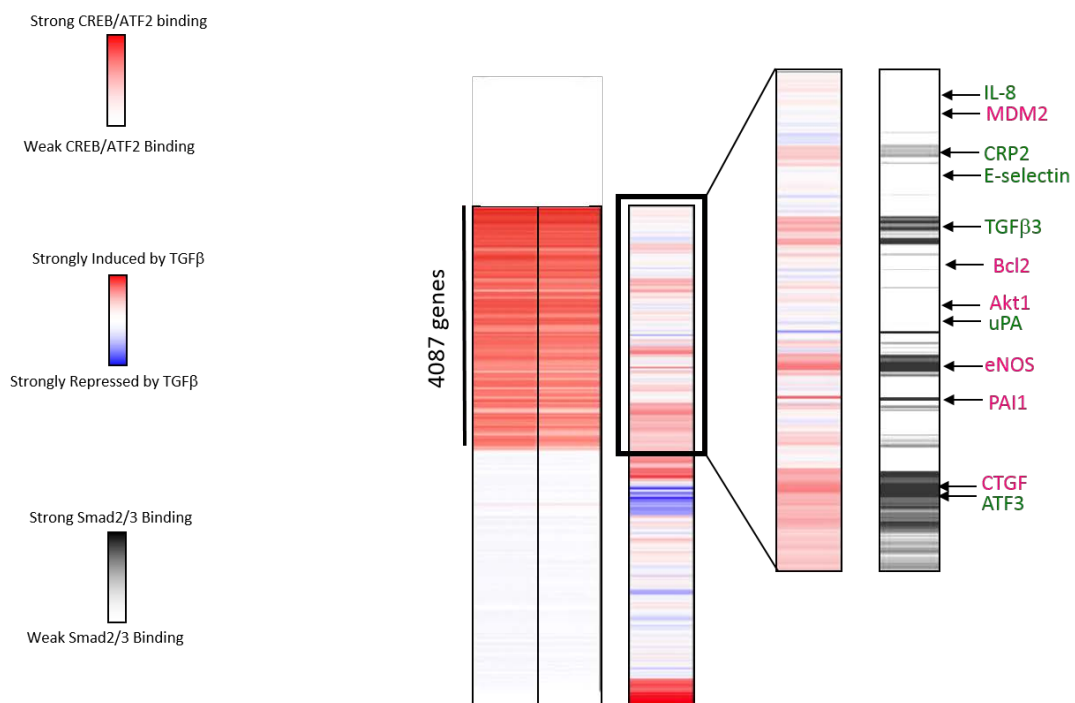


Figure 7.8. Of promoters bound by CREB, only those additionally bound by Smads are induced by TGF β . (Left) False colour images comparing ChIP on chip analysis of CREB and pCREB chromatin binding to DNA microarray gene induction analysis. (Right) Of CREB-binding promoters, TGF β gene induction is compared to ChIP on chip analysis of Smad3 binding after TGF β stimulation. Arrows indicate promoter/gene sequences associated with ATF2 (green) and CREB (pink) regulated genes.

Examination comparing the promoter sequences of induced genes with uninduced genes reveals a clear pattern. In induced gene promoters (regulated by ATF-CREB), there are clusters of Smad Binding Elements closely surrounding ATF-CREB binding elements (see Fig 7.9). Only a subset of TGF β induced genes are regulated by ATF-CREB and manual inspection of individual sequences revealed that even those that showed a pronounced impact of ATF-CREB on their induction still had some Smad Binding Elements that weren't contained in close proximity to ATF-CREB binding

elements. The number of these ATF-CREB independent Smad Binding Elements inversely correlated with the extent nuclear receptor phosphorylation of ATF-CREB impacted TGF β -mediated induction. Certainly, many of these Smad Binding Elements (even in genes not impacted by ATF-CREB or nuclear receptors) were clustered around binding elements for other transcription factors (data not shown).



Figure 7.9 Multiple Smad Binding Elements are clustered around CREB binding elements in PAI-1 promoter. The Promoter of mouse PAI1 gene with CREB binding element consensus sequences highlighted in enlarged dark blue, while Smad binding element consensus sequences are highlighted in orange.

One possible model that incorporates these findings suggests that phosphorylated ATF2 and CREB (phosphorylated by nuclear TGF β R1) has increased HAT activity and acetylates histones in gene promoters containing ATF-CREB binding elements, loosening the chromatin. Of these promoters, a number contain Smad Binding Elements that have become exposed surrounding the sites of ATF-CREB binding, and can be bound by phosphorylated, nuclear Smads. In support of this model, chromatin immunoprecipitation experiments confirm the level of Smad3 binding to ATF2 and CREB gene promoters is drastically reduced in cells expressing TGF β receptors that fail to translocate to the nucleus, and subsequently fail to phosphorylate and activate the HAT activities and DNA binding potential of ATF2 and CREB (Fig 7.10).

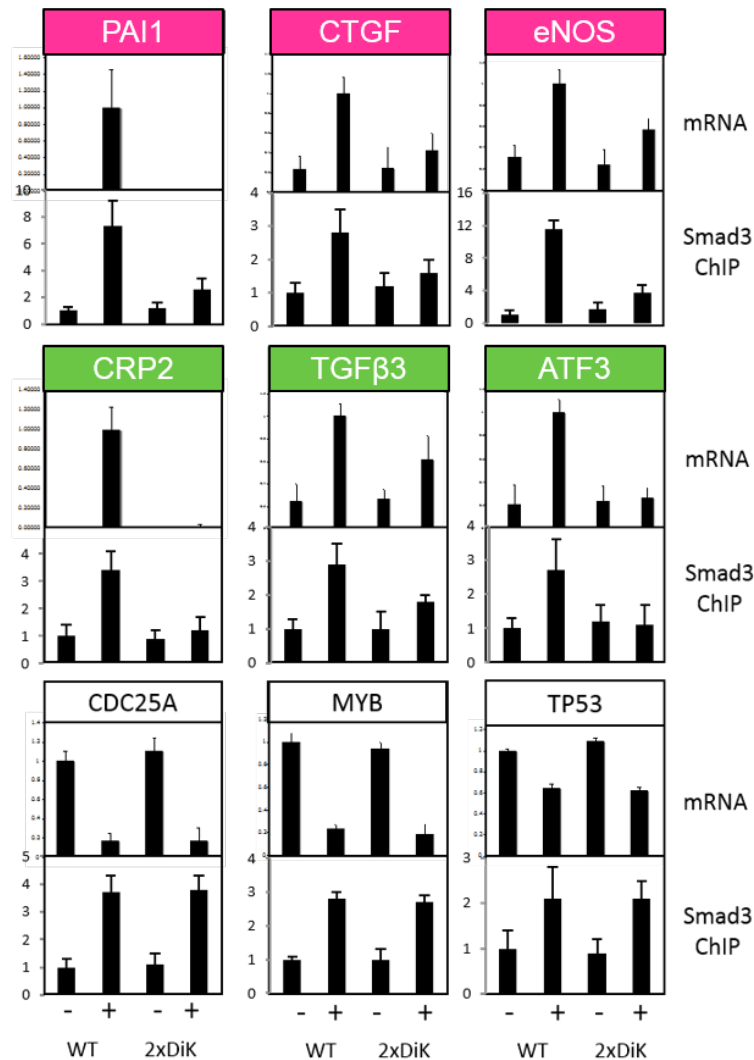


Figure 7.10 Correlation between gene induction and presence of Smad3 on promoters in the presence and absence of nuclear TGFβ Receptors. Mv1Lu epithelial cells expressing either wild type TGFβR1 (WT) or mutant TGFβR1 unable to traffic to the nucleus (2xDiK) were unstimulated or stimulated with TGFβ for 24 hours. Lysates were subjected to qRT-PCR directly (top panels) or chromatin Immunoprecipitation with Smad3 prior to qRT-PCR (bottom panels) examining recognized TGFβ-responsive genes. PAI1, CTGF and eNOS require CREB, ATF3, TGFβ3 and CRP2 require ATF2 and CDC25A, MYB and TP53 require ETF4A for full responsiveness to TGFβ.

7.4 DISCUSSION

TGFβR2 is a constitutively active kinase, the activity of which is essential for clathrin-mediated endocytosis of the receptors (Anders 1998) and being that clathrin-mediated endocytosis is the first step in delivering TGFβ receptors to the nucleus (Fig 6.6), it was not surprising the kinase activity of TGFβR2 was required for Golgi, ER and subsequent nuclear delivery of the TGFβ receptors (Fig 7.2). The kinase activity of

TGF β R1 was not required for nuclear delivery (Fig 7.2). However, while not required for nuclear delivery, the kinase activity of TGF β R1 was not attenuated during delivery of TGF β receptors from the plasma membrane, through the Golgi and ER, to the nucleus with receptors purified from the plasma membrane and the nucleus having no detectable difference in their ability to phosphorylate either Smad3 or ATF2 (Figs 7.3 and 7.4B).

In our studies, surface-derived TGF β R1 did not directly bind chromatin (Fig 6.17), suggesting any nuclear impact is not through the action of the receptors as transcription factors *per se*. This contrasts with EGFR which binds DNA directly upon nuclear entry, and influences gene expression of a number of genes, including Cyclin D (Hong 2011). Chandra and colleagues similarly observed full length TGF β R1 in the nucleus had no DNA binding, but report robust interaction with RNA containing the consensus sequence AGGAGGAG (Chandra 2012). However, binding to the TGF β R1 promoter by a cleaved form of TGF β R1 has also been reported in transformed but not untransformed cell lines (Gudey 2014) collectively suggesting nuclear TGF β receptors may potentially impact signalling through various mechanisms in different cellular conditions.

Although the impacts of inhibiting nuclear entry of TGF β receptors on TGF β -induced gene modulation has not been performed at the genome-wide level, we have investigated the role of nuclear TGF β receptors on select TGF β -induced genes. Our observations clearly indicate exclusion of TGF β receptors from the nucleus has significant impacts on a subset of TGF β -induced genes, while having no impact on others (Fig 7.6).

Transcriptional regulation by Smad proteins requires interactions with various other factors and Smad Binding Elements confer very limited transcriptional modulation in isolation (Seoane 2004). Smad interactions with numerous transcription factors have been documented, including some that have been reported as being phosphorylated in response to TGF β (Jungert 2006, Poncelet and Schnaper 2001, Ellenrieder 2008). The kinases responsible for phosphorylating these nuclear transcription factors were unknown, allowing us to speculate about a potential role for nuclear TGF β receptors as candidate kinases. We report nuclear TGF β R1 phosphorylates CREB, ATF2 and Sp1

both *in vitro* and *in vivo*, while not recognizing E2F4, Elk1, Fos, NFκB, P300 or Stat6 as substrates (Figs 7.4-7). Admittedly, our screen of phosphorylated transcription factors was limited to those reported to be involved in TGFβ signalling, but of those we found to be nuclear receptors substrates, all have been documented as Smad binding partners (Kang 2003, Topper 1998, Warner 2004).

At a gene expression level, genes that were induced by TGFβ with a reported requirement for CREB and ATF2, showed significantly reduced induction when the nuclear trafficking of TGFβ receptors was inhibited (Fig 7.6). This suggests phosphorylation of the transcription factors by nuclear TGFβR1 directly impacts their transcriptional activity. Evidence to support the role of phosphorylation of ATF2 and/or CREB (and not another indirect consequence downstream of TGFβ receptor nuclear localization) as being the critical mechanism in facilitating induction of the associated genes is through the ability of ATF2 and CREB proteins bearing mutations that mimic the phosphorylated forms to rescue of gene induction of ATF2 and CREB dependent genes in cells where TGFβ receptor nuclear trafficking is inhibited (Fig 7.6B).

Indeed, phosphorylation of the ATF2 and CREB by TGFβR1 caused an increase in P300 binding (Fig 7.5) and histone acetylation transferase (HAT) activity (Fig 7.7) yet this did not transfer to a genome-wide induction of ATF-CREB genes (Fig 7.8). Further examination, by alignment of genome-wide chromatin immunoprecipitation arrays of both Smad and ATF-CREB with genome-wide gene array data after TGFβ stimulation, indicated that only those ATF-CREB gene promoters that also shared Smad Binding Elements were induced in response to TGFβ (Fig 7.8). Interestingly, the majority TGFβ-induced gene promoters have several Smad Binding Elements clustered around binding sites for other transcription factors (as seen in Fig 7.9), not just ATF2 and CREB. How the binding of other transcription factors to these promoters is unknown, but we propose nuclear TGFβR1 phosphorylates ATF2 and CREB, which leads to an increase in P300 binding and HAT activity. When these activated transcription factors acetylate histones in the chromatin, Smad Binding Elements are exposed and are quickly occupied by phosphorylated Smad complexes, leading to full induction in response to TGFβ (presented diagrammatically in Fig 7.11).

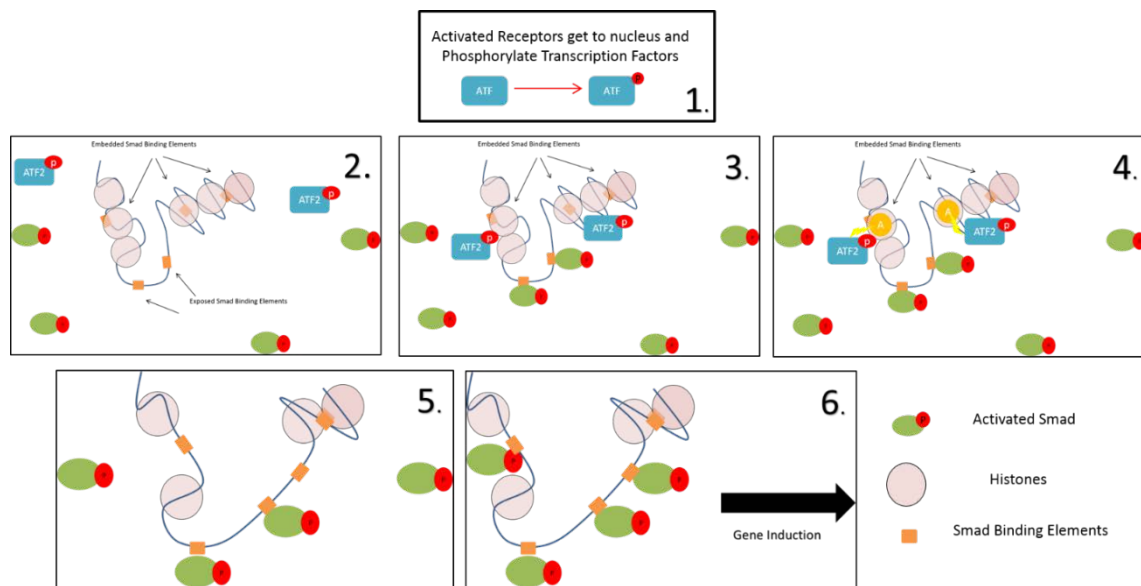


Figure 7.11 Model of proposed mechanism of nuclear receptor crosstalk with Smads at the promoter level. (1) Once the receptors enter the nucleus they can phosphorylate transcription factors such as ATF2 that enhances histone acetyltransferase activity. (2) Phosphorylated Smads are already in the nucleus and able to bind exposed Smad Binding Elements. (3) Phosphorylated transcription factors recognize histones surrounding their binding sites. (4) Histones around consensus binding sites are acetylated leading to (5) unwinding of the heterochromatin and exposing new Smad Binding Elements. (6) Newly exposed Smad binding Elements are bound by phosphorylated Smads and full gene induction follows.

While the preliminary data presented supports this model (Fig 7.11) much work remains to fully validate it and there are a number of complications that need to be addressed. A large problem stems from the complexity of many gene promoters. Most promoters are regulated by numerous transcription factors and can possess multiple consensus sequences to facilitate binding. A promoter with three CREB binding sites might also possess SP1, ETF2, and Elk binding sites each contributing some degree of regulation over the gene. While this offers infinite degrees of regulation for the cell to respond to external stimuli, it makes determining broad regulatory roles for individual transcription factors quite challenging. Comprehensive, genome wide chromatin immunoprecipitation mapping of numerous transcription factors in response to TGF β with nuclear trafficking of receptors blocked, would be required for a thorough understanding at a genome wide level.

A more attainable goal in the short term would be to focus on individual genes that are induced by TGF β and are impacted by nuclear receptors. The gene of interest may be associated with a particular clinically or biologically relevant phenotype. One such set of relevant genes are classical EMT markers E-cadherin and Vimentin. TGF β induces EMT in select epithelial lines and in doing so E-cadherin (an epithelial marker) expression is lost and Vimentin (a mesenchymal marker) levels are gained. Smads and the transcription factor SP1 have been strongly implicated in these events and because SP1 was another transcription we found to be phosphorylated (and gained HAT activity) by nuclear TGF β R1 phosphorylation, we believe both of these promoters are likely candidates for a similar regulation as described above. However, in a twist of the theme, it's not the Vimentin and E-cadherin promoters themselves that are being impacted by phosphorylated SP1, but instead the genes twist, snail and slug. It appears the nuclear receptors play a role in the induction of these three related genes which then serve as transcriptional master regulators of Vimentin, E-cadherin and a host of other EMT-related genes.

Because our ability to make accurate, broad conclusions on the role of TGF β receptors in the nucleus is dependent on examination of every gene regulated by TGF β in all cell types in diseased and normal conditions, it will take some time for a thorough understanding. Our initial examination of a small subset of TGF β -modulated genes provides a degree of insight, but no doubt our understanding will greatly improve as the impact nuclear TGF β receptors have on more and more genes is examined. While we have focused our investigations on the kinase activity of the receptors, others have found a role of nuclear receptors in binding and regulating RNA (Chandra 2012) and although we find no evidence to support direct association of receptors with DNA, a more comprehensive investigation may yet uncover cellular conditions that support it. This study has shed light on a mechanism of TGF β signal regulation previously unknown, and opens a whole new avenue of questioning, the answers to which have the potential to provide significant clinical and intellectual insight.

The central dogma of TGF β signalling is that Smad2 and Smad3 are central. However Smads are phosphorylated in all cell types in which receptors are expressed (Massagué 2005) and both bind the same consensus sequence in the DNA (Massagué 2005). So how can TGF β exert such a myriad of responses in different cell types and during different stages of their development? The presence of TGF β R1 in the nucleus

has been reported to be elevated in numerous cancer cell lines (Mu 2011, Chandra 2012) and perhaps this increase in active receptors in the nucleus leads to increased HAT activity in CREB, ATF2, sp1 and other transcription factors. The increase in HAT activity may lead to chromatin rearrangements in proximity of the transcription factor binding sites that may expose SBE elements that would have been otherwise masked (see Fig 7.9). Our data would support such a model as smad binding at the promoters of CREB, ATF2 and sp1-dependent genes is significantly reduced in the absence of nuclear receptor-induced transcription factor phosphorylation (Fig 7.7). Our studies were unable to demonstrate any differences in the levels of nuclear receptors between cancerous and healthy cell lines (Fig 6.4).

However, while we document a role for nuclear TGF β R1 as a kinase for these transcription factors, certainly other environmental cues could lead to phosphorylation of ATF-CREB, or any number of other histone acetyltransferases or deacetyltransferases that could modulate the chromatin to expose or conceal Smad Binding Elements. The destiny of Smad DNA binding more dependent on cellular impacts on chromatin arrangements than a pre-programmed message initiated by the ligand. In this way the response to TGF β the ligand is very much adapted to the cell that is exposed to it.

Indeed a more comprehensive screen of nuclear proteins that could be phosphorylated by an activated TGF β R1 in the nucleus may reveal other unknown aspects of TGF β signalling. Furthermore, while TGF β R2 is a constitutive kinase and is considered unmodulated by the addition of ligand, it is omitted from the nucleus in an unstimulated state. Perhaps the nucleus yields substrates to this kinase only once TGF β R2 is localized to the nucleus?

Furthermore, the activation of Smad2 and Smad3 occurs with both TGF β and Activin, yet cells respond differently to the two ligands. One possible explanation for this is that nuclear trafficking of TGF β receptors (and subsequent phosphorylation of transcription factors) leads to chromatin rearrangements exposing a different subset of Smad Binding Elements for the phosphorylated Smads. In this way an overlapping but somewhat different profile of genes would be induced, which is indeed what is observed. If this is indeed the case remains to be examined experimentally.

Interestingly, the inhibition of PML body formation with Ginkgolic acid resulted in only mild diminution of genes influenced by nuclear TGF β R1 (Fig. 7.5), suggesting PML bodies are not essential for transcription factor phosphorylation and substantial signalling can occur from within the inner nuclear membrane. Without a doubt, uncovering the details of what nuclear receptors are doing and how their trafficking is regulated will shed insight into the greater TGF β picture and hopefully provide opportunities to exploit in developing therapies for treatment of the many TGF β -driven diseases.

CHAPTER 8

GENERAL DISCUSSION

CHAPTER 8: GENERAL DISCUSSION

The four studies presented in this dissertation are united by a common thread. Each is an example of how the TGF β signal is actively regulated at the level of nuclear import. Because many of the factors involved in nuclear import are shared by many other signalling pathways they provide ideal platforms to provide cross talk to TGF β signals, allowing fine tuning of the signal to take into account cell context and other cellular stimuli. As the concepts of tumour microenvironment and epigenetics begin to influence our thoughts on all aspects of molecular biology, so too our view that individual ligands do not deliver a fixed message, but rather deliver specific messages to different cells, differing in type, space and time.

TGF β has long been known to cause dramatically different cellular responses depending on the cell type it is stimulating (Shi 2003) and our understanding of the factors determining these differences remain incomplete. Cell type specific activation of unique signalling and trafficking moieties almost certainly play some role in mediating these pleotropic effects, but more likely, small modifications within the basic framework of receptor and Smad signalling and transcription factor coupling provide a malleable framework within which, evolution can fine tune incrementally to adapt to the specific needs of each cell type. Simply determining IF TGF β activation is occurring in a disease process is likely to have limited value in informing the pathways controlling disease. Significant effort has been spent using genetic and biochemical approaches to compare expression levels of TGF β receptors and Smad proteins and to compare the extent of Smad phosphorylation between healthy and diseased states with limited clinical application. Smad4 and TGF β R2 mutations do occur with some frequency in cancers (particularly colon cancer) but mutations in other TGF β signalling mediators are rare (Fleming 2013) and significant correlates of disease or poor prognosis have not been identified (Piek 1999). The mechanisms that regulate and balance the various components of the TGF β pathway potentially hold the key to meaningful understanding of HOW the TGF β message is signalling in healthy and diseased cells and will provide insight into therapeutic approaches to manipulate these imbalances and engineer a favourable outcome for patients. It is our contention that one such regulatory checkpoint is nuclear entry of TGF β receptors.

TGF β signalling molecules as therapeutic targets

Both the beneficial and detrimental outcomes of TGF β signals are initiated by Smad2 and Smad3 phosphorylation by TGF β receptors. TGF β receptors cannot differentiate Smad2 from Smad3 and therefore phosphorylation of one Smad from the other by the TGF β receptors CANNOT be uncoupled. Furthermore preventing one Smad or the other from binding Smad Binding Elements (SBEs) in the nucleus is not possible as each forms heteromers with Smad4 and binding to the SBE can occur through any of the Smads in the complex. Hence, if we seek to impact the downstream effects of either Smad over the other our only option is to prevent the nuclear entry of one Smad over the other. The nuclear pore Importin- β is essential for all phosphorylated and unphosphorylated Smads to enter the nucleus (Figs 4.14 and 4.15) making it a poor choice as an inhibitory target. We showed that Importin8 was required for phosphorylated Smad3 nuclear entry but did not impact unphosphorylated Smad3 or both forms of Smad2 (Figs 4.13 and 4.14). However because Importin8 has roles not exclusively restricted to pSmad3 nuclear entry, targeting its function or expression would certainly have off-target effects. In TGF β signalling SNX9 plays a similar role as the importins by facilitating rapid targeting of pSmad3 to the nuclear pore and similarly, targeting SNX9 expression has limited potential as a therapy due to essential roles at the plasma membrane in endocytosis (Childress 2006, Lundmark 2009).

Because all of the individual components discussed above are involved in numerous essential functions independent of TGF β signalling targeting their expression is not a viable therapeutic option but approaches designed to antagonise the interactions between particular components (i.e. between pSmad3 and SNX9 or pSmad3/SNX9 and Imp8) is more likely to specifically target the role these proteins play in TGF β signalling without disrupting other vital cellular roles. The binding of SNX9 to phosphorylated Smad3 can only occur in the context of TGF β signalling (NB: Smad3 is only phosphorylated when cells are stimulated with TGF β) so targeted disruption of pSmad3 binding to SNX9 should lead to a decrease of pSmad3 entering the nucleus, while maintaining the fibrosis- and tumour-suppressive/homeostatic effects of pSmad2 signalling.

One approach to prevent/reduce the interaction between SNX9 and pSmad3 would be by using an antagonist: the ultimate goal being to design a small peptide inhibitor to

antagonize SNX9/pSmad3 interactions in patients with fibrosis and cancer. This could be achieved by generating compounds to either mimic/outcompete the region of SNX9 that associates with pSmad3, or compounds that mimic/outcompete the region of pSmad3 that associates with SNX9. In Chapter 4 we identified the region in SNX9 required for association with pSmad3 (12-20 amino acids towards the amino end of the protein within the SH3 domain). Utilizing the TAT delivery method for introducing peptides made up of this short region of SNX9 directly into cells (Chapter 4) would determine if the presence of such a peptide could outcompete for binding to pSmad3 with endogenous SNX9 and inhibit downstream pSmad3 events. Optimization of peptide length and determining of the exact sequence required for maximal inhibition would be necessary and studies using TGF β /pSmad3-driven disease models in animal models would further test efficacy and provide proof of concept for clinical trials.

SNX9 recognition of pSmad3 for nuclear delivery

There has been considerable controversy and debate as to whether Smad nuclear accumulation is due to increased nuclear trafficking *or* increased nuclear retention (reduced nuclear export). As this was relevant to our investigation of mechanisms controlling TGF β signals we sought to examine the role of SNX9 in Smad trafficking into the nucleus. While we fully acknowledge we have not examined Smad2, our results do not favour one side of the debate over the other. In fact, we observed an increased rate of phospho-Smad3 nuclear entry AND pronounced nuclear retention (Figs 4.7 and 4.8). While SNX9 dramatically impacts nuclear entry it has no impact on the kinetics of export, suggesting the two mechanisms are independent. In fact, even the pSmad3 that entered the cell in the absence of SNX9 was retained much longer than unphosphorylated Smad3. It is unclear why a cell would need two mechanisms to increase Smad accumulation. Perhaps they co-evolved or perhaps only one mechanism is specific to Smad3 and therefore able to regulate the Smad2/Smad3 balance? These questions are likely to be answered by further studies using strategies and tools similar to those presented in this study.

How SNX9 differentiates between phosphor-Smad2 and phosphor-Smad3 is perplexing. The region of Smad2 and Smad3 that is phosphorylated by the TGF β receptors is identical between the two proteins (Piek 1999) and the proteins share significant sequence homology, particularly in regions that associate with the receptors

and other Smads (Wrana 2013). When we examined the kinetics of pSmad3 nuclear entry following TGF β stimulation we unexpectedly showed that the peak nuclear import of pSmad3 in SNX9 wild type cells occurred approximately 30 minutes post stimulation whereas the peak nuclear import in SNX9 depleted cells (which was significantly reduced) occurred at 90 minutes (Figs 4.7 and 4.8). This peak at 90 minutes corresponded with the peak nuclear translocation of non-phosphorylated Smads. There are two possibilities to explain this result: (1) an experimental artefact due to incomplete ³²Phosphate labelling of Smad3 with unlabelled Smad3 comprising the second peak or; (2) there are two pools of pSmad3, differing in some way. The first possibility was excluded as we subsequently showed that Smad3 in the second peak retained ³²Phosphate counts suggesting two pools of pSmad3 exist within the cell.

Crystallography and energetic studies (Shi 1997, Wu 2001, Chacko 2004, Massagué 2005) indicate unphosphorylated R-Smads energetically favour monomers, while phosphorylated R-Smads can form homotrimers, heterotrimers (with a single Smad4), dimers or monomers. The favoured form is the trimer with the heterotrimer being somewhat favoured over the homotrimer. Perhaps the observed peak in the absence of SNX9 is a monomeric form of phospho-Smad3? If this is indeed the case, we should revise our view of SNX9 as having a preferential affinity for phosphorylated over non-phosphorylated Smad3, instead noting an affinity for trimeric rather than monomeric forms. More credence to this model comes from the fact that the phosphorylated residues of the pSmad3 molecules are embedded in the trimeric complex and not readily available for SNX9 binding (Chacko 2004). Size exclusion chromatography may offer one way to examine the specific complex composition associated with (or without) SNX9.

While this may indicate that SNX9 does NOT recognize the phosphorylated residues of pSmad3 to differentiate it from unphosphorylated Smad3, the question of why SNX9 does not associate with pSmad2 remains unresolved. There is experimental evidence supporting the concept that pSmad2 translocates to the nucleus faster than unphosphorylated Smad2 (Schmierer 2008) but to answer the question definitively would require an experiment similar to Figures 4.7 and 4.8 using phosphorylated and unphosphorylated Smad2-TAT rather than Smad3-TAT. Assuming there are differences, the next step would be identifying candidates involved in the process.

Because Smads crossing into the nucleus is a dynamic and rapid process, it is likely only a small percentage of pSmad2 will be bound to its nuclear trafficking partners at any given time. To screen for pSmad2 nuclear trafficking factors we could utilize the knowledge that Importin- β is required for nuclear import of both Smad2 and Smad3. Cell lines with Importin- β knocked down essentially trap Smads in the nuclear membrane, which SHOULD result in an enrichment of machinery involved in nuclear trafficking prior to Importin- β . Theoretically, purified nuclear membrane from cells stimulated with TGF β will provide a substantial yield of enriched pSmad2/nuclear trafficking partner complexes. Mass spectrometry analysis may identify unknown pSmad2 partners.

Do phosphoinositides in the nuclear membrane impact on SNX9 targeting and pSmad3 or TGF β signalling?

As unexpected as finding a role for SNX9 in differentially regulating Smad2 and Smad3 nuclear trafficking, was uncovering a role for SNX9 at the nuclear membrane. Previous reports indicate SNX9 is a soluble, cytosolic monomeric protein but exists as a homodimer with high specificity for the curvature of the plasma membrane and early endosomes (Worby 2002, Shin 2008, Yasar 2008, Lundmark 2009) with no reports of nuclear association. Our data indicated that SNX9 is not found as a homodimer at the nuclear membrane after TGF β stimulation (it was not found at the nuclear membrane at all in the absence of ligand). We propose the membrane seeking properties of the PX-BAR domain of SNX9 are engaged upon pSmad3 binding but the membrane specificity generated in homodimers to target to early endosomes and plasma membrane is lost when bound to pSmad3. Using an unknown mechanism pSmad3 binding redirects the SNX9 to the nuclear membrane, specifically to phosphoinositide-2-phosphate (PIP₂) embedded nuclear membrane. Whether other binding partners of SNX9 can redirect it to the nuclear membrane, or if SNX9 is involved in regulating nuclear transport of other molecules is currently unknown.

It has been reported extensively that phosphoinositides are excluded from the nuclear membrane. No phosphoinositide kinases have been identified that could generate these phospholipids in the nuclear membrane (Shah 2013) but accumulating evidence suggests that phosphoinositides can be found in the nuclear membrane, however their

source is unclear. The level of these phosphoinositides appears to be elevated substantially in many cancer cells (Fiume 2012, Shah 2013), low in normal cells, and virtually undetectable in stem cells and during early development (Fiume 2012).

As discussed previously there is growing evidence that TGF β -driven cancer and fibrosis can be considered an imbalance of pSmad2 and pSmad3 signalling, with a more pronounced pSmad3 response driving the disease as it overcomes the fibrosis and tumour suppressive action of pSmad2 (Feng 2005, Hoot 2008, Meng 2010). While our study indicates the role for SNX9 in facilitating pSmad3 nuclear entry is by bringing pSmad3 to the nuclear membrane by specifically binding to phosphoinositides, one question that arises is whether differing levels of phosphoinositides in the nuclear membrane has any impact on pSmad3 or TGF β signalling? One might predict that if nuclear membrane phosphoinositides were abundant (like in many cancer cells) pSmad3 signalling and resulting cell phenotypes and biology might be different than cells with lower nuclear membrane phosphoinositides. In contrast, during early development, Smad3 appears to play a distinctly limited role in TGF β signalling. Smad3 Null mice develop normally with a very mild phenotype whereas Smad2 Null mice are embryonically lethal (Feng 2005). During development, Smad2 seems to be most important, whereas Smad3 is the primary player in disease and tissue culture models. Could an absence of phosphoinositides in the nuclear membranes of cells during early development substantially favour pSmad2 signalling? This is an interesting possibility.

As discussed above understanding the subtle regulation mechanisms of TGF β signalling will likely provide more meaningful therapies than pan TGF β inhibitors. The balance between Smad2 and Smad3 signalling has significant impacts on homeostasis and disease. For example, blockage of all TGF β signalling may well alleviate Smad3-driven lung fibrosis (Yamamoto 1999, Santiago 2005), but without the protective Smad2 signal that accompanies it, wound healing or immune responses may well be disrupted leading to carcinogenesis or other disruptive complications (Hoot 2008, Meng 2010). The problem is not TGF β , but rather the way problematic cells are responding to it.

Phosphorylation and dephosphorylation of Smads by PAK2 determines nuclear retention

Like proteins flowing through any cellular compartment, the amount of the protein of interest contained within the compartment at any given time, is dependent on both the flow into, and the flow out of that compartment. Microscopy and fractionation experiments indicate TGF β stimulation results in virtually all cellular Smad2/3 amassing in the nucleus. While we document a role of SNX9 in increasing the rate in which Smad3 flows INTO the nucleus, we and others have also noted a reduction in the rate in which Smads flow OUT of the nucleus (Fig 4.7 and Schmierer and Hill 2005, Schmierer 2008).

SNX9 was found associated with the outer nuclear membrane and not complexed with pSmad3 at the nuclear pore or upon entry into the nucleus (Figs 4.18). While we propose no role for SNX9 in nuclear retention or export of Smads, any increase in the duration of “activated” (i.e. phosphorylated) Smads in the nucleus will clearly have an impact on the TGF β signal. Smad nuclear export is facilitated by RanBP1 that recognises dephosphorylated (or unphosphorylated) Smad2 and Smad3 and utilizes the hydrolysis of GTP of the small GTPase Ran (Dai 2009). RanBP1 is unable to recognize phosphorylated forms of Smad2 and Smad3, indicating the phosphorylation of these proteins is the marker for nuclear retention. Smad4 nuclear export is independent of Smad2/3 and is reliant upon CRM1 (Pierreux 2000), suggesting the Smads separate into monomers after dephosphorylation of Smad2/3 before export from the nucleus. A phosphatase found exclusively in the nucleus is responsible for dephosphorylating Smad2 and Smad3. PPM1A is expressed ubiquitously and its activity has not been reported to be modified by any post-translational modifications (Lin 2006).

However, dramatic differences in the duration of Smad2 and Smad3 phosphorylation in nuclei of different cell types has been observed (Rahimi 2007, Andrihafanana 2013) indicating, as with other components of the signalling pathway, the balance between phosphorylation and dephosphorylation of Smads in the nucleus is actively regulated, and differs between cell types. In fibroblast lines, Smad2 (and Smad3) phosphorylation at the sites recognized by the receptors lasted considerably longer than in epithelial

cells (Rahimi 2007, Andrihafanana 2013) despite both lines expressing comparable levels of receptors, Smads and the Smad phosphatase PPM1A.

A number of fibroblast cell lines activate the kinase PAK2 in response to TGF β and this correlated with the cells that had extended Smad2 phosphorylation in the nucleus (Wilkes 2003, Rahimi 2007, Andrihafanana 2013). PAK2 activation lead to the phosphorylation of Smad2 at a site (T430) separate from the sites recognized and phosphorylated by the receptors (S465/467). Phosphorylation at the threonine site prevented the binding, and subsequent dephosphorylation of Smads at the receptor serine residues causing an increase in nuclear retention (Fig 5.4).

PAK2 is just one of many kinases that have been shown to phosphorylate non-receptor sites of Smads, with roles as diverse as cytoplasmic retention (Shi 2003), transcription factor binding (Massagué 2005) and degradation (Wrighton 2009). Our observations chronicle how the phosphorylation of a nearby site by PAK2 can directly affect the receptor phosphorylated sites by blocking the phosphatase from reaching them. While we cannot rule out the PAK2 phosphorylation site may impact other nuclear interactions and/or either phosphorylation or dephosphorylation of other Smad sites, we found no impacts on the nuclear delivery of the Smads to the nucleus. Perhaps the ability to impact nuclear delivery is restricted to phosphorylation events in the linker region.

While the presented data documents the role of PAK2 to directly phosphorylate Smad2 at Thr430, PAK2 activation has also been shown to be required for other players that can phosphorylate R-Smads. In AKR-2B fibroblasts PAK2 phosphorylates Raf which acts in concert with Ras to activate Raf kinase activity (Suzuki 2007, Hough 2012). Raf phosphorylates MEK and MEK phosphorylates ERK (Chang 2003) which can phosphorylate a number of sites on the linker region (Fig 2.9) that can impact nuclear translocation (Shi 2003) or increase the duration of receptor mediated phosphorylation (Hough 2012) depending if ERK phosphorylates the Smads in the cytosol or nucleus. Expression of a dominant negative PAK2 did not impact Smad nuclear translocation but does prevent TGF β mediated proliferation (Wilkes 2003) suggesting PAK2 activated ERK must reside within the nucleus and phosphorylate already nuclear

localized Smads (Hough 2012). A number of other kinases reported to phosphorylate non-receptor sites of Smads have been reported to be activated by TGF β in certain cell types, including JNK (Santibañez 2006) and p38 (Yamashita 2008). The activation of these Smad-independent factors by TGF β is just one more mechanism a cell may utilize to impact the basic Smad signalling framework. While many of the phosphorylation sites are conserved on both Smad2 and Smad3, a number are not. Perhaps these sites serve as another way the cell can regulate the Smad2/Smad3 balance after TGF β stimulation.

Where and when PAK2 phosphorylates Smads is another unanswered question. Localization studies have reported either an ER (Huang 2003) or cytosolic (Jakobi 2003) distribution of unstimulated full-length PAK2, however it was noted a NLS (nuclear localization sequence) is contained within the C-terminal that is ordinarily masked by the autoinhibitory domain (Jakobi 2003). Certainly in the case of caspase-mediated cleavage of the AID the NLS leads to rapid nuclear localization of the active fragment of PAK2 (Jakobi 2003) but it is plausible a nuclear translocation event occurs during other mechanisms of activation. Although not conclusively verified, it is interesting to note PAK2 nuclear translocation after TGF β treatment has been observed (Doré, Memorial University of Newfoundland, *pers comm*). Comparing the kinetics of activation of PAK2 and Smads adds more confusion than insight as Smad phosphorylation and nuclear accumulation is maximal between 20 – 30 minutes, while PAK2 activity isn't detected at high levels until 30 – 40 minutes (Wilkes 2003). Even the sites of activation between the two proteins differ as Smad phosphorylation occurs only after receptors have internalized from the plasma membrane while PAK2 activation occurs while the receptors are at the cell surface prior to internalization (Wilkes 2006).

Although not observed during TGF β -mediated activation of PAK2 in AKR-2B fibroblasts, activated PAK2 has been reported to activate other kinases, including JNK (Chan 2007) and p38 (Wu 2010), that are reported to phosphorylate the linker region of Smad proteins. PAK2 and other kinases that can impact Smad signalling can be activated in many cell types and just because PAK2 isn't activated by TGF β doesn't mean PAK2 activation by another means isn't impacting the signal. Epithelial cells, for example, do not activate PAK2 in response to TGF β but EGF rapidly induces both

PAK1 and PAK2 activity (Roig 2001). Interestingly, when PAK2 is activated (by expressing a constitutively active PAK2 mutant) and then stimulated with TGF β , rather than combining to produce a fibroblast-like response to TGF β (as one might predict) the cells actually behave in a new, unpredicted manner. Clearly, the levels of cross-talk and fine-tuning of TGF β signalling is tremendously complex.

Direct links to deregulation of linker region phosphorylation in human disease have yet to be reported, in large part because deregulation of cellular factors like ERK, GSK3 β and cyclin dependent kinases have a plethora of destructive forces other than just altering Smad phosphorylation. Extensive phosphorylation at the PAK2 site in Smad3 (Thr388) has been reported in the kidneys of animals in a model of renal fibrosis (Qu 2014) while in healthy littermates the phosphorylation was almost undetectable. The role of this phosphorylation in the aetiology of fibrosis is unclear. Likewise, why prominent phosphorylation of Smad3 at this site occurs only in the disease state is unclear.

Kidney fibrosis is one example of a disease linked to phosphorylation at the linker site. TGF β and PAK2 activation have been strongly linked to lung fibrosis (Daniels 2004, Wang 2005, Wilkes 2006, Wang 2009, Andrianifahanana 2013) and scleroderma (Bhattacharyya 2009, Hinchcliff 2012) as well as hematoma (Sato 2013) and glioblastoma progression. Screening diseased tissue and comparing it to healthy sections for Smad phosphorylation at the PAK2 site may indeed be a helpful diagnostic tool. Normal epithelial cells do not activate PAK2 nor demonstrate Smad phosphorylation at the PAK2 site in response to TGF β , so how would one interpret it if tissues showed signs of phosphorylation? Could it be indicative of epithelial cells becoming more mesenchymal, undergoing EMT, or becoming tumorigenic? Could it be a sign of fibroblast infiltrating a space they shouldn't be to establish a fibrotic foci? Or simply an indication of active TGF β signalling in mesenchymal tissue? All of these possibilities could forewarn of serious clinical outcomes. Even in the event of diagnosed disease, in the age of individualized medicine, the presence of PAK site phosphorylation of Smads may provide potential insight into the feasibility of anti-TGF β or anti-PAK2 therapeutic strategies. Screening existing tissue banks may shed light on correlations beyond our foresight and once we start determining these correlations, we can begin developing focused therapies to correct specific imbalances that have

occurred in the TGF β pathway in patients suffering from specific TGF β -driven diseases.

Upon phosphorylation, Smads enter the nucleus and bind DNA (Massagué 2005). However, Smads are not the only proteins modified from one signalling state to another in response to TGF β . PAK2, c-Abl and other kinases can become modified and become enzymatically active (Wilkes 2003, Daniels 2004, Wilkes 2005), small GTPases such as Ras (Suzuki 2007), Rac (Wilkes 2003) and Rho (Kamaraju 2005) show increase GTP loading and activity and a variety of proteins translocate to new cellular locales, including Dab2 (Hocevar 1999) and Hrs (Attisano and Wrana, 2002). As described above, many of these modifications have impacts on Smads, but it is highly likely many of these proteins transmit a message to the nucleus independently of the Smads. PAK2, c-Abl, ERK, JNK, p38 (Jakobi 2003, Roig 2000, Chang 2003) are all recognized as translocating to or from the nucleus upon stimulation with significant transcriptional impacts, although this hasn't been specifically examined in a TGF β context.

TGF β receptors enter the nucleus and impact Smad DNA binding and subsequent gene expression

The theoretical plausibility of transmembrane receptors becoming soluble proteins within the nucleus has been a fiercely contested debate that has raged for some time. The reason for contention centres around the transmembrane domain/s, specifically, how to extract them from membranes and how they can solubilize. In order to insert into a lipid membrane, a transmembrane region (usually approximately 20 amino acids) must consist of mostly hydrophobic residues (Fariselli 2003). These hydrophobic regions are necessary within a membrane but dramatically impair solubility in hydrophilic conditions such as the cytosol. During synthesis and folding within the ER, these regions are accompanied by chaperones (such as HSP70 chaperones) to prevent aggregation (Yoshida 2010). Once a protein is embedded into a membrane it remains there; secreted in vesicles, endocytosed in vesicles and targeted to the lysosome or proteasome still embedded in vesicles. Within these biophysical constraints, reconciling a formerly transmembrane protein solubilized in the nucleus is problematic.

Despite the biophysical constraints, evidence has continued to accumulate of transmembrane receptors including TGF β receptors ending up soluble in the nucleus. Our studies did not determine TGF β receptors to be soluble. Instead, we observed both TGF β R1 and TGF β R2 exit the inner nuclear membrane into polymyeloid leukaemia (PML) bodies (Figs 6.18-19). Whether this can be extrapolated to other receptors remains to be determined.

While our studies did not focus specifically on the role of TGF β receptors in the nucleus we did observe a strong interaction between the impacts of nuclear receptors and Smads on numerous TGF β influenced genes. Transcription factors phosphorylated by nuclear receptors bound regions of gene promoters surrounded by SBEs (Figs 7.9 and 7.10). Even more striking, these SBEs were barely occupied by Smads in the absence of nuclear receptors. Just as the balance between pSmad2 and pSmad3 in the nucleus could influence the cellular response to TGF β from a non-transformed to transformed phenotype, the balance between activated TGF β receptors sorted for degradation versus those trafficked to the nucleus may greatly influence the cellular response to TGF β . While our study failed to observe significant differences in the levels of nuclear receptors between transformed and untransformed cells, other groups have examined various cancer tissues and observed a significant increase in nuclear TGF β receptors in comparison to healthy tissue (Mu 2011). The increased presence of EGFR nuclear receptors in cancerous cells is well established and there is a high likelihood that an imbalance in a hypothetical general receptor nuclear trafficking mechanism (NB: many of the factors involved in TGF β receptors and EGFR are the same) would have deleterious impacts on the cell and organism as a whole.

TGF β R2 as a nuclear signalling molecule

Our studies focussed on nuclear receptors as a component of the TGF β ligand-induced signal and were limited to nuclear trafficking in response to ligand. There are currently no documented enzymatic or signalling roles for TGF β receptors that have not been stimulated by ligand, however there may be cancer related roles for nuclear receptors distinct from ligand stimulation awaiting discovery. This is a particularly intriguing idea considering TGF β R2 is a constitutively active kinase that is excluded

from the nucleus in healthy cells. Although our observations of TGF β R2 nuclear entry were limited to conditions of TGF β stimulation and the presence of TGF β R1, deregulated entry into the nucleus would expose this active kinase to potential new substrates with unknown consequences in the absence of TGF β ligand.

Fate of TGF β receptors in the nucleus

Our study was specifically designed to follow the journey of TGF β receptors from the cell surface into the nucleus. Surface-derived receptors trafficked to, and remained present in, the nucleus of non-transformed AKR-2B and Cos7 cells for at least 12 hours after TGF β stimulation (Fig 6.4) but receptor abundance was declining over time, suggesting nuclear receptors were being degraded in this cell type. As discussed for Smad proteins, the absolute number of receptors present in the nucleus is not only impacted by the rate of receptor import, but also the rate of export/degradation. In AKR-2B and Cos7 cells we can conclude that nuclear receptor levels are reduced with time, presumably through degradation. Designing experiments with a specific focus on elucidating the fate of nuclear receptors, including extending the duration of these studies and comparisons across the different cell types could significantly extend our understanding of the regulation of nuclear receptors. If (as we determined using our techniques), the rate of nuclear entry of TGF β receptors is the same in normal and cancer cells, but the rate of degradation is slower in cancer cells, the total numbers of receptors in cancer cells would be significantly higher at any given point in time. While the experimental techniques utilized by Mu et al. (Mu 2011) and Gudey et al. (Gudey 2014) measured all receptors present in the nucleus at the time of analysis, our techniques were designed only to capture receptors at the cell surface at the moment the cells were stimulated with TGF β and subsequently follow their journey into the nucleus. Receptors already present in the nucleus would not be observed. This may reconcile our observations (no increased rate of nuclear trafficking between normal and cancer cells) with the results from other studies concluding cancer cells express higher levels of nuclear TGF β receptors. The increase observed by others would not be due to an increase in nuclear trafficking, but rather a decrease in degradation of nuclear receptors, a phenomenon our assays would be unable to detect.

In this study we determined that TGF β receptors in the nucleus are in either the inner nuclear membrane or PML nuclear bodies (Figs 6.18-19) but it doesn't answer where

the receptors signal from, or where the receptors traffic to. In regards to signalling, prevention of PML body formation with Ginkgolic acid had only a mild impact on the ability of nuclear receptors to impact gene induction (Fig 7.6) suggesting phosphorylation of transcription factors can occur while receptors reside within the inner nuclear membrane. Perhaps PML bodies have no role in TGF β signalling with one potential hypothesis that PML bodies are required to clear or degrade nuclear receptors.

TGF β receptors that enter the nucleus retain kinase activity (Fig 7.3) however it is not known how this biologically active signal is eventually resolved. Receptors could be dephosphorylated and recycled back to the ER, exported to other compartments, or degraded. Immunofluorescence microscopy, fractionation and western blot analysis all indicate that at later time points (beyond 6-8 hours) the only receptors remaining intact in the cell are contained within the nucleus (Fig 6.4) and as levels decrease in the nucleus they are not appearing in other cellular compartments.

But could receptors be degraded in the nucleus and do PML bodies play any role in this? It has long been documented that degradation of TGF β receptors has both lysosomal and proteosomal components (Huang 2012), but to date the nuclear receptors have not been specifically examined. Pharmacological inhibition of proteosomal and lysosomal degradation (by lactacystin and leupeptin respectively) should determine the impact these two pathways have on nuclear TGF β receptor turnover and subsequent downstream events.

The potential of proteosomal degradation of receptors within the nucleus is supported by observations of significant numbers of proteasomes within the nucleus actively degrading proteins (von Mikecz 2008). The presence of lysosomes within the nucleus has not been documented to date. Furthermore, PML bodies are degraded exclusively through proteasomes. It is the extensive SUMOylation of PML protein that is required for the formation of PML bodies (and that is inhibited by Ginkgolic acid) and when PML bodies can't form (or proteosomal degradation is blocked) the half-life of PML protein is dramatically increased (Hands 2014). Arsenic has been demonstrated to increase PML body formation (Hands 2014) and may increase degradation of nuclear receptors in normal and/or diseased cells but this remains to be tested. Ubiquitination has also

been demonstrated in PML bodies, another hallmark of proteins with roles in proteosomal degradation (Perusina Lanfranca 2013). Whether PML bodies serve to facilitate nuclear receptor degradation or act as a signalling platform remains to be conclusively demonstrated but determining the mechanism that regulates the duration and activity of activated TGF β receptors is being actively pursued.

Determining the fate of nuclear receptors is just as important as understanding their delivery. Presumably deregulation of the amount of receptors in the nucleus will have adverse effects on cell biology and, as discussed, could also occur by defects in the degradation pathway as the mechanism of delivery. However, defining the adverse effects of deregulation remains a critical area of study. Similarly, as the additional post-translational modifications on Smads can influence the duration of Smad phosphorylation and duration of the Smad signal in the nucleus, similar events may influence the duration of TGF β receptor signalling in the nucleus by delaying or accelerating dephosphorylation/degradation of the nuclear pool of receptors. The balance of TGF β signalling molecules transported to, and the time they are present within, the nucleus is evidently highly regulated.

The question of how TGF β receptors in the nucleus contribute to the TGF β signal is not clearly defined in normal or disease states. In synergy with the RNA-binding factor hnRNP A1, nuclear TGF β R1 has been reported to bind RNA at a purine-rich consensus sequence to influence nuclear RNA processing (Chandra 2012). Neither this study, nor ours found any evidence of receptors binding DNA or chromatin however others have shown that TGF β R1 could be detected by chromatin immunoprecipitation to the TGF β -regulated *Snail* promoter and in association with the transcriptional regulator p300 (Mu 2011).

Indeed our study determined a number of transcription factors were phosphorylated by nuclear TGF β R1 (Figs 7.4, 7.5 and 7.7) leading to increase association with p300 and associated DNA binding elements (Fig 7.5). We specifically examined recognized TGF β transcription factors known to be phosphorylated in response to ligand, but a comprehensive transcription factor screen would provide a fuller understanding of the impacts of TGF β R1 as a kinase within the nucleus. Limiting screens to TGF β R1 would be remiss because, as discussed above, while kinase activity is not impacted by

ligand, potential substrates in the nucleus only become available after stimulation causes nuclear entry.

Conclusion

The central aim of this study was to examine the role of nuclear trafficking machinery on the TGF β receptors and signalling molecules activated in response to TGF β stimulation. However, despite each study yielding significant and unexpected results, a common theme underlies them all: TGF β stimulation may result in a multitude of different cellular outcomes depending on the cell context, but TGF β intracellular signalling is restricted to a small subset of molecules. The balance of these signalling molecules within the nucleus is critical to the cellular outcome and much of this balance is regulated by interactions with nuclear trafficking machinery.

Our determination that SNX9 is critical in facilitating the nuclear import of phosphorylated Smad3 (but not phosphorylated Smad2) for the first time provides insight into the molecular mechanism of how cells differentiate between Smad2 and Smad3. This reconciles gene knockdown studies that define independent roles for Smad2 and Smad3 that could not be explained by our previous understanding of TGF β signalling at the molecular level (i.e. no differences in Smad2 and Smad3 signalling had been observed). We extended these findings to define the role of SNX9 in pSmad3 nuclear delivery to the nuclear membrane and nuclear pore machinery and it is hoped that approaches that disrupt SNX9 binding to pSmad3 will provide therapies in TGF β -driven diseases in which the pro-fibrotic and oncogenic properties of pSmad3 need to be reduced while leaving the fibro-protective and tumour-suppressive properties of pSmad2 intact (such as carcinomas, glioblastomas, sarcomas and fibrotic disorders).

Fibroblasts and epithelial cell responses to TGF β are significantly different (fibroblasts transform and form tumours while epithelial cells growth arrest) with almost identical TGF β receptor and Smad expression levels and signalling. The duration of Smad phosphorylation is extended in fibroblasts and the kinase PAK2 is activated. In this study we have documented PAK2 phosphorylation of Smad2 (and presumably Smad3) at a site distinct from the TGF β R1 site preventing the phosphatase PPM1A from binding and dephosphorylating the TGF β R1 sites and is the first reported case of

crosstalk between the Smad and Smad-independent pathways and is another example of cells regulating the Smad pathway in a specific context by regulating Smad nuclear localization.

While the presence of TGF β receptors in the nucleus has been reported by others, our examination extends this contentious observation to robustly define the kinetics, trafficking route and elements within the receptors that support nuclear translocation of both TGF β R1 and TGF β R2. We definitively document a subset of activated TGF β receptors are sorted by the retromer complex before delivery to the PML bodies, remaining embedded within lipid membrane throughout the process. Furthermore, we document TGF β R1 retains kinase activity in the nucleus and phosphorylates a number of transcription factors (including ATF2, CREB) leading to an increase in the acetyltransferase activity of the transcription factors, loosening of the chromatin around the transcription factor binding sites and the exposure of many SBEs. Exposure of SBEs in gene promoters results in gene induction.

Our examination of the nuclear trafficking machinery involved in regulating TGF β signalling has defined new models in the regulation of TGF β action. Signalling events initiated by the TGF β receptors both proximal to the plasma membrane and from within the nucleus have an obligate requirement for a functional nuclear pore and an array of accessory trafficking factors. While some factors are common to each of the signalling molecules (eg. Importin β) others only interact with individual signalling factors or even those containing specific post-translational modifications (e.g. SNX9). In this way, a balance of which TGF β signalling molecules are present in the nucleus, the post-translational status of these molecules, and the duration these molecules remain present and/or active within the nucleus can be regulated with a high degree of variability. We contend that fine tuning the balance of TGF β signalling factors present in the nucleus after TGF β stimulation is a major influence on the response of the cell, which is tremendously varied depending on the cell type and disease status. Despite considerable focus on identifying the activation unique signalling factors to account for the differences in cellular responses to TGF β , we offer that much of the variability stems not from a multitude of different signalling molecules being activated in different cell types, but rather from cell-specific regulatory machinery that influences the balance of a small number activated proteins within the nucleus.

REFERENCES

- Aaronson, R.P. and Blobel, G. (1975). "Isolation of nuclear pore complexes in association with a lamina." Proc Natl Acad Sci U S A **72**: 1007-1011.
- Agas, D., Sabbieti, M.G., Marchetti, L., Xiao, L. and Hurley, M.M. (2013). "FGF-2 enhances Runx-2/Smads nuclear localization in BMP-2 canonical signaling in osteoblasts." J Cell Physiol **228**(11): 2149-2158.
- Agricola, E., Randall, R.A., Gaarenstroom, T., Dupont, S. and Hill, C.S. (2011). "Recruitment of TIF1gamma to chromatin via its PHD finger-bromodomain activates its ubiquitin ligase and transcriptional repressor activities." Mol Cell **43**(1): 85-96.
- Alarcón, C., Zaromytidou, A.I., Xi, Q., Gao, S., Yu, J., Fujisawa, S., Barlas, A., Miller, A.N., Manova-Todorova, K., Macias, M.J., Sapkota, G., Pan, D. and Massagué, J. (2009). "CDK8/9 drive Smad transcriptional action, turnover and YAP interactions in BMP and TGFβ pathways." Cell **139**: 757-776.
- Alarcón, C., Zaromytidou, A.I., Xi, Q., Gao, S., Yu, J., Fujisawa, S., Barlas, A., Miller, A.N., Manova-Todorova, K., Macias, M.J., Sapkota, G., Pan, D. and Massagué, J. (2009). "Nuclear CDKs drive Smad transcriptional activation and turnover in BMP and TGF-beta pathways." Cell **139**(4): 757-769.
- Alliston, T., Choy, L., Ducey, P., Karsenty, G. and Derynck, R. (2001). "TGF-beta-induced repression of CBFA1 by Smad3 decreases cbfa1 and osteocalcin expression and inhibits osteoblast differentiation." EMBO J **20**(9): 2254-2272.
- Al-Salihi, M.A., Herhaus, L. and Sapkota, G.P. (2012). "Regulation of the transforming growth factor beta pathway by reversible ubiquitylation." Open Biol **2**(5): 120082.
- Alves, R.D., Eijken, M., Bezstarosti, K., Demmers, J.A. and van Leeuwen, J.P. (2013). "Activin A suppresses osteoblast mineralization capacity by altering extracellular matrix (ECM) composition and impairing matrix vesicle (MV) production." Mol Cell Proteomics **12**(10): 2890-2900.
- Anders, R.A., Arline, S.L., Dore Jr, J.J. and Leof, E.B. (1997). "Distinct endocytic responses of heteromeric and homomeric transforming growth factor beta receptors." Mol Biol Cell **8**(11): 2133-2143.
- Anders, R.A. and Leof, E.B. (1996). "Chimeric granulocyte/macrophage colony-stimulating factor/transforming growth factor-β (TGF-β) receptors define a model system for investigating the role of homomeric and heteromeric receptors in TGF-β signaling." J Biol Chem **271**: 21758-21766.
- Andrianifahanana, M., Wilkes, M.C., Gupta, S.K., Rahimi, R.A., Repellin, C.E., Edens, M., Wittenberger, J., Yin, X., Maidl, E., Becker, J. and Leof, E.B. (2013).

- "Profibrotic TGF β responses require the cooperative action of PDGF and ErbB receptor tyrosine kinases." FASEB J **27**(11): 4444-4454.
- Aragon, E., Goerner, N., Zaromytidou, A.I., Xi, Q., Escobedo, A., Massague, J. and Macias, M.J. (2011). "A Smad action turnover switch operated by WW domain readers of a phosphoserine code." Genes Dev **25**(12): 1275-1288.
- Asano, Y., Ihn, H., Yamane, K., Kubo, M. and Tamaki, K. (2004). "Impaired Smad7-Smurf-mediated negative regulation of TGF-beta signaling in scleroderma fibroblasts." J Clin Invest **113**(2): 253-264.
- Assoian, R.K., Komoriya, A., Meyers, C.A., Miller, D.M. and Sporn, M.B. (1983). "Transforming growth factor-beta in human platelets. Identification of a major storage site, purification, and characterization." J Biol Chem **258**(11): 7155-7160.
- Attisano, L. and Wrana, J.L. (1996). "Signal transduction by members of the transforming growth factor-beta superfamily." Cytokine Growth Factor Rev **7**(4): 327-339.
- Attisano, L. and Wrana, J.L. (1998). "Mads and Smads in TGF beta signaling." Curr Opin Cell Biol **10**: 188-194.
- Aubin, J., Davy, A. and Soriano, P. (2004). "*In vivo* convergence of BMP and MAPK signaling pathways: impact of differential Smad1 phosphorylation on development and homeostasis." Genes Dev **18**(12): 1482-1494.
- Babitt, J.L., Huang, F.W., Wrighting, D.M., Xia, Y., Sidis, Y., Samad, T.A., Campagna, J.A., Chung, R.T., Schneyer, A.L., Woolf, C.J., Andrews, N.C. and Lin, H.Y. (2006). "Bone morphogenetic protein signaling by hemojuvelin regulates hepcidin expression." Nat Genet **38**(5): 531-539.
- Babitt, J.L., Zhang, Y., Samad, T.A., Xia, Y., Tang, J., Campagna, J.A., Schneyer, A.L., Woolf, C.J. and Lin, H.Y. (2005). "Repulsive guidance molecule (RGMa), a DRAGON homologue, is a bone morphogenetic protein co-receptor." J Biol Chem **280**(33): 29820-29827.
- Badour, K., McGavin, M.K., Zhang, J., Freeman, S., Vieira, C., Filipp, D., Julius, M., Mills, G.B. and Siminovitch, K.A. (2007). "Interaction of the Wiskott-Aldrich syndrome protein with sorting nexin 9 is required for CD28 endocytosis and cosignaling in T cells." Proc Natl Acad Sci U S A **104**: 1593-1598.
- Bai, R.Y., Koester, C., Ouyang, T., Hahn, S.A., Hammerschmidt, M., Peschel, C. and Duyster, J. (2002). "SMIF, a Smad4-interacting protein that functions as a co-activator in TGFbeta signalling." Nat Cell Biol **4**(3): 181-190.
- Baker, J.C. and Harland, R.M. (1996). "A novel mesoderm inducer, Madr2, functions in the activin signal transduction pathway." Genes Dev **10**: 1880-1889.
- Bakin, A.V., Tomlinson, A.K., Bhowmick, N.A., Moses, H.L. and Arteaga, C.L. (2000).

- "Phosphatidylinositol 3-kinase function is required for transforming growth factor beta-mediated epithelial to mesenchymal transition and cell migration." J Biol Chem **275**(47): 36803-36810.
- Bakkebo, M., Huse, K., Hilden, V.I., Forfang, L., Myklebust, J.H., Smeland, E.B. and Oksvold, M.P. (2012). "SARA is dispensable for functional TGF-beta signaling." FEBS Lett **586**(19): 3367-3372.
- Baldys, A. and Raymond, J.R. (2009). "Critical role of ESCRT machinery in EGFR recycling." Biochemistry **48**(40): 9321-9323.
- Bannister, A.J. and Kouzarides, T. (1996). "The CBP co-activator is a histone acetyltransferase." Nature **384**(6610): 641-643.
- Barrios-Rodiles, M., Brown, K.R., Ozdamar, B., Bose, R., Liu, Z., Donovan, R., Shinjo, F., Liu, Y., Dembowy, J., Taylor, I.W., Luga, V., Przulj, N., Robinson, M., Suzuki, H., Hayashizaki, Y., Jurisica, I. and Wrana, J.L. (2005). "High-throughput mapping of a dynamic signaling network in mammalian cells." Science **307**: 1621-1625.
- Batut, J., Schmierer, B., Cao, J., Raftery, L.A., Hill, C.S. and Howell, M. (2008). "Two highly related regulatory subunits of PP2A exert opposite effects on TGF-beta/Activin/Nodal signalling." Development **135**(17): 2927-2937.
- Baumann, C., Lindholm, C.K., Rimoldi, D. and Levy, F. (2010). "The E3 ubiquitin ligase Itch regulates sorting nexin 9 through an unconventional substrate recognition domain." FEBS J **277**: 2803-2814.
- Becker-Hapak, M., McAllister, S.S. and Dowdy, S.F. (2001). "TAT-mediated protein transduction into mammalian cells." Methods Enz **24**: 247-256.
- Bellone, G., Gramigni, C., Vizio, B., Mauri, F.A., Prati, A., Solerio, D., Dughera, L., Ruffini, E., Gasparri, G. and Camandona, M. (2010). "Abnormal expression of Endoglin and its receptor complex (TGF-beta1 and TGF-beta receptor II) as early angiogenic switch indicator in premalignant lesions of the colon mucosa." Int J Oncol **37**(5): 1153-1165.
- Bertolino, P., Deckers, M., Lebrin, F. and ten Dijke, P. (2005). "Transforming growth factor-beta signal transduction in angiogenesis and vascular disorders." Chest **128**(6 Suppl): 585S-590S.
- Bhattacharyya, S., Ishida, W., Wu, M., Wilkes, M.C., Mori, Y., Hinchcliff, M., Leof, E.B. and Varga, J. (2009). "A non-Smad mechanism of fibroblast activation by transforming growth factor-beta via c-Abl and Egr-1; selective modulation by imatinib mesylate." Oncogene **28**: 1285-1297.
- Biederer, T., Volkwein, C. and Sommer, T. (1997). "Role of Cue1p in ubiquitination and degradation at the ER surface." Science **278**(5344): 1806-1809.

- Blanachette, F., Rivard, N., Rudd, P., Grondin, F., Attisano, L. and Dubois, C.M. (2001). "Cross-talk between the p42/p44 MAP kinase and Smad pathways in Transforming Growth Factor β 1-induced Furin transactivation." J Biol Chem **276**: 33986-33994.
- Boeuf, S., Bovee, J.V., Lehner, B., van den Akker, B., van Ruler, M., Cleton-Jansen, A.M. and Richter, W. (2012). "BMP and TGFbeta pathways in human central chondrosarcoma: enhanced endoglin and Smad 1 signaling in high grade tumors." BMC Cancer **12**: 488.
- Bonifacino, J.S. and Rojas, R. (2006). "Retrograde transport from endosomes to the trans-Golgi network." Nat Rev Mol Cell Biol **7**(8): 568-579.
- Bornancin, F. and Parker, P.J. (1996). "Phosphorylation of threonine 638 critically controls the dephosphorylation and inactivation of protein kinase Calpha." Curr Biol **6**(9): 1114-1123.
- Bourd-Boittin, K., Bonnier, D., Leyme, A., Mari, B., Tuffery, P., Samson, M., Ezan, F., Baffet, G. and Theret, N. (2011). "Protease profiling of liver fibrosis reveals the ADAM metallopeptidase with thrombospondin type 1 motif, 1 as a central activator of transforming growth factor beta." Hepatology **54**(6): 2173-2184.
- Brand, T.M., Iida, M., Li, C. and Wheeler, D.L. (2011). "The nuclear epidermal growth factor receptor signaling network and its role in cancer." Discov Med **12**(66): 419-432.
- Bray, S.J. (2006). "Notch signalling: a simple pathway becomes complex." Nat Rev Mol Cell Biol **7**(9): 678-689.
- Breen, M.J., Moran, D.M., Liu, W., Huang, X., Vary, C.P. and Bergan, R.C. (2013). "Endoglin-mediated suppression of prostate cancer invasion is regulated by activin and bone morphogenetic protein type II receptors." PLoS One **8**(8): e72407.
- Brodin, G., Ahgren, A., ten Dijke, P., Heldin, C.H. and Heuchel, R. (2000). "Efficient TGF-beta induction of the Smad7 gene requires cooperation between AP-1, Sp1, and Smad proteins on the mouse Smad7 promoter." J Biol Chem **275**(37): 29023-29030.
- Bruce, D.L. and Sapkota, G.P. (2012). "Phosphatases in SMAD regulation." FEBS Lett **586**(14): 1897-1905.
- Bryant, D.M. and Stow, J.L. (2005). "Nuclear translocation of cell-surface receptors: lessons from fibroblast growth factor." Traffic **6**(10): 947-954.
- Burd, C. and Cullen, P.J. (2014). "Retromer: a master conductor of endosome sorting." Cold Spring Harb Perspect Biol **6**(2).
- Cai, J., Jiang, W.G., Grant, M.B. and Boulton, M. (2006). "Pigment epithelium-derived

- factor inhibits angiogenesis via regulated intracellular proteolysis of vascular endothelial growth factor receptor 1." J Biol Chem **281**(6): 3604-3613.
- Cao, H., Lei, Z.M., Bian, L. and Rao, C.V. (1995). "Functional nuclear epidermal growth factor receptors in human choriocarcinoma JEG-3 cells and normal human placenta." Endocrinology **136**(7): 3163-3172.
- Capdevila, J., Tsukui, T., Rodriguez Esteban, C., Zappavigna, V. and Izpisua Belmonte, J.C. (1999). "Control of vertebrate limb outgrowth by the proximal factor Meis2 and distal antagonism of BMPs by Gremlin." Mol Cell **4**(5): 839-849.
- Carlton, J., Bujny, M., Rutherford, A. and Cullen, P. (2005). "Sorting nexins--unifying trends and new perspectives." Traffic **6**: 75-82.
- Carpenter, G. and Liao, H.J. (2009). "Trafficking of receptor tyrosine kinases to the nucleus." Exp Cell Res **315**(9): 1556-1566. .
- Cerdan, C., McIntyre, B.A., Mechael, R., Levadoux-Martin, M., Yang, J., Lee, J.B. and Bhatia, M. (2012). "Activin A promotes hematopoietic fated mesoderm development through upregulation of brachyury in human embryonic stem cells." Stem Cells Dev **21**(15): 2866-2877.
- Ceresa, B.P. (2006). "Regulation of EGFR endocytic trafficking by rab proteins." Histol Histopathol **21**(9): 987-993.
- Chacko, B.M., Qin, B.Y., Tiwari, A., Shi, G., Lam, S., Hayward, L.J., De Caestecker, M.P. and Lin, K. (2004). "Structural basis of heteromeric smad protein assembly in TGF-beta signaling." Mol Cell **15**(5): 813-823.
- Challen, G.A., Boles, N.C., Chambers, S.M. and Goodell, M.A. (2010). "Distinct hematopoietic stem cell subtypes are differentially regulated by TGF-beta1." Cell Stem Cell **6**(3): 265-278.
- Chan, W.H., Wu, H.J. and Shiao, N.H. (2007). "Apoptotic signaling in methylglyoxal-treated human osteoblasts involves oxidative stress, c-Jun N-terminal kinase, caspase-3, and p21-activated kinase 2." J Cell Biochem **100**(4): 1056-1069.
- Chandra, M., Zang, S., Li, H., Zimmerman, L.J., Champer, J., Tsuyada, A., Chow, A., Zhou, W., Yu, Y., Gao, H., Ren, X., Lin, R.J. and Wang, S.E. (2012). "Nuclear translocation of type I transforming growth factor β receptor confers a novel function in RNA processing." Mol Cell Biol **32**(12): 2183-2195.
- Chang, F., Steelman, L.S., Lee, J.T., Shelton, J.G., Navolanic, P.M., Blalock, W.L., Franklin, R.A. and McCubrey, J.A. (2003). "Signal transduction mediated by the Ras/Raf/MEK/ERK pathway from cytokine receptors to transcription factors: potential targeting for therapeutic intervention." Leukemia **17**(7): 1263-1293.
- Chang, H.M., Lin, Y.Y., Tsai, P.C., Liang, C.T. and Yan, Y.T. (2014). "The FYVE domain of Smad Anchor for Receptor Activation (SARA) is required to prevent

- skin carcinogenesis, but not in mouse development." PLoS One **9**(8): e105299.
- Chen, F., Ogawa, K., Liu, X., Stringfield, T.M. and Chen, Y. (2002). "Repression of Smad2 and Smad3 transactivating activity by association with a novel splice variant of CCAAT-binding factor C subunit." Biochem J **364**: 571-577.
- Chen, G., Ghosh, P. and Longo, D.L. (2011). "Distinctive mechanism for sustained TGF-beta signaling and growth inhibition: MEK1 activation-dependent stabilization of type II TGF-beta receptors." Mol Cancer Res **9**(1): 78-89.
- Chen, H.B., Rud, J.G., Lin, K. and Xu, L. (2005). "Nuclear targeting of transforming growth factor-beta-activated Smad complexes." J Biol Chem **280**: 21329-21336.
- Chen, H.B., Shen, J., Ip, Y.T. and Xu, L. (2006). "Identification of phosphatases for Smad in the BMP/DPP pathway." Genes Dev **20**(6): 648-653.
- Chen, X., Rubock, M.J. and Whitman, M. (1996). "A transcriptional partner for MAD proteins in TGF-beta signalling." Nature **383**(6602): 691-696.
- Chen, X. and Xu, L. (2010). "Specific nucleoporin requirement for Smad nuclear translocation." Mol Cell Biol **30**(16): 4022-4034.
- Chen, Y.G., Hata, A., Lo, R.S., Wotton, D., Shi, Y., Pavletich, N. and Massague, J. (1998). "Determinants of specificity in TGF-beta signal transduction." Genes Dev **12**(14): 2144-2152.
- Chen, Y.G. and Massague, J. (1999). "Smad1 recognition and activation by the ALK1 group of transforming growth factor-beta family receptors." J Biol Chem **274**(6): 3672-3677.
- Cheng, Q.C., Tikhomirov, O., Zhou, W. and Carpenter, G. (2003). "Ectodomain cleavage of ErbB-4: characterization of the cleavage site and m80 fragment." J Biol Chem **278**(40): 38421-38427.
- Cheng, S., Guo, J., Yang, Q. and Han, L. (2015). "Crk-like adapter protein is required for TGF-beta-induced AKT and ERK-signaling pathway in epithelial ovarian carcinomas." Tumour Biol **36**(2): 915-919.
- Chia, P.Z. and Gleeson, P.A. (2011). "The regulation of endosome-to-Golgi retrograde transport by tethers and scaffolds." Traffic **12**(8): 939-947.
- Childress, C., Lin, Q. and Yang, W. (2006). "Dimerization is required for SH3PX1 tyrosine phosphorylation in response to epidermal growth factor signalling and interaction with ACK2." Biochem J **394**: 693-698.
- Choi, M.E., Ding, Y. and Kim, S.I. (2012). "TGF-beta signaling via TAK1 pathway: role in kidney fibrosis." Semin Nephrol **32**(3): 244-252.
- Chudakov, D.M., Matz, M.V., Lukyanov, S. and Lukyanov, K.A. (2010). "Fluorescent proteins and their applications in imaging living cells and tissues." Physiol Rev **90**(3): 1103-1163.

- Cingolani, G., Petosa, C., Weis, K. and Muller, C.W. (1999). "Structure of importin-beta bound to the IBB domain of importin-alpha." Nature **399**(6733): 221-229.
- Cloughesy, T.F., Cavenee, W.K. and Mischel, P.S. (2014). "Glioblastoma: from molecular pathology to targeted treatment." Annu Rev Pathol **9**: 1-25.
- Cordenonsi, M., Dupont, S., Maretto, S., Insinga, A., Imbriano, C. and Piccolo, S. (2003). "Links between tumor suppressors: p53 is required for TGF-beta gene responses by cooperating with Smads." Cell **113**(3): 301-314.
- Cullen, P.J. (2008). "Endosomal sorting and signalling: an emerging role for sorting nexins." Nat Rev Mol Cell Biol **9**: 574-582.
- Dahlin, J.L., Chen, X., Walters, M.A. and Zhang, Z. (2015). "Histone-modifying enzymes, histone modifications and histone chaperones in nucleosome assembly: Lessons learned from Rtt109 histone acetyltransferases." Crit Rev Biochem Mol Biol **50**(1): 31-53.
- Dai, F., Chang, C., Lin, X., Dai, P., Mei, L. and Feng, X. (2007). "Erbin inhibits Transforming Growth Factor β signaling through a novel Smad-interacting domain." Mol. Cell. Biol 6183-6194.
- Dai, F., Lin, X., Chang, C. and Feng, X.H. (2009). "Nuclear export of Smad2 and Smad3 by RanBP3 facilitates termination of TGF-beta signaling." Dev Cell **16**(3): 345-357.
- Dai, F., Shen, T., Li, Z., Lin, X. and Feng, X.H. (2011). "PPM1A dephosphorylates RanBP3 to enable efficient nuclear export of Smad2 and Smad3." EMBO Rep **12**(11): 1175-1181.
- Dallas, S.L., Rosser, J.L., Mundy, G.R. and Bonewald, L.F. (2002). "Proteolysis of latent transforming growth factor-beta (TGF-beta)-binding protein-1 by osteoclasts. A cellular mechanism for release of TGF-beta from bone matrix." J Biol Chem **277**(24): 21352-21360.
- D'Angelo, M.A. and Hetzer, M.W. (2008). "Structure, dynamics and function of nuclear pore complexes." Trends Cell Biol **18**(10): 456-466.
- Daniels, C.E., Wilkes, M.C., Edens, M., Kottom, T.J., Murphy, S.J., Limper, A.H. and Leof, E.B. (2004). "Imatinib mesylate inhibits the profibrogenic activity of TGF-beta and prevents bleomycin-mediated lung fibrosis." J Clin Invest **114**(9): 1308-1316.
- Davis, M.E., Hsieh, P.C., Grodzinsky, A.J. and Lee, R.T. (2005). "Custom design of the cardiac microenvironment with biomaterials." Circ Res **97**(1): 8-15.
- Dean, D.B., Watson, J.T., Jin, W., Peters, C., Enders, J.T., Chen, A., Moed, B.R. and Zhang, Z. (2010). "Distinct functionalities of bone morphogenetic protein antagonists during fracture healing in mice." J Anat **216**(5): 625-630.

- Dekker, F.J. and Haisma, H.J. (2009). "Histone acetyl transferases as emerging drug targets." Drug Discov Today **14**(19-20): 942-948.
- Derynck, R., Muthusamy, B.P. and Saeteurn, K.Y. (2014). "Signaling pathway cooperation in TGF- β -induced epithelial-mesenchymal transition." Curr Opin Cell Biol **31C**: 56-66.
- Di Guglielmo, G.M., Le Roy, C., Goodfellow, A.F. and Wrana, J.L. (2003). "Distinct endocytic pathways regulate TGF-beta receptor signalling and turnover." Nat Cell Biol **5**(5): 410-421.
- Diaz-Meco, M.T. and Moscat, J. (2001). "MEK5, a new target of the atypical protein kinase C isoforms in mitogenic signaling." Mol Cell Biol **21**(4): 1218-1227.
- Diniz, L.P., Almeida, J.C., Tortelli, V., Vargas Lopes, C., Setti-Perdigao, P., Stipursky, J., Kahn, S.A., Romao, L.F., de Miranda, J., Alves-Leon, S.V., de Souza, J.M., Castro, N.G., Panizzutti, R. and Gomes, F.C. (2012). "Astrocyte-induced synaptogenesis is mediated by transforming growth factor beta signaling through modulation of D-serine levels in cerebral cortex neurons." J Biol Chem **287**(49): 41432-41445.
- Dittmann, K., Mayer, C., Fehrenbacher, B., Schaller, M., Raju, U., Milas, L., Chen, D.J., Kehlbach, R. and Rodemann, H.P. (2005). "Radiation-induced epidermal growth factor receptor nuclear import is linked to activation of DNA-dependent protein kinase." J Biol Chem **280**(35): 31182-31189.
- Dore Jr, J.J., Yao, D., Edens, M., Garamszegi, N., Sholl, E.L. and Leaf, E.B. (2001). "Mechanisms of transforming growth factor-beta receptor endocytosis and intracellular sorting differ between fibroblasts and epithelial cells." Mol Biol Cell **12**(3): 675-684.
- Duan, X., Liang, Y.Y., Feng, X.H. and Lin, X. (2006). "Protein serine/threonine phosphatase PPM1A dephosphorylates Smad1 in the bone morphogenetic protein signaling pathway." J Biol Chem **281**(48): 36526-36532.
- Dubinski, W., Gabriel, M., Iakovlev, V.V., Scorilas, A., Youssef, Y.M., Faragalla, H., Kovacs, K., Rotondo, F., Metias, S., Arsanious, A., Plotkin, A., Girgis, A.H., Streutker, C.J. and Yousef, G.M. (2012). "Assessment of the prognostic significance of endoglin (CD105) in clear cell renal cell carcinoma using automated image analysis." Hum Pathol **43**(7): 1037-1043.
- Dunn, N.R., Koonce, C.H., Anderson, D.C., Islam, A., Bikoff, E.K. and Robertson, E.J. (2005). "Mice exclusively expressing the short isoform of Smad2 develop normally and are viable and fertile." Genes Dev **19**(1): 152-163.
- Dupont, S., Zacchigna, L., Cordenonsi, M., Soligo, S., Adorno, M., Rugge, M. and Piccolo, S. (2005). "Germ-layer specification and control of cell growth by

- Ectodermin, a Smad4 ubiquitin ligase." Cell **121**(1): 87-99.
- Ebisawa, T., Fukuchi, M., Murakami, G., Chiba, T., Tanaka, K., Imamura, T. and Miyazono, K. (2001). "Smurf1 interacts with transforming growth factor-beta type I receptor through Smad7 and induces receptor degradation." J Biol Chem **276**(16): 12477-12480.
- Ellenrieder, V. (2008). "TGFbeta regulated gene expression by Smads and Sp1/KLF-like transcription factors in cancer." Anticancer Res **28**(3A): 1531-1539.
- Elliott, R.L. and Blobe, G.C. (2005). "Role of transforming growth factor beta in human cancer." J Clin Oncol **23**: 2078-2093.
- Engel, M.E., Datta, P.K. and Moses, H.L. (1998). "Signal transduction by transforming growth factor-beta: a cooperative paradigm with extensive negative regulation." J Cell Biochem Suppl **30-31**: 111-122.
- Estrada, K.D., Retting, K.N., Chin, A.M. and Lyons, K.M. (2011). "Smad6 is essential to limit BMP signaling during cartilage development." J Bone Miner Res **26**(10): 2498-2510.
- Eyler, C.E. and Rich, J.N. (2012). "Looking in the miR-ror: TGF- β -mediated activation of NF- κ B in glioma." J Clin Invest **122**(10): 3473-3475.
- Fan, W., Zhang, J., Zhang, Z., Wang, Q. and Cao, F. (2013). "Adaptive inflammatory microenvironment for cell-based regeneration in ischemic cardiovascular disease." Organogenesis **9**(3): 121-124.
- Fariselli, P., Finelli, M., Marchignoli, D., Martelli, P.L., Rossi, I. and Casadio, R. (2003). "MaxSubSeq: an algorithm for segment-length optimization. The case study of the transmembrane spanning segments." Bioinformatics **19**(4): 500-505.
- Fell, V.L. and Schild-Poulter, C. (2012). "Ku regulates signaling to DNA damage response pathways through the Ku70 von Willebrand A domain." Mol Cell Biol **32**(1): 76-87.
- Feng, X.-H. and Derynck, R. (2005). "Specificity and versatility in TGF-b signaling through Smads." Annu Rev Cell Dev Biol **21**: 659-693.
- Fiume, R., Keune, W.J., Faenza, I., Bultsma, Y., Ramazzotti, G., Jones, D.R., Martelli, A.M., Somner, L., Follo, M.Y., Divecha, N. and Cocco, L. (2012). "Nuclear phosphoinositides: location, regulation and function." Subcell Biochem **59**: 335-361.
- Fleming, N.I., Jorissen, R.N., Mouradov, D., Christie, M., Sakthianandeswaren, A., Palmieri, M., Day, F., Li, S., Tsui, C., Lipton, L., Desai, J., Jones, I.T., McLaughlin, S., Ward, R.L., Hawkins, N.J., Ruzkiewicz, A.R., Moore, J., Zhu, H.J., Mariadason, J.M., Burgess, A.W., Busam, D., Zhao, Q., Strausberg, R.L., Gibbs, P. and Sieber, O.M. (2013). "SMAD2, SMAD3 and SMAD4 mutations in

- colorectal cancer." Cancer Res **73**(2): 725-735.
- Fransz, P. and de Jong, H. (2011). "From nucleosome to chromosome: a dynamic organization of genetic information." Plant J **66**(1): 4-17.
- Fuentealba, L.C., Eivers, E., Ikeda, A., Hurtado, C., Kuroda, H., Pera, E.M. and De Robertis, E.M. (2007). "Integrating patterning signals: Wnt/GSK3 regulates the duration of the BMP/Smad1 signal." Cell **131**(5): 980-993.
- Fukasawa, H., Yamamoto, T., Togawa, A., Ohashi, N., Fujigaki, Y., Oda, T., Uchida, C., Kitagawa, K., Hattori, T., Suzuki, S., Kitagawa, M. and Hishida, A. (2004). "Down-regulation of Smad7 expression by ubiquitin-dependent degradation contributes to renal fibrosis in obstructive nephropathy in mice." Proc Natl Acad Sci U S A **101**(23): 8687-8692.
- Fukushima, T., Liu, R.Y. and Byrne, J.H. (2007). "Transforming growth factor-beta2 modulates synaptic efficacy and plasticity and induces phosphorylation of CREB in hippocampal neurons." Hippocampus **17**(1): 5-9.
- Funaba, M., Zimmerman, C.M. and Mathews, L.S. (2002). "Modulation of Smad2-mediated signaling by extracellular signal-regulated kinase." J Biol Chem **277**(44): 41361-41368.
- Gaarenstroom, T. and Hill, C.S. (2014). "TGF-beta signaling to chromatin: how Smads regulate transcription during self-renewal and differentiation." Semin Cell Dev Biol **32**: 107-118.
- Gal, A., Sjoblom, T., Fedorova, L., Imreh, S., Beug, H. and Moustakas, A. (2008). "Sustained TGF beta exposure suppresses Smad and non-Smad signalling in mammary epithelial cells, leading to EMT and inhibition of growth arrest and apoptosis." Oncogene **27**(9): 1218-1230.
- Gao, S., Alarcon, C., Sapkota, G., Rahman, S., Chen, P.Y., Goerner, N., Macias, M.J., Erdjument-Bromage, H., Tempst, P. and Massague, J. (2009). "Ubiquitin ligase Nedd4L targets activated Smad2/3 to limit TGF-beta signaling." Mol Cell **36**(3): 457-468.
- Garamszegi, N., Dore Jr, J.J., Penheiter, S.G., Edens, M., Yao, D. and Leof, E.B. (2001). "Transforming growth factor beta receptor signaling and endocytosis are linked through a COOH terminal activation motif in the type I receptor." Mol Biol Cell **12**(9): 2881-2893.
- Gatza, C.E., Holtzhausen, A., Kirkbride, K.C., Morton, A., Gatza, M.L., Datto, M.B. and Blobe, G.C. (2011). "Type III TGF-beta receptor enhances colon cancer cell migration and anchorage-independent growth." Neoplasia **13**(8): 758-770.
- Ghaemmaghami, S., Huh, W.K., Bower, K., Howson, R.W., Belle, A., Dephoure, N., O'Shea, E.K. and Weissman, J.S. (2003). "Global analysis of protein expression

- in yeast." Nature **425**(6959): 737-741.
- Giri, D.K., Ali-Seyed, M., Li, L.Y., Lee, D.F., Ling, P., Bartholomeusz, G., Wang, S.C. and Hung, M.C. (2005). "Endosomal transport of ErbB-2: mechanism for nuclear entry of the cell surface receptor." Mol Cell Biol **25**(24): 11005-11018.
- Gleason, R.J., Akintobi, A.M., Grant, B.D. and Padgett, R.W. (2014). "BMP signaling requires retromer-dependent recycling of the type I receptor." Proc Natl Acad Sci U S A **111**(7): 2578-2583.
- Glenn, G. and van der Geer, P. (2007). "CSF-1 and TPA stimulate independent pathways leading to lysosomal degradation or regulated intramembrane proteolysis of the CSF-1 receptor." FEBS Lett **581**(28): 5377-5381.
- Goldberg, J. (1999). "Structural and functional analysis of the ARF1-ARFGAP complex reveals a role for coatamer in GTP hydrolysis." Cell **96**(6): 893-902.
- Gonzales, C.B., Simmons, D. and MacDougall, M. (2010). "Competing roles of TGFbeta and Nma/BAMBI in odontoblasts." J Dent Res **89**(6): 597-602.
- Griswold-Prenner, I., Kamibayashi, C., Maruoka, E.M., Mumby, M.C. and Derynck, R. (1998). "Physical and functional interactions between type I transforming growth factor beta receptors and Balpha, a WD-40 repeat subunit of phosphatase 2A." Mol Cell Biol **18**(11): 6595-6604.
- Gronroos, E., Hellman, U., Heldin, C.H. and Ericsson, J. (2002). "Control of Smad7 stability by competition between acetylation and ubiquitination." Mol Cell **10**(3): 483-493.
- Gruenberg, J. and Stenmark, H. (2004). "The biogenesis of multivesicular endosomes." Nat Rev Mol Cell Biol **5**(4): 317-323.
- Gudey, S.K., Sundar, R., Mu, Y., Wallenius, A., Zang, G., Bergh, A., Heldin, C.H. and Landstrom, M. (2014). "TRAF6 stimulates the tumor-promoting effects of TGFbeta type I receptor through polyubiquitination and activation of presenilin 1." Sci Signal **7**(307): ra2.
- Gudey, S.K., Sundar, R., Mu, Y., Wallenius, A., Zang, G., Bergh, A., Heldin, C.H. and Landström, M. (2014). "TRAF6 stimulates the tumor-promoting effects of TGFβ type I receptor through polyubiquitination and activation of presenilin 1." Sci Signal **7**(307): ra2.
- Hanai, J., Chen, L.F., Kanno, T., Ohtani-Fujita, N., Kim, W.Y., Guo, W.H., Imamura, T., Ishidou, Y., Fukuchi, M., Shi, M.J., Stavnezer, J., Kawabata, M., Miyazono, K. and Ito, Y. (1999). "Interaction and functional cooperation of PEBP2/CBF with Smads. Synergistic induction of the immunoglobulin germline Calpha promoter." J Biol Chem **274**(44): 31577-31582.
- Hands, K.J., Cuchet-Lourenco, D., Everett, R.D. and Hay, R.T. (2014). "PML isoforms

- in response to arsenic: high-resolution analysis of PML body structure and degradation." *J Cell Sci* **127**(Pt 2): 365-375.
- Hara, H. (2012). "Endoglin (CD105) and claudin-5 expression in cutaneous angiosarcoma." *Am J Dermatopathol* **34**(7): 779-782.
- Harbour, M.E., Breusegem, S.Y., Antrobus, R., Freeman, C., Reid, E. and Seaman, M.N. (2010). "The cargo-selective retromer complex is a recruiting hub for protein complexes that regulate endosomal tubule dynamics." *J Cell Sci* **123**(Pt 21): 3703-3717.
- Hastie, C.J., McLauchlan, H.J. and Cohen, P. (2006). "Assay of protein kinases using radiolabeled ATP: a protocol." *Nat Protoc* **1**(2): 968-971.
- Hata, A., Lagna, G., Massague, J. and Hemmati-Brivanlou, A. (1998). "Smad6 inhibits BMP/Smad1 signaling by specifically competing with the Smad4 tumor suppressor." *Genes Dev* **12**(2): 186-197.
- Hata, A., Seoane, J., Lagna, G., Montalvo, E., Hemmati-Brivanlou, A. and Massagué, J. (2000). "OAZ uses distinct DNA- and protein-binding zinc fingers in separate BMP-Smad and Olf signaling pathways." *Cell* **100**(2): 229-240.
- Hayashi, A., Yamauchi, N., Shibahara, J., Kimura, H., Morikawa, T., Ishikawa, S., Nagae, G., Nishi, A., Sakamoto, Y., Kokudo, N., Aburatani, H. and Fukayama, M. (2014). "Concurrent activation of acetylation and tri-methylation of H3K27 in a subset of hepatocellular carcinoma with aggressive behavior." *PLoS One* **9**(3): e91330. .
- Hayes, S., Chawla, A. and Corvera, S. (2002). "TGF β receptor internalization into EEA1-enriched early endosomes: role in signaling to Smad2." *J Cell Biol* **158**: 1239-1249.
- Hedigan, K. (2010). "Fibrotic disease: Targeting the microenvironment." *Nat Rev Drug Discov* **9**(11): 840-841.
- Heikkinen, P.T., Nummela, M., Jokilehto, T., Grenman, R., Kahari, V.M. and Jaakkola, P.M. (2010). "Hypoxic conversion of SMAD7 function from an inhibitor into a promoter of cell invasion." *Cancer Res* **70**(14): 5984-5993.
- Herhaus, L., Al-Salihi, M., Macartney, T., Weidlich, S. and Sapkota, G.P. (2013). "OTUB1 enhances TGF β signalling by inhibiting the ubiquitylation and degradation of active SMAD2/3." *Nat Commun* **4**: 2519.
- Hill, C.S. (2009). "Nucleocytoplasmic shuttling of Smad proteins." *Cell Res* **19**(1): 36-46.
- Hiller, M.M., Finger, A., Schweiger, M. and Wolf, D.H. (1996). "ER degradation of a misfolded luminal protein by the cytosolic ubiquitin-proteasome pathway." *Science* **273**(5282): 1725-1728.

- Hilton, T.L., Li, Y., Dunphy, E.L. and Wang, E.H. (2005). "TAF1 histone acetyltransferase activity in Sp1 activation of the cyclin D1 promoter." Mol Cell Biol **25**(10): 4321-4332.
- Hinchcliff, M., Huang, C.C., Ishida, W., Fang, F., Lee, J., Jafari, N., Wilkes, M.C., Bhattacharyya, S., Leof, E.B. and Varga, J. (2012). "Imatinib mesylate causes genome-wide transcriptional changes in systemic sclerosis fibroblasts *in vitro*." Clin Exp Rheumatol **30**: S86-S96.
- Hobmayer, B., Rentzsch, F. and Holstein, T.W. (2001). "Identification and expression of HySmad1, a member of the R-Smad family of TGFbeta signal transducers, in the diploblastic metazoan Hydra." Dev Genes Evol **211**(12): 597-602.
- Hocevar, B.A., Brown, T.L. and Howe, P.H. (1999). "TGF-beta induces fibronectin synthesis through a c-Jun N-terminal kinase-dependent, Smad4-independent pathway." EMBO J **18**(5): 1345-1356.
- Holden, J.M., Koreny, L., Kelly, S., Chait, B.T., Rout, M.P., Field, M.C. and Obado, S.O. (2014). "Touching from a distance." Nucleus **5**(4): 304-310.
- Hong, M., Wilkes, M.C., Penheiter, S.G., Gupta, S.K., Edens, M. and Leof, E.B. (2011). "Non-Smad transforming growth factor- β signaling regulated by focal adhesion kinase binding the p85 subunit of phosphatidylinositol 3-kinase." J Biol Chem **286**(20): 17841-17850.
- Hoot, K.E., Lighthall, J., Han, G., Lu, S.L., Li, A., Ju, W., Kulesz-Martin, M., Bottinger, E. and Wang, X.J. (2008). "Keratinocyte-specific Smad2 ablation results in increased epithelial-mesenchymal transition during skin cancer formation and progression." J Clin Invest **118**: 2722-2732.
- Hough, C., Radu, M. and Dore Jr, J.J. (2012). "TGF-beta induced Erk phosphorylation of Smad linker region regulates Smad signaling." PLoS One **7**: e42513.
- Howe, P.H., Draetta, G. and Leof, E.B. (1991). "Transforming growth factor beta 1 inhibition of p34cdc2 phosphorylation and histone H1 kinase activity is associated with G1/S-phase growth arrest." Mol Cell Biol **11**: 1185-1194.
- Huang, F. and Chen, Y.G. (2012). "Regulation of TGF- β receptor activity." Cell Biosci **15**(2): 9.
- Huang, Z., Ling, J. and Traugh, J.A. (2003). "Localization of p21-activated protein kinase gamma-PAK/Pak2 in the endoplasmic reticulum is required for induction of cytostasis." J Biol Chem **278**(15): 13101-13109.
- Huovila, A.P., Turner, A.J., Pelto-Huikko, M., Karkkainen, I. and Ortiz, R.M. (2005). "Shedding light on ADAM metalloproteinases." Trends Biochem Sci **30**(7): 413-422.
- Iemura, S., Yamamoto, T.S., Takagi, C., Kobayashi, H. and Ueno, N. (1999). "Isolation

- and characterization of bone morphogenetic protein-binding proteins from the early *Xenopus* embryo." J Biol Chem **274**(38): 26843-26849.
- Inman, G.J., Nicolas, F.J. and Hill, C.S. (2002). "Nucleocytoplasmic shuttling of Smads 2, 3, and 4 permits sensing of TGF-beta receptor activity." Mol Cell **10**: 283-294.
- Isgro, T.A. and Schulten, K. (2007). "Cse1p-binding dynamics reveal a binding pattern for FG-repeat nucleoporins on transport receptors." Structure **15**(8): 977-991.
- Ishtiaq Ahmed, A.S., Bose, G.C., Huang, L. and Azhar, M. (2014). "Generation of mice carrying a knockout-first and conditional-ready allele of transforming growth factor beta2 gene." Genesis **52**(9): 817-826.
- Ito, I., Hanyu, A., Wayama, M., Goto, N., Katsuno, Y., Kawasaki, S., Nakajima, Y., Kajiro, M., Komatsu, Y., Fujimura, A., Hirota, R., Murayama, A., Kimura, K., Imamura, T. and Yanagisawa, J. (2010). "Estrogen inhibits transforming growth factor beta signaling by promoting Smad2/3 degradation." J Biol Chem **285**(19): 14747-14755.
- Itoh, S., Ericsson, J., Nishikawa, J., Heldin, C.H. and ten Dijke, P. (2000). "The transcriptional co-activator P/CAF potentiates TGF-beta/Smad signaling." Nucleic Acids Res **28**(21): 4291-4298.
- Jackson, M.R., Nilsson, T. and Peterson, P.A. (1990). "Identification of a consensus motif for retention of transmembrane proteins in the endoplasmic reticulum." EMBO J **9**(10): 3153-3162.
- Jakobi, R., McCarthy, C.C., Koepfel, M.A. and Stringer, D.K. (2003). "Caspase-activated PAK-2 is regulated by subcellular targeting and proteasomal degradation." J Biol Chem **278**(40): 38675-38685.
- Jalali, A., Zhu, X., Liu, C. and Nawshad, A. (2012). "Induction of palate epithelial mesenchymal transition by transforming growth factor beta3 signaling." Dev Growth Differ **54**(6): 633-648.
- Jarosch, E., Taxis, C., Volkwein, C., Bordallo, J., Finley, D., Wolf, D.H. and Sommer, T. (2002). "Protein dislocation from the ER requires polyubiquitination and the AAA-ATPase Cdc48." Nat Cell Biol **4**(2): 134-139.
- Jin, Q., Gao, G. and Mulder, K.M. (2009). "Requirement of a dynein light chain in TGFbeta/Smad3 signaling." J Cell Physiol **221**: 707-715.
- Jobling, M.F., Mott, J.D., Finnegan, M.T., Jurukovski, V., Erickson, A.C., Walian, P.J., Taylor, S.E., Ledbetter, S., Lawrence, C.M., Rifkin, D.B. and Barcellos-Hoff, M.H. (2006). "Isoform-specific activation of latent transforming growth factor beta (LTGF-beta) by reactive oxygen species." Radiat Res **166**(6): 839-848.
- Jones, F.E. (2008). "HER4 intracellular domain (4ICD) activity in the developing mammary gland and breast cancer." J Mammary Gland Biol Neoplasia **13**(2):

247-258.

- Jonk, L.J., Itoh, S., Heldin, C.H., ten Dijke, P. and Kruijer, W. (1998). "Identification and functional characterization of a Smad binding element (SBE) in the JunB promoter that acts as a transforming growth factor-beta, activin, and bone morphogenetic protein-inducible enhancer." J Biol Chem **273**(33): 21145-21152.
- Juan, H., Reddy, M.A., Sun, G., Lanting, L., Wang, M., Kato, M. and Natarajan, R. (2013). "Involvement of p300/CBP and epigenetic histone acetylation in TGF- β 1-mediated gene transcription in mesangial cells." Am J Physiol Renal Physiol **1**(304): F601-F613.
- Jungert, K., Buck, A., Buchholz, M., Wagner, M., Adler, G., Gress, T.M. and Ellenrieder, V. (2006). "Smad-Sp1 complexes mediate TGFbeta-induced early transcription of oncogenic Smad7 in pancreatic cancer cells." Carcinogenesis **27**(12): 2392-2401.
- Kaitu'u-Lino, T.J., Palmer, K.R., Whitehead, C.L., Williams, E., Lappas, M. and Tong, S. (2012). "MMP-14 is expressed in preeclamptic placentas and mediates release of soluble endoglin." Am J Pathol **180**(3): 888-894.
- Kamaraju, A.K. and Roberts, A.B. (2005). "Role of Rho/ROCK and p38 MAP kinase pathways in transforming growth factor-beta-mediated Smad-dependent growth inhibition of human breast carcinoma cells *in vivo*." J Biol Chem **280**(2): 1024-1036.
- Kamiya, Y., Miyazono, K. and Miyazawa, K. (2010). "Smad7 inhibits transforming growth factor-beta family type I receptors through two distinct modes of interaction." J Biol Chem **285**(40): 30804-30813.
- Kang, Y., Chen, C.R. and Massague, J. (2003). "A self-enabling TGFbeta response coupled to stress signaling: Smad engages stress response factor ATF3 for Id1 repression in epithelial cells." Mol Cell **11**(4): 915-926.
- Kang, Y., Chen, C.R. and Massagué, J. (2003). "A self-enabling TGFbeta response coupled to stress signaling: Smad engages stress response factor ATF3 for Id1 repression in epithelial cells." Mol Cell **11**(4): 915-926.
- Kasuga, K., Kaneko, H., Nishizawa, M., Onodera, O. and Ikeuchi, T. (2007). "Generation of intracellular domain of insulin receptor tyrosine kinase by gamma-secretase." Biochem Biophys Res Commun **360**(1): 90-96.
- Kato, Y., Habas, R., Katsuyama, Y., Naar, A.M. and He, X. (2002). "A component of the ARC/Mediator complex required for TGF beta/Nodal signalling." Nature **418**(6898): 641-646.
- Katsu, K., Tatsumi, N., Niki, D., Yamamura, K. and Yokouchi, Y. (2013). "Multi-modal effects of BMP signaling on Nodal expression in the lateral plate mesoderm

- during left-right axis formation in the chick embryo." Dev Biol **374**(1): 71-84.
- Kavsak, P., Rasmussen, R.K., Causing, C.G., Bonni, S., Zhu, H., Thomsen, G.H. and Wrana, J.L. (2000). "Smad7 binds to Smurf2 to form an E3 ubiquitin ligase that targets the TGF beta receptor for degradation." Mol Cell **6**(6): 1365-1375.
- Kershaw, R.M., Siddiqui, Y.H., Roberts, D., Jayaraman, P.S. and Gaston, K. (2014). "PRH/HHex inhibits the migration of breast and prostate epithelial cells through direct transcriptional regulation of Endoglin." Oncogene **33**(49): 5592-5600.
- Kim, S.I., Kwak, J.H., Na, H.J., Kim, J.K., Ding, Y. and Choi, M.E. (2009). "Transforming growth factor-beta (TGF-beta1) activates TAK1 via TAB1-mediated autophosphorylation, independent of TGF-beta receptor kinase activity in mesangial cells." J Biol Chem **284**(33): 22285-22296.
- Klein, D., Mendoza, V., Pileggi, A., Molano, R.D., Barbe-Tuana, F.M., Inverardi, L., Ricordi, C. and Pastori, R.L. (2005). "Delivery of TAT/PTD-fused proteins/peptides to islets via pancreatic duct." Cell Transplant **14**(5): 241-248.
- Knockaert, M., Sapkota, G., Alarcon, C., Massague, J. and Brivanlou, A.H. (2006). "Unique players in the BMP pathway: small C-terminal domain phosphatases dephosphorylate Smad1 to attenuate BMP signaling." Proc Natl Acad Sci U S A **103**(32): 11940-11945.
- Kobe, B. (1999). "Autoinhibition by an internal nuclear localization signal revealed by the crystal structure of mammalian importin alpha." Nat Struct Biol **6**(4): 388-397.
- Koenig, P. and Ploegh, H.L. (2014). "Protein quality control in the endoplasmic reticulum." F1000Prime Rep **6**.
- Koinuma, D., Tsutsumi, S., Kamimura, N., Imamura, T., Aburatani, H. and Miyazono, K. (2009). "Promoter-wide analysis of Smad4 binding sites in human epithelial cells." Cancer Sci **100**(11): 2133-2142.
- Koopmann, J.O., Albring, J., Hüter, E., Bulbuc, N., Spee, P., Neefjes, J. and Hämmerling, G.J. (2000). "Export of antigenic peptides from the endoplasmic reticulum intersects with retrograde protein translocation through the Sec61p channel." Immunity **13**(1): 117-127.
- Kretzschmar, M., Doody, J. and Massagué, J. (1997). "Opposing BMP and EGF signalling pathways converge on the TGF-beta family mediator Smad1." Nature **389**(6651): 618-622.
- Kroesen, M., Gielen, P., Brok, I.C., Armandari, I., Hoogerbrugge, P.M. and Adema, G.J. (2014). "HDAC inhibitors and immunotherapy; a double edged sword?" Oncotarget **5**(16): 6558-6572.
- Kuratomi, G., Komuro, A., Goto, K., Shinozaki, M., Miyazawa, K., Miyazono, K. and Imamura, T. (2005). "NEDD4-2 (neural precursor cell expressed,

- developmentally down-regulated 4-2) negatively regulates TGF-beta (transforming growth factor-beta) signalling by inducing ubiquitin-mediated degradation of Smad2 and TGF-beta type I receptor." Biochem J **386**(Pt 3): 461-470.
- Kurisaki, A., Kose, S., Yoneda, Y., Heldin, C.H. and Moustakas, A. (2001). "Transforming growth factor-beta induces nuclear import of Smad3 in an importin-beta1 and Ran-dependent manner." Mol Biol Cell **12**: 1079-1091.
- Kurisaki, A., Kurisaki, K., Kowanetz, M., Sugino, H., Yoneda, Y., Heldin, C.H. and Moustaka, s.A. (2006). "The mechanism of nuclear export of Smad3 involves exportin 4 and Ran." Mol Cell Biol **26**(4): 1318-1332.
- Labbe, E., Silvestri, C., Hoodless, P.A., Wrana, J.L. and Attisano, L. (1998). "Smad2 and Smad3 positively and negatively regulate TGF beta-dependent transcription through the forkhead DNA-binding protein FAST2." Mol Cell **2**: 109-120.
- Lack, J., O'Leary, J.M., Knott, V., Yuan, X., Rifkin, D.B., Handford, P.A. and Downing, A.K. (2003). "Solution structure of the third TB domain from LTBP1 provides insight into assembly of the large latent complex that sequesters latent TGF-beta." J Mol Biol **334**(2): 281-291.
- Ladinsky, M.S., Mastronarde, D.N., McIntosh, J.R., Howell, K.E. and Staehelin, L.A. (1999). "Golgi structure in three dimensions: functional insights from the normal rat kidney cell." J Cell Biol **144**(6): 1135-1149.
- Lange, A., Mills, R.E., Lange, C.J., Stewart, M., Devine, S.E. and Corbett, A.H. (2007). "Classical nuclear localization signals: definition, function, and interaction with importin alpha." J Biol Chem **282**(8): 5101-5105.
- Lanoix, J., Ouwendijk, J., Stark, A., Szafer, E., Cassel, D., Dejgaard, K., Weiss, M. and Nilsson, T. (2001). "Sorting of Golgi resident proteins into different subpopulations of COPI vesicles: a role for ArfGAP1." J Cell Biol **155**(7): 1199-1212. .
- Lee, K.B., Folger, J.K., Rajput, S.K. and Smith, G.W. (2014). "Temporal regulation of mRNAs for select bone morphogenetic proteins (BMP), BMP receptors and their associated SMAD proteins during bovine early embryonic development: effects of exogenous BMP2 on embryo developmental progression." Reprod Biol Endocrinol **12**: 67.
- Lee, N.Y., Ray, B., How, T. and Blobel, G.C. (2008). "Endoglin promotes transforming growth factor beta-mediated Smad 1/5/8 signaling and inhibits endothelial cell migration through its association with GIPC." J Biol Chem **283**(47): 32527-32533.
- Leonard, M., Song, B.D., Ramachandran, R. and Schmid, S.L. (2005). "Robust colorimetric assays for dynamin's basal and stimulated GTPase activities."

Methods Enzymol **404**: 490-503.

- Li, C.F., Fang, F.M., Wang, J.M., Tzeng, C.C., Tai, H.C., Wei, Y.C., Li, S.H., Lee, Y.T., Wang, Y.H., Yu, S.C., Shiue, Y.L., Chu, P.Y., Wang, W.L., Chen, L.T. and Huang, H.Y. (2012). "EGFR nuclear import in gallbladder carcinoma: nuclear phosphorylated EGFR upregulates iNOS expression and confers independent prognostic impact." Ann Surg Oncol **19**(2): 443-454.
- Li, C.W. and Ge, W. (2013). "Regulation of the activin-inhibin-follistatin system by bone morphogenetic proteins in the zebrafish ovary." Biol Reprod **89**(3): 55.
- Li, L., Xin, H., Xu, X., Huang, M., Zhang, X., Chen, Y., Zhang, S., Fu, X.Y. and Chang, Z. (2004). "CHIP mediates degradation of Smad proteins and potentially regulates Smad-induced transcription." Mol Cell Biol **24**(2): 856-864.
- Li, Z., Zhang, L.J., Zhang, H.R., Tian, G.F., Tian, J., Mao, X.L., Jia, Z.H., Meng, Z.Y., Zhao, L.Q., Yin, Z.N. and Wu, Z.Z. (2014). "Tumor-derived transforming growth factor-beta is critical for tumor progression and evasion from immune surveillance." Asian Pac J Cancer Prev **15**(13): 5181-5186.
- Liang, M., Liang, Y.Y., Wrighton, K., Ungermannova, D., Wang, X.P., Brunicardi, F.C., Liu, X., Feng, X.H. and Lin, X. (2004). "Ubiquitination and proteolysis of cancer-derived Smad4 mutants by SCFSkp2." Mol Cell Biol **24**(17): 7524-7537.
- Liao, H.J. and Carpenter, G. (2007). "Role of the Sec61 translocon in EGF receptor trafficking to the nucleus and gene expression." Mol Biol Cell **18**(3): 1064-1072.
- Lim, J., Park, S.J., Hwang, H., Park, E.J., Nam, J.H., Kim, J. and Park, S.I. (2005). "TGF- β 1 induces cardiac hypertrophic responses via PKC-dependent ATF-2 activation." J Mol Cell Cardiol **39**: 627-636.
- Lin, S.Y., Makino, K., Xia, W., Matin, A., Wen, Y., Kwong, K.Y., Bourguignon, L. and Hung, M.C. (2001). "Nuclear localization of EGF receptor and its potential new role as a transcription factor." Nat Cell Biol **3**(9): 802-808.
- Lin, X., Duan, X., Liang, Y., Su, Y., Wrighton, K.H., Long, J., Hu, M., Davis, C.M., Wang, J., Brunicardi, F.C., Shi, Y., Chen, Y., Meng, A. and Feng, X. (2006). "PPM1A functions as a Smad phosphatase to terminate TGF β signaling." Cell **125**: 915-928.
- Lipponen, P. and Eskelinen, M. (1994). "Expression of epidermal growth factor receptor in bladder cancer as related to established prognostic factors, oncoprotein (c-erbB-2, p53) expression and long-term prognosis." Br J Cancer **69**(6): 1120-1125.
- Litterst, C., Georgakopoulos, A., Shioi, J., Ghersi, E., Wisniewski, T., Wang, R., Ludwig, A. and Robakis, N.K. (2007). "Ligand binding and calcium influx induce distinct ectodomain/gamma-secretase-processing pathways of EphB2 receptor."

- J Biol Chem **282**(22): 16155-16163.
- Liu, X., Sun, Y., Constantinescu, S.N., Karam, E., Weinberg, R.A. and Lodish, H.F. (1997). "Transforming growth factor β -induced phosphorylation of Smad3 is required for growth inhibition and transcriptional induction in epithelial cells." Proc Natl Acad Sci U S A **94**: 10669-10674.
- Liu, Y., Wang, Z., Wang, J., Lam, W., Kwong, S., Li, F., Friedman, S.L., Zhou, S., Ren, Q., Xu, Z., Wang, X., Ji, L., Tang, S., Zhang, H., Lui, E.L. and Ye, T. (2013). "A histone deacetylase inhibitor, largazole, decreases liver fibrosis and angiogenesis by inhibiting transforming growth factor-beta and vascular endothelial growth factor signalling." Liver Int **33**(4): 504-515.
- Lo, H.W., Hsu, S.C., Ali-Seyed, M., Gunduz, M., Xia, W., Wei, Y., Bartholomeusz, G., Shih, J.Y. and Hung, M.C. (2005). "Nuclear interaction of EGFR and STAT3 in the activation of the iNOS/NO pathway." Cancer Cell **7**(6): 575-589.
- Lo, R.S. and Massague, J. (1999). "Ubiquitin-dependent degradation of TGF-beta-activated Smad2." Nat Cell Biol **1**(8): 472-478.
- Lo, R.S., Wotton, D. and Massague, J. (2001). "Epidermal growth factor signaling via Ras controls the Smad transcriptional co-repressor TGIF." EMBO J **20**(1-2): 128-136.
- Lombardi, D., Soldati, T., Riederer, M.A., Goda, Y., Zerial, M. and Pfeffer, S.R. (1993). "Rab9 functions in transport between late endosomes and the trans Golgi network." EMBO J **12**(2): 677-682.
- Luga, V., McLean, S., Le Roy, C., O'Connor-McCourt, M.D., Wrana, J.L. and Di Guglielmo, G.M. (2009). "The extracellular domain of the TGFbeta type II receptor regulates membrane raft partitioning." Biochem J **421**(1): 119-131.
- Lundmark, R. and Carlsson, S.R. (2009). "SNX9 - a prelude to vesicle release." J Cell Sci **122**: 5-11.
- Mandon, E.C., Trueman, S.F. and Gilmore, R. (2009). "Translocation of proteins through the Sec61 and SecYEG channels." Curr Opin Cell Biol **21**(4): 501-507.
- Mansfeld, J., Guttinger, S., Hawryluk-Gara, L.A., Pante, N., Mall, M., Galy, V., Haselmann, U., Muhlhauser, P., Wozniak, R.W., Mattaj, I.W., Kutay, U. and Antonin, W. (2006). "The conserved transmembrane nucleoporin NDC1 is required for nuclear pore complex assembly in vertebrate cells." Mol Cell **22**(1): 93-103.
- Marcías-Silva, M., Abdollah, S., Hoodless, P.A., Pirone, R., Attisano, L. and Wrana, J.L. (1996). "MADR2 is a substrate of the TGF β receptor and its phosphorylation is required for nuclear accumulation and signaling." Cell **87**: 1215-1224.
- Marioni, G., Marino, F., Giacomelli, L., Staffieri, C., Mariuzzi, M.L., Violino, E. and De

- Filippis, C. (2006). "Endoglin expression is associated with poor oncologic outcome in oral and oropharyngeal carcinoma." Acta Otolaryngol **126**(6): 633-639.
- Marron, M.B., Singh, H., Tahir, T.A., Kavumkal, J., Kim, H.Z., Koh, G.Y. and Brindle, N.P. (2007). "Regulated proteolytic processing of Tie1 modulates ligand responsiveness of the receptor-tyrosine kinase Tie2." J Biol Chem **282**(42): 30509-30517.
- Marsh, M. and Helenius, A. (2006). "Virus entry: open sesame." Cell **124**(4): 729-740.
- Marti, U., Ruchti, C., Kampf, J., Thomas, G.A., Williams, E.D., Peter, H.J., Gerber, H. and Burgi, U. (2001). "Nuclear localization of epidermal growth factor and epidermal growth factor receptors in human thyroid tissues." Thyroid **11**(2): 137-145.
- Massague, J. (2003). "Integration of Smad and MAPK pathways: a link and a linker revisited." Genes Dev **17**(24): 2993-2997.
- Massagué, J. (1998). "TGF-beta signal transduction. ." Annu Rev Biochem **67**: 753-791.
- Massague, J., Seoane, J. and Wotton, D. (2005). "Smad transcription factors." Genes Dev **19**: 2783-2810.
- Matlack, K.E., Mothes, W. and Rapoport, T.A. (1998). "Protein translocation: tunnel vision." Cell **92**(3): 381-390.
- Matsumura, N., Huang, Z., Mori, S., Baba, T., Fujii, S., Konishi, I., Iversen, E.S., Berchuck, A. and S.K., M. (2011). "Epigenetic suppression of the TGF-beta pathway revealed by transcriptome profiling in ovarian cancer." Genome Res **21**: 74-82.
- Matsuura, I., Denissova, N.G., Wang, G., He, D., Long, J. and Liu, F. (2004). "Cyclin-dependent kinases regulate the antiproliferative function of Smads." Nature **430**(6996): 226-231.
- Matsuura, I., Wang, G., He, D. and Liu, F. (2005). "Identification and characterization of ERK MAP kinase phosphorylation sites in Smad3." Biochemistry **44**: 12546-12553.
- Mayor, S. and Pagano, R.E. (2007). "Pathways of clathrin-independent endocytosis." Nat Rev Mol Cell Biol **8**(8): 603-612.
- McMahon, J.A., Takada, S., Zimmerman, L.B., Fan, C.M., Harland, R.M. and McMahon, A.P. (1998). "Noggin-mediated antagonism of BMP signaling is required for growth and patterning of the neural tube and somite." Genes Dev **12**(10): 1438-1452.
- McNiven, M.A. (1998). "Dynamin: a molecular motor with pinchase action." Cell **94**(2):

151-154.

- Meng, X.M., Huang, X.R., Chung, A.C., Qin, W., Shao, X., Igarashi, P., Ju, W., Bottinger, E.P. and Lan, H.Y. (2010). "Smad2 protects against TGF-beta/Smad3-mediated renal fibrosis." J Am Soc Nephrol **21**: 1477-1487.
- Meyer, H.A., Grau, H., Kraft, R., Kostka, S., Prehn, S., Kalies, K.U. and Hartmann, E. (2000). "Mammalian Sec61 is associated with Sec62 and Sec63." J Biol Chem **275**(19): 14550-14557.
- Meyers-Wallen, V.N., Lee, M.M., Manganaro, T.F., Kuroda, T., Maclaughlin, D. and Donahoe, P.K. (1993). "Mullerian inhibiting substance is present in embryonic testes of dogs with persistent mullerian duct syndrome." Biol Reprod **48**(6): 1410-1418.
- Mine, N., Anderson, R.M. and Klingensmith, J. (2008). "BMP antagonism is required in both the node and lateral plate mesoderm for mammalian left-right axis establishment." Development **135**(14): 2425-2434.
- Mitchell, H., Choudhury, A., Pagano, R.E. and Leof, E.B. (2004). "Ligand-dependent and -independent transforming growth factor-beta receptor recycling regulated by clathrin-mediated endocytosis and Rab11." Mol Biol Cell **15**(9): 4166-4178.
- Mitsui, H., Shibata, K., Mano, Y., Suzuki, S., Umezumi, T., Mizuno, M., Yamamoto, E., Kajiyama, H., Kotani, T., Senga, T. and Kikkawa, F. (2013). "The expression and characterization of endoglin in uterine leiomyosarcoma." Clin Exp Metastasis **30**(6): 731-740.
- Miyazono, K. (2000). "Positive and negative regulation of TGF-beta signaling." J Cell Sci **113** (Pt 7): 1101-1109.
- Miyazono, K., Ichijo, H. and Heldin, C.H. (1993). "Transforming growth factor-beta: latent forms, binding proteins and receptors." Growth Factors **8**(1): 11-22.
- Miyazono, K., Kamiya, Y. and Morikawa, M. (2010). "Bone morphogenetic protein receptors and signal transduction." J Biochem **147**(1): 35-51.
- Moremen, K.W., Tiemeyer, M. and Nairn, A.V. (2012). "Vertebrate protein glycosylation: diversity, synthesis and function." Nat Rev Mol Cell Biol **13**(7): 448-462.
- Moren, A., Imamura, T., Miyazono, K., Heldin, C.H. and Moustakas, A. (2005). "Degradation of the tumor suppressor Smad4 by WW and HECT domain ubiquitin ligases." J Biol Chem **280**(23): 22115-22123.
- Morris, D.G., Huang, X., Kaminski, N., Wang, Y., Shapiro, S.D., Dolganov, G., Glick, A. and Sheppard, D. (2003). "Loss of integrin alpha(v)beta6-mediated TGF-beta activation causes Mmp12-dependent emphysema." Nature **422**(6928): 169-173.
- Mosammaparast, N. and Pemberton, L.F. (2004). "Karyopherins: from nuclear-

- transport mediators to nuclear-function regulators." Trends Cell Biol **14**(10): 547-556.
- Moses, H.L., Branum, E.L., Proper, J.A. and Robinson, R.A. (1981). "Transforming growth factor production by chemically transformed cells." Cancer Res. **41**: 2842-2848.
- Moustakas, A. and Heldin, C.H. (2008). "Dynamic control of TGF-beta signaling and its links to the cytoskeleton." FEBS Lett **582**: 2051-2065.
- Mu, Y., Sundar, R., Thakur, N., Ekman, M., Gudey, S.K., Yakymovych, M., Hermansson, A., Dimitriou, H., Bengoechea-Alonso, M.T., Ericsson, J., Heldin, C.H. and Landström, M. (2011). "TRAF6 ubiquitinates TGFβ type I receptor to promote its cleavage and nuclear translocation in cancer." Nat Commun **2**: 330.
- Mulder, K.M. (2000). "Role of Ras and Mapks in TGFβ signaling." Cytokine Growth Factor Rev **11**: 23-25.
- Mulder, K.M. and Morris, S.L. (1992). "Activation of p21ras by transforming growth factor beta in epithelial cells." J Biol Chem **267**(8): 5029-5031.
- Mullen, A.C., Orlando, D.A., Newman, J.J., Lovén, J., Kumar, R.M., Bilodeau, S., Reddy, J., Guenther, M.G., DeKoter, R.P. and Young, R.A. (2011). "Master transcription factors determine cell-type-specific responses to TGF-β signaling." Cell **147**: 565-576.
- Munger, J.S. and Sheppard, D. (2011). "Cross talk among TGF-beta signaling pathways, integrins, and the extracellular matrix." Cold Spring Harb Perspect Biol **3**(11): a005017.
- Nagarajan, R.P., Chen, F., Li, W., Vig, E., Harrington, M.A., Nakshatri, H. and Chen, Y. (2000). "Repression of transforming-growth-factor-beta-mediated transcription by nuclear factor kappaB." Biochem J **348 Pt 3**: 591-596.
- Nakatsukasa, K. and Brodsky, J.L. (2008). "The recognition and retrotranslocation of misfolded proteins from the endoplasmic reticulum." Traffic. **9**(6): 861-870. .
- Ng, W., Sergeyenko, T., Zeng, N., Brown, J.D. and Romisch, K. (2007). "Characterization of the proteasome interaction with the Sec61 channel in the endoplasmic reticulum." J Cell Sci **120**(Pt 4): 682-691.
- Nicolas, F.J., De Bosscher, K., Schmierer, B. and Hill, C.S. (2004). "Analysis of Smad nucleocytoplasmic shuttling in living cells." J Cell Sci **117**: 4113-4125.
- Nolan, K. and Thompson, T.B. (2014). "The DAN family: modulators of TGF-beta signaling and beyond." Protein Sci **23**(8): 999-1012.
- O.H., G. and Gurdon, J.B. (2002). "Nuclear exclusion of Smad2 is a mechanism leading to loss of competence." Nat Cell Biol **4**: 519-522.
- Ohtsubo, M., Okazaki, H. and Nishimoto, T. (1989). "The RCC1 protein, a regulator for

- the onset of chromosome condensation locates in the nucleus and binds to DNA." J Cell Biol **109**(4 Pt 1): 1389-1397.
- Orth, J.D., Krueger, E.W., Weller, S.G. and McNiven, M.A. (2006). "A novel endocytic mechanism of epidermal growth factor receptor sequestration and internalization." Cancer Res **66**(7): 3603-3610.
- Ostermann, J., Orci, L., Tani, K., Amherdt, M., Ravazzola, M., Elazar, Z. and Rothman, J.E. (1993). "Stepwise assembly of functionally active transport vesicles." Cell **75**(5): 1015-1025.
- Panopoulou, E., Gillyooly, D.J., Wrana, J.L., Zerial, M., Stenmark, H., Murphy, C. and Fotsis, T. (2002). "Early endosomal regulation of Smad-dependent signaling in endothelial cells." J Biol Chem **277**(20): 18046-18052.
- Pappa, C.A., Alexandrakis, M.G., Boula, A., Psarakis, F.E., Kolovou, A., Bantouna, V., Stavroulaki, E. and Tsirakis, G. (2013). "Emerging roles of endoglin/CD105 and angiogenic cytokines for disease development and progression in multiple myeloma patients." Hematol Oncol **31**(4): 201-205.
- Parks, W.T., Frank, D.B., Huff, C., Renfrew Haft, C., Martin, J., Meng, X., de Caestecker, M.P., McNally, J.G., Reddi, A., Taylor, S.I., Roberts, A.B., Wang, T. and Lechleider, R.J. (2001). "Sorting nexin 6, a novel SNX, interacts with the transforming growth factor-beta family of receptor serine-threonine kinases." J Biol Chem **276**: 19332-19339.
- Patel, S.S., Belmont, B.J., Sante, J.M. and Rexach, M.F. (2007). "Natively unfolded nucleoporins gate protein diffusion across the nuclear pore complex." Cell **129**(1): 83-96.
- Penheiter, S.G., Mitchell, H., Garamszegi, N., Edens, M., Dore Jr, J.J. and Leof, E.B. (2002). "Internalization-dependent and -independent requirements for transforming growth factor beta receptor signaling via the Smad pathway." Mol Cell Biol **22**(13): 4750-4759.
- Perusina Lanfranca, M., Mostafa, H.H. and Davido, D.J. (2013). "Two overlapping regions within the N-terminal half of the herpes simplex virus 1 E3 ubiquitin ligase ICP0 facilitate the degradation and dissociation of PML and dissociation of Sp100 from ND10." J Virol **87**(24): 13287-13296.
- Piccolo, S., Sasai, Y., Lu, B. and De Robertis, E.M. (1996). "Dorsoventral patterning in *Xenopus*: inhibition of ventral signals by direct binding of chordin to BMP-4." Cell **86**(4): 589-598.
- Piek, E., Heldin, C.H. and Ten Dijke, P. (1999). "Specificity, diversity, and regulation in TGF-beta superfamily signaling." FASEB J **13**(15): 2105-2124.
- Pierreux, C.E., Nicolas, F.J. and Hill, C.S. (2000). "Transforming growth factor beta-

- independent shuttling of Smad4 between the cytoplasm and nucleus." Mol Cell Biol **20**(23): 9041-9054.
- Poncelet, A.C. and Schnaper, H.W. (2001). "Sp1 and Smad proteins cooperate to mediate transforming growth factor-beta 1-induced alpha 2(I) collagen expression in human glomerular mesangial cells." J Biol Chem **276**(10): 6983-6992.
- Pouponnot, C., Jayaraman, L. and Massagué, J. (1998). "Physical and functional interaction of SMADs and p300/CBP." J Biol Chem **273**(36): 22865-22868.
- Psyrrri, A., Yu, Z., Weinberger, P.M., Sasaki, C., Haffty, B., Camp, R., Rimm, D. and Burtness, B.A. (2005). "Quantitative determination of nuclear and cytoplasmic epidermal growth factor receptor expression in oropharyngeal squamous cell cancer by using automated quantitative analysis." Clin Cancer Res **11**(16): 5856-5862.
- Pusch, S., Dissmeyer, N. and Schnittger, A. (2011). "Bimolecular-fluorescence complementation assay to monitor kinase-substrate interactions *in vivo*." Methods Mol Biol **779**: 245-257.
- Qu, X., Li, X., Zheng, Y., Ren, Y., Puelles, V.G., Caruana, G., Nikolic-Paterson, D.J. and Li, J. (2014). "Regulation of renal fibrosis by Smad3 Thr388 phosphorylation." Am J Pathol **184**: 944-952.
- Rahimi, R.A. and Leof, E.B. (2007). "TGF-beta signaling: A tale of two responses." J Cell Biochem **102**: 593-608.
- Rapoport, T.A. (2008). "Protein transport across the endoplasmic reticulum membrane." FEBS J **275**(18): 4471-4478.
- Restrepo, R., Zhao, X., Peter, H., Zhang, B.Y., Arvan, P. and Nothwehr, S.F. (2007). "Structural features of vps35p involved in interaction with other subunits of the retromer complex." Traffic **8**(12): 1841-1853.
- Ribbeck, K. and Gorlich, D. (2001). "Kinetic analysis of translocation through nuclear pore complexes." EMBO J **20**(6): 1320-1330.
- Roberts, A.B., and Wakefield, L.M. (2003). "The two faces of transforming growth factor b in carcinogenesis." Proc Natl Acad Sci U S A **100**: 8621-8623.
- Roberts, A.B., Anzano, M.A., Lamb, L.C., Smith, J.M. and Sporn, M.B. (1981). "New class of transforming growth factors potentiated by epidermal growth factors: Isolation from non-neoplastic tissues." Proc Natl Acad Sci USA **78**: 5339-5343.
- Rodriguez Esteban, C., Capdevila, J., Economides, A.N., Pascual, J., Ortiz, A. and Izpisua Belmonte, J.C. (1999). "The novel Cer-like protein Caronte mediates the establishment of embryonic left-right asymmetry." Nature **401**(6750): 243-251.
- Roelen, B.A., Cohen, O.S., Raychowdhury, M.K., Chadee, D.N., Zhang, Y., Kyriakis,

- J.M., Alessandrini, A.A. and Lin, H.Y. (2003). "Phosphorylation of threonine 276 in Smad4 is involved in transforming growth factor-beta-induced nuclear accumulation." Am J Physiol Cell Physiol **285**(4): C823-830.
- Rogge, G., Shen, L.L. and Kuhar, M.J. (2010). "Chromatin immunoprecipitation assays revealed CREB and serine 133 phospho-CREB binding to the CART gene proximal promoter." Brain Res **1344**: 1-12.
- Roig, J. and Traugh, J.A. (2001). "Cytostatic p21 G protein-activated protein kinase gamma-PAK." Vitam Horm **62**: 167-198.
- Roig, J., Tuazon, P.T., Zipfel, P.A., Pendergast, A.M. and Traugh, J.A. (2000). "Functional interaction between c-Abl and the p21-activated kinase gamma-PAK." Proc Natl Acad Sci U S A **97**: 14346-14351.
- Rombouts, K. and Carloni, V. (2013). "The fibrotic microenvironment as a heterogeneity facet of hepatocellular carcinoma." Fibrogenesis Tissue Repair **6**(1): 17.
- Ross, S. and Hill, C.S. (2008). "How the Smads regulate transcription." Int J Biochem Cell Biol **40**: 383-408.
- Ruggiano, A., Foresti, O. and Carvalho, P. (2014). "Quality control: ER-associated degradation: protein quality control and beyond." J Cell Biol **204**(6): 869-879.
- Samuel, G., Miller, D. and Saint, R. (2001). "Conservation of a DPP/BMP signaling pathway in the nonbilateral cnidarian *Acropora millepora*." Evol Dev **3**(4): 241-250.
- Santiago, B., Gutierrez-Cañas, I., Dotor, J., Palao, G., Lasarte, J.J., Ruiz, J., Prieto, J., Borrás-Cuesta, F. and Pablos, J.L. (2005). "Topical application of a peptide inhibitor of transforming growth factor-beta1 ameliorates bleomycin-induced skin fibrosis." J Invest Dermatol **125**(3): 450-455.
- Santibañez, J.F. (2006). "JNK mediates TGF-beta1-induced epithelial mesenchymal transdifferentiation of mouse transformed keratinocytes." FEBS Lett **580**(22): 5385-5391.
- Santibanez, J.F., Quintanilla, M. and Bernabeu, C. (2011). "TGF-beta/TGF-beta receptor system and its role in physiological and pathological conditions." Clin Sci (Lond) **121**(6): 233-251.
- Sapkota, G., Alarcon, C., Spagnoli, F.M., Brivanlou, A.H. and Massague, J. (2007). "Balancing BMP signaling through integrated inputs into the Smad1 linker." Mol Cell **25**(3): 441-454.
- Sapkota, G., Knockaert, M., Alarcon, C., Montalvo, E., Brivanlou, A.H. and Massague, J. (2006). "Dephosphorylation of the linker regions of Smad1 and Smad2/3 by small C-terminal domain phosphatases has distinct outcomes for bone

- morphogenetic protein and transforming growth factor-beta pathways." J Biol Chem **281**(52): 40412-40419.
- Sardi, S.P., Murtie, J., Koirala, S., Patten, B.A. and Corfas, G. (2006). "Presenilin-dependent ErbB4 nuclear signaling regulates the timing of astrogenesis in the developing brain." Cell **127**(1): 185-197.
- Sariola, H. and Saarma, M. (2003). "Novel functions and signalling pathways for GDNF." J Cell Sci **116**(Pt 19): 3855-3862.
- Sato, M., Matsuda, Y., Wakai, C., Kubota, M., Osawa, M., Fujimaki, S., Sanpei, A., M. Takamura, M., Yamagiwa, S. and Aoyagi, Y. (2013). "p21-activated kinase-2 is a critical mediator of transforming growth factor- β -induced hepatoma cell migration." J Gastroenterol Hepatol **28**: 1047-1055.
- Scherner, O., Meurer, S.K., Tihaa, L., Gressner, A.M. and Weiskirchen, R. (2007). "Endoglin differentially modulates antagonistic transforming growth factor-beta1 and BMP-7 signaling." J Biol Chem **282**(19): 13934-13943.
- Schmierer, B., and Hill, C.S. (2007). "TGFbeta-SMAD signal transduction: molecular specificity and functional flexibility. ." Nat Rev Mol Cell Biol **8**: 970-982.
- Schmierer, B., Tournier, A.L., Bates, P.A., and Hill, C.S. (2008). "Mathematical modeling identifies Smad nucleocytoplasmic shuttling as a dynamic signal-interpreting system. ." Proc Natl Acad Sci U S A **105**: 6608-6613.
- Schmierer, B. and Hill, C.S. (2005). "Kinetic analysis of Smad nucleocytoplasmic shuttling reveals a mechanism for transforming growth factor beta-dependent nuclear accumulation of Smads." Mol Cell Biol **25**: 9845-9858.
- Schmitz, A., Herrgen, H., Winkeler, A. and Herzog, V. (2000). "Cholera toxin is exported from microsomes by the Sec61p complex." J Cell Biol **148**(6): 1203-1212.
- Schnell, D.J. and Hebert, D.N. (2003). "Protein translocons: multifunctional mediators of protein translocation across membranes." Cell **112**(4): 491-505.
- Sekiya, T., Adachi, S., Kohu, K., Yamada, T., Higuchi, O., Furukawa, Y., Nakamura, Y., Nakamura, T., Tashiro, K., Kuhara, S., Ohwada, S. and Akiyama, T. (2004). "Identification of BMP and activin membrane-bound inhibitor (BAMBI), an inhibitor of transforming growth factor-beta signaling, as a target of the beta-catenin pathway in colorectal tumor cells." J Biol Chem **279**(8): 6840-6846.
- Seoane, J., Le, H.V., Shen, L., Anderson, S.A. and Massague, J. (2004). "Integration of Smad and forkhead pathways in the control of neuroepithelial and glioblastoma cell proliferation." Cell **117**(2): 211-223.
- Sflomos, G., Kostaras, E., Panopoulou, E., Pappas, N., Kyrkou, A., Politou, A.S., Fotsis, T. and Murphy, C. (2011). "Erbin is a new SARA-interacting protein:

- competition between SARA and Smad2 and Smad3 for binding to erbin." J Cell Sci **124**: 3209-3222.
- Shah, S., Lee, S.F., Tabuchi, K., Hao, Y.H., Yu, C., LaPlant, Q., Ball, H., Dann, C.E., 3rd, Sudhof, T. and Yu, G. (2005). "Nicastrin functions as a gamma-secretase-substrate receptor." Cell **122**(3): 435-447.
- Shah, Z.H., Jones, D.R., Sommer, L., Foulger, R., Bultsma, Y., D'Santos, C. and Divecha, N. (2013). "Nuclear phosphoinositides and their impact on nuclear functions." FEBS J **280**(24): 6295-6310.
- Shav-Tal, Y. and Zipori, D. (2002). "The role of activin a in regulation of hemopoiesis." Stem Cells **20**(6): 493-500.
- Shi, W., Sun, C., He, B., Xiong, W., Shi, X., Yao, D. and Cao, X. (2004). "GADD34-PP1c recruited by Smad7 dephosphorylates TGFbeta type I receptor." J Cell Biol **164**(2): 291-300.
- Shi, Y. (2001). "Structural insights on Smad functions in TGFβ signaling." BioEssays **23**: 223-232.
- Shi, Y., Hata, A., Lo, R.S., Massagué, J. and Pavletich, N.P. (1997). "A structural basis for mutational inactivation of the tumour suppressor Smad4." Nature **388**(6637): 87-93.
- Shi, Y. and Massagué, J. (2003). "Mechanisms of TGF-beta signaling from cell membrane to the nucleus." Cell **113**(6): 685-700.
- Shi, Y., Wang, Y.F., Jayaraman, L., Yang, H., Massagué, J. and Pavletich, N.P. (1998). "Crystal structure of a Smad MH1 domain bound to DNA: insights on DNA binding in TGF-beta signaling." Cell **94**(5): 585-594.
- Shimizu, K., Bourillot, P.Y., Nielsen, S.J., Zorn, A.M. and Gurdon, J.B. (2001). "Swift is a novel BRCT domain coactivator of Smad2 in transforming growth factor beta signaling." Mol Cell Biol **21**(12): 3901-3912.
- Shin, N., Ahn, N., Chang-Ileto, B., Park, J., Takei, K., Ahn, S.G., Kim, S.A., Di Paolo, G. and Chang, S. (2008). "SNX9 regulates tubular invagination of the plasma membrane through interaction with actin cytoskeleton and dynamin 2." J Cell Sci **121**: 1252-1263.
- Shin, N., Lee, S., Ahn, N., Kim, S.A., Ahn, S.G., YongPark, Z. and Chang, S. (2007). "Sorting nexin 9 interacts with dynamin 1 and N-WASP and coordinates synaptic vesicle endocytosis." J Biol Chem **282**(39): 28939-28950.
- Shioda, T., Lechleider, R.J., Dunwoodie, S.L., Li, H., Yahata, T., de Caestecker, M.P., Fenner, M.H., Roberts, A.B. and Isselbacher, K.J. (1998). "Transcriptional activating activity of Smad4: roles of SMAD hetero-oligomerization and enhancement by an associating transactivator." Proc Natl Acad Sci U S A **95**(17):

9785-9790.

- Simonsson, M., Heldin, C.H., Ericsson, J. and Gronroos, E. (2005). "The balance between acetylation and deacetylation controls Smad7 stability." J Biol Chem **280**(23): 21797-21803.
- Sirard, C., Kim, S., Mirtsos, C., Tadich, P., Hoodless, P.A., Itie, A., Maxson, R., Wrana, J.L. and Mak, T.W. (2000). "Targeted disruption in murine cells reveals variable requirement for Smad4 in transforming growth factor beta-related signaling." J Biol Chem **275**(3): 2063-2070.
- Siu, M.K., Wong, E.S., Chan, H.Y., Kong, D.S., Woo, N.W.S., Tam, K.F., Ngan, H.Y., Chan, Q.K., Chan, D.C., Chan, K.Y. and Cheung, A.N. (2009). "Differential expression and phosphorylation of Pak1 and Pak2 in ovarian cancer; effects on prognosis and cell invasion." Int J Cancer **127**: 21-31.
- Sohn, K., Orci, L., Ravazzola, M., Amherdt, M., Bremser, M., Lottspeich, F., Fiedler, K., Helms, J.B. and Wieland, F.T. (1996). "A major transmembrane protein of Golgi-derived COPI-coated vesicles involved in coatamer binding." J Cell Biol **135**(5): 1239-1248.
- Song, B.D., Yarar, D. and Schmid, S.L. (2004). "An assembly-incompetent mutant establishes a requirement for dynamin self-assembly in clathrin-mediated endocytosis *in vivo*." Mol Biol Cell **15**: 2243-2252.
- Sönnichsen, B., Watson, R., Clausen, H., Misteli, T. and Warren, G. (1996). "Sorting by COP I-coated vesicles under interphase and mitotic conditions." J Cell Biol **134**(6): 1411-1425.
- Soond, S.M. and Chantry, A. (2011). "Selective targeting of activating and inhibitory Smads by distinct WWP2 ubiquitin ligase isoforms differentially modulates TGFbeta signalling and EMT." Oncogene **30**(21): 2451-2462.
- Sorkin, A. (2004). "Cargo recognition during clathrin-mediated endocytosis: a team effort." Curr Opin Cell Biol **16**(4): 392-399.
- Sorkin, A. and Goh, L.K. (2009). "Endocytosis and intracellular trafficking of ErbBs." Exp Cell Res **315**(4): 683-696.
- Soulet, F., Yarar, D., Leonard, M. and Schmid, S.L. (2005). "SNX9 regulates dynamin assembly and is required for efficient clathrin-mediated endocytosis." Mol Biol Cell **16**(4): 2058-2067.
- Stabile, H., Mitola, S., Moroni, E., Belleri, M., Nicoli, S., Coltrini, D., Peri, F., Pessi, A., Orsatti, L., Talamo, F., Castronovo, V., Waltregny, D., Cotelli, F., Ribatti, D. and Presta, M. (2007). "Bone morphogenic protein antagonist Drm/gremlin is a novel proangiogenic factor." Blood **109**(5): 1834-1840.
- Starczynowski, D.T., Lockwood, W.W., Delehouzee, S., Chari, R., Wegryzn, J., Fuller,

- M., Tsao, M.S., Lam, S., Gazdar, A.F., Lam, W.L. and Karsan, A. (2011). "TRAF6 is an amplified oncogene bridging the RAS and NF-kappaB pathways in human lung cancer." J Clin Invest **121**(10): 4095-4105.
- Stepanov, V.A. (2010). "Genomes, populations and diseases: ethnic genomics and personalized medicine." Acta Naturae **2**(4): 15-30.
- Strom, A.C. and Weis, K. (2001). "Importin-beta-like nuclear transport receptors." Genome Biol **2**: REVIEWS3008.
- Sun, H., Li, X., Fan, L., Wu, G., Li, M. and Fang, J. (2014). "TRAF6 is upregulated in colon cancer and promotes proliferation of colon cancer cells." Int J Biochem Cell Biol **53**: 195-201.
- Sun, Y., Liu, X., Eaton, E.N., Lane, W.S., Lodish, H.F. and Weinberg, R.A. (1999). "Interaction of the Ski oncoprotein with Smad3 regulates TGF-beta signaling." Mol Cell **4**(4): 499-509.
- Sundqvist, A., Zieba, A., Vasilaki, E., Herrera Hidalgo, C., Söderberg, O., Koinuma, D., Miyazono, K., Heldin, C.H., Landegren, U., Ten Dijke, P. and van Dam, H. (2013). "Specific interactions between Smad proteins and AP-1 components determine TGFβ-induced breast cancer cell invasion." Oncogene **32**(31): 3606-3615.
- Suzuki, K., Kobayashi, T., Funatsu, O., Morita, A. and Ikekita, M. (2010). "Activin A induces neuronal differentiation and survival via ALK4 in a SMAD-independent manner in a subpopulation of human neuroblastomas." Biochem Biophys Res Commun **394**(3): 639-645.
- Suzuki, K., Wilkes, M.C., Garamszegi, N., Edens, M. and Leof, E.B. (2007). "Transforming growth factor beta signaling via Ras in mesenchymal cells requires p21-activated kinase 2 for extracellular signal-regulated kinase-dependent transcriptional responses." Cancer Res **67**(8): 3673-3682.
- Suzuki, M., Shigematsu, H., Shames, D.S., Sunaga, N., Takahashi, T., Shivapurkar, N., Lizasa, T., Frenkel, E.P., Minna, J.D., Fujisawa, T. and Gazdar, A.F. (2005). "DNA methylation-associated inactivation of TGFβ-related genes DRM/Gremlin, RUNX3, and HPP1 in human cancers." Br J Cancer **93**: 1029-1037.
- Taketo, T., Saeed, J., Manganaro, T., Takahashi, M. and Donahoe, P.K. (1993). "Mullerian inhibiting substance production associated with loss of oocytes and testicular differentiation in the transplanted mouse XX gonadal primordium." Biol Reprod **49**(1): 13-23.
- Tamiya, T., Ichiyama, K., Kotani, H., Fukaya, T., Sekiya, T., Shichita, T., Honma, K., Yui, K., Matsuyama, T., Nakao, T., Fukuyama, S., Inoue, H., Nomura, M. and Yoshimura, A. (2013). "Smad2/3 and IRF4 play a cooperative role in IL-9-

- producing T cell induction." J Immunol **191**(5): 2360-2371.
- Tervahauta, A., Syrjanen, S. and Syrjanen, K. (1994). "Epidermal growth factor receptor, c-erbB-2 proto-oncogene and estrogen receptor expression in human papillomavirus lesions of the uterine cervix." Int J Gynecol Pathol **13**(3): 234-240.
- Topper, J.N., DiChiara, M.R., Brown, J.D., Williams, A.J., Falb, D., Collins, T. and Gimbrone Jr, M.A. (1998). "CREB binding protein is a required coactivator for Smad-dependent, transforming growth factor beta transcriptional responses in endothelial cells." Proc Natl Acad Sci U S A **95**(16): 9506-9511.
- Tran, N.D., Correale, J., Schreiber, S.S. and Fisher, M. (1999). "Transforming growth factor-beta mediates astrocyte-specific regulation of brain endothelial anticoagulant factors." Stroke **30**(8): 1671-1678.
- Tsai, B. and Rapoport, T.A. (2002). "Unfolded cholera toxin is transferred to the ER membrane and released from protein disulfide isomerase upon oxidation by Ero1." J Cell Biol **159**(2): 207-216.
- Tuazon, P.T., Spanos, W.C., Gump, E.L., Monnig, C.A. and Traugh, J.A. (1997). "Determinants for substrate phosphorylation by p21-activated protein kinase (gamma-PAK)." Biochemistry **36**: 16059-16064.
- Varelas, X., Sakuma, R., Samavarchi-Tehrani, P., Peerani, R., Rao, B.M., Dembowy, J., Yaffe, M.B., Zandstra, P.W. and Wrana, J.L. (2008). "TAZ controls Smad nucleocytoplasmic shuttling and regulates human embryonic stem-cell self-renewal." Nat Cell Biol **10**: 837-848.
- Vecchi, M., Baulida, J. and Carpenter, G. (1996). "Selective cleavage of the heregulin receptor ErbB-4 by protein kinase C activation." J Biol Chem **271**(31): 18989-18995.
- Verges, M. (2007). "Retromer and sorting nexins in development." Front Biosci **12**: 3825-3851.
- von Mikecz, A., Chen, M., Rockel, T. and Scharf, A. (2008). "The nuclear ubiquitin-proteasome system: visualization of proteasomes, protein aggregates, and proteolysis in the cell nucleus." Methods Mol Biol **463**: 191-202.
- Wain, K.E., Ellingson, M.S., McDonald, J., Gammon, A., Roberts, M., Pichurin, P., Winship, I., Riegert-Johnson, D.L., Weitzel, J.N. and Lindor, N.M. (2014). "Appreciating the broad clinical features of SMAD4 mutation carriers: a multicenter chart review." Genet Med **16**(8): 588-593.
- Wang, G., Matsuura, I., He, D. and Liu, F. (2009). "Transforming Growth Factor- β -inducible phosphorylation of Smad3." J Biol Chem **284**: 9663-9673.
- Wang, S., Wilkes, M.C., Leof, E.B., Hirschberg, R. (2009). "Noncanonical TGF- β pathways, mTORC1 and Abl, in renal interstitial fibrogenesis." Am J Physiol

- Renal Physiol **298**: F142-F149.
- Wang, S., Wilkes, M.C., Leof, E.B. and Hirschberg, R. (2005). "Imatinib mesylate blocks a non-Smad TGF- β pathway and reduces renal fibrogenesis *in vivo*." FASEB Journal **19**: 1-11.
- Wang, Y.N. and Hung, M.C. (2012). "Nuclear functions and subcellular trafficking mechanisms of the epidermal growth factor receptor family." Cell Biosci **2**(1): 13.
- Wang, Y.N., Lee, H.H., Lee, H.J., Du, Y., Yamaguchi, H. and Hung, M.C. (2012). "Membrane-bound trafficking regulates nuclear transport of integral epidermal growth factor receptor (EGFR) and ErbB-2." J Biol Chem **287**(20): 16869-16879.
- Wang, Y.N., Wang, H., Yamaguchi, H., Lee, H.J., Lee, H.H. and Hung, M.C. (2010). "COPI-mediated retrograde trafficking from the Golgi to the ER regulates EGFR nuclear transport." Biochem Biophys Res Commun **399**(4): 498-504.
- Warner, D.R., Bhattacharjee, V., Yin, X., Singh, S., Mukhopadhyay, P., Pisano, M.M. and Greene, R.M. (2004). "Functional interaction between Smad, CREB binding protein, and p68 RNA helicase." Biochem Biophys Res Commun **324**(1): 70-76.
- Weiss, A. and Attisano, L. (2013). "The TGF β superfamily signaling pathway." Wiley Interdiscip Rev Dev Biol **2**(1): 47-63.
- Wilkes, M.C., Repellin, C.E., Hong, M., Bracamonte, M., Penheiter, S.G., Borg, J.P., Leof, E.B. (2009). "Erbin and the NF2 Tumor Suppressor Merlin Cooperatively Regulate Cell Type-specific Activation of PAK2 by TGF- β ." Dev Cell **16**: 433-444.
- Wilkes, M.C. and Leof, E.B. (2006). "Transforming growth factor beta activation of c-Abl is independent of receptor internalization and regulated by phosphatidylinositol 3-kinase and PAK2 in mesenchymal cultures." J Biol Chem **281**(38): 27846-27854.
- Wilkes, M.C., Mitchell, H., Penheiter, S.G., Dore Jr, J.J., Suzuki, K., Edens, M., Sharma, D.K., Pagano, R.E. and Leof, E.B. (2005). "Transforming growth factor-beta activation of phosphatidylinositol 3-kinase is independent of Smad 2 and Smad3 and regulates fibroblast responses via p21-activated kinase-2." Cancer Res **65**: 10431-10440.
- Wilkes, M.C., Murphy, S.J., Garamszegi, N. and Leof, E.B. (2003). "Cell-type-specific activation of PAK2 by transforming growth factor β independent of Smad2 and Smad3." Mol Cell Biol **23**: 8878-8889.
- Willis, S.A. and Mathews, L.S. (1997). "Regulation of activin type I receptor function by phosphorylation of residues outside the GS domain." FEBS Lett **420**(2-3): 117-120.
- Worby, C.A. and Dixon, J.E. (2002). "Sorting out the cellular functions of sorting nexins." Nat Rev Mol Cell Biol **3**: 919-931.

- Wrana, J.L. (2013). "Signaling by the TGF β superfamily." Cold Spring Harb Perspect Biol **5**(10).
- Wrana, J.L., Attisano, L., Wieser, R., Ventura, F. and Massagué, J. (1994). "Mechanism of activation of the TGF-beta receptor." Nature **370**(6488): 341-347.
- Wrighton, K.H., Lin, X. and Feng, X.H. (2009). "Phospho-control of TGF-beta superfamily signaling." Cell Res **19**(1): 8-20.
- Wrighton, K.H., Willis, D., Long, J., Liu, F., Lin, X. and Feng, X.H. (2006). "Small C-terminal domain phosphatases dephosphorylate the regulatory linker regions of Smad2 and Smad3 to enhance transforming growth factor-beta signaling." J Biol Chem **281**(50): 38365-38375.
- Wu, J.W., Hu, M., Chai, J., Seoane, J., Huse, M., Li, C., Rigotti, D.J., Kyin, S., Muir, T.W., Fairman, R., Massagué, J. and Shi, Y. (2001). "Crystal structure of a phosphorylated Smad2. Recognition of phosphoserine by the MH2 domain and insights on Smad function in TGF-beta signaling." Mol Cell **8**: 1277-1289.
- Wu, R., Abramson, A.L., Symons, M.H. and Steinberg, B.M. (2010). "Pak1 and Pak2 are activated in recurrent respiratory papillomas, contributing to one pathway of Rac1-mediated COX-2 expression." Int J Cancer **127**(9): 2230-2237.
- Wu, X., Zhang, N. and Lee, M.M. (2012). "Mullerian inhibiting substance recruits ALK3 to regulate Leydig cell differentiation." Endocrinology **153**(10): 4929-4937.
- Wu, Z.B., Cai, L., Lin, S.J., Lu, J.L., Yao, Y. and Zhou, L.F. (2013). "The miR-92b functions as a potential oncogene by targeting on Smad3 in glioblastomas." Brain Res **1529**: 16-25.
- Xia, W., Wei, Y., Du, Y., Liu, J., Chang, B., Yu, Y.L., Huo, L.F., Miller, S. and Hung, M.C. (2009). "Nuclear expression of epidermal growth factor receptor is a novel prognostic value in patients with ovarian cancer." Mol Carcinog **48**(7): 610-617.
- Xia, Y., Yu, P.B., Sidis, Y., Beppu, H., Bloch, K.D., Schneyer, A.L. and Lin, H.Y. (2007). "Repulsive guidance molecule RGMA alters utilization of bone morphogenetic protein (BMP) type II receptors by BMP2 and BMP4." J Biol Chem **282**(25): 18129-18140.
- Xiao, Z., Liu, X. and Lodish, H.F. (2000). "Importin beta mediates nuclear translocation of Smad 3." J Biol Chem **275**: 23425-23428.
- Xu, L., Alarcon, C., Col, S., and Massague, J. (2003). "Distinct domain utilization by Smad3 and Smad4 for nucleoporin interaction and nuclear import." J Biol Chem **278**: 42569-42577.
- Xu, L., Kang, Y., Col, S. and Massague, J. (2002). "Smad2 nucleocytoplasmic shuttling by nucleoporins CAN/Nup214 and Nup153 feeds TGFbeta signaling complexes in the cytoplasm and nucleus " Mol Cell **10**: 271-282.

- Xu, L., Yao, X., Chen, X., Lu, P., Zhang, B. and Ip, Y.T. (2007). "Msk is required for nuclear import of TGF- β /BMP-activated Smads." *J Cell Biol* **178**(6): 981-994.
- Xu, Y., Wang, D., Zhao, L.M., Zhao, X.L., Shen, J.J., Xie, Y., Cao, L.L., Chen, Z.B., Luo, Y.M., Bao, B.H. and Liang, Z.Q. (2013). "Endoglin is necessary for angiogenesis in human ovarian carcinoma-derived primary endothelial cells." *Cancer Biol Ther* **14**(10): 937-948.
- Yagi, K., Goto, D., Hamamoto, T., Takenoshita, S., Kato, M. and Miyazono, K. (1999). "Alternatively spliced variant of Smad2 lacking exon 3. Comparison with wild-type Smad2 and Smad3." *J Biol Chem* **274**(2): 703-709.
- Yamamoto, T.S., Takagawa, S., Katayama, I. and Nishioka, K. (1999). "Anti-sclerotic effect of transforming growth factor-beta antibody in a mouse model of bleomycin-induced scleroderma." *Clin Immunol* **92**(1): 6-13.
- Yamashita, M., Fathyol, K., Jin, C., Wang, X., Liu, Z. and Zhang, Y.E. (2008). "TRAF6 mediates Smad-independent activation of JNK and p38 by TGF-beta." *Mol Cell* **31**(6): 918-924.
- Yan, X., Pan, J., Xiong, W., Cheng, M., Sun, Y., Zhang, S. and Chen, Y. (2014). "Yin Yang 1 (YY1) synergizes with Smad7 to inhibit TGF-beta signaling in the nucleus." *Sci China Life Sci* **57**(1): 128-136.
- Yan, X., Zhang, J., Sun, Q., Tuazon, P.T., Wu, X., Traugh, J.A. and Chen, Y.G. (2012). "p21-Activated kinase 2 (PAK2) inhibits TGF-beta signaling in Madin-Darby canine kidney (MDCK) epithelial cells by interfering with the receptor-Smad interaction." *J Biol Chem* **287**(17): 13705-13712.
- Yang, X., Teng, Y., Hou, N., Fan, X., Cheng, X., Li, J., Wang, L., Wang, Y., Wu, X. and Yang, X. (2011). "Delayed re-epithelialization in Ppm1a gene-deficient mice is mediated by enhanced activation of Smad2." *J Biol Chem* **286**(49): 42267-42273.
- Yao, D., Dore Jr, J.J. and Leof, E.B. (2000). "FKBP12 is a negative regulator of transforming growth factor-beta receptor internalization." *J Biol Chem* **275**(17): 13149-13154.
- Yao, X., Chen, X., Cottonham, C. and Xu, L. (2008). "Preferential utilization of Imp7/8 in nuclear import of Smads." *J Biol Chem* **283**(33): 22867-22874. .
- Yarar, D., Surka, M.C., Leonard, M.C. and Schmid, S.L. (2008). "SNX9 activities are regulated by multiple phosphoinositides through both PX and BAR domains." *Traffic* **9**: 133-146.
- Yin, X., Murphy, S.J., Wilkes, M.C., Ji, Y. and Leof, E.B. (2013). "Retromer maintains basolateral distribution of the type II TGF-beta receptor via the recycling endosome." *Mol Biol Cell* **24**(2285-2298.).
- Ying, S.X., Hussain, Z.J. and Zhang, Y.E. (2003). "Smurf1 facilitates myogenic

- differentiation and antagonizes the bone morphogenetic protein-2-induced osteoblast conversion by targeting Smad5 for degradation." *J Biol Chem* **278**(40): 39029-39036.
- Ying, S.Y. (1988). "Inhibins, activins, and follistatins: gonadal proteins modulating the secretion of follicle-stimulating hormone." *Endocr Rev* **9**(2): 267-293.
- Yokouchi, Y., Vogan, K.J., Pearse, R.V., 2nd and Tabin, C.J. (1999). "Antagonistic signaling by Caronte, a novel Cerberus-related gene, establishes left-right asymmetric gene expression." *Cell* **98**(5): 573-583.
- Yoshida, Y. and Tanaka, K. (2010). "Lectin-like ERAD players in ER and cytosol." *Biochim Biophys Acta* **1800**(2): 172-180.
- Yoshitomi, H., Kobayashi, S., Ohtsuka, M., Kimura, F., Shimizu, H., Yoshidome, H. and Miyazaki, M. (2008). "Specific expression of endoglin (CD105) in endothelial cells of intratumoral blood and lymphatic vessels in pancreatic cancer." *Pancreas* **37**(3): 275-281.
- Yu, D., Zhuang, L., Sun, X., Chen, J., Yao, Y., Meng, K. and Ding, Y. (2007). "Particular distribution and expression pattern of endoglin (CD105) in the liver of patients with hepatocellular carcinoma." *BMC Cancer* **7**: 122.
- Yu, J., Pan, L., Qin, X., Chen, H., Xu, Y., Chen, Y. and Tang, H. (2010). "MTMR4 attenuates transforming growth factor beta (TGFbeta) signaling by dephosphorylating R-Smads in endosomes." *J Biol Chem* **285**(11): 8454-8462.
- Yu, L., Hébert, M.C. and Zhang, Y.E. (2002). "TGF- β receptor-activated p38 MAP kinase mediates Smad-independent TGF- β responses." *EMBO J* **21**(3749-3759).
- Yu, P.B., Beppu, H., Kawai, N., Li, E. and Bloch, K.D. (2005). "Bone morphogenetic protein (BMP) type II receptor deletion reveals BMP ligand-specific gain of signaling in pulmonary artery smooth muscle cells." *J Biol Chem* **280**(26): 24443-24450.
- Yuzawa, H., Koinuma, D., Maeda, S., Yamamoto, K., Miyazawa, K. and Imamura, T. (2009). "Arkadia represses the expression of myoblast differentiation markers through degradation of Ski and the Ski-bound Smad complex in C2C12 myoblasts." *Bone* **44**(1): 53-60.
- Zawel, L., Dai, J.L., Buckhaults, P., Zhou, S., Kinzler, K.W., Vogelstein, B. and Kern, S.E. (1998). "Human Smad3 and Smad4 are sequence-specific transcription activators." *Mol Cell* **1**(4): 611-617.
- Zhang, W., Jiang, Y., Wang, Q., Ma, X., Xiao, Z., Zuo, W., Fang, X. and Chen, Y.G. (2009). "Single-molecule imaging reveals transforming growth factor-beta-induced type II receptor dimerization." *Proc Natl Acad Sci U S A* **106**(37): 15679-15683.

- Zhang, Y., Feng, X.H. and Derynck, R. (1998). "Smad3 and Smad4 cooperate with c-Jun/c-Fos to mediate TGF-beta-induced transcription." Nature **394**(6696): 909-913.
- Zhu, H., Kavsak, P., Abdollah, S., Wrana, J.L. and Thomsen, G.H. (1999). "A SMAD ubiquitin ligase targets the BMP pathway and affects embryonic pattern formation." Nature **400**(6745): 687-693.
- Zimmerman, L.B., De Jesus-Escobar, J.M. and Harland, R.M. (1996). "The Spemann organizer signal noggin binds and inactivates bone morphogenetic protein 4." Cell **86**(4): 599-606.
- Zwaagstra, J.C., El-Alfy, M. and O'Connor-McCourt, M.D. (2001). "Transforming growth factor (TGF)-beta 1 internalization: modulation by ligand interaction with TGF-beta receptors types I and II and a mechanism that is distinct from clathrin-mediated endocytosis." J Biol Chem **276**(29): 27237-27245.
- Zwaagstra, J.C., Guimond, A. and O'Connor-McCourt, M. (2000). "Predominant intracellular localization of the type I transforming growth factor-beta receptor and increased nuclear accumulation after growth arrest." Exp Cell Res **258**(1): 121-134.

APPENDICES

Appendix I: Gene Silencing

Gene silencing was achieved primarily by lentiviral transduction of shRNA sequences supplied by Sigma's MISSION library purchased from the Mayo Clinic Jacksonville RNA Interference Technology Resource. In the case of silencing components of the coatamer complex, generation of stable knockdown clones using shRNA was unsuccessful so transient expression of siRNA to Cop β was introduced by transfection with Lipofectamine® 2000 (Invitrogen, Carlsbad, California).

Gene Silencing Constructs

Gene Silence Target	Pool	Sequence	Silencing Method
Sorting Nexin 9 (SNX9)	Pool 77	CCTGACTTGGATTTGATAGAA	Short Hairpin RNA
Sorting Nexin 9 (SNX9)	Pool 78	CCTACTGACTACGTGGAAATT	Short Hairpin RNA
Importin 8 (Imp8)	Pool 89	GCACATTGTTAGAGAGACAAT	Short Hairpin RNA
Importin β (Imp β)	Pool 5	GCGCTGTTAGACATGAGCTAA	Short Hairpin RNA
Sec 61 (Sec61)		TGGCGATTCTACACGGAAGAT	Short Hairpin RNA
Non Targeting (NT)	NT	CGAAAGTAGGTACATCCCTTA	Short Hairpin RNA
Coatamer β (Cop β)	Transient	AAAAGCCGTCTCCTTTGACTC	Short Inhibitory RNA
Scrambled	Transient	GTACAGACTATTGCCTCTCGA	Small Inhibitory RNA

Appendix II: Site – Directed Mutagenesis

Site-directed Mutagenesis Primer Sequences

SNX9 BAR Mut	Forward	GCACTGGAAGCGATGCACAGGGCCCT TACCCAGGAGTATTCAGCAGATAGGGAAG
SNX9 BAR Mut	Reverse	CGTGACCTTCGCTAGGTGTCCCGGA
SNX9 RYK Mut	Forward	AAACCACAAAGATGACCACTTTGA
SNX9 RYK Mut	Reverse	TTTGGTGTCTACTGGTGAACT
SNX9 delta13C	Forward	GAAACAATCGCATAATAGCTGAGG
SNX9 delta13C	Reverse	CCTCAGCTATTATGCGATTGTTTC
SNX9 esc	Forward	CCTGATTTGGATTTAATAGAG
SNX9 esc	Reverse	GGACTAACCTAAATTATCTC

Mutagenesis

Introducing directed point mutants in existing constructs has become standard and quite reliable using commercially available kits. Quikchange® II XL (Agilent Technologies, Santa Clara, California) site-directed mutagenesis kits offer fast, reliable and inexpensive mutagenesis. The most problematic step of the process is ensuring high quality primers. Sometimes, more than one set of primers were designed to yield a suitable PCR product. Primers are recommended to be between 25 and 45 base pairs but I have opted for primers approximately 30 residues long and ending in a G or C. The T_M (melting temperature) should be greater than 77°C and to calculate melting temperature I used the equation: $T_m = 81.5 + 0.41(\%GC) - 675/N - \% \text{ mismatch}$, where N = primer length. A GC content of 40% is optimal but not essential. In the case of insertions, I included 12-15 bases of correct sequence flanking either side of the inserted sequence. The Mutagenesis PCR Reaction Mix was then prepared in a PCR tube and placed in a thermocycler with hot top assembly. Cycling parameters are listed below.

Mutagenesis PCR Reaction Mix.

Mutagenesis

Cycling Parameters for site-directed

Component	Final Concentration
10X reaction buffer	1X (5 µl)
dsDNA	50 ng
Forward Primer	125 ng
Reverse Primer	125 ng
dNTP Mix	1 µl
Water	Bring up to 50 µl
Pfu Turbo DNA polymerase	1 µl

Segment	Cycles	Temp	Time
1	1	95°C	30 seconds
2	16	95°C	30 seconds
		55°C	1 minute
		68°C	1 minute/kb of plasmid
Hold	Hold	4°C	Indefinite

To ensure the methylated, non-mutated parental DNA is no longer present in with the amplified mutants, 1 µl of the restriction enzyme *Dpn1* (New England Biolabs, Ipswich, Massachusetts) was added to the mix and incubated at 37°C for 1 hour. Finally the mix was transformed into the supplied XL1-Blue competent cells (Agilent

Technologies, Santa Clara, California) and plated on LB-Ampicillin plates with 80 µg/ml X-gal and 20 mM isopropyl β-d-thiogalactopyranoside (IPTG) (Sigma-Aldrich, St Louis, Missouri) added. Blue colonies represent those containing the desired mutation.

Appendix III: Cell Culture

Culture Conditions

Standard cell culture techniques were employed and all assays were carried out in sterile flow hoods while cells were maintained at 37°C with 5% Carbon dioxide and fixed humidity. Cell lines were cultured in culture media recommended for optimal growth by the supplier and supplemented with 10% Fetal Bovine Serum (FBS) (Gibco® Life Technologies, Grand Island, New York) in 75cm² flasks with regular passaging (as per ATCC suggestions) before expansion in 75 cm² flasks for freezing down stocks or experimental manipulation. When generating and maintaining stably selection of plasmids carrying antibiotic resistance, antibiotics were added as described in Appendix XI. Once a large seed stock (approximately 20 cryovials) was banked in liquid nitrogen storage, dividing cultures were never passaged more than three times, thus ensuring all experiments were performed on cells with a similar genetic background and not introducing genetic drift to the experiments. Upon the third passage, cells were discarded with a new seed stock thawed to replace it. Cultures underwent regular inspection for signs of transformation, multi-nucleation, excessive blebbing, drifting or contamination with cultures immediately discarded if any warning signs were observed.

Passaging consisted of 2 washes with sterile Phosphate Buffered Saline (PBS – see Appendix IV) followed by a 6 minute incubation in 0.05% Trypsin (Gibco® Life Technologies, Grand Island, NY) in PBS. Trypsin digestion was halted through the addition of 10X 10% FBS-Dulbecco's Modified Eagle (DME) (Gibco® Life Technologies, Grand Island, New York) media and cells were pipetted into a 15 ml tube for counting (using a haemocytometer or simply split 1:5 vol/vol).

Appendix IV: Buffer Recipes

Phosphate-Buffered Saline for Cell Culture

Component	Final Concentration	Added for 1 L (1X)
NaCl	137 mM	8 g
KCl	2.7 mM	0.2 g
Na ₂ HPO ₄	10 mM	1.44 g
KH ₂ PO ₄	1.8 mM	0.24 g
Sterile Water	N/A	Up to 1 L

DNA Restriction Digest Reaction

Component	Amount Added
DNA (insert or plasmid)	1 – 2 µg
Restriction Enzyme 1	1 µl
Restriction Enzyme 2	1 µl
10X Reaction Buffer	3 µl
Water	Up to 30 µl
BSA (if required)	As suggested by manufacturer

DNA Ligation Reaction

Component	Amount Added
Plasmid DNA	25 ng
Insert DNA	75 ng
5X Ligation Buffer	2 µl
T4 DNA Ligase	1 µl
water	Bring up to 10 µl

DNA Sequencing Reaction Mix

Component	Final Concentration
DNA	25 x (kb of PCR product or plasmid) ng
10X Sequencing Buffer	1 µl
Primer	3.2 pmol
Sterile water	Up to 10 µl

Tris-acetate-EDTA (TAE) Buffer 50X stock

Component	Amount Added for 1 L
Tris-HCl	242 g
Glacial Acetic Acid	57.1 ml
EDTA (pH 8.0)	100 ml
Water	Up to 1 L

DNA/RNA Agarose gel Composition.

Agarose Gel	1.0 %	1.2 %	1.5 %
TAE Buffer	Bring up to 100 ml	Bring up to 100 ml	Bring up to 100 ml
Agarose	1 g	1.2 g	1.5 g
Ethidium bromide	30 µg	30 µg	30 µg

DNA Sample Buffer (6X Stock).

Component	Amount Added
Glycerol	3 ml
Bromophenol Blue	25 mg
Water	Bring up to 10 ml

SOC Bacterial Growth Media

Component	Add for 1 L
Bacto-tryptone	20 g
Yeast Extract	5 g
NaCl	2 ml (5M stock)
KCl	2.5 ml (1M stock)
MgCl ₂	10 ml (1M stock)
MgSO ₄	10 ml (1M stock)
Glucose	20 ml (1M stock)
Water	Up to 1 L

Liquid Broth Bacterial Growth Media

Component	Added for 1 mL
Bacto-Tryptone	10 g
Yeast Extract	5 g
NaCl	10 g
Water	Bring up to 1 L
Antibiotic (Amp/Kan)	50 µg/ml

STE Buffer for suspension of bacterial pellets

STE buffer Component	Final Concentration
Tris-HCl (pH 8.0)	10 mM
NaCl	150 mM
EDTA	1 mM
Lysozyme	100 µg/ml

Elution Buffer for GST protein elution

Elution Buffer Component	Final Concentration
Tris-HCl (pH 8.0)	100 mM
Triton-X	0.1%
NaCl	150 mM
Glutathione	15 mM

Storage Buffer for Purified GST Proteins

Component of Storage Buffer	Final Concentration
Tris-HCl (pH 7.5)	20 mM
Glycerol	20% (by volume)
KCl	150 mM
Dithiothreitol (DTT)	0.5 mM
Complete® Protease Inhibitor	1X

Hypotonic Buffer for Nuclei Purification

Components	Final Concentration
HEPES (pH 7.9)	10 mM
MgCl ₂	1.5 mM
KCl	10 mM
Phenylmethylsulfonyl fluoride (PMSF)	0.2 mM
Dithiothreitol (DTT)	0.5 mM

Disruption Buffer for Organelle Fractionation

Component	Final Concentration
Tris HCl (pH 8.5)	8 mM
MgCl ₂	0.1 mM
2-mercaptoethanol	11 mM
Sucrose	0.25 M
Pancreatic DNase I	1 µg/ml

Envelope Buffer for Organelle Fractionation

Component	Final Concentration
Tris HCl (pH 7.5)	10 mM
MgCl ₂	0.1 mM
2-mercaptoethanol	14 mM
Sucrose	0.25 M
Pancreatic DNase I	1 µg/ml

Lipid Solubilizing Buffer for Organelle Fractionation

Components	Final Concentration
Sucrose	0.25 M
Tris HCl (pH 7.5)	50 mM
KCl	25 mM
MgCl ₂	5 mM
Triton X-100	2 %

Chromatin Solubilizing Buffer for Nuclear Fractionation

Component	Final Concentration
Sucrose	0.25 M
Tris HCl (pH 7.5)	50 mM
KCl	25 mM
MgCl ₂	0.3 M

Inner Nuclear Membrane Buffer A

Component	Final Concentration
Sucrose	0.25 M
Tris HCl (pH 7.4)	50 mM
MgCl ₂	10 mM
Dithiothreitol (DTT)	1 mM
Complete® protease inhibitor	1 X

1X Laemmli Buffer for Co-Immunoprecipitation.

Component of 1X Laemmli Buffer	Final Concentration
Sodium dodecylsulfate (SDS)	2 %
Tris-HCl (pH 6.8)	63 mM
β-mercaptoethanol	0.1 %
Glycerol	10 %
Bromophenol Blue	0.0025%

Modified RIPA Buffer for Cell Lysis.

Component	Final Concentration
Tris-HCl (pH 7.4)	50 mM
Triton X100	1 %
sodium deoxycholate	0.25 %
sodium chloride	150 mM
EDTA (pH 8.0)	1 mM
sodium fluoride	10 mM
PMSF	50 µg/ml
sodium vanadate	100 µM
Leupeptin	1 µg/ml

6X Laemmli Buffer.

Component of 6X Laemmli Buffer	Final Concentration	Amount for 10 ml
Sodium dodecylsulfate (SDS)	6 %	600 mg
Tris-HCl (pH 6.8)	375 mM	591 mg
β-mercaptoethanol	9 %	900 µl (14.7M stock)
Glycerol	48%	4.8 ml
Bromophenol Blue	0.03%	3 mg

SDS PAGE Running Buffer

Component	Final Concentration	Amount for 1 L (10X Stock)
Glycine	192 mM	144 g
Tris-HCl	25 mM	30.2 g
SDS	0.1 %	10.0 g

SDS PAGE Gel and Stack Recipes

<u>Running Gel</u>	8 %	10 %	12 %	15 %
30% Polyacrylamide	13.3 ml	16.7 ml	20.0 ml	25.0 ml
1M Tris (pH6.8)	12.5 ml	12.5 ml	12.5 ml	12.5
10% Ammonium sulphate	500 µl	500 µl	500 µl	500 µl
10% SDS	500 µl	500 µl	500 µl	500 µl
TEMED	30 µl	30 µl	30 µl	30 µl
dH₂O	23.16 ml	19.83 ml	16.5 ml	11.5 ml
Total Volume	50 ml	50 ml	50 ml	50 ml

<u>Stack (4%)</u>	<u>Acrylamide</u>	<u>1M Tris</u>	<u>10% AP</u>	<u>10% SDS</u>	<u>TEMED</u>	<u>dH₂O</u>	<u>Total</u>
<u>Reagent</u>	<u>850 µl</u>	<u>625 µl</u>	<u>50 µl</u>	<u>50 µl</u>	<u>5 µl</u>	<u>3.4 ml</u>	<u>5 ml</u>

SDS PAGE Transfer Buffer

Component	Final Concentration	Added for 1 L
Tris-HCl	25 mM	3.03 g
Glycine	192 mM	14.4 g
Water	50 %	500 ml
Methanol	20 %	200 ml
SDS (Optional)	0.025 - 0.1 %	2.5 – 10 ml (10% Stock)

Tris-Buffered Saline with Tween (TBST) Buffer

Component	Final Concentration	Added for 1 L (pH 7.6)
Tris-HCl	50 mM	24.23 g
NaCl	150 mM	80.06 g
Water	N/A	To 1 L
Tween-20	0.01 %	1 ml

Histone Lysis Buffer

Component	Final Concentration
Tris-Cl (pH 8.0)	20 mM
NaCl	250 mM
Triton X100	0.1%
EDTA (pH 8.0)	5 mM
NaF	5 mM
Aprotinin	0.1 Trypsin Inhibitor Unit (TAU)
Leupeptin	1 µg/µl
Sodium orthovanadate	100 µM
Phenylmethylsulfonyl fluoride (PMSF)	50 µg/ml

Kinase Buffer

Component	Final Concentration
Tris-HCl (pH 7.4)	25 mM
MgCl ₂	10 mM
Dithiothreitol (DTT)	1 mM

Gel Destain Buffer

Component	Final Concentration
Methanol	50 %
Acetic Acid	40 %
Water	10 %

GST Lysis Buffer

Component	Final Concentration
Tris-Cl (pH 8.0)	20 mM
NaCl	200 mM
EDTA (pH 8.0)	1 mM
Nonident P-40	0.5%
Aprotinin (Sigma-Aldrich, St Louis, Missouri)	2 µg/µl
Leupeptin (Sigma-Aldrich, St Louis, Missouri)	1 µg/µl
Pepstatin (Sigma-Aldrich, St Louis, Missouri)	0.7 µg/ml
Phenylmethylsulfonyl fluoride (PMSF)	25 µg/ml

HEPES Liposome Buffer

Component	Final Concentration
HEPES (pH 7.50)	50 mM
KCl	150 mM
Aprotinin	0.1 Trypsin Inhibitor Units (TIU)
NaF	50 mM
PMSF	50 µg/ml
Sodium vanadate	100 µM
Leupeptin	1 µg/ml

Soft Agar Plates

Per 6-well dish	Base (Bottom) Plug	Top Layer
Agarose (DNA grade)	700 µl of 1.6 %	450 µl of 0.8 %
2X DME	700 µl	450 µl
Fetal Bovine Serum	100 µl	100 µl
AKR-2B Cells	-	4000 cells/well
TGFβ (as required)	-	10 ng/ml

Chromatin Immunoprecipitation Elution Buffer

Component	Final Concentration
Sodium Docecyl Sulfate	1%
NaHCO ₃	100 mM

Appendix V: Quantitative Reverse Transcriptase Polymerase Chain Reaction

qRT-PCR Primer Sequences

Gene	qRT-PCR primer sequence	Amplicon (bp)
PAI-1 forward.1	GAAAGGGACACGCATTGGTAA	94
PAI-1 reverse.1	GATGGTGCTGTTCCAAA	
PAI-1 forward.2	GAAAGGGCACGCATTGGTAA	
PAI-1 reverse.2	GATGGTGCTGTTCCAAA	
Furin forward	GAGACTTCTTCTTCTTCGGCG	
Furin reverse	CCAGGATGTTGTGCGATGCTGA	
MixL forward	ATCCCCTGGGCCTTCTTACT	
MixL reverse	GGGAAACTGAGTCAAGCCGA	
Goosecoid fwd	GCTGTCCTGGAATTTCTCTGT	
Goosecoid rvs	GTGTGTCCACAGCACTTCCC	
CTGF forward	GCATCCTCCTACCGCGTC	107
CTGF reverse	CAGTCCTGGCCCATAGCAG	
eNOS forward	TACGCACCCAGAGCTTTTCTT	108
eNOS reverse	GGGAGGAAGACTGTCAGGAAC	
CRP2 forward	CCCGGACCTCGAGACCTAA	107
CRP2 reverse	GAGTGAGGTGGCGTCCACAG	
TGFβ3 forward	TAGAGGCGGCCAAGCATTTT	99
TGFβ3 reverse	TGCAGAAAGAACGGATTGTCC	
ATF3 forward	TCTGTCCCAGAATGACTGTGC	102
ATF3 reverse	ACTCCCGGAAAAATCATGCCA	
CDC25A for	GTGAAGGTTTCTTCTCTGCGA	100
CDC25A rev	CCGTGGAGGAAGAGTCTTGAG	
MYB forward	ATGTTTCATCCGTTTGGGCGT	91
MYB reverse	CAGGAACCACGAGGCAGTT	
TP53 forward	CCCAGCCAAAGAAGAAACA	98
TP53 reverse	GTTCCAAGGCCTCATTGAGCT	
Smad7 forward	GACGAAGAGAGTCTCCGAGG	
Smad7 reverse	GCTCTCATGAGCTGCTGGC	
GAPDH forward	CCACCCATGGCAAATTCCATGGCA	
GAPDH reverse	TCTAGACGGCAGGTCAGGTCCACC	
MDM2 forward	GGATTTTCGGACGGCTCTCGC	164
MDM2 reverse	CGCGCAGCGTTCACACTAGTG	
Bcl2 forward	CTCGTCGCTACCGTCGTGACTTCG	106
Bcl2 reverse	CAGATGCCGTTTCAGGTAAGTACAGTC	
Akt1 forward	GCACAAACGAGGGGAGTACAT	113
Akt1 reverse	CCTCACGTTGGTCCACATC	
IL-8 forward	ATGACTTCCAAGCTGGCCGTGGCT	106
IL-8 reverse	TCTCAGCCCTCTTCAAAAATTCTC	
E-Selectin for	CCTCTGACAGAGGAAGCTCAGAACT	126
E-Selectin rev	TCCACTCTCCAGAGGACGTACACCG	
uPA forward	GAGCAGCTCATCTTGCACGAATAC	98
uPA reverse	GCCAGTGATCTCACAGTCTGAACC	

Total RNA was extracted from the cells one of two ways, depending on availability of reagents, either using Trizol® (Invitrogen, Carlsbad, California) or using the RNeasy Plus Mini Kit with gDNA eliminator spin columns to remove genomic DNA (QIAGEN, Velno, The Netherlands).

Trizol® Extraction Method

Cells were grown in 6-well plates and lysed directly on the plate using 1 ml of Trizol® and pipetted up and down several times to ensure thorough lysis before adding to a microfuge tube. After 5 minutes at room temperature to ensure complete dissociation of the nucleoprotein complex, 200 µl of chloroform was added with vigorous shaking for 10-15 seconds followed by an incubation of 2-3 minutes at room temperature. After incubation, the mix was separated into 3 phases by centrifugation at 12000 x g for 15 minutes at 4°C. The upper (colourless) aqueous phase contained the RNA and was approximately 50% of the solution. A lower red phenol-chloroform phase and interphase contain protein and DNA and were discarded while the aqueous phase was pipetted into a new microfuge tube for RNA isolation.

To the aqueous phase, 500 µl of 100% isopropanol was added and incubated at room temperature for 10 minutes followed by centrifugation at 12000 x g for 10 minutes at 4°C. A small opaque pellet formed to the outside of centre of the tube and after removal of the supernatant, the pellet was washed with 1 ml of 75% ethyl-alcohol prior to a brief vortex and centrifugation at 7500 x g for 5 minutes at 4°C with the supernatant discarded. The pellet was air dried with the absence of the smell of alcohol determining the evaporation process was complete. RNA was re-suspended in 50 µl of sterile water and incubated at 60°C for 10 minutes.

RNeasy®-Plus-Mini (QIAGEN, Velno, The Netherlands)

Cells were grown in 6 wells and plated at 2.5×10^5 and left overnight to divide and attach, prior to experimental manipulation. Media was removed, followed by washing with PBS and cells lifted from the plate with 6 minute treatment with 0.5% Trypsin in PBS. Digestion was halted with addition of 1 ml 10%FBS-DME, pipetted up and down several times and added to a diethylpyrocarbonate (DEPC) -treated microfuge tube followed by centrifuge at 300 x g for 5 minutes and aspiration of all supernatant.

Disruption and homogenization of the cells was achieved through the addition of the supplied RLT Plus Buffer (with β-mercaptoethanol added) with 500 µl added to each tube. The mix was added directly into a QIAshredder® spin column (QIAGEN, Venlo, The Netherlands) and centrifuged at 13000 x g for 2 minutes at 4°C. 500 µl of 70% ethanol was added to the flow through and transferred to an RNeasy® spin column and centrifuged at 8000 x g for 15 seconds, and discarding the flow through. 700 µl of supplied Buffer RW1 was added to the column and another 15 second spin. The process was repeated using 500 µl of supplied Buffer RPE followed by a more stringent 2 minute wash with 500 µl Buffer RPE. A fresh DEPC-treated tube was added to the column and RNA eluted with 50 µl sterile water and a 1 minute spin at 8000 x g.

RNA was converted to cDNA for quantitative PCR using Superscript III Reverse Transcriptase (Life Technologies, Grand Island, New York). For each reaction, 5 µg of total RNA, 50 µM oligo (dT) (Invitrogen, Carlsbad, California) and 10 mM dNTP mix were incubated in 10 µl sterile water at 65°C for 5 minutes. After 5 minutes the tube was placed on ice for 1 minute prior to the addition of 10 µl cDNA Synthesis Mix, mixed gently and incubated at 50°C for 50 minutes. The reaction was terminated by raising

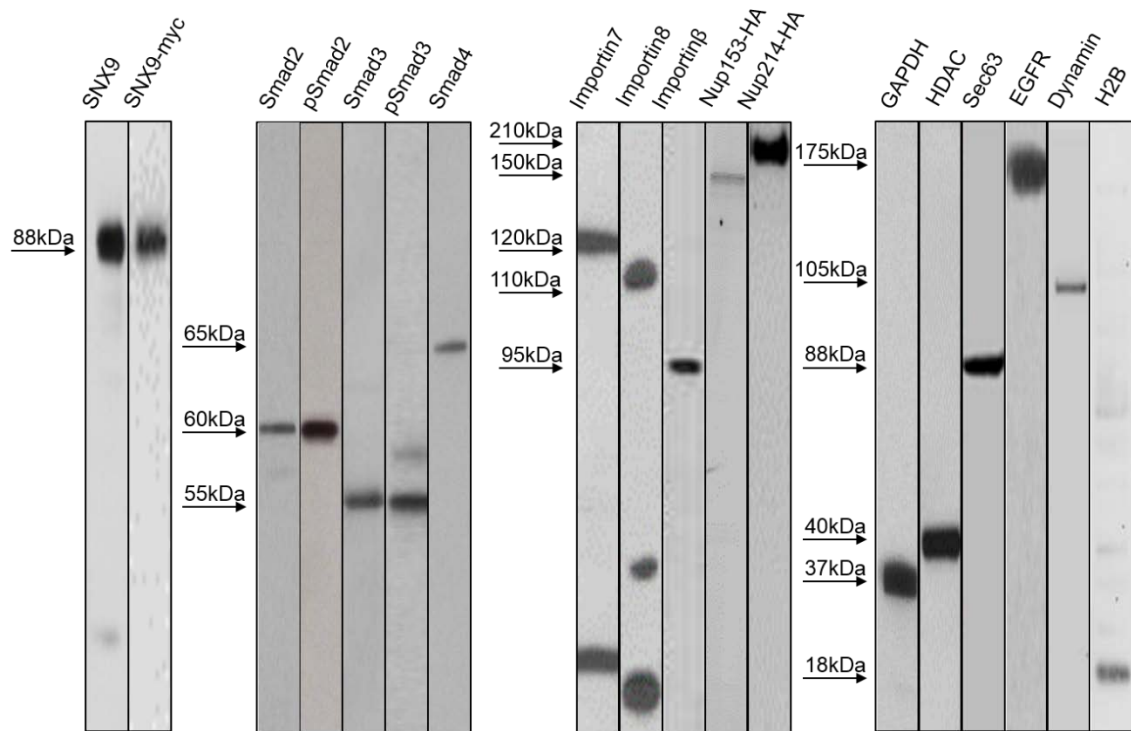
the temperature to 85°C for 5 minutes and 1 µl per reaction of RNase H was added and incubated for 20 minutes at 37°C.

cDNA Synthesis Mix for Reverse Transcriptase PCR

cDNA Synthesis Mix Component	Added per Reaction
10X RT Buffer	2 µl
25 mM MgCl ₂	4 µl
100 mM DTT	2 µl
RNaseOUT™ (40U/µl)	1 µl
Superscript® III Reverse Transcriptase (200U/µl)	1 µl

Quantitative real-time PCR was performed using the CFX96 Real-Time PCR detection system (Bio-Rad, Hercules, California). The cDNA samples were diluted 1:5 with water and a 50th used as template. The amplified nucleic acids were quantified using the SYBR® Green PCR Master Mix (Life Technologies, Grand Island, New York). The conditions for the PCR reactions were as follows: 50°C for 2 minutes, 95°C for 2 minutes, and 40 cycles of 95°C for 15 seconds, 60°C for 30 seconds, and 72°C for 30 seconds and SYBR® quantification. Primers were at 0.2 µM final concentration. To determine the relative expression levels of TGFβ-regulated genes, the mRNA levels were normalized to the level of GAPDH mRNA using the comparative threshold cycle (CT) method, in which the fold difference is $2^{-\Delta\Delta CT}$ (ΔCT of target gene - ΔCT of reference gene)

Appendix VI: Antibody Validation



Appendix VII: Bolton-Hunter Reaction

Prior to the labelling, water-soluble Bolton-Hunter reagent (Pierce) was dissolved in dimethyl sulfoxide (DMSO) at 1.5 mmol/L (0.55 mg/mL) and Na¹²⁵I was neutralized before use by adding 3 µmol/L phosphoric at a vol/vol ratio of 1:3 of Na¹²⁵I:acid.

To begin the reaction process, 20 µl of chloramine -T (5 mg/mL in PBS) were added to the neutralized Na¹²⁵I, followed by addition of 2 µL water-soluble Bolton-Hunter reagent. The reaction was allowed to proceed for 1 min, then stopped by the addition of 20 µL sodium metabisulphite (12 mg/mL in PBS). This was immediately followed by addition of the 100 µg of purified TAT-Smad3 in 0.5 mol/L borate (pH 9.2) and the reaction was allowed to proceed for 1 hour. The reaction was stopped by the addition of 600 µL of 0.2 mol/L glycine in 0.2 mol/L borate (pH 8.0). Labelled TAT-Smad3 was purified by spinning repeatedly through a Microcon concentrator (Millipore) and dialysis.

Appendix VII: Statistical Calculations for Chapter 4

Fig 4.2A

Soft Agar Assays			
NT+ / 77+	p=0.00049	Significant	n=12
NT+ / 78+	p=0.00081	Significant	n=12

Fig 4.2B

Growth Arrest Assays			
NT+ / 77+	p=0.00078	Significant	n=8
NT+ / 78+	p=0.00067	Significant	n=8

Fig 4.2C

qRT-PCR			
Goosecoid	p=0.00755	Significant	n=6
MixL1	p=0.90897	Not Significant	n=6
Furin	P=0.0326	Significant	n=3
Serpine	p=0.01812	Significant	n=6
Smad7	p=0.00178	Significant	n=6
CTGF	p=0.00525	Significant	n=6

Fig 4.3B Soft Agar Assay			
WT+/PX+	p=0.03472	Significant	n=3
WT+/SH+	p=0.04520	Significant	n=3
Fig 4.3C Luciferase Assays (shRNA)			
3TP	p=0.00085	Significant	n=15
SBE	p=0.03754	Significant	n=9
ARE	p=0.35943	Not Significant	n=12
Fig 4.3D 3TP Luciferase Assay (DNs)			
WT/PX	p=0.00133	Significant	n=3
WT/SH3	p=0.00855	Significant	n=3
SBE Luciferase Assay (DNs)			
WT/PX	p=0.00770	Significant	n=3
WT/SH3	p=0.00823	Significant	n=3
ARE Luciferase Assay (DNs)			
WT/PX	p=0.08974	Not Significant	n=3
WT/SH3	p=0.13284	Not Significant	n=3

Fig 4.4B

Smad2 Phosphorylation			
NT/sh 0	p=0.8075	Not Significant	n=9
NT/sh 30	p=0.68404	Not Significant	n=9
NT/sh 60	p=0.73513	Not Significant	n=9
Smad3 Phosphorylation			
NT/sh 0	p=0.97455	Not Significant	n=11
NT/sh 30	p=0.33528	Not Significant	n=11
NT/sh 60	p=0.69529	Not Significant	n=11
Smad2 Nuclear Accumulation			
NT/sh 0	p=0.26209	Not Significant	n=8
NT/sh 30	p=0.06745	Not Significant	n=8
NT/sh 60	p=0.50004	Not Significant	n=8
NT/sh120	p=0.29986	Not Significant	n=8
Smad3 Nuclear Accumulation			
NT/sh 0	p=0.1522	Not Significant	n=8
NT/sh 30	p=0.00346	Significant	n=8
NT/sh 60	p=0.00110	Significant	n=8
NT/sh120	p=0.00538	Significant	n=8

Fig 4.4D

Fig 4.5A

Smad2 Phosphorylation			
WT/PX20	p=0.14236	Not Significant	n=3
WT/PX60	p=0.22230	Not Significant	n=3
WT/SH20	p=0.53442	Not Significant	n=3
WT/SH60	p=0.44444	Not Significant	n=3
Smad3 Phosphorylation			
WT/PX20	p=0.47031	Not Significant	n=3
WT/PX60	p=0.52912	Not Significant	n=3
WT/SH20	p=0.34503	Not Significant	n=3
WT/SH60	p=0.62433	Not Significant	n=3
Smad2 Nuclear Accumulation			
WT/PX20	p=0.06431	Not Significant	n=3
WT/PX60	p=0.13002	Not Significant	n=3
WT/SH20	p=0.32054	Not Significant	n=3
WT/SH60	p=0.74327	Not Significant	n=3
Smad3 Nuclear Accumulation			
WT/PX20	p=0.00993	Significant	n=3
WT/PX60	p=0.00651	Significant	n=3
WT/SH20	p=0.08300	Significant	n=3
WT/SH60	p=0.00963	Significant	n=3
Smad2 Nuclear Staining			
WT+/PX+	p=0.77931	Not Significant	n=3
Smad3 Nuclear Staining			
WT+/PX+	p=0.01264	Significant	n=3

Fig 4.5B

Fig 4.5C

Fig 4.10B

SNX9:smad3 Co-localization			
AKR-2B	p=0.00213	Significant	n=18
NIH3T3	p=0.00631	Significant	n=9
WI 38	p=0.01004	Significant	n=10
NMuMg	p=0.00894	Significant	n=12
Eph4	p=0.00164	Significant	n=14

Fig 4.14B

- TGF β Smad2 Nuclear Staining			
NT/SNX	p=0.24312	Not Significant	n=18
NT/Imp8	p=0.06871	Not Significant	n=18
NT/Imp β	p=0.03248	Significant	n=18
- TGF β Smad3 Nuclear Staining			
NT/SNX	p=0.12633	Not Significant	n=18
NT/Imp8	p=0.09438	Not Significant	n=18
NT/Imp β	p=0.03618	Significant	n=18

Fig 4.15

+ TGFβ Smad2 Nuclear Staining			
NT/SNX	p=0.84271	Not Significant	n=18
NT/Imp8	p=0.88230	Not Significant	n=18
NT/Impβ	p=0.00653	Significant	n=18
+ TGFβ Smad3 Nuclear Staining			
NT/SNX	p=0.03461	Significant	n=18
NT/Imp8	p=0.02833	Significant	n=18
NT/Impβ	p=0.00844	Significant	n=18

Fig 4.16B

3TP Luciferase Assays			
KD+/WT+	p=0.0016	Significant	n=3
KD+/Mut+	p=0.0786	Not Significant	n=3
KD+/13C	p=0.0010	Significant	n=3
WT+/Mut+	p=0.0047	Significant	n=3
WT+/13C+	p=0.0418	Significant	n=3

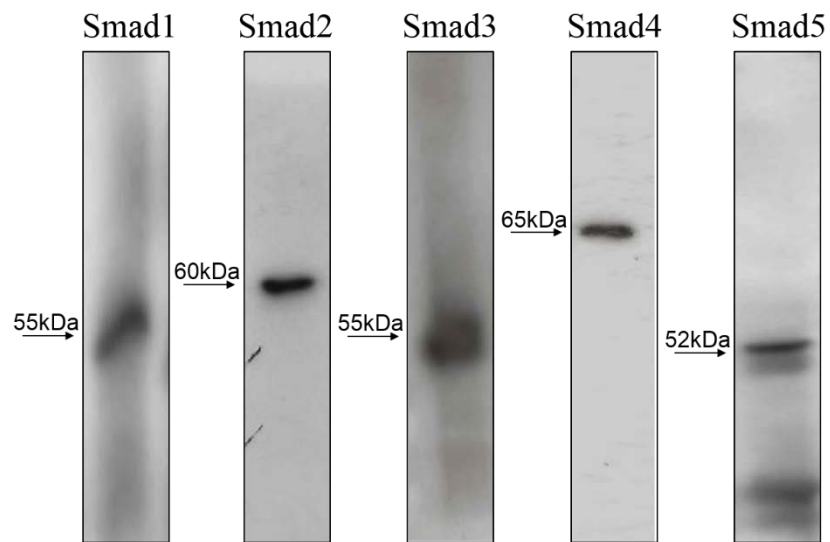
Fig 4.16C

ARE Luciferase Assays			
KD+/WT+	p=0.0931	Not Significant	n=3
KD+/Mut+	p=0.2461	Not Significant	n=3
KD+/13C	p=0.1640	Not Significant	n=3
WT+/Mut+	p=0.6322	Not Significant	n=3
WT+/13C+	p=0.7211	Not Significant	n=3

Fig 4.16D

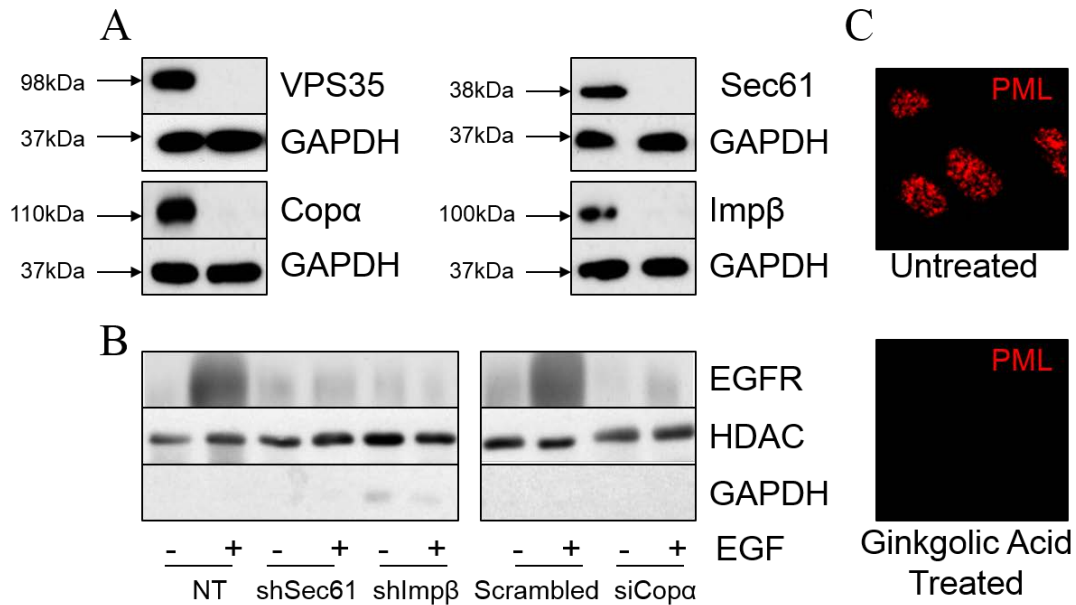
Liposome Assays			
KD-/KD+	p=0.0613	Not Significant	n=3
WT-/WT+	p=0.0015	Significant	n=3
Mut-/Mut+	p=0.0625	Not Significant	n=3
13C-/13+	p=0.0009	Significant	n=3
KD+/WT+	p=0.0016	Significant	n=3
KD+/Mut+	p=0.0531	Not Significant	n=3
KD+/13C	p=0.0006	Significant	n=3
Dynamin GTPase Assays			
KD / WT	p=0.0015	Significant	n=3
KD / Mut	p=0.0663	Not Significant	n=3
KD / 13C	p=0.1032	Not Significant	n=3

Appendix IX: Validating Smad Purity of Immunoprecipitation



Validation of Smad enrichment after Immunoprecipitation. After immunoprecipitation with relevant antibody, the purity of each immunoprecipitation was determined with predicted size of each Smad depicted to the left of each panel. Antibody details are supplied in Table 3.3.

Appendix X: Validating Disruption of Trafficking Compartments.



Validation of efficient gene knockdown and loss-of-function after gene silencing and pharmacological inhibition of retromer, COPI vesicles, retrotranslocon, nuclear pore and PML bodies. (A) Top-Left; Expression of Vps35 and GAPDH in MDCK cells stably infected with shRNA to Vps35. Bottom Left; Expression of Copα and GAPDH and transient transfection of Cos7 cells with siRNA to Copα. Top Right; Expression of Sec61 and GAPDH in AKR2B cells stably infected with shRNA to Sec61. Bottom Right; Expression of Importin-β and GAPDH in AKR2B cells stably infected with shRNA to Importin-β. (B) Left panels; Nuclear fractions indicating the nuclear presence of EGFR after 45 minutes of no treatment (-) or 50 ng/ml EGF stimulation (+) in AKR2B cells stably expressing non-targetting (NT), shRNA to Sec61 (shSec61) or shRNA to Importin-β (shImpβ). Right Panels; Nuclear fractions of Cos7 cells transiently transfected with either scrambled sequence siRNA or siRNA against Copα were treated as with shRNA infected cells. Top panels indicate levels of EGFR present in the nucleus while purity of the nuclear fractions is determined by the enrichment of HDAC and exclusion of GAPDH. (C) AKR2B cells were left untreated (top) and exposed to Ginkgolic Acid (bottom);(as per Chapter 3) and PML Nuclear bodies visualized by immunofluorescence confocal microscopy.

Appendix XI: Pharmacological Inhibitor Protocols

Cellular Trafficking Disruption

Pharmacological Inhibitor	Concentration Utilized
chlorpromazine (CPZ)	10 µg/ml
nystatin	25 µg/ml
Ginkgolic Acid	10 µM

Antibiotic Selection and Maintenance

Maintenance of stably integrated genes was achieved through the use of antibiotic selection. Unlike others, I choose not to maintain cells in culture media with a low level of antibiotic (as I feel this promotes selection of spontaneously generated antibiotic resistant clones). Instead I add a high (same concentration used to select clones originally) every third or fourth passage if there is a need to maintain a long-term culture. As mentioned above, generally, lines are not maintained longer than 3 passages and in that case cells are brought up in a high concentration of selective media until confluent, and then antibiotic is not added for the remaining passages.

When transient expression or gene silencing was sufficient, we utilized transient transfection or adenoviral infection, depending on the specific experimental requirements. For each cell line a kill curve was established to ensure effective target selection. Below are the antibiotics utilized and the range of concentrations used across the cell types. Hygromycin (50 - 200 µg/ml) (Sigma-Aldrich, St Louis, Missouri), Neomycin (0.5 - 2.0 mg/ml) (Life Technologies, Grand Island, New York) and Puromycin (1.0 -1.2 µg/ml) (Sigma-Aldrich, St Louis, Missouri).

Appendix XII: Bead Preparation for Chromatin Immunoprecipitation Assay

Blocking Protein A beads is required previous to use in ChIP assays.

1. Wash beads in RIPA buffer three times.
2. Aspirate RIPA buffer and add single stranded herring sperm DNA to 75 ng/ul of beads and BSA to a final concentration 0.1 ug/ul beads.
3. Add RIPA to twice the bead volume and incubate 30 minutes with rotation at room temp.
4. Wash once with RIPA, then add RIPA to bring volume up to twice the bead volume.